Investigation of riboswitches as new antibacterial targets

Identification and characterization of novel synthetic and natural riboswitch modulators with effect on bacterial cell growth

Dissertation

zur
Erlangung des Doktorgrades (Dr. rer. nat.)
der
Mathematisch-Naturwissenschaftlichen Fakultät
der
Rheinischen Friedrich-Wilhelms-Universität Bonn

vorgelegt von

Christina E. Lünse

aus

Quedlinburg

Bonn 2012

Angefertigt mit Genehmigung der Mathematisch-Naturwissenschaftlichen Fakultät der
Rheinischen Friedrich-Wilhelms-Universität Bonn

IV

Contents

Contents

X

List of Tables

List of Tables

List of Figures

Acknowledgements

There are many people without whom this work would not have been possible and to whom I am greatly indebted.

First of all, I owe my earnest thankfulness to Professor Dr. Günter Mayer, who has not only been my supervisor during the past three years, but who has become my mentor. I am grateful for his constant support, for his valuable suggestions and constructive criticism. Moreover, I would like to express my sincere appreciation for his encouragement of my career aspirations, his enthusiastic fostering of new project ideas as well as our vivid discussions.

Furthermore, I am indebted to Professor Dr. Michael Famulok, who has known me from the very beginning of my scientific career and for whose inestimable support and example I am very grateful.

I would also like to acknowledge them and the other co-assessors for their willingness to appraise this dissertation.

Additionally, there are many people whose collaborative contributions have been invaluable for my PhD research. These include Professor Dr. Gabriele Bierbaum and Professor Dr. Hans-Georg Sahl and their labs who have helped me with all microbiological experimentation, Professor Dr. Valentin Wittmann and Dr. Magnus Schmidt who synthesized the GlcN6P analog library and supplied Carba-sugars, Professor Dr. Colin Suckling and Fraser Scott who synthesized the triazolethiamine library and supplied triazolethiamine derivatives, Professor Dr. Louis Reymond and Lars Ruddigkeit who performed the *in silico* screening for GlcN6P analogs, PD Dr. Thomas Letzel and Dr. Giorgia Greco who performed the HILIC/MS analysis and PD Dr. Jens Müller for advice concerning quantitative real-time PCRs.

Moreover, I would like to thank all my interns, undergraduates and masterstudents for their contributions, in particular Alexander Müller, Anna Schüller and Jens Hör.

In addition, it is a great pleasure to thank the members of the Mayer and Famulok as well as the Sahl and Bierbaum groups for their help and support and the great times we shared in the lab. This includes in particular Barbara Albertoni, Anne Berscheid, Volkmar Fieberg, Nicole Florin, Jeff Hannam, Mohammed Hussein, Nicole Krämer, Björn Niebel, Falk Rohrbach, Anton Schmitz, Jan Vinkenborg, Benjamin Weiche, Miriam Wilmes, Christine Wosnitza and Bernhard Wulffen.

I am truly indebted and thankful to Dr. Jan L. Vinkenborg for his conscientuous proof-reading of my thesis, his helpful comments and suggestions.

Acknowledgements

Furthermore, I would like to express my heart-felt gratitude to my parents, my brother and my sister as well as to my "extended" family, the Armstrongs, for their love and support. In particular, I am deeply obliged to my mother, who has supported and encouraged me my entire life with care, love, good advice and honest words.

Ultimately, I would like to thank Anne Mai Wassermann, Christian Lentz, Katharina Hochheiser and Christine Wosnitza for their loving friendship, care and advice which accompanied me not only during the past three years, but throughout my entire studies in Bonn. The same is true for Ulrike Vogt, Franziska Briegnitz and Simone Kühn-Simon whom I am happy to know amongst my closest friends for more than 15 years.

Abstract

The increase in bacterial resistances and the decrease in available antibacterial substances against multi-drug resistant pathogens calls for an intensified search for novel antibiotics. Therefore, in this study riboswitches were investigated as new antibacterial drug targets.

Riboswitches, which are RNA elements mostly found in the 5' UTR of bacterial mRNA, consist of a metabolite-binding aptamer domain and an expression platform. They regulate up to 4 % of all bacterial genes, either by inhibiting transcription or translation initiation. As many of the genes regulated by riboswitches are essential for bacterial functioning, manipulation of riboswitch activation may enable control over bacterial growth and viability. In this study, two riboswitches with distinct regulatory mechanisms were investigated: the glmS ribozyme and a *thi*-box riboswitch. The glmS ribozyme is a catalytically active RNA that regulates gene expression by recognition of glucosamine-6-phosphate (GlcN6P), subsequent self-cleavage, and degradation of glmS mRNA. *Thi*-box riboswitches recognize thiamine pyrophosphate (TPP) and are involved in the regulation of TPP-biosynthesis genes. While TPP is a fundamental cofactor for the crucial function of many bacterial proteins, GlcN6P is an important precursor of cell wall biosynthesis.

Here, it was sought to identify modulators for these two riboswitch classes based on different strategies. Firstly, *in silico* predicted riboswitch ligands were validated *in vitro*. Secondly, *in vitro* and *in vivo* screenings were performed using rationally designed libraries of compounds with structural analogy to their natural ligand. Finally, also natural products were investigated for riboswitch modulation.

The screening of designed compound analogs identified carba-sugars as potent activators of the glmS ribozyme of *Staphylococcus aureus*. These GlcN6P analogs activate the ribozyme to a level comparable with the natural metabolite *in vitro* and revealed inhibition of bacterial growth of a vancomycin-intermediate resistant *S. aureus* strain. Furthermore, compounds suggested by virtual screening, and natural substances such as aminoglycosides were shown to be inhibitors of glmS ribozyme cleavage. Finally, a natural GlcN-nitrosourea-derivative revealed glmS ribozyme activating potential *in vitro*, albeit at higher concentrations than carba-sugars.

The *E. coli thi*-box riboswitch thiM was shown to be modulated by triazolethiamine (TT) and derivatives *in vivo* and increasing concentrations of TT led to a decrease in *E. coli* growth. Additionally, thiamine analogs containing metal-chelating groups that mimic the pyrophosphate moiety of TPP revealed efficient activation the *thi*-box riboswitch *in vivo*.

This study describes the discovery and characterization of the first glmS ribozyme activating compound with effects on bacterial growth as well as thiM riboswitch activators that act through a distinct mechanism in comparison to the already described thiamine analog pyrithiamine (PT). The different screening assays applied as well as the compounds identified in this study enabled a thorough investigation of riboswitches and their artificial regulation. In the future, some of these promising riboswitch modulators may serve as lead structures for novel antibacterials to combat the increasing number of multi-drug resistant pathogens.

Abstract

Zusammenfassung

Durch die Zunahme bakterieller Resistenzen stehen immer weniger antibiotisch wirksame Substanzen gegen multiresistente Bakterienstämme zur Verfügung. Diese Tatsache begründet die fortlaufende, intensive Suche nach neuen Antibiotika. Im Fokus dieser Suche liegen neben Substanzen mit neuen Wirkungsmechanismen auch solche, die neue Zielstrukturen angreifen. In der vorliegenden Arbeit wurden RNA-Schalter (Riboswitches) als neue Zielstrukturen für die Entwicklung antibakterieller Wirkstoffe untersucht.

Riboswitches sind RNA-Elemente, die zumeist in der 5' untranslatierten Region bakterieller mRNA zu finden sind und aus einer Metabolit-bindenden Aptamerdomäne und einer Expressionsdomäne bestehen. Diese RNA-Strukturen regulieren bis zu 4 % aller bakteriellen Gene, entweder durch vorzeitiges Beenden der Transkription oder Hemmung der Translationsinitiation. Da viele Riboswitch-regulierte Gene essentiell für bakterielle Funktionen sind, ermöglicht die Manipulation der Riboswitch-Aktivierung eventuell die Kontrolle von Bakterienwachstum und -überleben.

In dieser Arbeit wurden zwei RNA-Schalter mit verschiedenen regulatorischen Mechanismen untersucht: der glmS-RNA-Schalter sowie ein *thi*-Box Riboswitch. Der glmS Riboswitch ist eine katalytisch aktive RNA (ein Ribozym), welche durch Erkennung von Glucosamin-6-phosphat (GlcN6P), anschließender Selbstspaltung und Abbau der glmS mRNA die Genexpression reguliert. *Thi*-Box RNA-Schalter erkennen Thiaminpyrophosphat (TPP) und sind an der Regulation von Genen der TPP-Biosynthese beteiligt. Während TPP ein wichtiger Cofaktor für entscheidende Funktionen vieler bakterieller Proteine ist, spielt GlcN6P eine bedeutende Rolle als Vorläufer der Zellwandbiosynthese.

In der hier vorliegenden Arbeit wurden verschiedene Strategien zur Identifikation von Modulatoren dieser Riboswitch-Klassen genutzt. Zum einen wurden *in silico* vorhergesagte Riboswitch-Liganden *in vitro* validiert. Zum anderen wurden *in vitro* und *in vivo* Screenings mit designten Bibliotheken unternommen, die strukturelle Ähnlichkeit zum natürlichen Liganden aufwiesen. Schließlich wurden auch natürliche Substanzen auf ihre Riboswitch-modulierenden Wirkungen hin untersucht.

Im Screening der rational designten Substanzanaloga wurden Carba-Zucker als potente Aktivatoren des glmS-Ribozyms von *Staphylococcus aureus* identifiziert. Diese GlcN6P-Analoga aktivieren das Ribozym *in vitro* fast genauso stark wie der natürliche Metabolit und hemmen das Wachstum eines intermediär Vancomycin-resistenten *S. aureus* Stammes. Darüber hinaus konnte gezeigt werden, dass Substanzen, die im virtuellen Screening gefunden worden, sowie bereits bekannte, natürliche Substanzen wie beispielsweise Aminoglycoside, die glmS-Ribozym-Selbstspaltung hindern können. Außerdem zeigte eine Glucosamin-Nitrosoharnstoff-Verbindung glmS-Ribozym-Aktivierung *in vitro*, jedoch bei höheren Konzentrationen als die Carba-Zucker.

Desweiteren wurde gezeigt, dass der *E. coli thi*-Box Riboswitch thiM *in vivo* durch Triazolthiamin (TT) und Derivate moduliert wird und steigende Konzentrationen von TT zu einer Verminderung des Bakterienwachstums führen. Zusätzlich aktivierten Thiaminanaloga mit Metall-chelatierenden Gruppen, welche möglicherweise das Pyrophosphat von TPP imitieren,

Zusammenfassung

den ThiM Riboswitch *in vivo*.

  Diese Arbeit beschreibt die Entdeckung und Charakterisierung der ersten synthetischen Substanz, die das glmS Ribozym aktiviert und Bakterienwachstum hemmt, sowie thiM Riboswitch-Aktivatoren, die wahrscheinlich über einen vom bekannten Thiaminanalogon Pyrithiamine (PT) abweichenden Mechanismus auf den Riboswitch wirken. Die genutzen, unterschiedlichen Screening-Systeme sowie die in dieser Studie entdeckten Substanzen ermöglichen eine fundierte Untersuchung von Riboswitches und ihrer künstlichen Regulation. In Zukunft könnten einige dieser vielversprechenden Substanzen als Leitstrukturen für neue Antibiotika genutzt werden, um die steigende Zahl an multi-resistenten Pathogenen zu bekämpfen.

1 Introduction

Genetic control has been presumed to result mostly from protein factors that act as transcriptional repressors or activators. However, over the past 15 years the role of non-coding RNAs (ncRNAs) in the control of bacterial gene expression has been unraveled (Dambach and Winkler, 2009). Among them are ncRNAs acting in trans, such as small RNAs (sRNAs), which interact with their target mRNAs through base-pairing (Repoila and Darfeuille, 2009), or affect gene expression by associating with RNA-binding proteins (Babitzke and Romeo, 2007) or with RNA polymerase (Storz et al., 2006). Furthermore, the 5' untranslated region (5'UTR) of the mRNA can often contain cis-acting regulatory elements which respond to many different types of effector signals (Figure 1.1). These include the recognition of metabolites (Figure 1.1 A), or metals (Figure 1.1 B), the detection of fluctuations in temperature (Figure 1.1 C, Narberhaus et al. (2006)), the recognition of RNA-binding proteins or trans-encoded RNAs (Figure 1.1 D & J, Irnov et al. (2006); Grundy and Henkin (1998); Dambach and Winkler (2009)) or combinations of these recognition mechanisms (Figure 1.1 E-J).

The metabolite-sensing RNAs which modulate many fundamental biochemical pathways and essential cellular functions constitute a major class among these cis-regulatory RNAs (Figure 1.1 A, B, E-I and Section 1.1). They are referred to as riboswitches (Section 1.1) and will be in the focus of this work. The detailed understanding of their structures and differential architectures, phylogenetic conservation and distribution, as well as the regulatory systems they use, will form the foundation for understanding the application of riboswitches as antibacterial targets particularly with respect to multi-drug resistant pathogens evolving (Section 1.4).
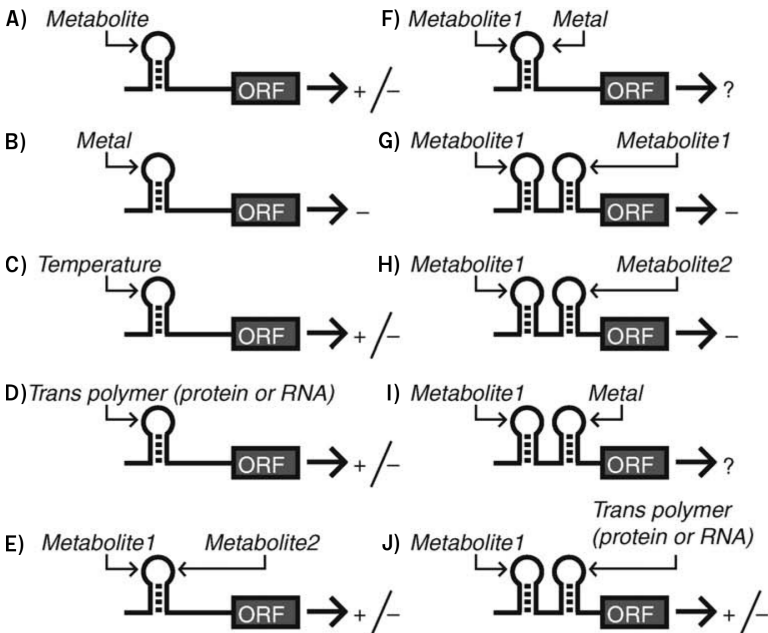
Figure 1.1: Posttranscriptional regulation of gene expression in bacteria.
Increased $(+)$ or decreased (-) gene expression by cis-regulatory RNAs (depicted as hairpins) in response to cognate stimulus (A-E). Hypothetical cis-regulatory RNA responding to a combination of metals and metabolite concentrations (F). Tandem riboswitches that respond to the same (G) or different metabolites (H, I). Possibly multiple, distinct posttranscriptional regulatory mechanisms cooperate in controlling downstream expression (J). Figure taken from Dambach and Winkler (2009).

5

1.1 Riboswitches

Riboswitches are RNA elements found in mRNAs and efficiently regulate gene expression within many fundamental metabolic pathways (Mandal et al., 2003). They have been identified not only in bacterial, but also in archaeal and eukaryotic genomes (Rodionov et al., 2002; Sudarsan et al., 2003a). Riboswitches consist of an aptamer domain and an expression platform. The natural aptamer recognizes the cognate ligand with high affinity and specificity. Binding of the ligand to this sensory domain induces a global secondary structure change, that also influences the expression platform of the riboswitch. These changes mostly lead to repression of gene expression by transcription termination or inhibition of translation initiation.

1.1.1 Classes of riboswitches

Riboswitches are grouped into different classes according to their sequence and structure conservation within the aptamer domain. At present more than 20 riboswitch classes are known, some of which represent orphan riboswitches, whose natural ligands remain unidentified to date. Among the known riboswitch classes are seven which respond to enzymatic cofactors, like adenosyl-cobalamine (AdoCbl, Nahvi et al. (2004)), thiamine pyrophosphate (TPP, Winkler et al. (2002a)), flavin mononucleotide (FMN, Winkler et al. (2002b)), S-adenosylhomocysteine (SAH, Wang and Breaker (2008); Wang et al. (2008)), molybdenum cofactor (Moco, Regulski et al. (2008)), S-adenosylmethionine (SAM, Grundy and Henkin (1998); Winkler et al. (2003)) and tetrahydrofolate (THF, Ames and Breaker (2010)). Three riboswitches were described that sense amino acids (glycine, glutamine, lysine Mandal et al. (2004); Ames and Breaker (2011); Sudarsan et al. (2003b)) and one recognizes an amino sugar, glucosamine-6-phosphate (GlcN6P, Winkler et al. (2004)). Moreover, there are several of these RNA elements that react to purines (adenine, Mandal and Breaker (2004) & guanine, Batey et al. (2004)) or other nucleobase containing ligands like deoxyguanosine (dG), prequeuosine (preQ$_1$, Roth et al. (2007)) or cyclic di-GMP (c-di-GMP, Sudarsan et al. (2008); Lee et al. (2010)). Finally, also ions like Mg^{2+} and F$^-$ can trigger riboswitch mediated gene regulation (Ramesh and Winkler, 2010; Baker et al., 2012).

The aptamer domains which determine the riboswitch class vary in length from about 30 nt (preQ$_1$ riboswitch, Roth et al. (2007)) to approx. 150 nt (TPP riboswitch), and also in secondary structure complexity (Dambach and Winkler, 2009). Some riboswitch sequences and structures are exceedingly well conserved among different species, e. g. the TPP riboswitch class (Breaker, 2011; Barrick and Breaker, 2007). Nevertheless, other metabolites can be recognized by several distinct aptamer folds. There are, for example, two different preQ$_1$ (Roth et al., 2007; Meyer et al., 2008) and two kinds of c-di-GMP riboswitches (Shanahan et al., 2011). However, the riboswitch that probably best exemplifies this variation in aptamer structure is the SAM-responsive element for which at least six subtypes are known (Winkler et al., 2003; Weinberg et al., 2008, 2010; Corbino et al., 2005; Poiata et al., 2009; Fuchs et al., 2006).

The specific discrimination of the appropriate riboswitch ligand under a pool of many, often very similar, metabolites is neccessary to allow precise gene regulation (Barrick and Breaker, 2007). Riboswitches are capable of this high selectivity through shape complementarity, and specific interactions (Serganov and Patel, 2012). The latter are usually established through numerous hydrogen bonds between aptamer and ligand, but can also include electrostatic,

van der Waals and stacking interactions. Riboswitch aptamers bind their target with high affinities that extend from the mid micromolar (glmS ribozyme, Winkler et al. (2004)) to the mid picomolar range (TPP, Welz and Breaker (2007) or FMN, Lee et al. (2009)). Finally, aptamers can be structurally preorganized in the absence of ligand, but because riboswitch ligands are usually well buried within a binding pocket (Breaker, 2008), ligand binding often induces structural rearrangement or stabilization of aptamer substructures (Breaker, 2010).

Frequently, cations aid in ligand recognition by shielding negative charges of the cognate molecule. Examples include the negatively charged pyrophosphate group of TPP which is coordinated by two Mg^{2+} ions (Edwards and Ferré-D'Amaré, 2006), or flouride which is only recognized by its riboswitch, when it interacts with three Mg^{2+} ions (Ren et al., 2012). Other cations, like potassium can also be required for metabolite binding as shown for the lysine riboswitch (Serganov et al., 2008).

1.1.2 Mechanisms of riboswitch-mediated gene control

Riboswitch-mediated gene regulation is facilitated by the concerted communication between aptamer domain and expression platform. Whereas the well-conserved aptamer domain is even used to categorize these RNA elements, the expression platforms are far less conserved. This is mainly due to the fact, that they harness folding differences which enable several different processes to interfere with gene expression efficiency (Breaker, 2010).

One of the most common mechanisms of riboswitch control involves the manipulation of transcription termination (Figure 1.2 A). Here, ligand binding induces a conformational change in the expression domain that creates a terminator stem followed by a stretch of five to nine uridines. Upon encountering this structure, the RNA polymerase pauses and eventually falls off its template, thus prematurely ending transcription. In the absence of ligand, a competing second structure or anti-terminator is formed that allows efficent mRNA production. Some riboswitch-RNA fragments generated by premature transcriptional arrests have been shown to be prone to degradation by specific RNases (Spinelli et al., 2008; Shahbabian et al., 2009).

Similarly to the transcription termination mechanism, gene expression can be regulated by riboswitches on the translation initiation level. Here, two altering RNA folds control ribosome access to the ribosome binding site (or Shine-Dalgarno (SD) sequence). In the presence of ligand, the anti-SD-sequence sequesters the ribosome binding site, which prevents association of the small ribosomal subunit and hence translation start. This mechanism of gene regulation by riboswitches is more commonly found in organisms that also make extensive use of the protein factor Rho (Figure 1.2 B, Barrick and Breaker (2007); Roth and Breaker (2009)), which is an RNA binding protein that enhances transcript termination in regions that are not masked by ribosomes (Ciampi, 2006).

In addition to these widespread mechanisms, there are riboswitches known that regulate splicing (Figure 1.2 C, Croft et al. (2007)), or gene expression via transcription interference or antisense action (Figure 1.2 D Breaker (2010); André et al. (2008)), dual transcription and translation control (Figure 1.2 E, Rodionov et al. (2004); André et al. (2008)) as well as RNA cleavage (Figure 1.2 F, Winkler et al. (2004)).

Splicing was found to be regulated by TPP riboswitches in plants and fungi (Figure 1.2 C, Sudarsan et al. (2003a); Cheah et al. (2007); Wachter et al. (2007); Kubodera et al. (2003)). *Thi*-box RNAs will be discussed in greater detail in Section 1.3 as will be the detailed gene regulatory mechanism employed by glmS ribozyme self-cleavage (Section 1.2, Figure 1.2 F, Winkler et al. (2004); Collins et al. (2007)).

Common mechanisms

Rare mechanisms

A) Transcription termination

D) Transcription interference or antisense

B) Translation initiation

E) Dual transcription/translation control

C) Splicing (eukarya)

F) Self-cleaving
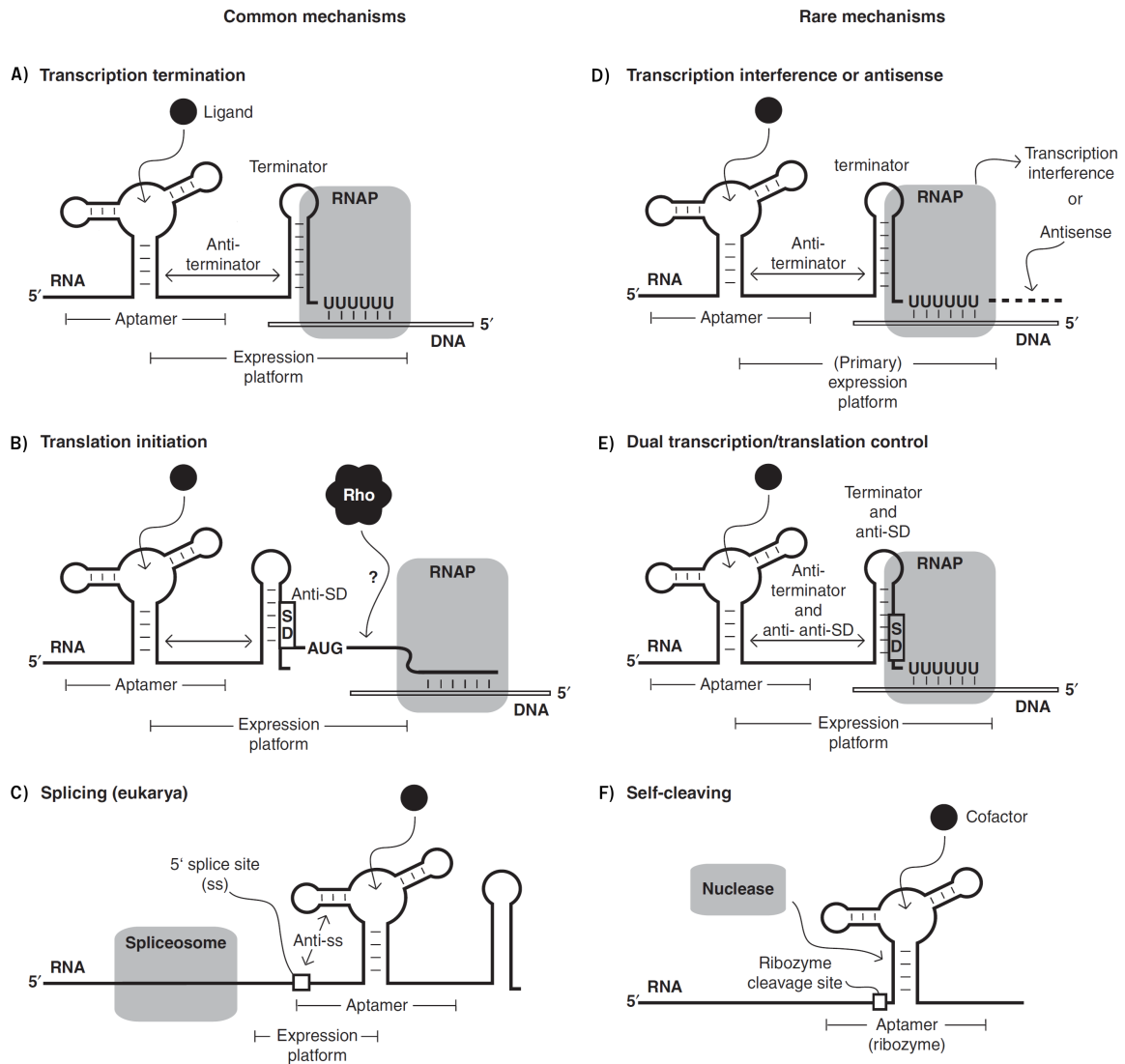
Figure 1.2: Established and predicted mechanisms of riboswitch-mediated gene regulation. Most common mechanisms are transcription termination (A), translation initiation – perhaps accompanied by Rho, which recognizes nascent mRNA that is not actively translated, thus causing transcription termination– (B), and splicing control in eukaryotes (C). More rare mechanisms observed or predicted in some bacterial species include transcription interference or possibly antisense action (D), dual transcription and translation control (E), and ligand-dependent self-cleaving ribozyme action (F). Figure taken from Breaker (2010).

Not depicted in detail is the mechanism of a SAM-I riboswitch in *Clostridium acetobutylicum*. This special riboswitch is encoded in trans downstream of an operon involved in the conversion of methionine to cysteine (Rodionov et al., 2004) and confers its gene regulatory function by controlling the production of antisense transcripts in cis, which interact with the mRNA like sRNAs to downregulate gene expression (André et al., 2008).

Riboswitches most often provide the means for negative feedback regulation of metabolic pathways, being placed upstream of those genes that produce the ligand by which they

are triggered. This allows the organisms to quickly react to changes in their environment. However, there are also two examples of positive feedback regulation: the glycine and adenine riboswitches. The latter RNA element, for example, is often found in front of genes that are only required when high adenine concentrations are encountered in the cell, such as adenine transporters or adenine deaminase (Mandal and Breaker, 2004; Mandal et al., 2004).

1.1.3 Stacking of riboswitch components

In addition to the varieties of aptamer structures and ligand specificities, the repertoire of gene regulatory function by riboswitches can be expanded to more complex architectures consisting of, e. g. several riboswitches in tandem (Figure 1.1 F-I), or multiple aptamer domains followed by a single expression domain. These sensory domains could recognize the same or a different ligand and bind them independently or in a cooperative manner. All these scenarios will influence gene regulation efficiency (explained in detail in Breaker (2010)).

Under the simplest conditions, where a gene is controlled by a riboswitch carrying only a single aptamer and expression platform, an 81-fold change in ligand concentration is needed to progress from 10 % to 90 % gene expression (Welz and Breaker, 2007; Breaker, 2010). When two or more riboswitches that sense the same ligand are placed in series, the system requires only a 40-fold change in ligand concentration to elicit the same change in gene expression (Breaker, 2008). However, this is merely the case if these tandem riboswitches are triggered with near-identical ligand concentrations and if triggering either one independently represses gene expression (Breaker, 2008).

Even more complex is the natural example of a Boolean operator, which consists of two different riboswitches specific for two different ligands. Binding of either ligand will cause the activation of gene regulatory processes. This case of riboswitch stacking has been observed for the metE mRNA in *Bacillus clausii* (Sudarsan et al., 2006).

A glycine riboswitch from *Vibrio cholerae* provides yet another example of architectural complexity, as it carries two similar aptamers and one expression platform (Barrick and Breaker, 2007; Mandal et al., 2004). If perfectly cooperative, then the riboswitch could overcome the 10 % to 90 % gene expression range with only a factor of 9 change in glycine concentration (Breaker, 2008). In this case perfect cooperativity means that ligand binding at either side improves affinity at the other.

1.1.4 Riboswitch folding and function

Riboswitch folding in bacteria is tightly coupled to transcription (Serganov, 2010) and was shown to contribute greatly to the efficiency of riboswitch mediated gene control. Hence, it is not surprising to find some aptamer domains that bind their ligand only when the expression domain has not yet been transcribed. However, there are two extremes of how riboswitches handle the concerted action of ligand binding and folding. The one extreme is represented by riboswitches which exist in a fairly well-defined, pre-organized conformation in the absence of ligand. Ligand-dependent conformational changes are limited to a region within or adjacent to the binding pocket (Montange and Batey, 2008). The glmS, purine and SAM-II riboswitches belong to this category. Even though the glmS and SAM-II riboswitches are rather rigid, there is a certain degree of pre-organization in apo-state of purine riboswitches, which oscillate between different non-binding structures and then likely use conformational selection for ligand recognition (Liberman and Wedekind, 2012). Therefore, when the ligand binds, the

aptamer structure continues to envelope the ligand by folding.

The other extreme of riboswitch folding is represented by those RNA structures that will undergo extensive changes in secondary and tertiary structure upon ligand recognition in addition to local changes near the binding pocket (Montange and Batey, 2008). The TPP, M-box and SAM-I riboswitch classes are members of this group. As binding pockets of these riboswitches are often split, significant conformational changes in the RNA are necessary to bring together distal elements of tertiary structure (Montange and Batey, 2008). These extensive structural changes are often supported by cations such as Mg^{2+}, which aid the folding of ligand-binding conformations and assist in ligand recognition, e. g. by the alignment of helical segments and thus the promotion of base pairing (Serganov and Patel, 2012).

1.1.5 Phylogenetic distribution of riboswitches

Since the aptamer domain has to use the limited diversity of only four nucleobases for target recognition, it is not surprising that its sequence is often well conserved. This sequence and structure conservation is used to assign riboswitches to distinct classes, but can also be used

Figure 1.3: Riboswitch distributions and phylogenetic conservation. Depicted is the phylogenetic tree with standard accepted branching for different organisms. The size of squares illustrates the frequency with which a given riboswitch occurs in the corresponding taxonomic group. The bar diagram on the right demonstrates the total number of nucleotides from each taxonomic division in the sequence databases that were searched. Figure taken from Barrick et al. (2007).
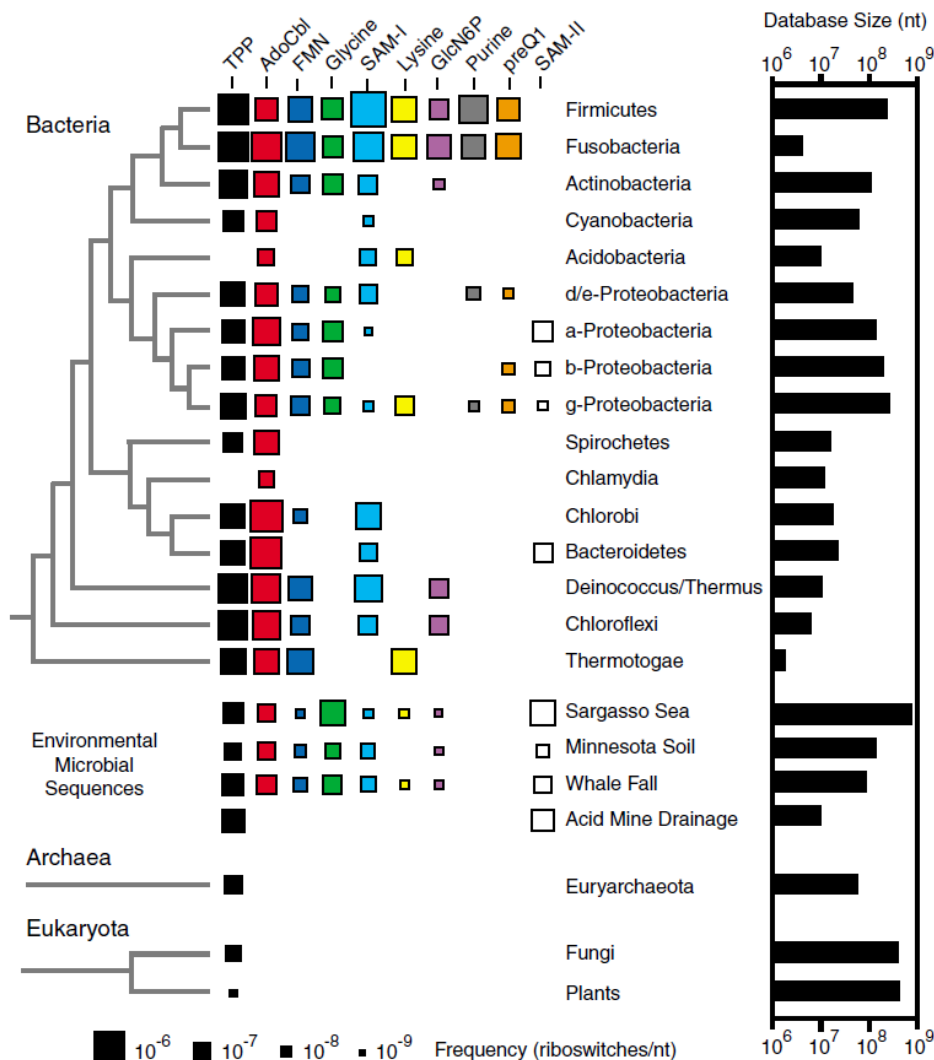
to estimate the phylogenetic distribution and conservation of these RNA elements (Figure 1.3, Barrick and Breaker (2007)).

The TPP riboswitch is the only class known to date that can be found in all three domains of life: bacteria, archeae and eukarya. The AdoCbl riboswitch is widely distributed among eubacteria and seems to be a key-regulator of this metabolite's biosynthesis. The glmS ribozyme recognizing GlcN6P is mainly found in Gram-positive bacteria, where it was predicted to exist in at least 18 other species apart from *Bacillus subtilis* (Barrick et al., 2004). Purine riboswitches are the least distributed and the preQ class is only found in proteobacteria. Interestingly, the distribution of SAM-I and SAM-II classes overlaps only slightly and indicates how these two classes rather complement each other in a variety of organisms. In proteobacteria for example, SAM-II dominates over the occurance of SAM-I, which is preferably found in firmicutes, fusobacteria, actinobacteria, cyanobacteria and acidobacteria, that do not regulate their SAM levels by SAM-II riboswitches. Although in some bacteria both SAM-sensing classes are found, no single bacterium carries both SAM-I and SAM-II riboswitch classes (Barrick and Breaker, 2007). Additionally, SAH riboswitches are predicted to be present in proteobacteria and SAM-IV RNA elements in actinobacteria (Weinberg et al., 2007).

Firmicutes, fusobacteria and γ-proteobacteria use riboswitch regulation extensively, even though the latter carry fewer representatives of each class (Barrick and Breaker, 2007).

Although, the appearance of these distributions may shift as new genomes are constantly sequenced and several new riboswitch classes have been discovered since this description was published by Barrick in 2007, Figure 1.3 still demonstrates how commonly riboswitches are used as regulatory tool in bacteria.

1.1.6 Riboswitches as new antibacterial drug targets

Antibiotics known to date address a relatively concise spectrum of targets (Figure 1.4). They interfere with important cellular processes like transcription (rifampicins), translation (aminoglycosides, macrolides, tetracycline, oxazolidinone), metabolic pathways, e.g. tetrahydrofolate synthesis (sulfonamides) as well as cell wall biosynthesis (β-lactam antibiotics, glycopeptides). Despite this collection of means employed and targets addressed, the development of resistances hampers the use of several antibiotics today. This rise in antibiotic resistances creates an urgent need for the development of antibacterial substances that address new targets and use novel modes of action.

Riboswitches constitute such a new promising target. This is not only due to the fact that structured RNA is a druggable entity in general (e.g. rRNA binding by aminoglycosides), but also because riboswitches naturally bind low molecular weight ligands with a distinction similar to that known by proteins (Blount and Breaker, 2006). Moreover, they are known to regulate up to 4% of all bacterial genes, many of which are essential. Finally, exept for TPP, riboswitches have mainly been identified in bacteria. And the TPP recognizing RNA elements present in eukarya exert regulatory mechanisms very distinct from the ones used by eubacteria (Section 1.1.2). In an agonistic fashion, riboswitch targeting compounds are thought to permanently activate the riboswitch and hence repress gene expression even under starvation from that metabolite (Blount et al., 2007), provided that the mimic cannot functionally replace the natural ligand. However, many of the essential metabolites whose production is regulated by riboswitches are also needed by mammals, e.g. the vitamin B_1, TPP. Hence, ligand analogs could not only act on riboswitches but also interfere with mammalian enzymes,
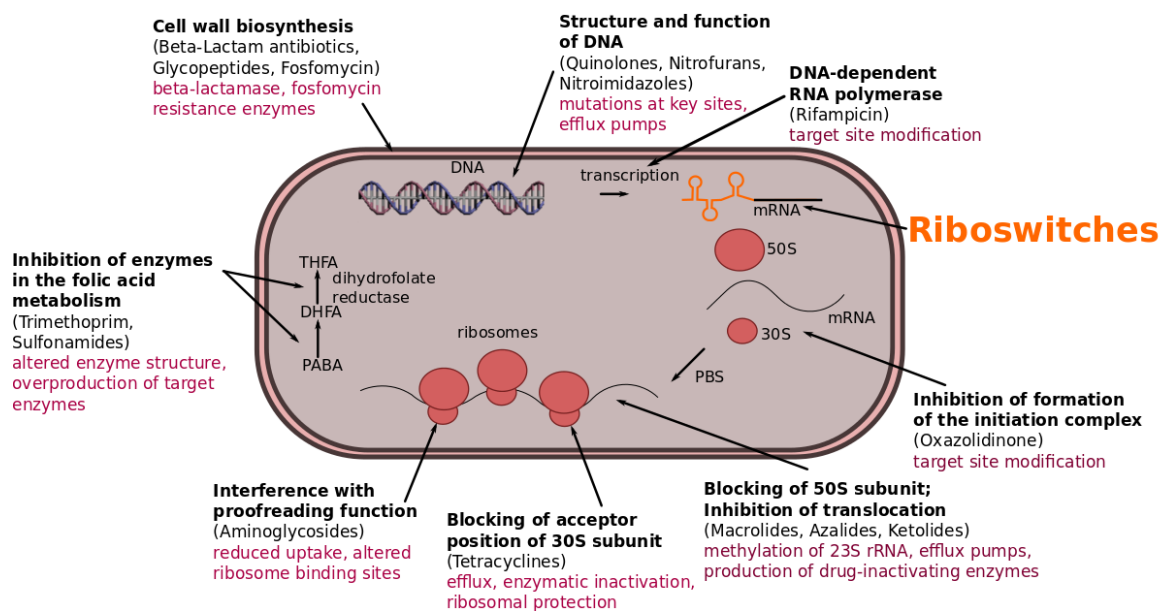
Figure 1.4: Antibiotic drug targets in bacteria. Schematic representation of a bacterial cell to illustrate different modes of action employed by known classes of antibiotics (black) with some substance representatives in brackets, and their most frequently used resistance mechanisms (red). Arrows point at target structures. The novel, promising target represented by riboswitches is highlighted in orange.

as known for pyrithiamine (PT, Koedam (1958)) and L-aminoethylcysteine (AEC, Girolamo et al. (1986)). Nevertheless, evidence exist that there are differences in recognition of cognate ligands by enzymes and riboswitches (Serganov et al., 2006; Lim et al., 2006), which opens up the possibility of finding compounds that only interact with the bacterial riboswitch. As riboswitches can also be located in front of several genes or controlling entire operons, the collective repression of these genes within a certain metabolic pathway could be deleterious.

Depending on their natural distribution substances targeting riboswitches could be used as broad-spectrum antibiotics (such as TPP or FMN riboswitches, Section 1.1.5) or as more selective drugs (like preQ or purine riboswitches, see Figure 1.3, Section 1.1.5).

Moreover, these RNA elements are compatible with the establishment of high-throughput screening systems (HTS) as shown for the glmS ribozyme by Blount et al. (2006); Mayer and Famulok (2006). Additionally, rational design approaches have proven to be indispensible for identifying novel riboswitch modulators (Blount et al., 2006; Lünse et al., 2011).

1.1.6.1 Riboswitch-targeting compounds

When searching for riboswitch activating drugs one has to overcome the challenge of finding chemical entities that are still close enough to the natural riboswitch ligand to be recognized, but as much dissimilar as possible to avoid resistance mechanisms or side effects.

The thiamine analog pyrithiamine (PT, Figure 1.5, A), whose mode of action remained elusive for decades, was finally shown to exert at least parts of its toxic effects by the interaction with *thi*-box riboswitches. Like thiamine, PT is taken up and phosphorylated to pyrithiamine pyrophosphate (PTPP, Iwashima et al. (1976)). As such, it acts on the riboswitch and represses the expression of thiamine biosynthesis and transport genes (Sudarsan et al.,

2005). PT resistant bacteria have been shown to contain mutations in the aptamer domain of *thi*-box riboswitches, which result in the inhibition of proper ligand recognition and efficient metabolite binding.

Screening of lysine related compounds resulted in the identification of several lysine analogs, e. g. L-aminoethylcysteine (AEC) and DL-4-oxalysine, able to repress gene expression (Blount et al., 2007). These compounds show affinities similar to that of the natural riboswitch ligand and the ones with K_d values closest to lysine revealed bacterial growth inhibition in the micromolar range (4-140 µg/ml, Figure 1.5, B). Point mutations in the aptamer domain of the lysine riboswitch upstream of *lysC* render *B. subtilis* cells resistant against riboswitch targeting compounds (Blount et al., 2007; Ataide et al., 2007).

Additionally, several guanine riboswitch targeting purine analogs (Figure 1.5, C) were described that do not only bind to the riboswitch *in vitro* but also inhibit bacterial growth *in vivo* (Kim et al., 2009; Mulhbacher et al., 2010).
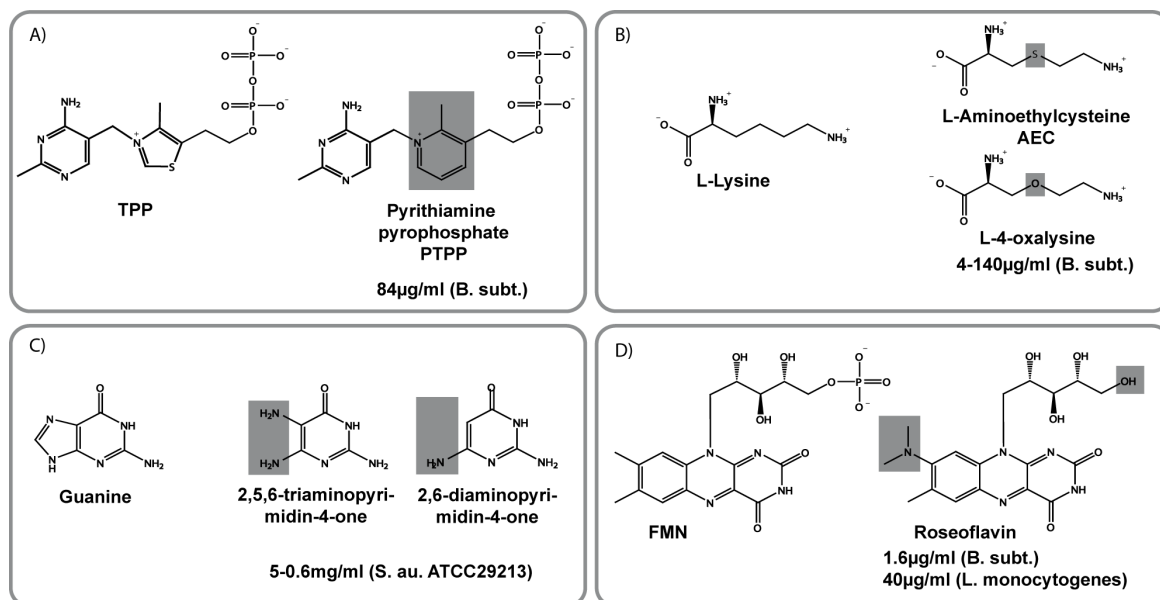
Figure 1.5: Array of non-metabolite riboswitch modulators. Shown are compounds acting on four different riboswitch classes. TPP with its analog pyrithiamine pyrophosphate (PTPP) (A). Amino acid analogs acting on the lysine riboswitch (B). Guanine and its analogs (C). Ligand for the FMN riboswitch and a naturally synthesized analog, Roseoflavin (D). Minimal inhibitory concentrations are stated below the riboswitch activating analog with the according microorganism in brackets.

Finally, the riboflavin analog Roseoflavin which is synthesized by *Streptomyces davawensis* has one additional dimethylamino group (Figure 1.5 D, Ott et al. (2009)) that is well accommodated by a space in the binding pocket of FMN riboswitches (Serganov et al., 2009). This provides evidence for the action of naturally occurring substances that act on riboswitches to interfere with bacterial growth.

1.2 The glmS ribozyme

In the following sections the gene regulatory mechanism of the glmS ribozyme is described in more detail. Special emphasis is put on riboswitch structure for ligand recognition and cofactor aided cleavage catalysis (Sections 1.2.2 and 1.2.3). Their precise knowledge is prerequisite for the successful identification of novel substances activating this riboswitch, which is able to discriminate close analogs of its cognate metabolite not only by potential differences in binding affinity, but also by requiring the ligand to catalyze RNA cleavage (Breaker, 2008).

1.2.1 Mechanism of glmS ribozyme-mediated gene regulation

Among the different classes of riboswitches introduced in Section 1.1.1, the glmS riboswitch assumes a unique role, as it does not only regulate gene expression in response to increasing metabolite concentrations, but it does so by an enzymatic activity. The glmS riboswitch is actually a ribozyme, i.e. a catalytically active RNA (Winkler et al., 2004) that irreversibly cleaves itself upon encountering its ligand. Depending on the experimental conditions the glmS ribozyme can enable a change in rate constants of 10^7 (Brooks and Hampel, 2009; Klein et al., 2007b).

The cognate ligand, glucosamine-6-phosphate (GlcN6P), is a central metabolite needed for bacterial cell wall assembly as it is the precursor of peptidoglycan biosynthesis (Section 1.2.4). When GlcN6P binds to the glmS ribozyme the RNA cleaves itself. This scission produces a short RNA fragment bearing a 2',3'-cyclic phosphate in addition to its 5' triphosphate, which caps all intact mRNAs, as well as a second product with a characteristic 5' hydroxyl terminus. These products are analogous to the ones produced by other ribozymes like the hammerhead, hairpin or hepatitis delta virus (HDV). This newly freed 5'-OH group is recognized by RNase J1, an RNase conserved among bacteria, which degrades the glmS mRNA (Collins et al., 2007). As the glmS protein is a preferred substrate for ClpP and hence for protein degradation (Kock et al., 2004), the down-regulation of its mRNA levels by glmS ribozyme activation

Figure 1.6: GlmS ribozyme consensus model and crystal structure. Consensus sequence and secondary structure model for glmS ribozymes (A). The asterisk denotes the site of ribozyme self-cleavage. Optional hairpins (i) or (ii) are present in some representatives. Figure adapted from McCown et al. (2011). Crystal structure of glmS ribozyme from Klein and Ferré-D'Amaré (2006) (B).
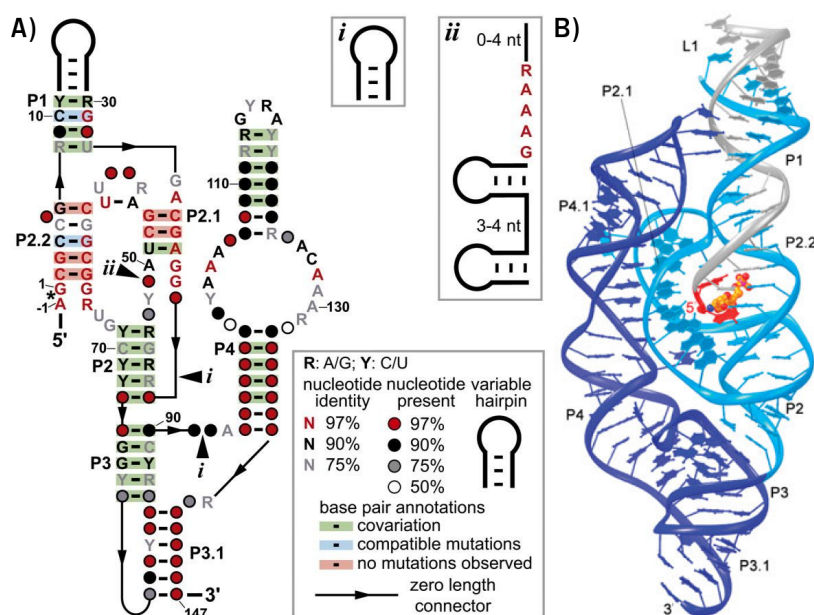
results in a decrease of enzymatic activity. This allows for negative feedback regulation by the glmS ribozyme.

Collins et al. impressively demonstrated the importance of glmS ribozyme cleavage *in vivo*, as ribozyme mutants incapable of self-cleavage resulted in a sporulation deficient phenotype in *Bacillus subtilis*. Additionally, Watson et al. showed that the glmS riboswitch is capable of integrating two signals: it is activated by GlcN6P, but at high concentrations of Glc6P, this metabolite can occupy the binding pocket and inhibit ribozyme mediated gene repression (Watson and Fedor, 2011).

Interestingly, ribozyme-dependent GlmS regulation seems to be fairly restricted to Gram-positive organisms (Barrick et al., 2004). Today 463 glmS riboswitch variants have been predicted of which only five were identified in Gram-negative species (mainly belonging to the phylum of synergestetes, McCown et al. (2011)). The paralogous GlmS enzymes of Gram-negative bacteria and eukaryotes are controlled on the protein level by the allosteric action of GlcN6P (Milewski, 2002; Ferré-D'Amaré, 2010). Moreover, trans-acting non-coding RNAs regulate the expression of GlmS in *Escherichia coli* (Görke and Vogel, 2008; Reichenbach et al., 2008).

1.2.2 Structure of the glmS ribozyme

The crystal structure revealed that the glmS ribozyme consists of three parallel helical stacks comprising three pseudoknots. The minimal functional core (Section 1.2.3) includes helices P1, P2, P2.1 and P2.2 (Figure 1.6), of which P1, P2 and P2.2 stack coaxially and pack side-by-side with the short P2.1 helix (Ferré-D'Amaré, 2010; Klein and Ferré-D'Amaré, 2006). The four helices of this compact, contiguous structure are connected by four strand crossovers that define two nested pseudoknots (Ferré-D'Amaré, 2010). GlcN6P and the scissile phosphate lie engulfed in the core structure. The exact metabolite binding site lies within the major groove of P2.2, also suggested by the highly conserved nucleotides in P2.1, P2.2 and the segments connecting the two helices (Klein and Ferré-D'Amaré, 2006).

The core domain of the riboswitch is stabilized by the associated peripheral domain (dark blue, Figure 1.6 B), which is formed by the coaxially stacked helices P4 and P4.1, which are covalently connected to the ribozyme core through helices P3 and P3.1. These interactions are supported by tertiary contacts, i. e. by helices P3 and P3.1 which form an H-type pseudoknot, that is defined by two helices and three connecting loops (Aalberts and Hodas, 2005).

1.2.3 The glmS ribozyme catalytic core & ribozyme action

Based on biochemical and structural data, GlcN6P acts as a cofactor in the glmS ribozyme catalysis rather than through an allosteric activation that would lead to a conformational change in the RNA structure (refer to Section 1.1.4, Klein and Ferré-D'Amaré (2006); McCarthy et al. (2005); Cochrane et al. (2007, 2009)). Three different experimental set-ups for glmS ribozyme crystallization yielded precisely superimposed structures for the ribozyme: I) in the absence of ligand, II) in the presence of glucose-6-phosphate (Glc6P), which does not activate the riboswitch, or III) in the presence of GlcN6P, however using an RNA construct point-mutated to be incabable of self-cleavage (Klein and Ferré-D'Amaré, 2006; Klein et al., 2007a). The structures show that an open, hydrated binding site, which is lined with phylogenetically conserved residues, accommodates GlcN6P thereby burying about 80 % of its solvent-accessible surface area (Klein and Ferré-D'Amaré, 2006). The fact that Glc6P,

which differs from GlcN6P only by having a hydroxyl group at the C2 position instead of an amine group, is not capable of activating the glmS ribozyme, points at the critical function of the amine group (Winkler et al., 2004; McCarthy et al., 2005).

The active site within the glmS ribozyme core brings the reactive groups of the substrate in a near in-line conformation. Since the conserved nucleobase A-1 makes a hydrogen bond to G65, the exchange of this adenosine for a guanosine results in a steric clash with G65 (Figure 1.6 A). Hence, this point mutation is often used to generate a minimally altered, but inactive glmS ribozyme variant (see Section 5.1.2).

GlcN6P binds to the glmS ribozyme exclusively in the α-anomeric conformation (Lim et al., 2006), which is supported by the fact that only compounds with the stereochemical arrangement of the anomeric hydroxyl group and the amine at position 2 are able to activate the RNA enzyme (e. g. ethanol vs. ethanolamine, McCarthy et al. (2005)). These groups make extensive use of hydrogen bonds to nucleobases in the ribozyme structure (Figure 1.7). Substituting the G1 residue with a series of natural and unnatural purine nucleotides revealed the importance of this imine-phosphate-group interaction. When G1 was replaced by inosine, GlcN6P was still able to activate the ribozyme. However, the use of 2-aminopurine or 6-dimethyladenine, whose N1 position is not protonated at neutral pH, rendered the ribozyme more active in the presence of GlcN instead of GlcN6P (Klein et al., 2007b). It is thought that the unprotonated imine results in a steric clash with the phosphate of GlcN6P. Therefore, GlcN can be bound more efficiently and lead to stronger activation of the mutated ribozyme.

Complex RNAs require divalent metal ions for folding and Mg^{2+}-ions have been shown to adopt this functional role for the glmS ribozyme. However, Mn^{2+}, Ca^{2+} and cobalt hexamine (trivalent) can substitute the role of Mg^{2+}. These ions which show a higher charge density than monovalent ions, solely support folding (Roth et al., 2006) and not catalysis. In part this is evidenced by the fact that no metal ions bind in the immediate vicinity of the scissile phosphate (Klein and Ferré-D'Amaré, 2006). Although it was shown that many riboswitches bind anionic ligands (Baker et al., 2012) as chelates of divalent cations, this does not seem to be the case for the phosphate group of GlcN6P in the glmS ribozyme. There are Mg^{2+} ions in the vicinity of the GlcN6P phosphate moiety, but the cations do not make inner-sphere (direct) coordination (Ferré-D'Amaré, 2010). Furthermore, the GlcN6P binding site is heavily hydrated, and the Mg^{2+} ions in it are surrounded by well-ordered water molecules, yet they do not have a largely preferred arrangement. Finally, none of the Mg^{2+} ions in this binding

Figure 1.7: Recognition of GlcN6P by the glmS ribozyme. Schematic depiction of interaction responsible for GlcN6P recognition by glmS ribozyme. Hydrogen bonds are shown as two-headed arrows. Stacking interaction occurs between the nucleobase of G1 and the sugar. Figure adapted from Ferré-D'Amaré (2010).
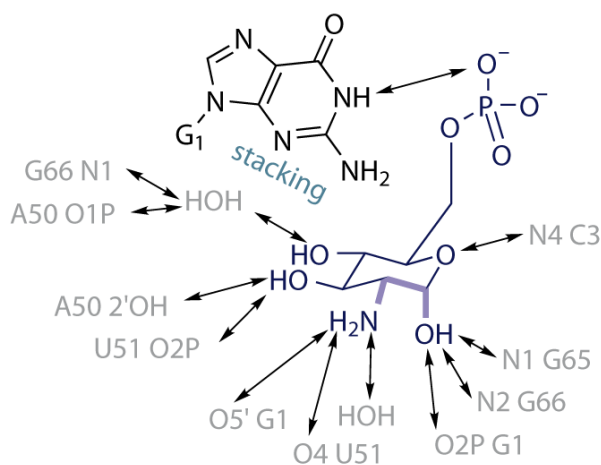
pocket have ligands that complete their octahedral coordination shell with good geometry (Klein et al., 2007b). This is in contrast to the higly ordered Mg^{2+} ion that coordinates the phosphates of C2, C36 and G37.

The necessity of GlcN6P for the scission is undoubtedly evident from the fact that despite the well pre-organized active site, in which the substrate is distorted to a near in-line conformation, no cleavage can be observed in the absence of GlcN6P. Nevertheless, there are different theories on how GlcN6P supports the glmS ribozyme cleavage reaction. According to the first theory GlcN6P could act as general acid-base catalyst (Figure 1.8 A). Here, it is thought to deprotonate the 2'OH nucleophile of A-1 through a proton relay employing two tightly bound water molecules. The resulting ammonium form of GlcN6P functions to stabilize the transition state as electrostatic catalyst. Additionally, the ammonium group could donate a proton to the 5'oxo leaving group thereby stabilizing it (Figure 1.8 A, Klein and Ferré-D'Amaré (2006); Ferré-D'Amaré (2010)). Another theory involves the G40 residue of which the N1 imine could function as general base catalyst deprotonating the A-1 2'OH nucleophile, whereas the ammonium form of GlcN6P functions as an electrostatic and/or general acid catalyst (Figure 1.8 B). This is supported by a G40A mutation which renders the ribozyme inactive even in the presence of GlcN6P, even though for the glmS ribozyme catalytic activity an interdependency seems to exist between GlcN6P and G40, as neither is functional in the absence of the other (Ferré-D'Amaré, 2010).
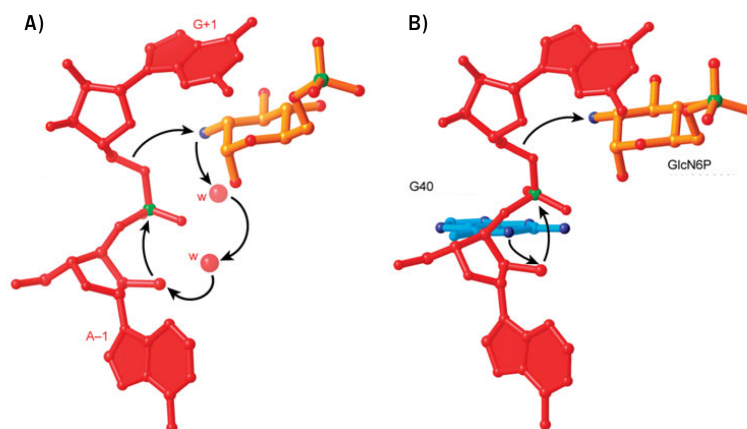
Figure 1.8: Catalytic mechanisms of the glmS ribozyme. GlcN6P deprotonates the 2'-OH nucleophile through a proton relay employing two tightly bound water molecules, functioning as a general base catalyst. The resulting ammonium form of GlcN6P functions to stabilize the transition state electrostatically and also donates a proton to the 5'-oxo leaving group, functioning as a general acid catalyst (A). The N1 imine of G40 functions as a general base catalyst (B). GlcN6P, in its ammonium form, functions as an electrostatic and general acid catalyst. The ribozyme is inactive in the absence of GlcN6P or if a G40A mutation is made. Figure adapted from Ferré-D'Amaré (2010)

Even though an RNA sequence ranging from nucleotide -1 to 75 has been shown to be able to perform the GlcN6P aided self-cleavage reaction, an RNA structure including nucleotides -1 to 145 will exhibit maximal activity (Figure 1.6 A). These observations led to the definition of the ribozyme core region (for the short RNA) and the glmS ribozyme motif (for the longer sequence). Furthermore, the glmS ribozyme can be split at L1 (Figure 1.6 B) into a bimolecular RNA construct allowing the performance of multiple turnover reactions in the presence of GlcN6P (Brooks and Hampel, 2009).

1.2.4 The GlmS protein

The glmS ribozyme regulates the expression of the enzyme glucosamine-6-phosphate synthase (Figure 1.9, (3), GlmS, L-glutamine:D-fructose-6-phosphate amidotransferase). This key enzyme of hexosamine metabolism is responsible for the utilization of the amide nitrogen of glutamine in the biosynthesis of amino sugars (Zalkin and Smith, 1998). GlmS catalyzes the conversion of fructose-6-phosphate (Fru6P) into glucosamine-6-phosphate (GlcN6P) in the presence of glutamine (Badet et al., 1987). The resulting GlcN6P is then isomerized into D-glucosamine-1-phosphate (GlcN1P) by the phosphoglucosamine mutase (Figure 1.9, (4) glmM) and further converted into uridine diphospho-N-acetyl-D-glucosamine (UDP-GlcNAc) by the GlcN1P acetyltransferase (Figure 1.9, (5) glmU, bi-functional N-acetylglucosamine-1-phosphate uridinyltransferase) via the intermediate N-acetyl-glucosamine-1-phosphate (Glc-NAc1P). UDP-GlcNAc itself is an essential precursor of peptidoglycan biosynthesis in Gram-positive organisms (as well as lipopolysaccharide biosynthesis in Gram-negative bacteria).
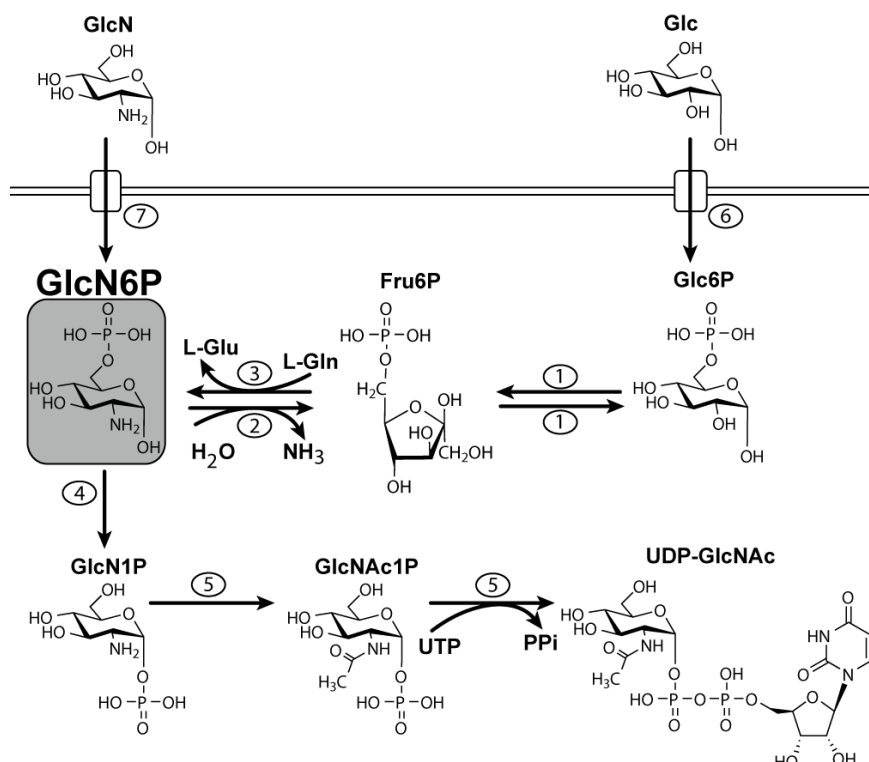
Figure 1.9: GlcN6P biosynthesis pathway in *S. aureus* Mu50. nagB codes for glucosamine-6-phosphate isomerase (2) which converts access GlcN6P to Fru6P. For further detailed description of GlcN6P biosynthesis and annotation of numbers refer to main text.

These pathways are fuelled by glucose (Glc), which is taken-up by *S. aureus* Mu50 via the ptsG phosphotransferase system (Figure 1.9, (6)) and thereby phosphorylated to glucose-6-phosphate (Glc6P). The glucose-6-phosphate isomerase (Figure 1.9, pgi, (1)) converts Glc6P to fructose-6-phosphate (Fru6P). When glucosamine (GlcN) is taken up by the glcA PTS transporter (Figure 1.9, (7)) it is directly phosphorylated to GlcN6P.

1.3 *thi*-box riboswitches

Thiamine pyrophosphate (vitamin B1) is an essential cofactor for several important enzymes of the carbohydrate metabolism. As a result the production of this vitamine has to be tightly regulated and many organisms employ regulatory RNAs, namely *thi*-box riboswitches for exactly this purpose.

Thi-box riboswitches belong to the most widespread class of regulatory RNAs. They are not only found in α-, β-, γ- and ϵ-proteobacteria, in cyanobacteria, the CFB group (Cytophaga-Flavobacteria-Bacteroides group), the *Thermus/Deinococcus* group, the *Bacillus/Clostridium* group, in actinomycetes and thermotogales (Figure 1.3, Rodionov et al. (2002)), but also in archeae (Miranda-Ríos et al., 2001), and they represent the only class also abundant in eukarya, were they were identified in fungi (Sudarsan et al., 2003a) and plants (Kubodera et al., 2003).

This riboswitch class controls the expression of genes involved in the biosynthesis, salvage and transport of thiamine and its precursors (Section 1.3.3) through a variety of different control mechanisms (Section 1.3.1). The higly conserved RNA structure (Section 1.3.2), which regulates gene expression differently in the absence or presence of thiamine, was first described by Miranda-Rios and co-workers in 2001. Later, Winkler et al. brought biochemical evidence of aptamer domains within bacterial mRNA that specifically bind to TPP, leading to a direct modulation of gene expression (Winkler et al., 2002a).

1.3.1 Mechanisms of *thi-box* riboswitch-mediated gene regulation

This riboswitch class concentrates the wealth of regulatory mechanisms that can be employed by these entirely RNA-based regulatory elements. There are *thi*-box riboswitches which inhibit translation initiation or stop transcription prematurely, others control splicing or processing and stability of mRNAs (Figure 1.10).

In eubacteria the most commonly encountered regulatory mechanisms comprise either the formation of a terminator stem or the sequestration of the SD-sequence (Section 1.1.2, Figure 1.10 A & B). However, in a variety of plant species TPP riboswitches were found to reside in the 3'UTR of *thiC* genes and it was shown that thiC transcripts with alternating 3'UTR lengths were produced dependent on riboswitch function (Figure 1.10 C, Wachter et al. (2007)).

Apart from the TPP riboswitch-mediated regulation of splicing and 3' end processing in plants, *thi*-box riboswitches in fungi, like *Neurospora crassa*, regulate the splicing of introns (Cheah et al., 2007). Metabolite binding alters the availability of alternative splice site and branch site components of an intron within the NMT1 mRNA, which codes for a protein involved in TPP metabolism (Figure 1.10 D).

1.3.2 Structure of *thi*-box riboswitches

Two crystal structures have been solved for the TPP riboswitch. The TPP-responsive regulatory element in front of *thiM* in *Escherichia coli* was crystallized by Serganov and coworkers, whereas Thore et al. obtained the *thi*-box riboswitch structure of *thiC* from *Arabidopsis thaliana* (Serganov et al., 2006; Thore et al., 2006).

The structures show a strong similarity and both fold into a tuning fork-like conformation that binds the ligand between its prongs. Five base-paired helical stems (P1-P5) are connected
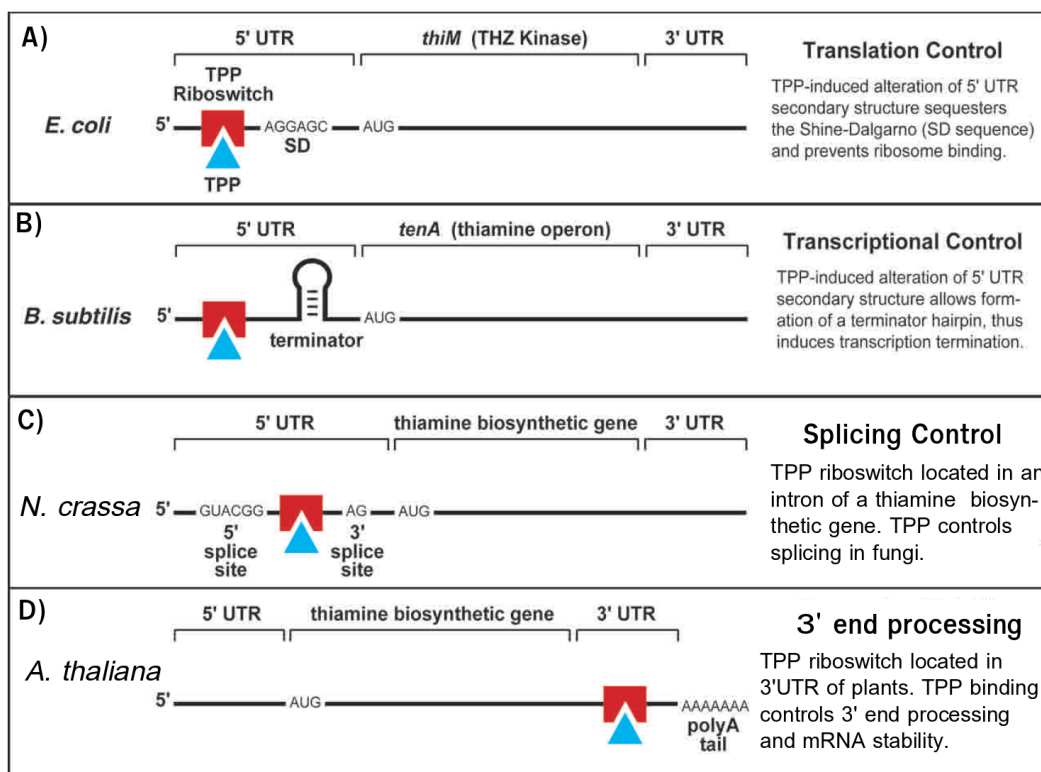
Figure 1.10: Mechanisms of riboswitch control employed by *thi*-box riboswitches. In bacteria, *thi*-box riboswitches usually reside in the 5'UTR and regulate gene expression either by inhibition of translation initiation through the sequestration of the Shine-Dalgarno sequence (A) or they prematurely halt transcription by enabling the formation of a terminator hairpin (B). In eukaryotes TPP riboswitches control splicing (C) or 3' end processing/RNA stability (D). Figure adapted from Sudarsan et al. (2003a).

via non-base-paired junctions and loops (Figure 1.11). The helix P1 is formed by the 5' and 3' end of the riboswitch RNA. Helices P1, P2, P4 and junctions J1/4 and J2/4 form a central three way junction (Thore et al., 2006). The two parallel helices each function by recognizing one part of TPP. Helix P2, J3/2, P3, L3 represents the pyrimidine sensor helix and helix P4, J4/5, P5, L5 comprises the pyrophosphate sensor helix. The actual binding sites are found in deep pockets which orient TPP perpendicular to the helices. Eukaryotic TPP riboswitches often contain variable lengths of the P3 stem, whereas in bacterial representatives a P3a stem is frequently present, but neither P3 nor P3a is directly involved in TPP binding (Edwards and Ferré-D'Amaré, 2006; Thore et al., 2006).

The pyrimidine part of vitamine B_1 is sensed by the J3/2 bulge within helix P2/3, which contains a conserved sequence (UGAGA, nucleotides 39-43, Figure 1.11 B, C, D). Residues U39 and A43 form a trans-Watson-Crick/Hoogsteen base pair that causes the extrusion of residues G40, A41 and G42. The pyrimidine ring itself is held between residues G42 and A43 by stacking interactions and the formation of two hydrogen bonds with residue G40 and one hydrogen bond between the N1 position of the TPP pyrimidine ring and the 2' oxygen of residue G19. Triples (G19·A47)·G42 and (G18·C48)·A41 further stabilize these arrangements (Serganov et al., 2006).

Using chemical and enzymatic probing analysis Rentmeister et al. showed that the pyrimi-
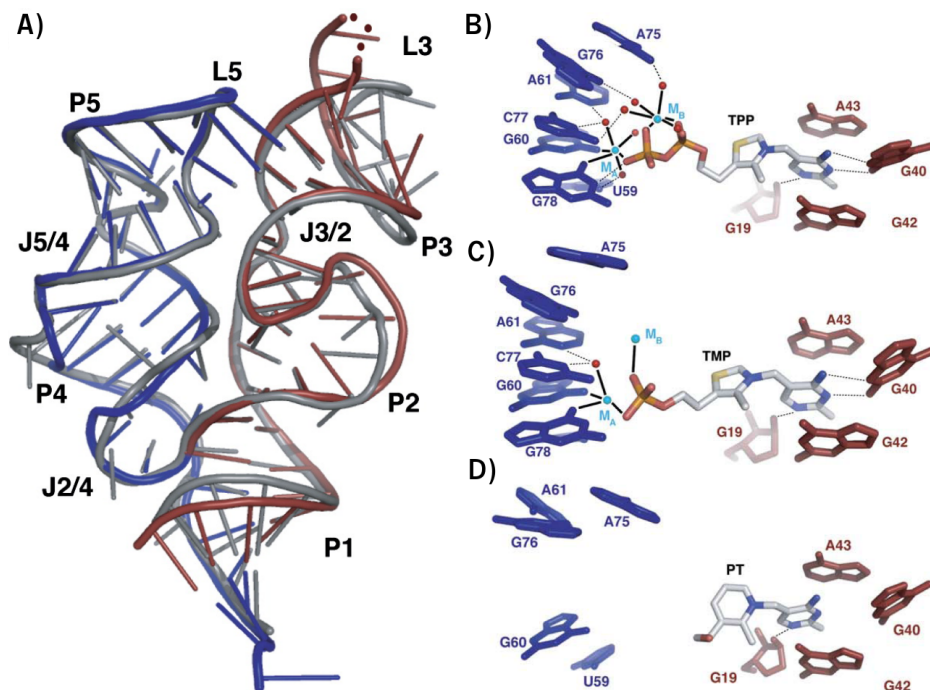
Figure 1.11: Crystal structure of the *E. coli* thiM riboswitch. Overall structure indicating helical, loop and junction regions of the *E. coli* thiM riboswitch (A). Gray structure indicates the *A. thaliana* thiC riboswitch (Thore et al., 2006). Close ups of TPP (B), TMP (C) or PT (D) binding contacts within the aptamer domain. Pyrimidine sensor helix colored in red and pyrophosphate sensor helix represented in blue. Metal ions are shown in light blue and water ions in red. Hydrogen bonds are represented as dashed and inner sphere metal coordinations as solid lines. Figures taken from Edwards and Ferré-D'Amaré (2006).

dine sensor helix was preformed to recognize the HMP moiety of TPP with the stem region P2/3 (Rentmeister et al., 2007). Once this part of the molecule is bound, a structural rearrangement that draws the pyrophosphate sensor helix near, is initiated. However, in the absence of a phosphate or pyrophosphate group this global conformational change does not occur (Rentmeister et al., 2007).

The pyrophosphate group of TPP is recognized by its according sensor helix in the J4/5 internal loop through interaction with divalent cations and their corresponding coordinated water molecules (Figure 1.11). Even though conflicting data exists, the current hypothesis involves the aid of two divalent ions for this interaction (Serganov et al., 2006; Edwards and Ferré-D'Amaré, 2006). The only residue making direct contact with the phosphate group is the highly conserved G78, which forms a hydrogen bond between its N1 proton and a nonbridging oxygen of the β-phosphate of TPP. Two more divalent ions are involved in correct folding of the RNA structure.

Finally, two tertiary interactions bring the pyrimidine and pyrophosphate sensor helix together. This is achieved by base-pairing between L5 & P3 on top of the helices, whereas the parallel alignment of both helices is due to a kink at residue A53 in the J2/4 bulge. This kink also allows the adaptation of the two helices to accommodate the ligand. Therefore, thiamine monophosphate (TMP) will lead to a more compact fold of the riboswitch's aptamer domain in comparison to TPP.

1.3.3 TPP biosynthesis and metabolism

Synthesis of the coenzyme thiamine pyrophosphate is accomplished in bacteria by the coupling of a pyrimidine and thiazole moiety (Figure 1.12). Each of these molecules is produced separately and then finally united.
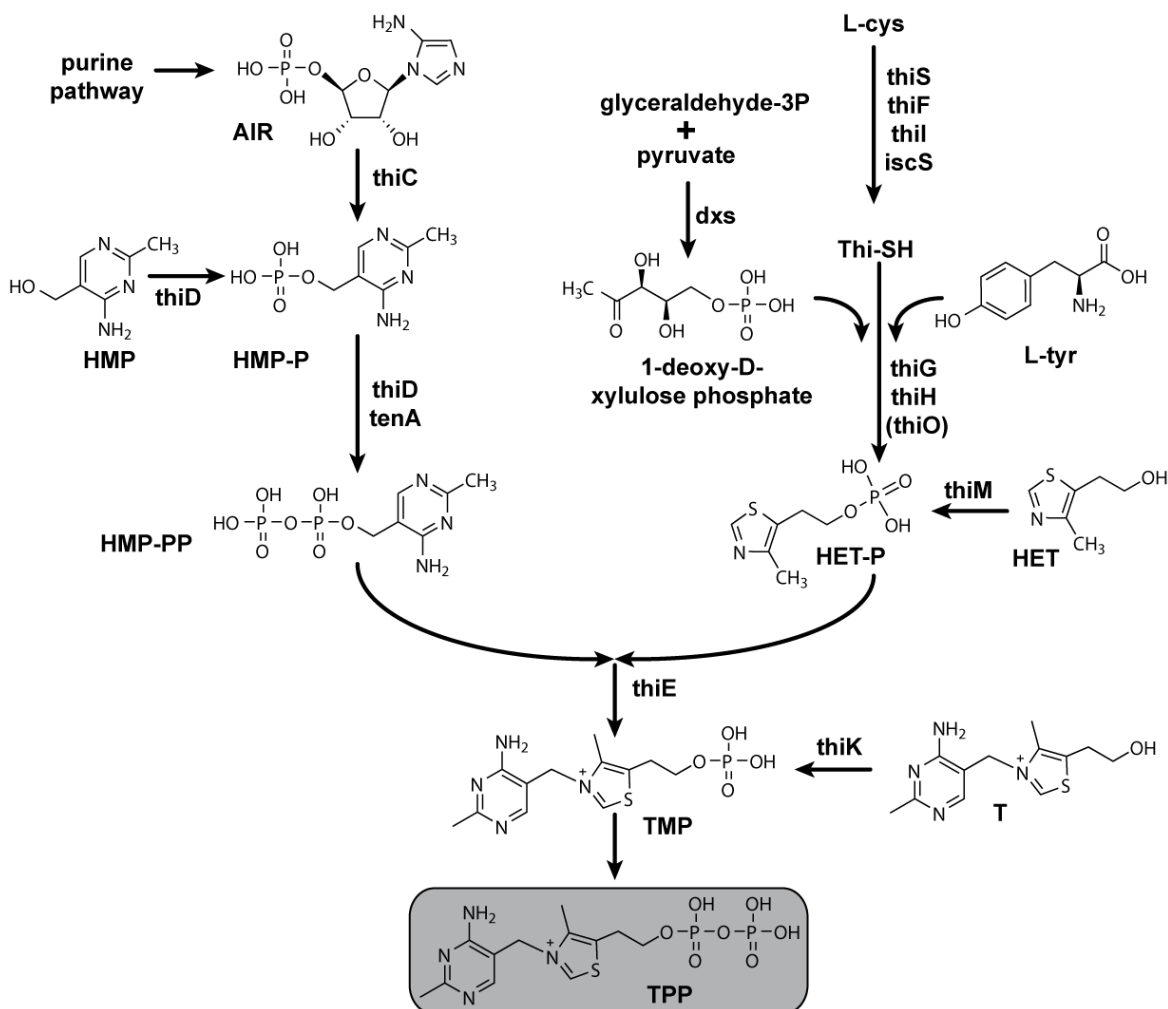
Figure 1.12: Schematic of the TPP biosythesis pathway in bacteria. For a detailed description refer to main text.

The biosynthesis of the pyrimidine moiety starts with aminoimidazole ribotide (AIR), an intermediate of the purine biosynthesis pathway. ThiC converts AIR to hydroxymethyl-pyrimidine-phosphate (HMP-P), which is then phosphorylated by the bifunctional HMP kinase/HMP-P kinase ThiD to yield hydroxymethyl-pyrimidine-pyrophosphate (HMP-PP, Figure 1.12).

In *E. coli*, the thiazole moiety of thiamine is derived from tyrosine, cysteine, and 1-deoxy-D-xylulose phosphate (DXP). An unresolved chain of reactions involving the thiF, thiS, thiG, thiH, and thiI gene products converts these reactants to the hydroxyethyl-thiazole phosphate product (HET-P). Thiazole synthase (ThiG) catalyzes an Amadori-type rearrangement of DXP via an imine intermediate (Dorrestein et al., 2004). DXP, whose production is catalyzed

by the dxs gene product, is also used in the nonmevalonate pathway and the pyridoxal biosynthesis (Begley et al., 1999; Rodionov et al., 2002). ThiF catalyzes adenylation of the sulfur carrier protein ThiS by ATP. In addition, ThiI and IscS, enzymes shared by the thiamine and 4-thiouridine biosynthetic pathways, may play a role in the sulfur transfer chemistry (Figure 1.12).

HMP-PP and HET-P are joined by one enzymatic step mediated by the ThiE protein, followed by phosphorylation of the formed TMP by ThiL to create TPP. Moreover, three distinct kinases, ThiM, ThiD, and ThiK, are involved in the salvage of HET, HMP, and thiamine, respectively, from the culture medium. Thiamine, thiamine phosphate, and thiamine pyrophosphate are actively transported in enteric bacteria using the ABC transport system ThiBPQ (Webb et al., 1997). At present, no other distinct thiamine transporters, neither HET nor HMP transport systems, have been identified in bacteria (Rodionov et al., 2002).

1.4 Multidrug-resistant pathogens

Antibiotics have become a valuable, yet habitually used defense against microbial infections. Hence, resistances have evolved to every antibiotic placed into clinical practice, irrespective of the chemical class or molecular target of the drug (Payne et al., 2007). The appearance and further evolution of multidrug-resistant (MDR) pathogens almost puts us into the perspective of the pre-antibiotic era, because only limited antibiotic means for sufficient cure exist against many of these pathogens. It seems nearly impossible to undertake today's surgical procedures, transplantations, cancer chemotherapy, or care of the critically ill or HIV-infected without effective antimicrobial agents (Arias and Murray, 2008). Bacteria have proven to be champions of evolution by adapting not only to challenging natural circumstances (extreme pH, salt, temperature), but also by establishing resistance strategies to circumvent the action of harmful substances targeted at them.

Among the Gram-positive organisms, especially methicillin-resistant *Staphylococcus aureus* and vancomycin-resistant enterococci impose therapeutic challenges, whereas multidrug-resistant *Pseudomonas aeroginosa* and acinetobacter, klebsiella, enterobacter and *Escherichia coli* assume this role for Gram-negatives.

As bacterial infections are the third-leading cause of death world wide (WHO, 2008), the search for novel antibacterial substances has to continue to provide the means for sufficient defense, not only, but particularly, against MDR pathogens.

1.4.1 Resistance mechanisms and the need for new antibacterial targets or compounds with new mechanisms of action

Resistance mechanisms are classically divided into two categories: Intrinsic resistance, which refers to a resistance against an antibacterial agent that is inherently present in a microorganism. This may be due to the drug-susceptible target not being present in the species (e. g. resistance of the penicillin-binding proteins of enterococci to the effects of cephalosporins), or an inherent characteristic of the organism may prevent the agent from reaching the target (e. g. resistance of Gram-negative bacteria to vancomycin because of the drug's inability to penetrate the Gram-negative outer membrane). The second, and most often referred to resistance mechanism in the discussion of MDR pathogens are acquired resistances. These occur from a change in the genetic composition of the microorganism either by mutation of important cellular structures or by changes in physiological processes. Genetic composition

can also be altered by acquisition of foreign resistance genes, so that a drug that once was effective is no longer active (Kaye and Kaye, 2000; Neu, 1992).

To combat or avoid these resistances which render many antibiotics useless, efforts have been focused on

- finding inhibitors of the enzymes that confer resistance

- chemically modifying existing antibiotic structures to prevent enzymatic modification

- designing inhibitors of bacterial efflux pumps

- developing new antibiotics with new modes of action (MoAs, Roemer et al. (2012); Payne et al. (2007)).

Nevertheless, these strategies should be aided by a prudent use of antibiotics, as it may avoid overmortality associated with infections due to MDR bacteria. Thus, the restrictive use of empirical antimicrobial therapy, short-duration treatments, and knowledge of pharmacological models, need to be encouraged in order to break the vicious circle of antibiotic overuse (Alvarez-Lerma et al., 2006; Leone et al., 2003, 2007). In addition, microbiological documentation before initiating empirical antimicrobial therapy should be an obligatory prerequisite to avoid fostering of new resistance development.

1.4.2 *Staphylococcus aureus* - a multi-drug resistant pathogen

Staphylococcus aureus, first isolated by Alexander Ogston in 1880 (Ogston, 1882), is a Gram-positive, facultative anaerobic, coccal bacterium that is frequently found as part of the normal skin flora and nasal passages (Kluytmans et al., 1997). Even though about one-fifth of the human population is a permanent carrier of this bacterium, some *S. aureus* strains can cause severe opportunistic, difficult to treat infections, due to their resistance against most antibiotics in use (methicillin-resistant or multi-drug resistant Staphylococcus aureus (MRSA)). Methicillin resistance is now a common problem for many hospitals around the world, and the recent emergence of community strains of *S. aureus* that are methicillin resistant, but also harbor genes associated with increased virulence impose the latest concern (Chambers, 2001, 1997). In 2002, an MRSA strain was isolated that is resistant against vancomycin, one of the last resort antibiotics applicable against these top causes for nosocomial infections (Weigel et al., 2003).

This rapid development of resistances calls for an ongoing search for alternative antibacterial substances that address novel targets and employ new modes of action. This is why RNA elements should be explored as antibacterial targets in these organisms which appear most difficult to target and most needy in obtaining adequate defense against.

1.4.3 Vancomycin-resistant *Staphylococcus aureus*

Vancomycin resistant *Staphylococcus aureus* (VRSA) evolved by acquisition of the vanA gene from enterococci, which are of significance as reservoir of resistance genes among Gram-positive bacterial pathogens (Leclercq et al., 1988). After the isolation of vancomycin-resistant *Staphylococcus aureus* (VRSA) in Japan in 1997 (Hiramatsu et al., 1997), several methicillin-resistant *S. aureus* (MRSA) strains with similar levels of vancomycin resistance have been isolated in other countries (Ploy et al., 1998; Boyle-Vavra et al., 2001; Chesneau et al., 2000;

Ferraz et al., 2000; Tenover et al., 1998; Walsh, 1999). The term VRSA is based on the vancomycin breakpoint set by the British Society for Chemotherapy, where a strain for which the minimal inhibitory concentration (MIC) is 8 µg/ml is defined as resistant. Since the same MIC is defined as an indicator for intermediate susceptibility by the Clinical and Laboratory Standards Institute (CLSI), these VRSA strains are called vancomycin-intermediate *S. aureus* (VISA) or glycopeptide- intermediate *S. aureus* (GISA) in the United States (Tenover et al., 1998). Both terms, GISA and VISA, have been used in the literature and in essence are interchangeable. Here, the CLSI classification and terminology is going to be used (Table 1.1).

Susceptibility classification	Vancomycin [µg/ml]
susceptible (VSSA)	≤ 2
intermediate (VISA)	4 - 8
resistant (VRSA)	≥ 16

Table 1.1: Terminology for *S. aureus* strains with reduced vancomycin susceptibility.

A subclass of VISA is formed by heterogeneous vancomycin-intermediate resistant *S. aureus* (hVISA), that show a vancomycin MIC within the susceptible range when tested by routine methods, but a proportion of the population of cells are in the vancomycin-intermediate range (Hiramatsu, 2001).

1.4.3.1 Resistance mechanisms

Main resistance mechanisms of VISA include changes in cell wall architecture, autolytic activity, and metabolism. Cell wall thickening is a consistent feature of VISA strains that may be associated with activated cell wall synthesis (Hanaki et al., 1998a), and is reduced when isolates are serially passaged in vancomycin free medium and resistance levels drop (Cui et al., 2003). Although the exact mechanisms leading to cell wall thickening have not been determined yet, the thickness is thought to prevent vancomycin from reaching its target (Sieradzki and Tomasz, 2003). In most isolates studied, common changes in cell wall structure include

- increased levels of abnormal muropeptides (Sieradzki and Tomasz, 1999)

- overexpression of PBP2 and PBP2' (Moreira et al., 1997; Hanaki et al., 1998a)

- reduced PBP4 expression levels (Sieradzki et al., 1999)

- increased levels of D-Ala-D-Ala residues

- increased glycan chain length (Komatsuzawa et al., 2002)

- decreased levels of the muropeptide amidation (Boyle-Vavra et al., 2001)

- reduced levels of peptidoglycan cross-linking (Moreira et al., 1997; Pfeltz et al., 2000; Sieradzki and Tomasz, 2003; Sieradzki and Tomasz., 1997).

For some VISA isolates a small increase in peptidoglycan cross-linking was found (Boyle-Vavra et al., 2001; Reipert et al., 2003). Additional common characteristics are a reduced growth

rate (Chuard et al., 1997) and reduced whole-cell lysostaphin susceptibility (Cui et al., 2006; Daum et al., 1992; Moreira et al., 1997). Furthermore, VISA strains often show a reduced acetate catabolism, which could lead to altered growth characteristics, antibiotic tolerance, changes in cell death, and increased polysaccharide intercellular adhesin synthesis according to Nelson et al. (2007). Finally, reduced autolytic activity is yet another mutual attribute of hVISA and VISA strains (Boyle-Vavra et al., 2001, 2003; Hanaki et al., 1998a; Koehl et al., 2004).

1.4.3.2 Mu50

In this study, the VISA strain Mu50 was used for all *in vivo* investigations related to the glmS ribozyme (Section 3.1.5 and 3.1.6).

Mu50 (ATCC 700699, vancomycin MIC of $8\,\mu g/ml$) was isolated in 1997 from a surgical wound infection from a 4-month-old individual who had undergone cardiac surgery, where vancomycin failed to cure the infection (Hiramatsu et al., 1997). Mu50 and its putative precursor strain Mu3, a hVISA (Hiramatsu et al., 1997), show increased cell wall synthesis. When compared with vancomycin-susceptible control strains (VSSA), they have enhanced incorporation of N-acetylglucosamine (GlcNAc) into the cell wall, an increased pool size of the cytoplasmic murein monomer precursor (UDP-N-acetylmuramyl-penta-peptide), an increased cell wall turnover rate, and increased production of penicillin-binding proteins PBP2 and PBP2' (Hanaki et al., 1998a,b; Hiramatsu, 1998). In addition to these shared features with hVISA strain Mu3, VISA strain Mu50 displays about a twofold increase in cell wall thickness, increased synthesis of nonamidated muropeptides and reduced peptidoglycan cross-linking which additionally contribute to vancomycin resistance as they enhance the affinity for trapping vancomycin (Cui et al., 2000). Subsequent investigation of isogenic cells with different cell wall thicknesses prepared from single colonies of Mu50 cells demonstrated that the cell wall thickening is the major contributor to vancomycin resistance of Mu50 (Cui et al., 2000).

Interestingly, Mu50 displays prolonged doubling times which suggests that their resistance comes at a great biological fitness cost. Compared with VSSA strains, Mu50 incorporates 2.3 times more glucose molecules into the cell wall peptidoglycan, where they constitute the aminosugar components of thickened cell wall (Cui et al., 2000). Although it was described that the rates of growth and cell wall synthesis of *S. aureus* are not correlated with each other (Wong et al., 1978), it might be that the increased use of glucose for cell wall components depletes the organism of energy and important metabolites. The prolonged doubling times of VISA strains explain why they do not quickly prevail in health care facilities and their detection is mostly confined to patients with MRSA infection undergoing long-term vancomycin therapy (Tenover, 1999).

2 Aim of this study

In the 1960's many antibiotics were discovered and their mode of action elucidated. In this Golden age of antibiotic research it was generally believed that the problem of bacterial infections was solved. This is why this research field was soon deserted and many pharmaceutical companies abandonned their anti-infectives programs. However, today the search for antibacterials has appeared back on the agenda, as resistances have evolved against every chemical entity in use as antibiotic. In this regard, bacterial species emerged, which have accumulated a variety of resistance mechanisms. These multi-drug resistant bacteria used to be confined to hospitals, although they are now increasingly found in community settings as well.

This combination of events calls for an ongoing search for new antibiotic substances that address novel targets and/or employ new modes of action. A quite recently discovered class of non-coding RNAs, coined "riboswitches", regulates gene expression in bacteria in response to binding to a cognate ligand. In this study, these riboswitches are investigated as promising, new antibacterial drug targets.

For this, two complementing strategies are followed: On the one hand a riboswitch class mainly found in Gram-positive organisms is investigated - the glmS riboswitch, whereas on the other hand a more widespread riboswitch class is studied for its use as antibacterial target - namely that of the *thi*-box riboswitches.

Different means were utilized to enable the identification of potential riboswitch modulators. *In silico* predictions and screenings of concise, rationally designed libraries of ligand analogs aimed at the detection of compounds that could interfere with riboswitch-mediated gene regulation. Furthermore, libraries of chemically synthesized, artificial entities as well as natural compounds were used for these investigations.

Newly identified compounds targeting riboswitches may provide a new class of antibacterial substances, employing novel modes of action and hence evading common resistance mechanisms. Therefore, these substances spur the hopes of defining a new class of last resort antibiotics urgently needed to fight multi-drug resistant pathogens.

Moreover, the identified riboswitch-targeting compounds can be used as tools for the investigation of RNA-small molecule interactions. Chemically and structurally related compounds and their potential of riboswitch modulation will provide a more detailed understanding of riboswitch-ligand recognition and tolerance. Furthermore, these riboswitch modulators can be used to investigate bacterial metabolic pathways and their regulatory networks. This could in turn aid in exploring riboswitch related virulence factors or resistance mechanisms in MDR pathogens.

3 Results

This chapter describes the search for artificial as well as natural riboswitch modulators. The validation of the *in silico* predicted glmS riboswitch is outlined in the first part (Section 3.1.1 and 3.1.2), culminating in its use for a screening system utilized to search for chemically synthesized glmS ribozyme activators (Section 3.1.3.1 and 3.1.3.2) as well as the testing of naturally occuring RNA interactors for their effect on ribozyme cleavage (Section 3.1.7.1 and 3.1.7.2).

The second part of this chapter applies concepts of riboswitch modulator identification to the most wide-spread class of riboswitches, namely the *thi*-box riboswitches (Section 3.2.1). Here, the validation and characterization of triazolethiamine compounds as thiM riboswitch activators is described (Section 3.2.2 and 3.2.3).

The chapter concludes with introducing a proof-of-principle study to enable the identification of preQ$_1$ riboswitch modulators (Section 3.3) by applying previously employed screening set-ups to new riboswitch classes.

3.1 The glmS ribozyme of *Staphylococcus aureus* Mu50 as antibacterial drug target

As the increasing occurence of bacterial resistances and the decrease of novel antibacterial structures imposes a serious threat on public health, there is an urgent need for the ongoing search for new antibiotics with novel modes of action. Therefore, the vancomycin-resistant staphylococcal strain Mu50 was used in this study as model organism for the screening and *in vitro* as well as *in vivo* characterization of compounds that modulate the glmS ribozyme.

The glmS ribozyme regulates expression of the enzyme glucosamine-6-phosphate synthase (GlmS), which catalyzes the conversion of fructose-6-phosphate to glucosamine-6-phosphate (GlcN6P, Section 1.2.4). Since GlcN6P is an important precursor of cell wall biosynthesis, manipulating the concerted synthesis of this essential metabolite promises maximal interference with bacterial growth and/or survival. Hence, targeting the regulatory element of the glmS gene, the glmS ribozyme, is a promising route for the development of novel antibacterial measures.

3.1.1 Validation of *in silico* predicted glmS ribozyme of *S. aureus* Mu50

Riboswitches usually reside in long intergenic regions (IGRs) and are characterized by their relatively well conserved aptamer domain. The Breaker laboratory created a database known as the Breaker Laboratory Intergenic Sequence Server (BLISS; http://bliss.biology.yale.edu) that integrates sequence similarity between IGRs from 91 microbial genomes (in 2004) with uniform predictions of gene functions and intrinsic transcription terminators to identify new riboswitches (Barrick et al., 2004). Riboswitch sequence alignments generated by BLISS usually show a collection of base-paired stems that are often supported by the presence

of nucleotide covariation. Moreover, search algorithms that use this secondary structure information and allow for the insertion of variable loops and incorporate predictions of intrinsic terminators, have been successfully employed to identify new examples of these RNA elements (Barrick et al., 2004).

Barrick et al. used this computational method not only for the discovery of a number of new riboswitches in IGRs, but also for the prediction of the presence of validated riboswitch structures in other organisms. Figure 3.1 shows the phylogenetic distribution of the glmS ribozyme which, according to their prediction, can be found in at least 18 other Gram-positive bacterial species. Among them is *Staphylococcus aureus* (secondary structure prediction shown in Figure 3.2 A), which allowed us to use the sequence alignment published in 2004 for the design of primers suitable for amplification of the putative glmS ribozyme sequence from *S. aureus* Mu50 genomic DNA (refer to Table 7.10 for primer sequences). The resulting genomic PCR product (217 bp) of the wild type glmS ribozyme version is shown in Figure 3.2 B. Additionally a longer version of the glmS ribozyme was designed (248 bp) and used for all following metabolite-induced self-cleavage assays (primers: 5'+T7 glmS Sau long & 3'Sau glmS neu) as this elongation allowed better separation and thus visibility of the cleavage fragment (Figure 3.2 C).

The RNA, which had been *in vitro* transcribed from the amplified DNA product, was subsequently dephosphorylated, radioactively labeled at its 5' end and finally tested in the so-called metabolite-induced self-cleavage assay for ribozymatic activity (Figure 3.2 C). In this assay, the RNA is incubated in the absence and presence of magnesium chloride as well as glucosamine-6-phosphate (GlcN6P), the natural ligand of the glmS ribozyme, and its
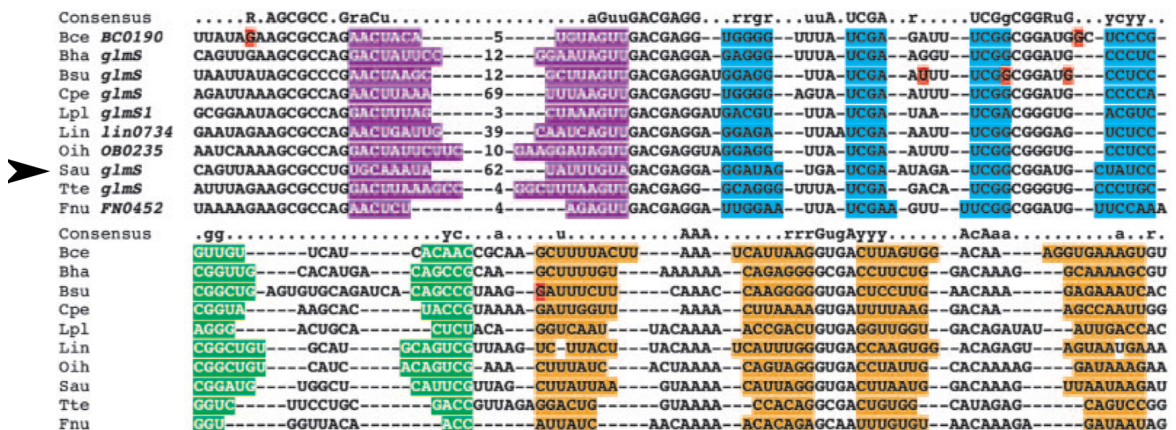
Figure 3.1: Phylogenetic distribution of the glmS ribozyme. Sequence alignment of the conserved element residing upstream of glmS gene homologs. Nucleotides shaded with purple, blue, green, and orange identify putative base-paired regions P1 through P4, respectively. Lowercase and uppercase letters of the consensus identify nucleotides that are conserved in 80 % and 95 % of the representatives. Nucleotides highlighted in red differ between the database sequence and the ones determined by the sequencing of clones for Bce and Bsu prepared by the Breaker laboratory. For each representative the organism and gene name are provided. Organism abbreviations: Bce, *Bacillus cereus*; Bha, *B. halodurans*; Bsu, *B. subtilis*; Cpe, *Clostridium perfringens*, Lpl, *Lactobacillus plantarum*; Lin, *Listeria innocua*; Oih, *Oceanobacillus iheyensis*; Sau, *Staphylococcus aureus*; Tte, *Thermoanaerobacter tengcongensis*; Fnu, *Fusobacterium nucleatum* (taken from Barrick et al. (2004)).
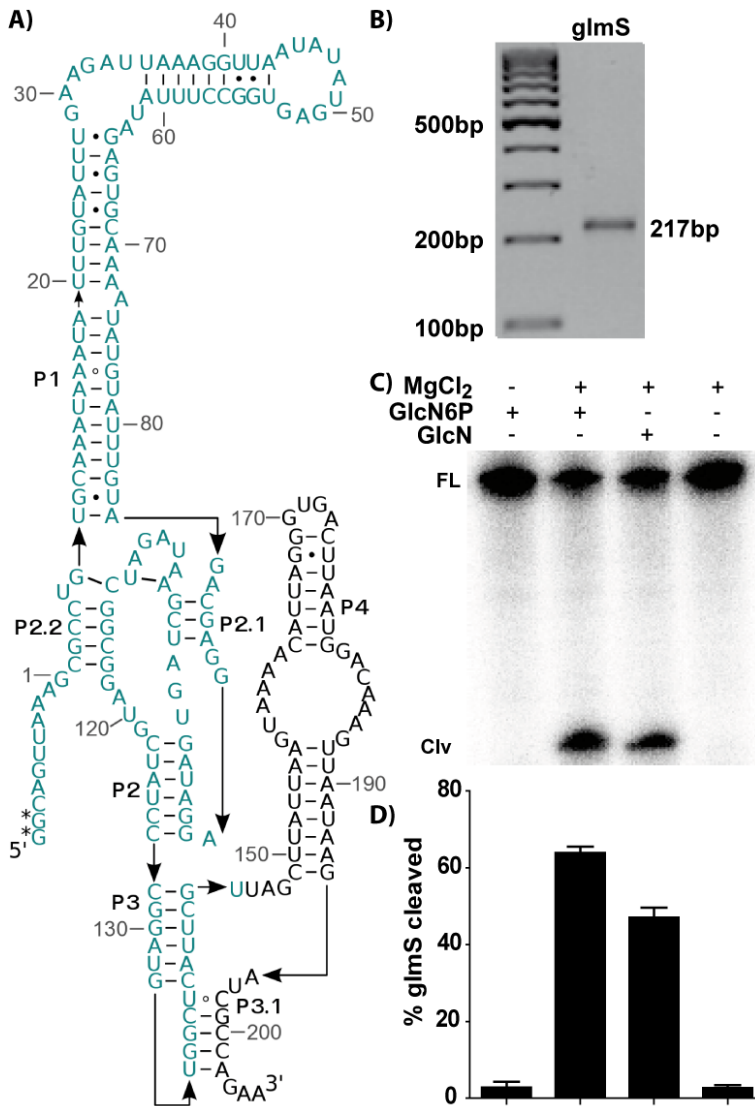
Figure 3.2: Amplification and verification of glmS ribozyme in *S. aureus* Mu50. Secondary structure of glmS riboswitch sequence including the ribozyme core (-10-145 nt, A, blue sequence) according to glmS consensus by McCown et al. (2011). Agarose gel analysis of glmS ribozyme amplification from genomic DNA of *S. aureus* Mu50. Primers 5'Sau glmS+T7 and 3'Sau glmS neu used for this PCR (B) were designed according to conserved sequences shown in Figure 3.1. GlmS ribozyme self-cleavage assay is shown in (C). GlmS RNA undergoes self-cleavage upon incubation with either its natural metabolite GlcN6P or the unphosphorylated aminosugar GlcN in the presence of $MgCl_2$. PAGE quantification results obtained by evaluation of band intensities of full length RNA (FL) and cleavage product (Clv) using AIDA software (D).

self-cleavage can be monitored by separating the labeled RNA fragments by PAGE (Figure 3.2 C). The predicted sequence from Barrick et al. showed enzymatic activity dependent on the presence of GlcN6P and Mg^{2+}-ions *in vitro*.

3.1.2 Characterization of the glmS ribozyme of *S. aureus* Mu50

The metabolite-induced self-cleavage assay was also employed to investigate certain characteristics of the *S. aureus* glmS riboswitch in comparison to its already described counterpart in *B. subtilis* (Winkler et al., 2004). Both riboswitches revealed very similar behaviour in their optimal cleavage temperature, the used pH for cleavage and their activating metabolites (Table 3.1 and compare to primary data shown in Figure 8.2 A-D). In summary, the optimal activity for the glmS ribozyme occurs under near physiological conditions for Mg^{2+}, pH and cleavage temperature. However, even though most of their properties were alike, the *S. aureus* glmS ribozyme needed higher magnesium chloride concentrations (9 mM) for cleavage than *B. subtilis* (5 mM, see Table 3.1 and Section 8.1 Figure 8.2 F), respectively. Furthermore, Co^{2+}

cannot replace Mg^{2+} in the self-cleavage reaction in *S. aureus* (Table 3.1 and Figure 8.2 E), whereas the divalent metal ions Ca^{2+}, Mn^{2+} and Sr^{2+} were able to substitute for Mg^{2+} in both organisms, however with decreasing potency.

Parameter	*S. aureus* Mu50	*B. subtilis*
pH	7	7
EC_{50} $MgCl_2$	9 mM	5 mM
Divalent cations accepted	Ca^{2+}, Mg^{2+}, Mn^{2+}, Sr^{2+}	Ca^{2+}, Co^{2+}, Mg^{2+}, Mn^{2+}, Sr^{2+}
Activating metabolites	GlcN6P, GlcN, GlcN6S, GlcNAc6P	GlcN6P, GlcN GlcN6S, GlcNAc6P
Optimal temperature	37 °C	37 °C

Table 3.1: Characteristics of glmS ribozymes of *S. aureus* and *B. subtilis*. Comparison between parameters influencing glmS cleavage such as optimal pH, $MgCl_2$ concentration, divalent cations accepted, activating metabolites and optimal reaction temperature is shown. All parameters for the *S. aureus* glmS were determined using the metabolite-induced self-cleavage assay (Section 6.2.4.1) and are compared to published results from Winkler et al. (2004), where same assay conditions were used. GlcN6P= glucosamine-6-phosphate, GlcN= glucosamine, GlcN6S= glucosamine-6-sulfate, GlcNAc6P= N-acetyl-glucosamine-6-phosphate.

The half maximal effective concentration (EC_{50}) was determined for the most potent glmS ribozyme activators (Table 3.2). For this, self-cleavage assays were performed with increasing concentrations of activator, and cleavage was stopped after 30 minutes of incubation. A dose-response curve was plotted and EC_{50}-values were calculated from non-linear regression, three-parameter fits (Section 6.2.4.2). The natural activator of the glmS riboswitch, GlcN6P, revealed the lowest EC_{50}-value of 3.6 µM. The unphosphorylated amino sugar GlcN, which has been known to activate the glmS ribozyme to a lesser degree, has an EC_{50}-value of 189 µM. This about 50 fold decrease in EC_{50} demonstrates the importance of the phosphate group for glmS ribozyme activation. Glucosamine-6-sulfate (GlcN6S), which contains a sulfate instead of a phosphate group, has a half maximal effective concentration in the same range as GlcN (160 µM, Table 3.2). This exchange of phosphate for sulfate also results in a decrease of EC_{50}-values (Table 3.2).

Activator	EC_{50} [µM]
GlcN6P	3.6 ± 0.4
GlcN	189 ± 22
GlcN6S	160 ± 14

Table 3.2: EC_{50}-values for *S. aureus* glmS riboswitch activating metabolites. Percentage of glmS cleavage was plotted against the logarithm of metabolite concentration used in the cleavage reaction, leading to a sigmoidal dose-response curve (Figure 8.1, Table 8.1 and Section 6.2.4.2).

3.1.3 Screening for artificial activators of *S. aureus* Mu50 glmS ribozyme

Different approaches can be employed when searching for chemical entities that activate riboswitches. One can search known metabolites and natural products to identify "natural" riboswitch activators or inhibitors (see Section 3.1.7.2 and 3.1.7.1). Or one could search through compounds that are not part of the metabolome of organisms, which would lead to

the identification of "artifical" riboswitch modulators. This approach can be pursued using a variety of strategies, such as the screening of libraries containing small molecules with certain characteristics, e. g. drug-like (Mayer and Famulok, 2006), FDA-approved (Blount et al., 2006; Lim et al., 2006), or *in silico* predicted (see Section 3.1.3.1). Furthermore, libraries can be screened that contain analogs of the cognate riboswitch ligand (Blount et al. (2006); Lünse et al. (2011), see Sections 3.1.3.2, 3.2.2 and 3.2.3).

In the following sections the search for artificial glmS ribozyme modulators will be discussed using *in silico* predicted (Section 3.1.3.1), as well as concise, rationally designed compound libraries (Section 3.1.3.2).

3.1.3.1 Screening of compounds with three-dimensional shapes similar to GlcN6P

Using the concept of 3D similarity, a virtual screening of commercially available compounds was performed in collaboration with Jean-Louis Reymond's group at the University of Berne. Their approach is distantly comparable to the already published strategy of "rapid overlay of chemical structures" (ROCS, (Nicholls et al., 2010)), which is a state-of-the-art 3D similarity method that allows the identificaton of the most active compounds in virtual screenings and having those molecules be diverse (Nicholls et al., 2010; McGaughey et al., 2007). Compared to ROCS however, Reymond's algorithm integrates the entire molecule shape instead of only matching atomic centers. Furthermore, hydrophobic areas as well as hydrogen acceptors and donors are taken into consideration by the program, but ionic interactions are disregarded.

In this *in silico* screening, 57 structures appeared as hits whose binding characteristics and molecular shape mimicked that of GlcN6P in three dimensional space (unpublished algorithm, personal communication Lars Ruddigkeit). These compounds, which are hereafter referred to as "Reymond compounds", were obtained from Princeton Biomolecular Research and subsequently tested for induction of glmS ribozyme cleavage, or for inhibition of GlcN6P-mediated glmS ribozyme activation. The metabolite-induced self-cleavage assay (see Sections 6.2.4.1 and 6.2.4.2 for experimental details) was utilized for these screenings.

Before screening the Reymond compound library, the assay was analyzed for its DMSO tolerance (Figure 8.3 E). Increasing concentrations of DMSO were tested and demonstrated that this solvent can be used to up to 2 % without strong effects on assay performance.

Screening for the activation of *S. aureus* Mu50 glmS ribozyme was performed in the presence of 2 mM compound in 2 % DMSO. Six hits were identified (compounds **D4**, **D7**, **E5**, **E6**, **E9** and **F5**) that showed at least 2 fold increase in cleavage above background cleavage in the absence of any metabolite (Figure 3.3 and Table 8.3). Compound **E6** (as well as **C6**, even though this compound did not appear as hit, compare percent glmS cleavage in Figure 3.3) showed RNase contamination or some kind of unspecific RNA interaction causing a smear of the full length glmS RNA in the polyacrylamide-gel (PA-gel). These two effects could lead to an artificial increase in band intensity, either for the cleavage product or the full length RNA, resulting in false positive hit-detection in the screening evaluation from quantification analysis data. Increased glmS cleavage detected for compounds **D4**, **D7**, **E5**, **E9** and **F5** (see Figure 3.3 for chemical formulas) was not due these effects. As compounds **D7** and **E5** showed highest activities, they should be investigated further, e. g. for concentration dependent and glmS ribozyme-specific cleavage activation. Furthermore, compounds structurally similar to the ones found in this screening should be investigated for their effects on ribozyme activation.

The screening was repeated under more stringent conditions, meaning at lower compound concentrations (500 µM compound) which also decreased the total DMSO content (0.5 %
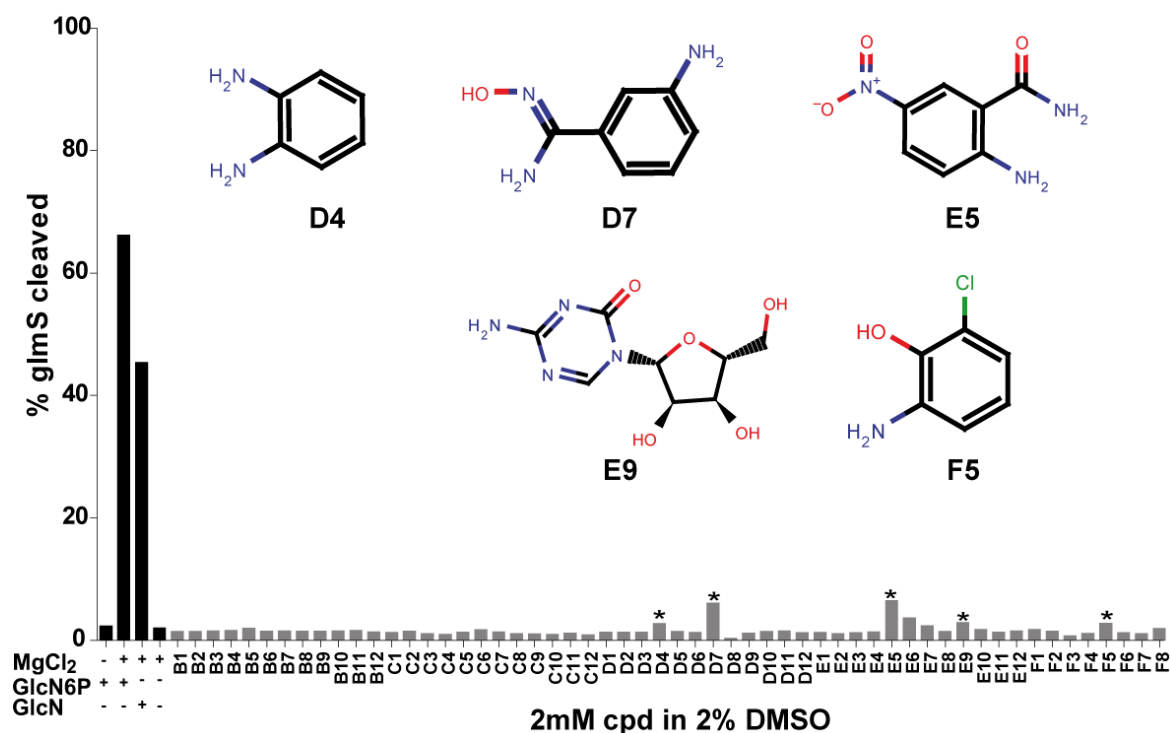
Figure 3.3: Screening of Reymond compounds for activation of *S. aureus* Mu50 glmS ribozyme. Screening outcome with controls as black bars on the left (reactions without metabolite and without $MgCl_2$ as negative control, reactions with divalent ions and metabolite as positive control). Chemical formulas of hit compounds are shown as inset. Compounds that were considered as hits after PAGE and band quantification analysis are marked with an asterisk.

DMSO, see Table 8.3). Those compounds revealing more than five fold background cleavage were deemed hits, namely **C1**, **C11**, **D1**, **D3** and **F2** (Figure 3.4, again background cleavage was defined as glmS cleavage in the absence of metabolite). Interestingly, not even the strongest activators from the first screening, compounds **D7** and **E5**, were confirmed under these conditions. This may be due to the decreased DMSO concentrations used here and the resulting changes in compound solubility (see detailed discussion in Section 4.2.1).

Additionally, a screening was performed using $20\,\mu M$ compound in $2\,\%$ DMSO (Figure 8.7). Here, the compound concentration was decreased further to identify inhibitors in the low micromolar range. At the same time the DMSO concentration was increased to the maximum of $2\,\%$, that is tolerable in terms of assay performance, to secure best-possible compound solubility. Under these conditions no compounds were identified that activated glmS ribozyme cleavage above background levels (Figure 8.7).

Moreover, a screening of Reymond compounds ($2\,mM$) in competition with GlcN6P ($200\,\mu M$) in a final DMSO concentration of $2\,\%$ was undertaken (Figure 3.5 A, and Table 8.3). Using a rather broad cut-off for hit definition at $40\,\%$ cleavage, substances were detected that reduce cleavage by at least $50\,\%$ compared to glmS activation observed in the mere presence of $200\,\mu M$ GlcN6P. In this respect, 13 compounds were deemed hits, namely **B7**, **C3**, **C6**, **C8**, **C9**, **D2**, **D6**, **D8**, **E6**, **E8**, **F6** as well as an accidental mixture of **F7/8** (Figure 3.5 B).

However, the effect observed for compound **E6** and **C6** was found to be unspecific as it was most likely due to an RNase contamination that diminished band intensity, and compound
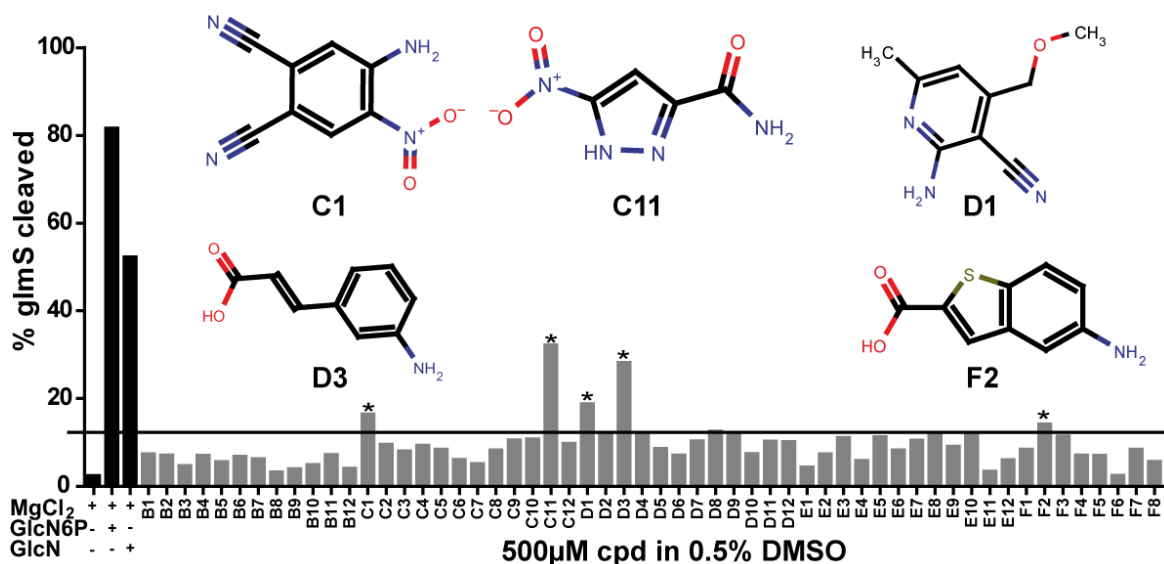
Figure 3.4: Screening of Reymond compounds for activation of *S. aureus* Mu50 glmS ribozyme. Screening outcome with controls on the left (black bars). Assay conditions are as described above (Figure 3.3), yet using 500 µM compound in 0.5 % DMSO instead of 2 µM in 2 % DMSO. Chemical formulas of hit compounds are shown as insets. The black line shows the cut-off for hit definition at about 12.5 % glmS cleavage. Compounds that were considered as hits after PAGE and band quantification analysis are marked with an asterisk.

D8 caused unspecific interactions with the RNA, so that the full length glmS could only be detected in the PA-gel pocket. This is why these compounds were excluded from the primary hits.

Due to structural similarity to **C9** and high activity, **D9** was also included in further characterizations of cleavage inhibition (Figure 3.5).

In addition to all the substances identified that block glmS cleavage, it was striking to find compound **D4** to increase glmS scission above percentages observed in the mere presence of GlcN6P (Figure 3.5). This compound had also been identified in the 2 mM in 2 % DMSO screening approach (see also Table 8.3). However, in a concentration dependent study of **D4** influence on glmS cleavage, no enhancement was observed (Figure 8.6 F). This finding suggests that the increased cleavage rates monitored in the presence of **D4** are merely due to unspecific effects (see detailed discussion Section 4.2.1).

Compounds **B7**, **C3**, **C6**, **C8**, **C9**, **D2** and **D4** were tested for effects on glmS cleavage in the presence of compound concentrations ranging from 25 nM to 2 mM (Figure 8.6 in Section 8.1). Compounds were not tested at concentrations exceeding 2 mM as this would have increased the final DMSO concentration above 2 %. In order to reach saturation, a lower concentration of GlcN6P was used, that is closer to the EC_{50}-value for glmS ribozyme activation of 3.6 µM. Under these conditions only **B7**, **C3**, **C6**, **C8** and **D2** revealed a concentration dependent cleavage inhibition in competition with 4 µM GlcN6P (Figure 8.6 A-E). For compound **D2** a dose-response curve could be fitted (R^2= 0.94) yielding an IC_{50}-value of 488 µM (Figure 8.6 E). For the other compounds a decrease in cleavage was observed at high compound concentrations, indicating a weaker affinity within the millimolar range.

Figure 3.5: Screening of Reymond compounds for competition with GlcN6P in glmS ribozyme cleavage activation. Screening outcome with controls on the left (black bars). Assay conditions are as described above (Figure 3.3). 200 μM GlcN6P were used in all competition reactions with 2 mM Reymond compound (2 % DMSO final). Black lines show the cut-off for hit definition at 40 % glmS cleavage. Compounds that were considered as hits after PAGE and band quantification analysis are marked with an asterisk (A). Chemical formulas of hit compounds are shown in (B). Due to structural similarity to **C9** and high activity, **D9** was also included in further characterizations of cleavage inhibition.

3.1.3.2 Screening of GlcN6P analogs for ribozyme activation

Several strategies have already been employed to search for glmS ribozyme activators. In 2006, Mayer et al. described a fluorescence polarization-based high-throughput-compatible screening assay to monitor GlcN6P-dependent glmS ribozyme self-cleavage of the minimal riboswitch from *B. subtilis* (Mayer and Famulok, 2006). A diverse library of small molecules was assembled to include mainly compounds that follow Lipinski's rule of five, thereby increasing the chances to obtain orally active drugs (Lipinski et al., 2001). However, none of the 5000 drug-like compounds showed activation of the glmS ribozyme (Lünse et al., 2011).

At the same time, Blount et al. performed a FRET-based screening to identify inhibitors of a bimolecular glmS ribozyme from *S. aureus* (Blount et al., 2006). A collection of rationally designed GlcN6P analogs as well as a library of 960 bioactive compounds was screened. Within the GlcN6P analog library, several substances with a potential for glmS ribozyme activation were discovered. Although the bioactive compound library was quite diverse, only one valuable hit was identified, whose binding and activation of the ribozyme was not due to unspecific RNA interactions (Blount et al., 2006). This compound was glucosamine - again a sugar, in structure very similar to the natural ligand of the glmS ribozyme.
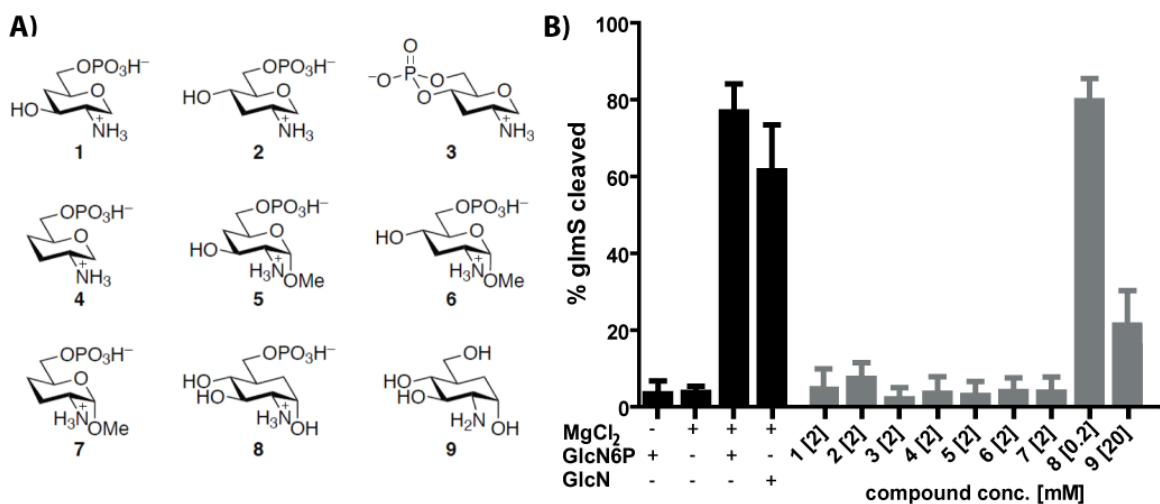
Figure 3.6: Screening of GlcN6P analogs for *S. aureus* Mu50 glmS ribozyme activation. Library of glucosamine-6-phosphate analogs used in this screening (A). Performance of glucosamine-6-phosphate and derivatives in the metabolite-induced self-cleavage assay (B). Cleavage of the glmS riboswitch induced by GlcN6P and GlcN (black bars, 0.2 mM) compared to a panel of compounds **1-9** (gray bars, concentration as indicated).

These different approaches indicate that screening distinct libraries of metabolite analogs can be very effective in riboswitch activator identification. Thus, a novel GlcN6P analog library was designed (Figure 3.6 A, compounds **1-9**). Compounds **1-4** were based 1-deoxyglucosamine-6-phosphate which has been shown previously to activate the glmS-riboswitch from *B. cereus* (Lim et al., 2006). Compounds **1-4** as well as the methyl glycosides **5-7** were designed to investigate the importance of the C-3 and C-4 hydroxy groups for *S. aureus* glmS ribozyme activation. Additionally, carba-sugars **8** and **9** were synthesized to address the role of the ring oxygen in riboswitch activation. This small compound library was synthesized by Valentin Wittmann's lab at the University of Konstanz. The synthesis of CGlcN6P (Figure 8.4) is described in detail in Schmidt (2010).

This series of structural and stereochemical GlcN6P isomers was subsequently investigated for glmS ribozyme activation using the metabolite-induced self-cleavage assay (Figure 3.6 B). Most strikingly, compound **8** activated the riboswitch to a comparable extent as does GlcN6P (control bar) demonstrated by 80 % cleavage at 200 µM. Compound **9**, which is the unphosphorylated form of compound **8**, activates glmS cleavage to about 20 %, yet at 100 fold higher concentrations (20 mM). Finally, compound **2**, which contains the minimal requirements for glmS ribozyme activation (Lim et al., 2006), also revealed a slight increase in ribozyme activity above background levels (approx. 10 %), that was found to be concentration dependent (Figure 8.3 D).

The other compounds tested revealed no significant increase in ribozyme activity. The derivatives of 1-deoxy-GlcN6P lacking the equatorial 4-hydroxy group are not active anymore (Figure 3.6, compound **4**). Similarly, variants with a cyclic phosphate (Figure 3.6, compound **3**) or a methylation at the 1-hydroxy functionality (Figure 3.6, compounds **5-7**) are also not effective in inducing glmS riboswitch hydrolysis.

3.1.4 Characterization of carba-sugars as novel glmS ribozyme activators

Carba-sugar **8**, from here on referred to as carba-glucosamine-6-phosphate (CGlcN6P) was shown to efficiently induce glmS riboswitch self-cleavage. Therefore, its cleavage characteristics were further investigated *in vitro*.

For this, EC_{50}-values for GlcN6P and GlcN as well as their carba-analogs were calculated by plotting the ratio of glmS cleaved against the logarithm of metabolite concentration used in the cleavage reaction, leading to a sigmoidal dose-response curve (Figure 8.1). In comparison to GlcN6P (Section 3.1.2), carba-glucosamine-6-phosphate's EC_{50}-value is less than two fold higher (EC_{50} GlcN6P= 3.6 µM vs. EC_{50}CGlcN6P= 6.2 µM, see also Table 3.2). Due to
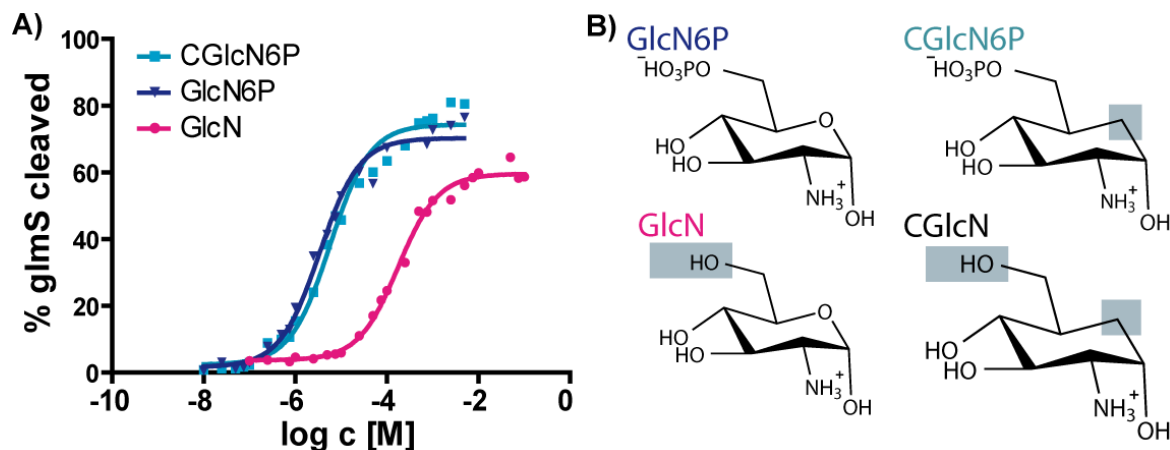
Figure 3.7: Concentration dependent cleavage of *S. aureus* Mu50 glmS ribozyme. GlcN6P, GlcN and artificial metabolite Carba-GlcN6P trigger concentration dependent cleavage of glmS ribozyme of *S. aureus* Mu50 (A). Dose-response curves from at least three independent experiments were used to calculate the EC_{50}. Error bars are omitted for clearer representation, but can be found in Figure 8.1. (B) Chemical formulas for natural metabolite GlcN6P (upper left) and its carba-analog CGlcN6P (upper right) as well as for the amino sugar GlcN (lower left) and its analog CGlcN (lower right). Differences in chemical structure from GlcN6P are highlighted in light blue.
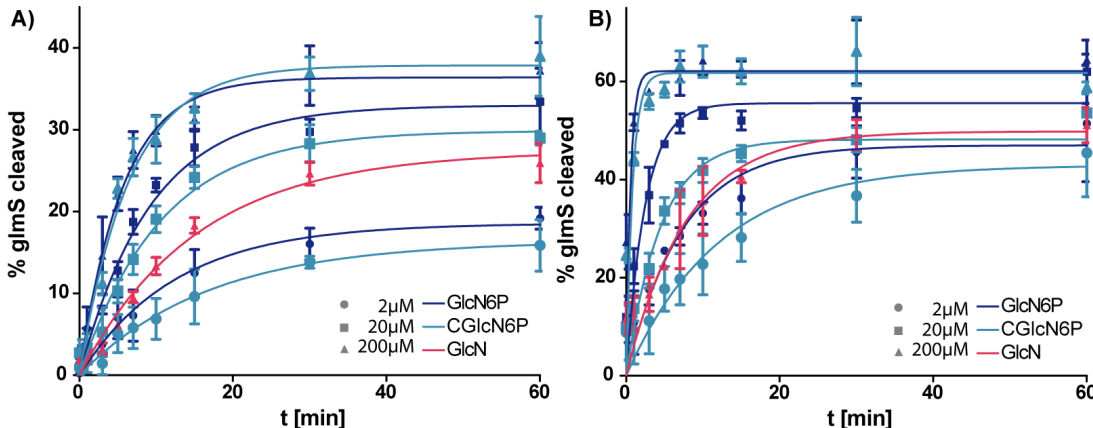
Figure 3.8: Determination of observed rate constant for glmS cleavage. K_{obs} determination of *S. aureus* Mu50 (A) and *B. subtilis* (B). Cleavage rates of the glmS-riboswitch at different concentrations (circles 2 µM; squares 20 µM; triangles 200 µM) of GlcN6P (blue), CGlcN6P (cyan), and GlcN (red). Plots of the fraction cleaved as a function of time are shown. Experiments were carried out in triplicates.

the mere exchange of the ring oxygen for a CH_2 group in the carba-sugar (Figure 3.7 B), the interaction the oxygen formes with the riboswitch is the only one lost in comparison to the natural metabolite. This most likely accounts for the similarity in half-maximal ribozyme activation. When the phosphate group is missing, like in GlcN (Figure 3.7 B), the concentration of half-maximal activation is about 50 fold higher. For its carba-analog, CGlcN, no EC_{50}-value could be determined as the assay set-up did not permit the use of compound concentrations high enough to reach saturation levels of maximal ribozyme cleavage. The highest CGlcN concentration assayed was 10 mM, which indicates that half maximal CGlcN triggered ribozyme activation must be in the millimolar range. Interestingly, the half maximal ribozyme activation by CGlcN6P is about three fold enhanced in *B. subtilis* (2.1 µM) in comparison to *S. aureus* (6.2 µM).

In order to evaluate how efficiently the glmS ribozyme cleaves upon encountering its cofactor or analogs, k_{obs} values were determined. By monitoring ribozyme cleavage over a time course of 90 minutes at defined metabolite concentrations, rate constants (k_{obs}) were determined using the fit for a one phase exponential association (Section 6.2.4.3).

The rate constants (k_{obs}) of metabolite-induced cleavage of the *S. aureus* glmS-riboswitch were found to be comparable for GlcN6P and CGlcN6P at all concentrations tested (200, 20, 2 µM, Table 3.3). For example, GlcN6P cleaves the *S. aureus* ribozyme at 200 µM with a rate constant of $0.18\,\mathrm{min}^{-1}$ and the carba-analog at a rate of $0.15\,\mathrm{min}^{-1}$. These data indicate

Concentration [µM]	*S. aureus* k_{obs} [min^{-1}]		*B. subtilis* k_{obs} [min^{-1}]	
	GlcN6P	**CGlcN6P**	**GlcN6P**	**CGlcN6P**
200	0.18	0.15	1.75	1.2
20	0.11	0.095	0.4	0.22
2	0.07	0.060	0.14	0.083

Table 3.3: k_{obs} values determined for glmS ribozyme cleavage of *S. aureus* and *B. subtilis*.

that the potential of CGlcN6P for riboswitch activation is very similar to that of the natural metabolite (Figure 3.8 A). The overall cleavage rates of the *S. aureus* glmS-riboswitch were found to be slower than those reported for glmS-riboswitches from other bacteria (k_{obs} at $200\,\mu$M GlcN6P $0.18\,min^{-1}$ in *S. aureus* and $1.75\,min^{-1}$ in *B. subtilis*, Table 3.3, Winkler et al. (2004)). Interestingly, the activation of the *B. subtilis* glmS-riboswitch was more disturbed by CGlcN6P as k_{obs}- values decreased in comparison to GlcN6P (k_{obs} at $200\,\mu$M CGlcN6P $1.2\,min^{-1}$ vs. $1.75\,min^{-1}$ for GlcN6P, Figure 3.8 B). Similarities in k_{obs} values determined for *S. aureus* GlcN6P versus CGlcN6P dependent cleavage are also reflected in obtained EC_{50}-values (see above). The three fold difference in EC_{50} of CGlcN6P between *S. aureus* and *B. subtilis* hints at the about 10 fold higher k_{obs} values determined for *B. subtilis*.

3.1.5 Antibacterial effects of carba-sugars on *S. aureus* Mu50

After CGlcN6P had shown similar behaviour to GlcN6P in activating the glmS ribozyme *in vitro*, the effect of carba-sugars on growth of the VISA strain Mu50 was investigated.

For these *in vivo* studies the use of CGlcN6P is not indicated because it is not very likely to pass the cell membrane due to its charged phosphate moiety (Figure 3.7 B). Different strategies will have to be utilized to possibly enable direct CGlcN6P take-up (McGuigan et al., 2008).

Gram-positive bacteria usually take up sugars by active transport through sugar specific phosphoenolpyruvate transfer systems (PTS, Reizer et al. (1988)). Staphylococci have PTS transporters for a variety of sugars, among them also glucosamine. Under the hypothesis that the PTS transporters responsible for GlcN uptake can also accept CGlcN, this carba-sugar was used for all *in vivo* investigations. When transferred across the cell membrane via a PTS, GlcN, and likely CGlcN, is phosphorylated at its C-6, resulting in GlcN6P or CGlcN6P, the more potent glmS ribozyme activator (Figure 3.9 A).

Two standard microbiological evaluations were performed to investigate and define an-
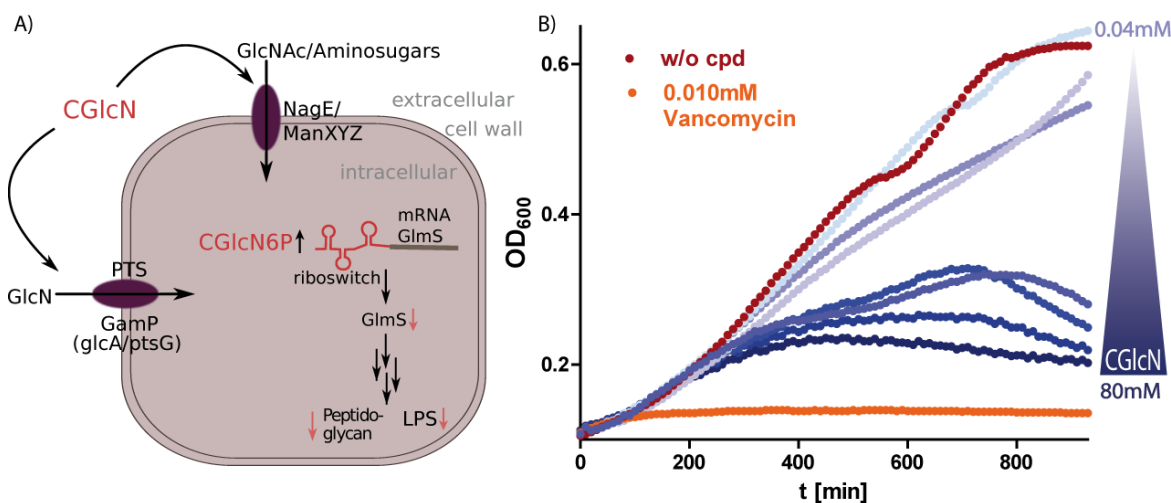
Figure 3.9: Effect of CGlcN on *S. aureus* Mu50 growth. Schematic of hypothesized carba-sugar transport and action inside bacteria (A). Increasing concentrations of CGlcN are shown in shades of blue, bacterial growth without compound is depicted in red and growth in the presence of high doses of vancomycin are orange (B).

tibacterial potency of CGlcN. On the one hand, the influence of CGlcN on *S. aureus* Mu50 growth was assessed by determining its minimal inhibitory concentration (MIC, experimental details are found in Section 6.3.5). The MIC marks the lowest compound concentration at which bacterial cells do not show growth after 24 h of incubation. This figure is often used to compare potencies of antibiotics with each other. Cells were grown in a chemical defined medium (CDM, Section 7.4) where amino acids were the sole carbon source. An inhibition in growth was observed at concentrations of 625 µM carba-glucosamine (133 µg/ml).

On the other hand, bacterial growth was measured directly upon addition of the carba-compound over a time course of 24 h. Vancomycin, used at elevated, clinically irrelevant, concentrations in this experiment, is a bactericidal antibiotic. Its killing effect is evident from the fact that the orange line, resembling *S. aureus* growth in the presence of vancomycin, only slightly elevates and then remains at the same absorption value (Figure 3.9 B). The CGlcN growth curves revealed that with increasing concentrations (40 µM-80 mM) a decrease in optical density was observed, which suggests that *Staphylococcus aureus* Mu50 cell count descreases (Figure 3.9 B). Whether this is due to a bactericidal or bacteriostatic effect needs to be further investigated (Section 5.1.5).

3.1.6 Synergistic effect of carba-sugars and vancomycin on *S. aureus* Mu50 growth inhibition

The vancomycin-resistant *Staphylococcus aureus* strain Mu50 shows increased cell wall synthesis (Section 1.4.3.2, Hanaki et al. (1998a)). The thickened cell wall of this strain is seen as a major contributor to vancomycin resistance (Breukink et al., 1999). In order to be able to synthesize a stronger cell wall, more precursors are needed. Several components of pathways involved in the making these precursors were shown to be upregulated in *S. aureus* Mu50 (Cui et al., 2000). This strain shows an increased uptake of GlcNAc, which can easily be converted to GlcN6P. Moreover, higher levels of glutamate synthase are found increasing the production of glutamate, which is necessary for the synthesis of GlcN6P from Fru6P with the help of
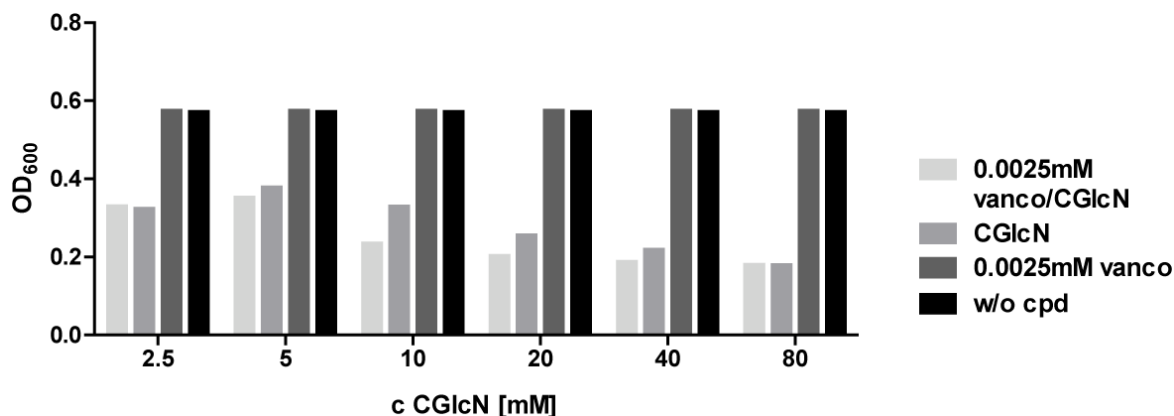
Figure 3.10: Synergistic effect of sub-inhibitory concentrations of vancomycin in combination with CGlcN. Bar graph depicts cell growth in the presence of either sub-inhibitory concentrations of vancomycin (2.5 µM) in combination with increasing concentrations of CGlcN (light gray) or increasing CGlcN concentrations (gray). Bacterial growth in chemically defined medium without any compound present (black) or upon addition of 2.5 µM vancomycin are shown as controls (dark gray).

glmS. And finally this enzyme, the GlcN6P synthase, has also been found to be more active thus producing more GlcN6P, which is the precursor of UDP-GlcNAc (Cui et al., 2000).

Therefore, sub-inhibitory concentrations of vancomycin were tested in combination with CGlcN to investigate any synergistic effects. A concentration of 2.5 µM vancomycin did not show any reduction in cell growth and was hence used as "sub-inhibitory" concentration (Figure 3.10). A decrease in cell growth was observed in the presence of 5-40 mM CGlcN in combination with 2.5 µM of the glycopeptide antibiotic, with the greatest difference to be observed at 10 mM CGlcN (Figure 3.10). In comparison to this, the mere use of CGlcN did not lead to such a strong abatement in bacterial growth. These results are preliminary, as this experiment could only be carried out once. Since CGlcN is not commercially available, but rather had to be synthesized, only limited amounts of compound were at hand for experimentation. However, the synergistic CGlcN-Vancomycin tendencies call for further evaluation of this phenomenon by future experiments.

3.1.7 Screening for natural activators of vancomycin-intermediate resistant *S. aureus* Mu50 glmS ribozyme

Apart from screening synthetic small molecule libraries or chemically synthesized metabolite analogs, natural products should be considered for interfering with glmS ribozyme activation. Hence, this Section will describe the investigation of aminoglycosides as glmS ribozyme regulators (Section 3.1.7.1) as well as the exploration of the naturally occuring substance Streptozotocin in its role of glmS riboswitch activation (Section 3.1.7.2).

3.1.7.1 Screening of aminoglycosides for activation or inhibition of the glmS ribozyme

Aminoglycosides are oligosaccharide antibiotics that were first discovered in 1944 in the group of Selman Waksman (Jones, 1944). These antibiotics are multiply charged compounds of high flexibility. Their positive charges are attracted to the negatively charged RNA backbone (Hermann and Westhof, 2000; Tor, 2003). The flexibility of the aminoglycosides facilitates accommodation into a binding pocket within internal loops of RNA helices or into ribozyme cores (Schroeder et al., 2000).

The conserved elements among aminoglycosides are highlighted in Figure 3.11 for Tobramycin. The 2-deoxystreptamine ring is common to all aminoglycosides. Moreover, the aminogroups at position 1 and 3 are conserved, as these elements are essential for binding to the decoding site of the 16S rRNA (Schroeder et al., 2000). Furthermore, the 2-deoxystreptamine ring is most commonly substituted, usually via O-glycosidic bonds, at positions 4 and 5, as in the neomycin class (Figure 3.11 H-L), or at positions 4 and 6, as in the gentamicin and kanamycin classes (Figure 3.11 A-D and Figure 3.13 B).

Aminoglycosides interact with ribosomal RNA at the A-site (Fourmy et al., 1996; Vicens and Westhof, 2002), which is the entry site for aminoacyl tRNAs (except for the first aminoacyl tRNA fMet, which enters at the P-site). Binding of the antibiotic induces a conformational change in the RNA, thereby switching the A-site into a high affinity state for mRNA–tRNA recognition and reducing the rejection rate of near-cognate tRNAs (Karimi and Ehrenberg, 1994; Fourmy and Puglisi, 1998). This increased affinity of the A-site for tRNAs in the presence of antibiotics results in misreading of the genetic code (Davies et al., 1964, 1965; Schroeder et al., 2000). In the presence of aminoglycosides, the level of translational accuracy was estimated to decrease from a normal frequency of 1×10^{-3}–10^{-4} misincorporation events
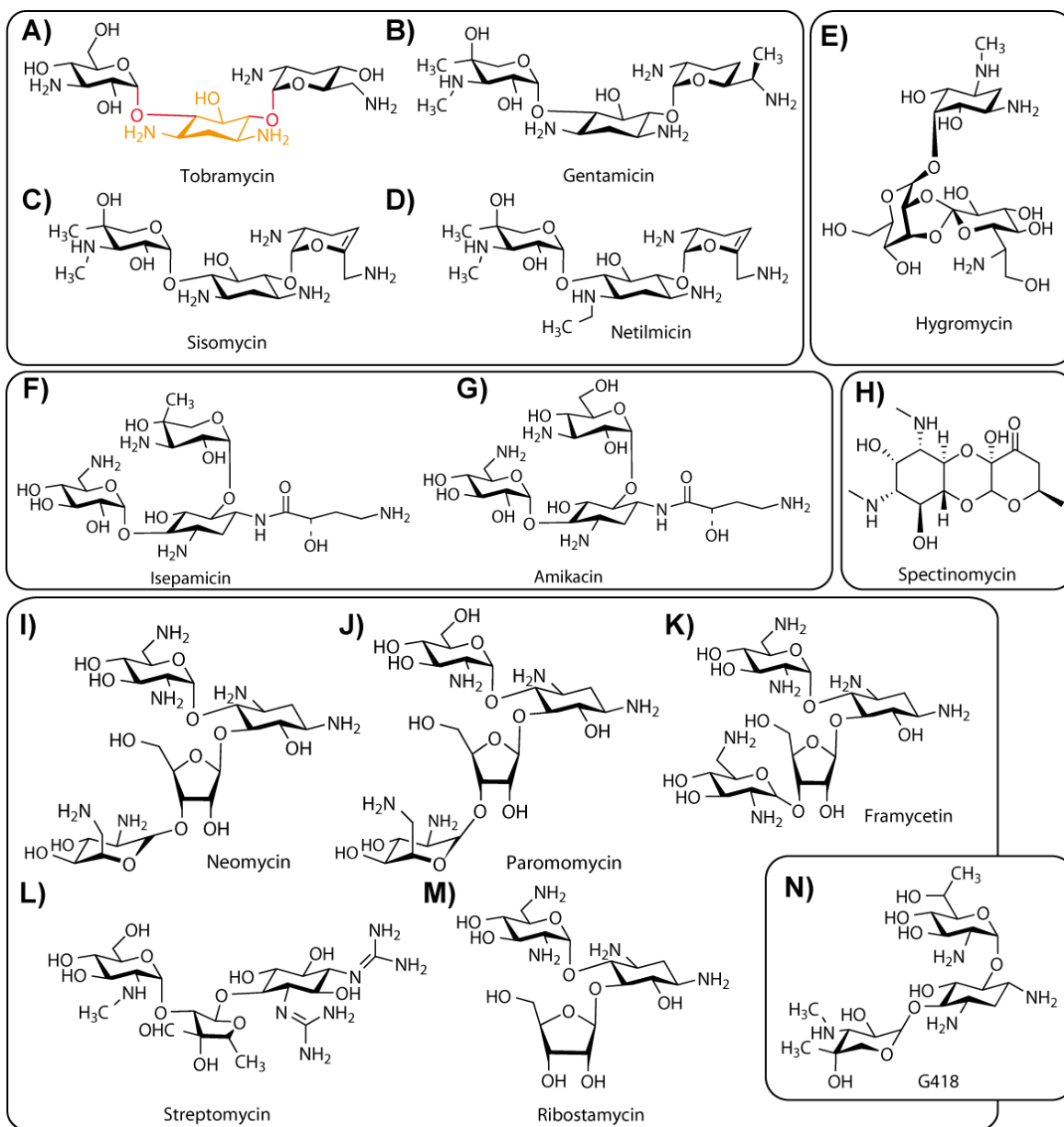
Figure 3.11: Chemical structures of aminoglycosides tested for glmS ribozyme interference in this study. In (A) the conserved streptamin ring is highlighted in orange, the O-glycosidic bonds in red.

per codon to as much 1 in 10^{-1}-10^{-2} (Zaher and Green, 2009).

Aminoglycosides are also known for interacting with catalytically active RNAs. Extensive studies have been performed on their influence on the hammerhead ribozyme, RNase P cleavage (Stage et al., 1995; Vioque, 1989), or group I intron splicing (von Ahsen et al., 1991).

Hence, aminoglycosides were tested for their ability to enhance or inhibit the activation of the glmS ribozyme of *S. aureus* Mu50. For this, the ribozyme was either incubated with the aminoglycoside alone or additionally in the presence of 200 µM GlcN6P. None of the aminoglycosides investigated showed any activation of glmS ribozyme cleavage (Figure

3.12). However, there were some amino sugars that interfered with proper ribozyme cleavage triggered by GlcN6P, namely Paromomycin, Tobramycin, Hygromycin B, and Neomycin. Although from the quantification data analysis it appears that Netilmicin decreases cleavage significantly, PAGE showed that this is merely due to unspecific interactions with the RNA, which retain it in the gel pockets (Figure 3.12 A).

The most prominent decrease in metabolite-induced self-cleavage showed Neomycin (Figure 3.12 B, Figure 3.11 I), which is similar in structure to Ribostamycin, Paromomycin and Framycetin (Figure 3.11 M, J & K and Figure 3.12 B). Paromomycin (Figure 3.12 A) and Ribostamycin (Figure 3.12 C, Schüller (2012)) revealed a slight inhibition of glmS cleavage. Framycetin was not available for testing, but should be investigated for its effect on glmS ribozyme inhibition. Tobramycin also interfered with ribozyme activity, however aminoglycosides similar in structure, like Gentamicin and Kanamycin A did not show any effect (Figure 3.11 A, B and 3.13 B). Slightly less closely related Sisomycin revealed moderate glmS cleavage inhibition (Figure 3.12 C and Figure 3.11 C, (Schüller, 2012)). Although, future experiments will have to uncover whether these effects are due to the same unspecific interactions observed for the structurally very closely related Netilmicin (Figure 3.11 D).

Moreover, Spectinomycin did not show any effect in glmS ribozyme cleavage inhibition (Figure 3.12 A and Figure 3.11 H). Compared to the aforementioned aminoglycodsides, it uses different mode of action on bacterial translation by inhibiting the translocation process (Brink et al., 1994). However, Hygromycin B which employs this mode of action also (Peske et al., 2004), revealed a very strong effect on ribozyme inhibition (Figure 3.12 A and Figure 3.11 E). Hence, those groups conferring the inhibition of the translocation process are either not necessarily the same ones that interfere with ribozyme action, or possibly secondary or tertiary RNA structures targeted by Spectinomycin and Hygromycin B in rRNA are not equally found in the glmS ribozyme.

Because different influences on ribozyme activation have been described in the literature for Kanamycin A and B, the latter was also tested for its ability to interfere with glmS ribozyme cleavage (Figure 3.13). Although the only difference between these antibiotics is the exchange of a hydroxyl group for an amino-group, this slight difference in structure leads to a strong reduction of glmS ribozyme cleavage by Kanamycin B (to about 20 %), whereas Kanamycin A shows no effect (Figure 3.13 A). In this regard, Kanamycin C (Figure 3.13 B) should be tested for its influence on ribozyme cleavage. This would allow to conclude whether the number or the position of amino-groups is critical for cleavage inhibition. Kanamycin B is also interesting, as it is very close in structure to Tobramycin (Figure 3.13 B and Figure 3.11 A), which contains a single hydroxy-group less.

To further investigate these observed phenomena, all aminoglycosides that revealed an inhibitory effect on cleavage were tested in a concentration dependent manner in competition with GlcN6P. Table 3.4 shows half-maximal inhibitory concentrations obtained from dose-response curves (Figure 8.11). Neomycin inhibited cleavage most potently of all examined aminoglycosides displaying an IC_{50} of 28.7 µM. Ribostamycin lacks one of the amino sugar rings compared to Neomycin, it has a less pronounced inhibitory activity (IC_{50} 2.03 mM). Interestingly, Paromomycin, which differs from Neomycin by the exchange of one amino-group for a hydroxyl group, is able to reduce ribozyme cleavage, but too subtle to determine IC_{50}-values from a proper dose-response curve. This indicates that its IC_{50}-value is more than 100 fold reduced compared to Neomycin. These findings underline the importance of the number of amino-groups carried by the aminoglycoside. A decrease in amino-groups is correlated with a decrease in ribozyme cleavage inhibition. Tobramycin inhibits glmS cleavage with an
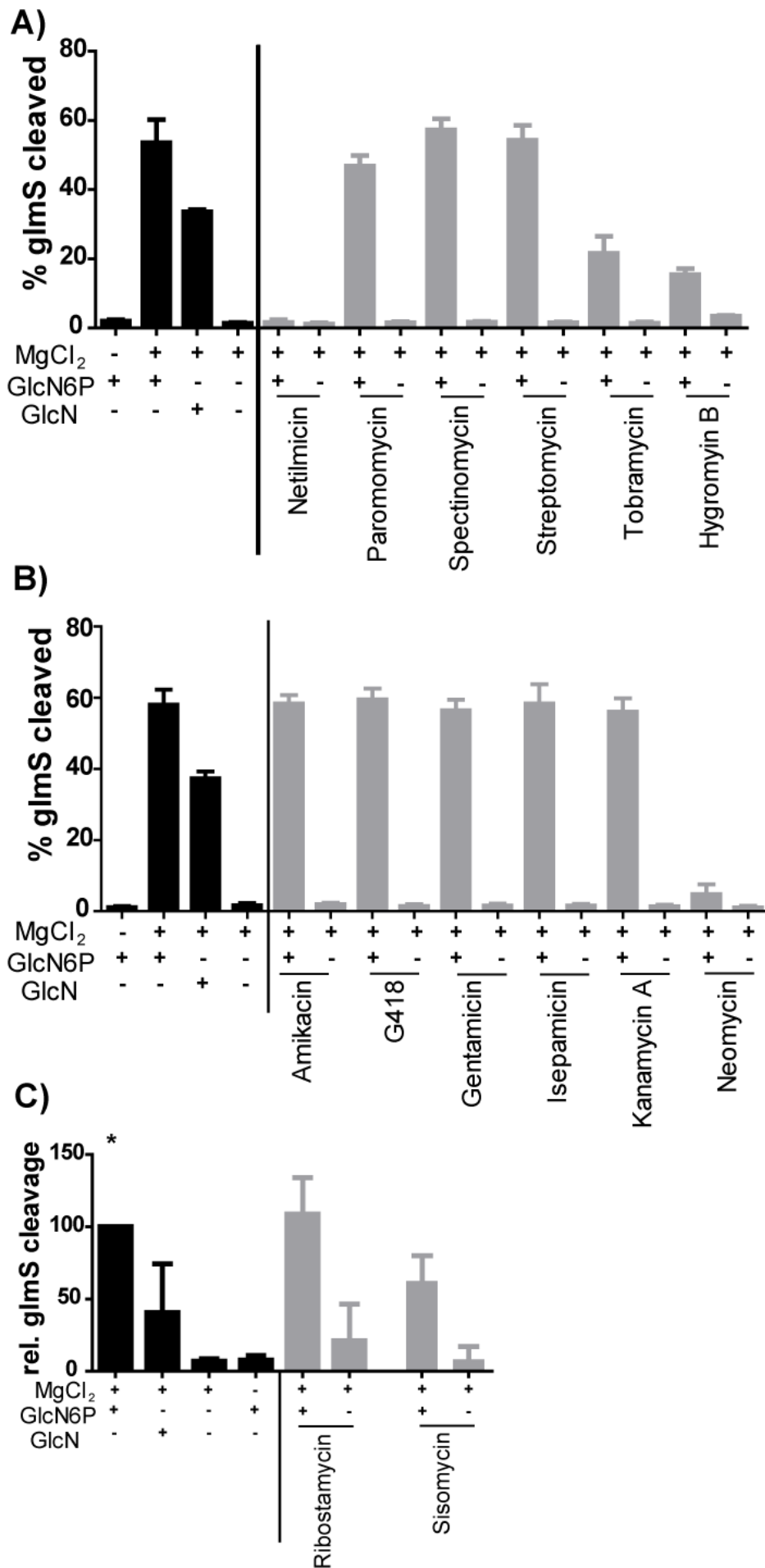
Figure 3.12: Screening of aminoglycosides for inhibition and activation of *S. aureus* glmS ribozyme cleavage. Aminoglycosides Netilmicin, Paromomycin, Spectinomycin, Streptomycin, Tobramycin and Hygromycin B were tested for activation of the glmS ribozyme at compound concentrations of 200 µM or for inhibition of glmS ribozyme cleavage in the presence of 200 µM GlcN6P (A). The same experimental setup as described in (A) was used to investigate characteristics of Amikacin, G418, Gentamicin, Isepamicin, Kanamycin A and Neomycin (B) as well as Ribostamycin and Sisomycin (C). Experiments carried out by Anna Schüller are marked with an asterisk.
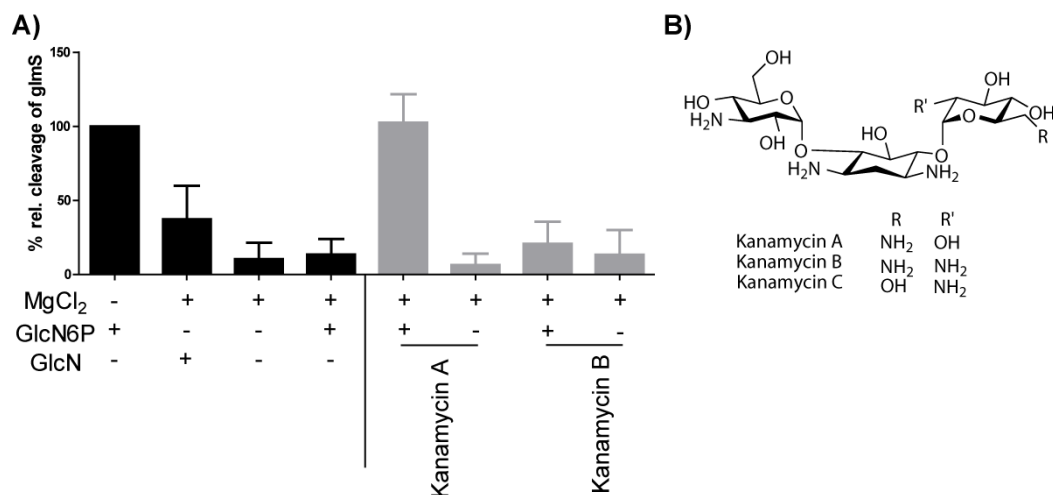
Figure 3.13: Influence of Kanamycin A and B on glmS ribozyme clevage. Metabolite-induced self-cleavage of glmS ribozyme in the presence of either aminoglycoside alone (200 µM) or in the presence of 200 µM GlcN6P (A). This assay was performed by Anna Schüller. Structure of Kanamycin A, B and C (B).

Aminoglycoside	IC$_{50}$ [µM]
Neomycin	28.7
Tobramycin	55.4
Paromomycin	n.a.
Ribostamycin	2030
Sisomycin	n.d.
Kanamycin B	43.4

Table 3.4: IC$_{50}$-values of aminoglycoside mediated glmS ribozyme inhibition. Kanamycin B and Ribostamycin values were calculated from aminoglycoside concentration dependent glmS ribozyme cleavage experiments performed by Anna Schüller. n. a.= not applicable, where fits could not be applied to insufficient dose-response curves, n. d.= not determined.

IC$_{50}$-value of 55.4 µM, thus about two fold less effectively than Neomycin. However, its value of half-maximal ribozyme inhibition lies in the same range as that observed for Kanamycin B, which was found to be 43.4 µM (Table 3.4). These two aminoglycosides are very similar in structure and only differ by an additional hydroxyl group carried by Kanamycin B (Figure 3.13 B and Figure 3.11 A).

The half-maximal inhibitory concentration of Sisomycin has not yet been determined, even though this aminoglycoside, in structure closely related to Netilmicin and quite similar to Tobramycin and Gentamicin (Figure 3.11 A-D), did show glmS cleavage inhibition comparable to Kanamycin B (Figure 3.12).

Additionally, cleavage rate contants were determined by Anna Schüller for GlcN6P induced glmS ribozyme cleavage in the presence of increasing concentrations of aminoglycosides (Table 3.5). These k$_{obs}$ values indicate the change in speed of the cleavage reaction in the presence of the antibiotic. In general, for all aminoglycoside antibiotics tested, increasing concentrations led to a decrease in the observed rate constants. Moreover, the differences in k$_{obs}$ are in line with inhibition tendencies observed in IC$_{50}$ measurements (Table 3.4).

Aminoglycoside	Concentration [µM]	k_{obs} [min^{-1}]
GlcN6P	2	0.068
	20	0.107
	200	0.177
Neomycin	2	0.155
	20	0.0726
	50	0.0414
	100	n. a.
Tobramycin	2	0.167
	20	0.098
	200	0.034
	2000	n. a.
Paromomycin	20	0.29
	200	0.22
	2000	0.151
Ribostamycin	-	n. d.
Sisomycin	20	0.193
	200	0.058
	2000	n. a.
Kanamycin B	20	0.154
	50	0.115
	100	0.039

Table 3.5: k_{obs} values determined for glmS cleavage reaction. k_{obs} measurements and calculations were performed by Anna Schüller (Schüller, 2012). Observed rate constants were obtained for reactions containing 200 µM GlcN6P and varying concentrations of aminoglycoside antibiotic (2 µM-2 mM). Metabolite-induced self-cleavage was monitored over a time course of 90 min (Figure 8.10 and Figure 8.9). n. d.= not determined, n. a.= not applicable, where fits could not be applied because of (near)-complete cleavage inhibition.

Exemplarily, an aminoglycoside concentration of 20 µM is chosen for comparison of k_{obs} values obtained in the presence of 200 µM GlcN6P. Under those conditions, observed rate constants for Sisomycin (0.193 min^{-1}) or Kanamycin B (0.154 min^{-1}) remain comparable to that observed for 200 µM GlcN6P alone (0.177min^{-1}, Table 3.5). The cleavage rate for Tobramycin (0.098 min^{-1}) and Neomycin (0.0726 min^{-1}) is 1.8-2.4 fold lower. Interestingly, Paromomycin enhances glmS ribozyme cleavage 1.6 fold, even though increasing Paromomycin concentrations still lead to a decrease in k_{obs} values.

The decreases in k_{obs} is even more pronounced at equimolar concentrations of aminoglycoside. At these concentrations the k_{obs} values are in the range of natural glmS ribozyme activation at 2 µM GlcN6P (Table 3.5).

3.1.7.2 Streptozotocin

This section describes the investigation of a naturally occurring GlcN analog, Streptozotocin, for its potential in glmS riboswitch activation. Streptozotocin (also known as Streptozocin and abbreviated Stz) is a monofunctional nitrosourea compound that was first isolated from *Streptomyces achromogenes* ssp. *streptozoticus* (C. Lewis, 1959/1960) and has been used as

broad spectrum antibiotic that is active against many Gram-positive and -negative bacteria. Streptozotocin or [2d-2-(3-methyl-3-nitrosoureido)-D-glucopyranoside] (Figure 3.14 A) is a derivative of 2d-glucose and similar in structure to D-glucosamine and N-acetyl-D-glucosamine (GlcNAc) (Ross R. Herr, 1967; Wiley, 1979). Stz is described as a mutagen, cancerogen, an antitumor agent (Wiley, 1979) and is also a widely distributed diabetogen (Rakieten and Nadkarni, 1963; Junod et al., 1967).

Stz is taken-up by *Escherichia coli* and other sensitive bacteria via a PTS transporter, nagE, which is naturally involved in N-acetyl-glucosamine (GlcNAc) uptake (Lengeler, 1979). Bacteria that show a mutation in the pts-operon transport enzyme or the gene nagE are not susceptible to Streptozotocin anymore (Ammer et al., 1979; Lengeler, 1980). This nitrosourea compound relies on its ability to be taken-up into cells, where it is broken down to yield the highly toxic compound diazomethane, which kills cells by excessive DNA alkylation (Wiley, 1979). Additionally, the phosphorylated derivative of Stz accumulates intracellularly, since it can neither be dephosphorylated nor deacetylated by metabolic enzymes.

3.1.7.2.1 *In vitro* activation of the glmS ribozyme of *S. aureus* Mu50 and *B. subtilis* by Streptozotocin

Considering the similarity in structure between glucosamine and Streptozotocin we hypothesized that this antibiotic might also affect glmS ribozyme cleavage. Therefore, the previously described riboswitches from *B. subtilis* and *S. aureus*, were used to assess ribozyme activation by increasing concentrations of Streptozotocin (Figure 3.14 B, C). Indeed, this antibiotic revealed concentration dependent effects leading to a half-maximal glmS activation of 104 mM in *S. aureus* and 956 mM in *B. subtilis*. It is not unexpected that these values lie in the millimolar range. Apart from the structural changes at the C-2 position, it is also known that the lack of the phosphate group at C-6 causes a significant decrease in ribozyme activation for GlcN and GlcN6P which differ 50 fold in EC_{50}-value (Table 3.2). Therefore, although these results do not appear promising at first sight, the phosphorylated variant might be interesting to investigate *in vitro*, especially since it is known that Streptozotocin is present in its phosphorylated form *in vivo*.

3.1.7.2.2 Antibacterial effects of Streptozotocin

To investigate the influence of Streptozotocin on bacterial growth, minimal inhibitory concentrations as well as growth curves were obtained for the VISA Mu50 strain. As a vancomycin susceptable control strain, SG511-Berlin was used, which displays increased sensitivity to antibiotic treatment (Sass and Bierbaum, 2009).

Minimal inhibitory concentrations (MICs) of Streptozotocin were determined as described before in different growth media, namely 2× chemically defined medium (2×CDM), 0.5× Mueller-Hinton (0.5×MH) broth, and brain-heart infusion (BHI).

BHI is a highly nutritious general purpose growth medium for fastidious as well as nonfastidious bacteria and is the richest medium used in this MIC-investigation. Mueller-Hinton medium consists of beef extract and acid hydrolysate of casein, which provide nitrogen, vitamins, carbon, and amino acids. Starch is added to absorb any toxic metabolites produced. Because of its composition and its use as half-concentrated solution, this medium is lower in glucose than the BHI-broth (Mueller and Hinton, 1941). The chemically defined medium
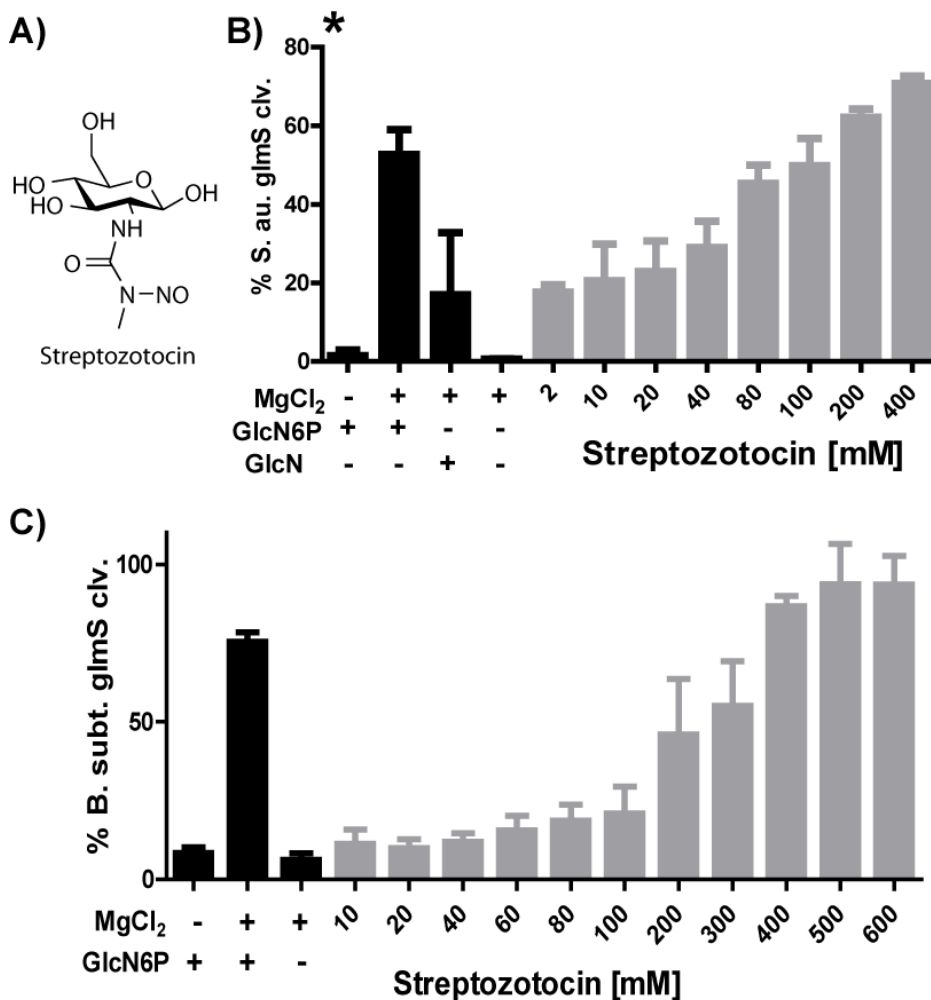
Figure 3.14: Activation of the glmS ribozyme by Streptozotocin. Studies of metabolite-induced self-cleavage by *S. aureus* (B) and *B. subtilis* (C) glmS ribozyme in the presence of controls GlcN and GlcN6P (black bars) as well as increasing concentrations of Streptozotocin (gray bars, 2-600 mM). Dose-response curves were used for EC$_{50}$-value determination as described before. *S. aureus* dose-response experiment marked with an asterisk was performed by Anna Schüller.

does not contain any glucose. Here, the bacteria use aminoacids as sole energy source.

In general, it can be observed that the richer the medium in aminosugar equivalents, like GlcN, the higher is the MIC (GlcN concentration in BHI $>0.5\times$MH $>2\times$CDM and according MICs are $18.75 > 9.4 > 0.29\,\mu$M, Table 3.6). This can be explained by the competition of (amino-) sugars with Streptozotocin for take-up by the same PTS transporters.

Strikingly, the vancomycin-resistant Mu50 strain has four fold lower MICs than the sensitive SG511 strain, which is known to be very susceptible to cell wall targeting antibiotics (e.g. in BHI $18.75\,\mu$M in Mu50 vs. $75\,\mu$M in SG511).

Medium	MIC Mu50 [µM]	Streptozotocin SG511 [µM]
BHI	18.75	75
0.5×MH	9.4	37.4
2×CDM	0.29	1.17

Table 3.6: Minimal inhibitory concentrations of Streptozotocin in different media in *S. aureus* Mu50 or SG511.

Figure 3.15:
**Growth of *S. au-*
reus Mu50 and
SG511 in the pres-
ence of increasing
Streptozotocin con-
centrations in BHI.**
Graphs show optical
density measured at
600 nm plotted against
the time. Bacterial
growth without Strep-
tozotocin added is
shown in magenta and
contamination controls
of BHI and Strepto-
zotocin solutions are
depicted in black and
gray.
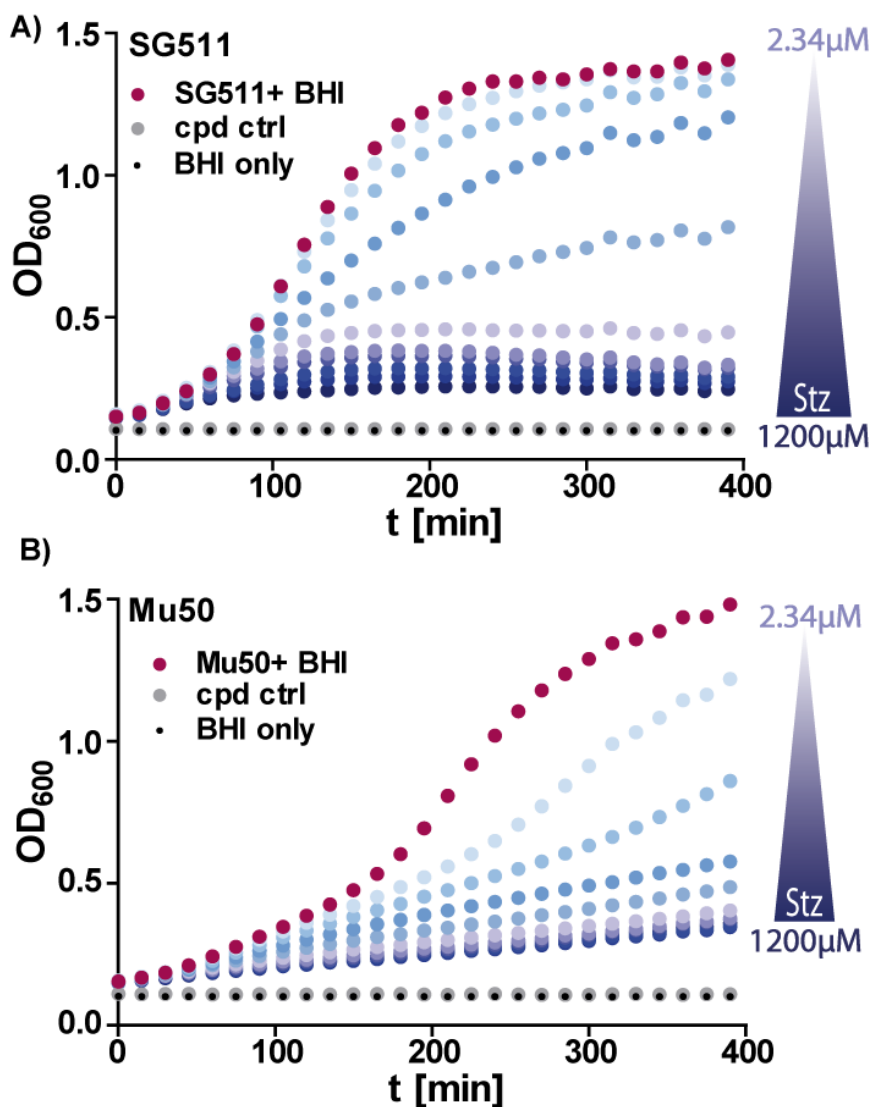
Measuring bacterial growth with increasing Streptozotocin concentrations revealed a strong inhibition at concentrations higher than 37.5 μM in the vancomycin-susceptible strain SG511 as well as the VISA strain Mu50 (Figure 3.15). In 0.5×MH or 2×CDM bacterial growth could be inhibited at even lower concentrations (Figure 8.12). However, with decreasing aminosugar concentrations in the medium, bacterial growth rates decrease as well. This is why, determinations of minimal inhibitory concentrations in 2×CDM were incubated for 48 h (Section 6.3.5 for experimental details).

3.2 The *thi*-box riboswitch as antibacterial drug target

Thi-box riboswitches are phylogenetically the most widely distributed (Rodionov et al., 2002), as they are found in all three domains of life (Miranda-Ríos et al., 2001; Sudarsan et al., 2003a; Kubodera et al., 2003). Therefore, they constitute a valuable target for the identification of novel antibacterial substances addressing a broad range of bacterial species.

So far, a pyrimidine analog of thiamine called pyrithiamine (PT, Figure 3.17 E) has been shown to bind to (Figure 1.11 D) and activate *thi*-box riboswitches in its phosphorylated form pyrithiamine pyrophosphate (PTPP, Sudarsan et al. (2005)). The phosphorylation of PT to PTPP is most likely accomplished with the help of thiamine pyrophosphorylase (thiK, Melnick et al. (2004)). This compound was synthesized and first described as means to study thiamine metabolism (Tracy and Elderfield, 1941), as it induces thiamine deficiency in mice and pigeons (Koedam et al., 1956). PT and PTPP are known to compete for thiamine and TPP binding sites on proteins (Woolley, 1951). Quickly after its discovery, PT was shown to be toxic in small doses to bacteria and fungi which need thiamine supplementation (Woolley and White, 1943; Robbins, 1941). At present, it is known that at least part of this antibacterial and antifungal activity is due to action on the riboswitch and interference with proper protein expression, because PT-resistant bacteria have mutations in their TPP riboswitch aptamer domain (Sudarsan et al., 2005).

3.2.1 Screening for thiM riboswitch activators

In order to screen for *thi*-box riboswitch activators, a reporter gene assay was designed, in which the thiM riboswitch from *E. coli* (Figure 3.16 A, Mayer et al. (2007)) was cloned into the 5´-UTR of the lacZ gene, coding for β-galactosidase (Figure 3.16 B, Simons et al. (1987)). Thiamine addition to the growth medium, leads to absorption and conversion to thiamine pyrophosphate (TPP). TPP binds to the aptamer domain of the thiM riboswitch, which induces a change in secondary structure that sequesters the Shine-Dalgarno sequence and subsequently downregulates reporter gene expression. The amount of β-galactosidase produced is measured by a colorimetric assay (see Section 6.3.7) in which the amount of cleaved O-nitrophenyl-β-galactopyranoside is detected by measuring absorption at 420 nm.

Two *E. coli* strains were transformed using the pRS414-thiM plasmid: the MG1655 strain, which is often referred to as the *E. coli* wild-type laboratory strain due to its few mutations (Table 7.5), and DH5αZ1 cells which are rendered dependent on thiamine uptake from the growth medium, because of the thi^{-1} mutation (Table 7.5). In these cells the amount of TPP is dependent on the amount of thiamine added to the growth medium. This enables direct external control of the availability of this vitamine. In MG1655 cells however, TPP amounts cannot be controlled from the outside, as these bacteria can synthesize it themselves from precursors.

Subsequent monitoring of β-galactosidase activity in the presence and absence of thiamine revealed a concentration dependent decrease in β-galactosidase expression with increasing amounts of thiamine (Figure 3.16 C & D, black curve). Evaluation of dose-response curves gave comparable IC$_{50}$-values for both strains in the nanomolar range (15 nM for DH5αZ1 and 21 nM for MG1655). For thiamine as well as pyrithiamine it is thought that they are likely to be taken-up and phosphorylated by the bacteria, hence probably act as TPP or PTPP on the riboswitch (Iwashima et al., 1976). However, both strains differ in the effect seen for pyrithiamine. Whereas this thiamine analog decreases reporter gene expression in MG1655 cells at concentrations above 50 µM, it does not show any influence on β-galactosidase expression in the thiamine dependent strain (Figure 3.16 C & D, gray curve).
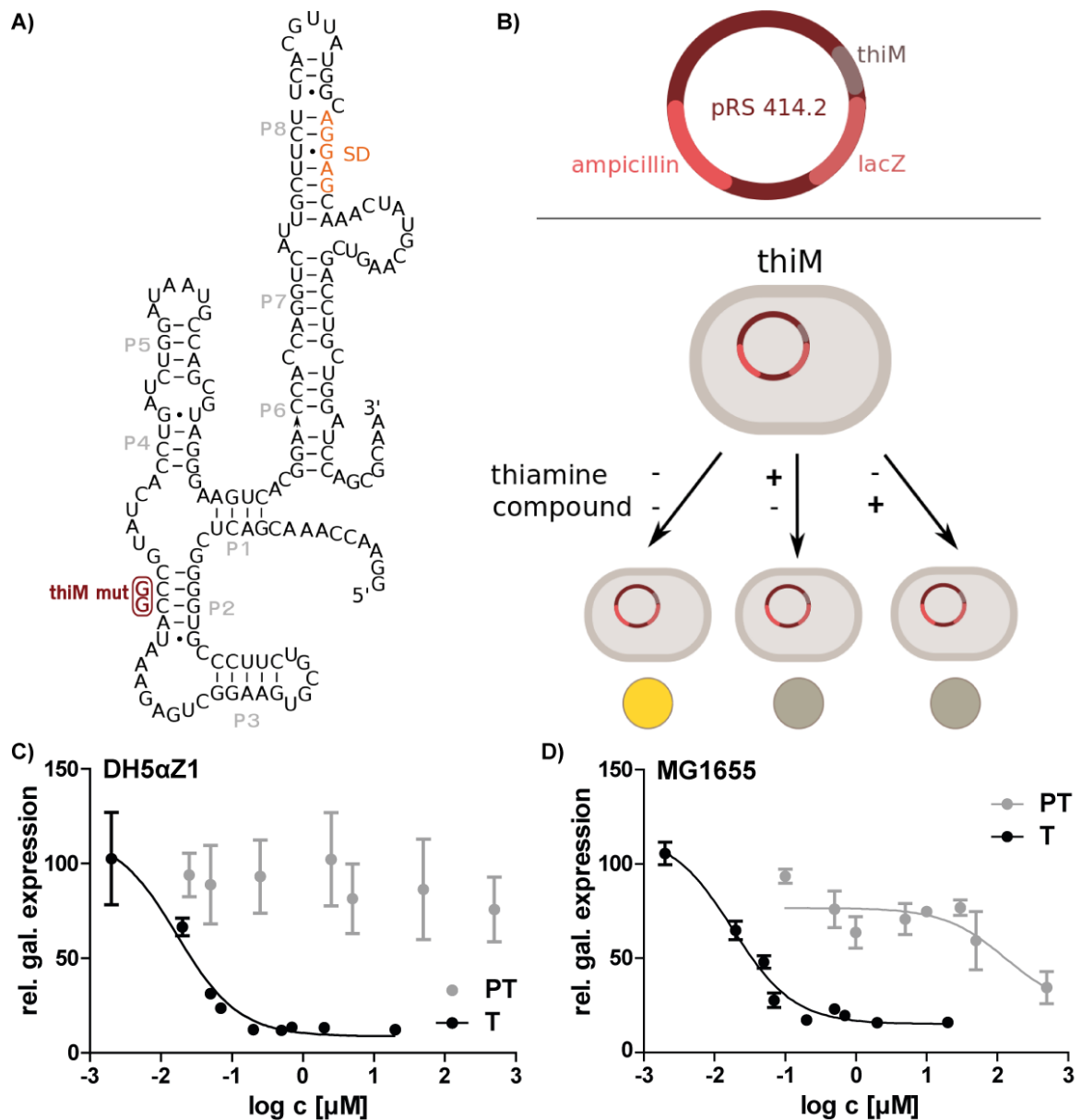
Figure 3.16: *In vivo* **screening system for thiM riboswitch activators.** Secondary structure prediction of *E. coli* thiM riboswitch (A). Shine-Dalgarno sequence is highlighted in orange and thiM mutation site is colored in red. Schematic representation of plasmid construct used for thiM riboswitch activator screening (B). pRS414 plasmid containing an ampicillin selection marker was used to construct a lacZ-fusion with the thiM riboswitch sequence. Transformed *E. coli* strains DH5αZ1 (C) and MG1655 (D), were utilized to report thiM riboswitch activation. TPP binds to and activates the thiM riboswitch, which results in a decrease in reporter gene expression measured by a colorimetric assay (6.3.7), whereas PT only decreases β-galactosidase expression in MG1655 cells.

3.2.2 Identification of triazolethiamine and close derivatives as new thiM riboswitch activators

The *thi*-box riboswitch has been shown to allow a greater degree of variation in its ligand interaction as exemplified by the TPP analog pyrithiamine (Thore et al., 2008). Therefore, thiamine analogs bearing a 1,2,3-triazole group instead of the thiazole heterocyclic moiety in thiamine were investigated for *in vivo thi*-box riboswitch activation using the aforementioned reporter gene assay (Section 3.2.1). Synthesis of these compounds was achieved using a "click" chemistry approach utilizing a common azide intermediate which was then reacted with the appropriate substituted alkyne (Figure 8.5). All triazolethiamine (TT) analogs, were synthesized by Colin Suckling's group (University of Strathclyde, Glasgow, UK, for detailed synthesis schemes refer to Scott (2012)).

Figure 3.17 A & B shows reporter gene activity in *E. coli* upon addition of thiamine, PT or the synthesized triazolethiamine compounds in relation to maximum β-galactosidase expression monitored without thiamine. These data indicate that TT (**10**) is able to repress reporter gene activity to about 5 % in the thiamine dependent strain or about 10 % in MG1655. As PT and TT-variants are likely to be phosphorylated *in vivo*, and thus activated to interact with the thiM riboswitch, they are capable of inducing the necessary conformational changes in the RNA to downregulate gene expression. In DH5αZ1 cells, triazolethiamine compound **11** reduces β-galactosidase expression to 40 %, compound **12** to 60 % and compound **13** to only about 80 % (Figure 3.17 A). Even though effects were pronounced in the wt *E. coli* strain, a reduction in reporter gene expression was observed for compounds **12** and **13** (Figure 3.17 B). Therefore, shortening (**11**) or elongating the alkyl side chain (**12** and **13**) results in a loss of activity. This is most likely due to reduced uptake and/or phosphorylation of these compounds *in vivo*. Interestingly, compound **14**, which bears an amino group instead of a hydroxyl residue on the ethyl-alkyl side chain of TT, also represses reporter gene activity to about 20 % (Figure 3.17 A) or 10 % (Figure 3.17 B). In order to efficiently activate the thiM riboswitch this compound would have to be phosphorylated, however by which biochemical pathways this is possibly achieved, remains to be elucidated. Compound **15** with its terminal carbonyl group reveals neither in *E. coli* wild-type MG1655 cells nor in the thiamine auxotrophic DH5αZ1 strain a strong thiM riboswitch activation. This compound was not further investigated, neither for concentration dependent effects in the reportger gene nor growth assay (for comparison of chemical formulas refer to Figure 3.17 E).

Except for the strikingly different effect of PT, the investigated compounds show similar tendencies of activating the riboswitch in both *E. coli* strains. However, in DH5αZ1 cells the compounds revealed a clear structure-activity relationship at concentrations of 500 µM (Figure 3.17 A), whereas in the strain MG1655 almost every compound was active with a slight decrease of activity when elongating the alkyl-side chain of TT (Figure 3.17 B). Generally, the triazolethiamine-analog-effect is always more pronounced for concentrations of 500 µM in *E. coli* MG1655 cells.

In order to evaluate whether the observed effects on β-galactosidase expression are solely due to activation of the riboswitch, a thiM riboswitch variant (thiM mut, Figure 3.16 A) was used. It has an alteration in its aptamer domain disrupting the P2 helix and has previously been described as rendering this riboswitch incapable of controlling β-galactosidase expression (Mayer et al., 2007). In both bacterial strains, thiamine and compound effects were abolished when the thiM mut construct is used in the reporter gene assay (Figure 3.17 C & D).
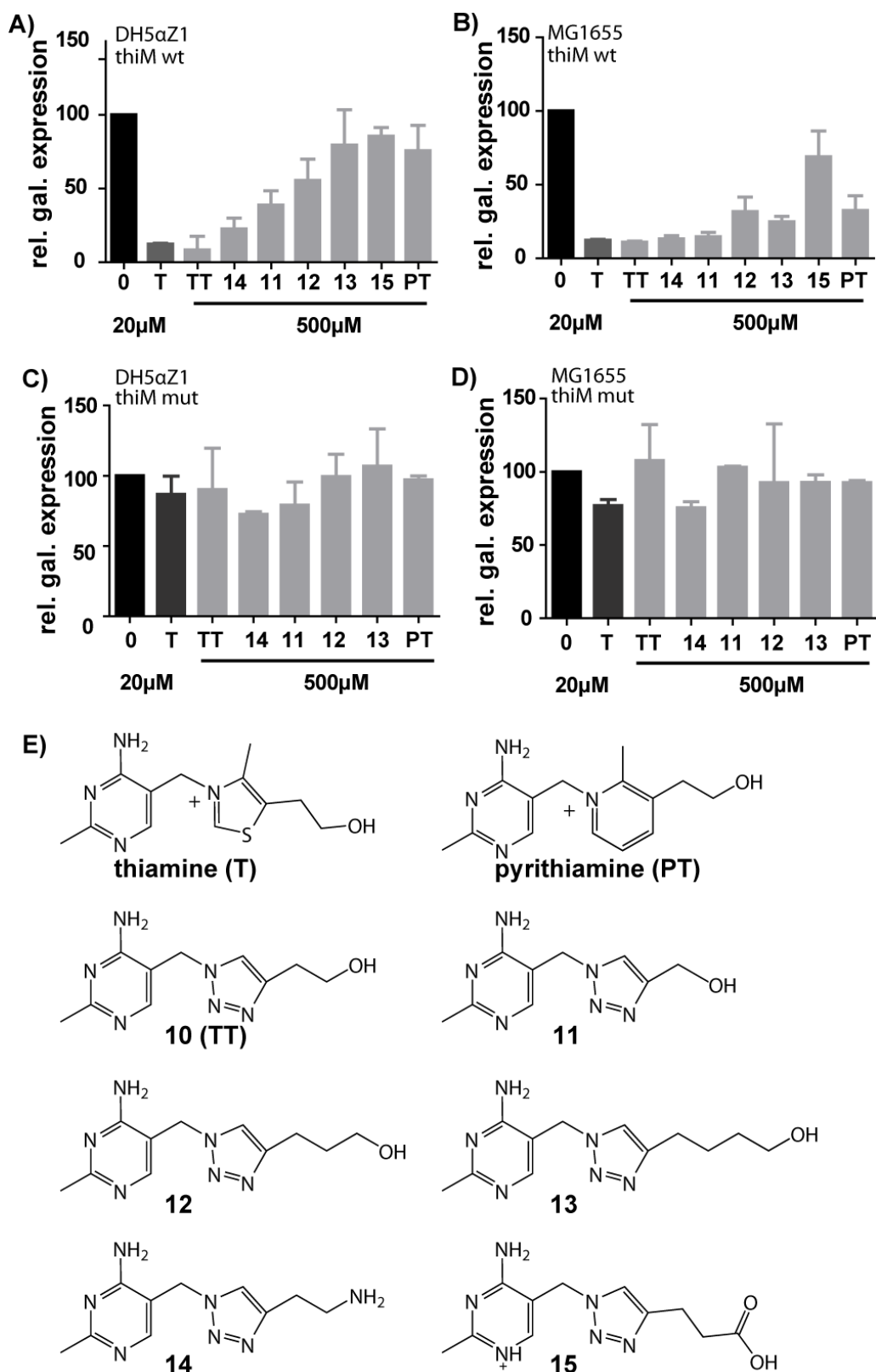
Figure 3.17: *In vivo* **screening of triazolethiamine analogs using a thiM riboswitch-dependent reporter gene assay.** β-galactosidase assay in DH5αZ1 (A) and MG1655 cells (B) in the presence of thiamine, PT or triazole compounds **10-15** shown as relative expression. C & D depict control assays using a reporter construct with a mutated thiM sequence. Chemical formulas for thiamine, pyrithiamine and triazole thiamine analogs (**10-15**) (E).

3.2.2.1 Concentration dependent influence of triazole-compounds on reporter gene expression in DH5αZ1 and MG1655

In support of the observed thiM riboswitch activation by TT compounds, IC$_{50}$-values were determined. All compounds (**10-14**) clearly indicated a concentration dependent repression of gene expression, however TT (**10**) revealed the strongest effect with an IC$_{50}$-value of 8.0 µM (Table 3.7) in DH5αZ1. For compounds with increasing alkyl-chain length (**12** and **13**) inhibition curves in DH5αZ1 cells did not reach maximum inhibition, hampering IC$_{50}$-value determination (Supplementary Figure 8.14). Where dose response fits were not applicable, the IC$_{50}$-value is above 500 µM. Also in wt *E. coli* only comparatively high IC$_{50}$-values were observed (213.5 µM for **12**, Table 3.7, Supplementary Figure 8.15). As expected, PT did not show any concentration dependent effect on β-galactosidase expression in DH5αZ1 cells, but in MG1655 cells repression of gene expression was detectable at concentrations above 100 µM (Table 3.7, Figure 3.17 B and C).

Compound	IC$_{50}$ [µM] DH5αZ1	IC$_{50}$ [µM] MG1655
thiamine	0.015 ± 0.001	0.021 ± 0.006
10 (TT)	8.01 ± 3.64	38.36 ± 4.7
11	38.95 ± 8.4	106.44 ± 23.98
12	n. a.	213.50 ± 2.69
13	n. a.	n. a.
14	73.59 ± 5.8	123.00 ± 28.99
PT	n. a.	n. a.

Table 3.7: IC$_{50}$-values for thiM riboswitch activating compounds 10-14. IC$_{50}$-values were calculated from dose-response curves of the inhibition of reporter gene expression in DH5αZ1 and MG1655 cells. Means and standard deviations of at least three independent experiments, measured in duplicates, are shown. n. a. = not applicable, TT = triazolethiamine, PT = pyrithiamine.

Furthermore, IC$_{50}$-values for TT compounds were found to differ 2-4 fold between both strains, which is likely to be caused by the differences in genetic background (Section 4.2.5). However, the relative order of half maximal inhibitory concentrations within the strains is the same (IC$_{50}$ thiamine < TT < **11** < **14** < **12**, Table 3.7).

3.2.2.2 Influence of TT compounds on bacterial growth in *E. coli* and *H. influenza* cells

The finding that triazolethiamine and some TT-based compounds activate the *thi*-box riboswitch and act as inhibitors of gene expression in *E. coli*, led to the investigation of their impact on bacterial growth (Figure 3.18).

Monitoring the ratio of bacterial growth in *E. coli* DH5αZ1 (growth in the presence of triazolethiamine derivative versus cell growth in the absence of compound) showed concentration dependent inhibition of bacterial growth by TT (Figure 3.18 A). It is noteworthy that this property was not seen for the shortened TT-variant **11** (Figure 3.18 B), even though this compound revealed moderate downregulation of reporter gene expression (Figure 3.17 A). In contrast, elongation of the alkyl-side chain renders **12** and **13** capable of interfering with bacterial growth. It is interesting that especially compound **13** whose activity in *thi*-box-dependent repression of gene expression was less prominent, still inhibits cell growth
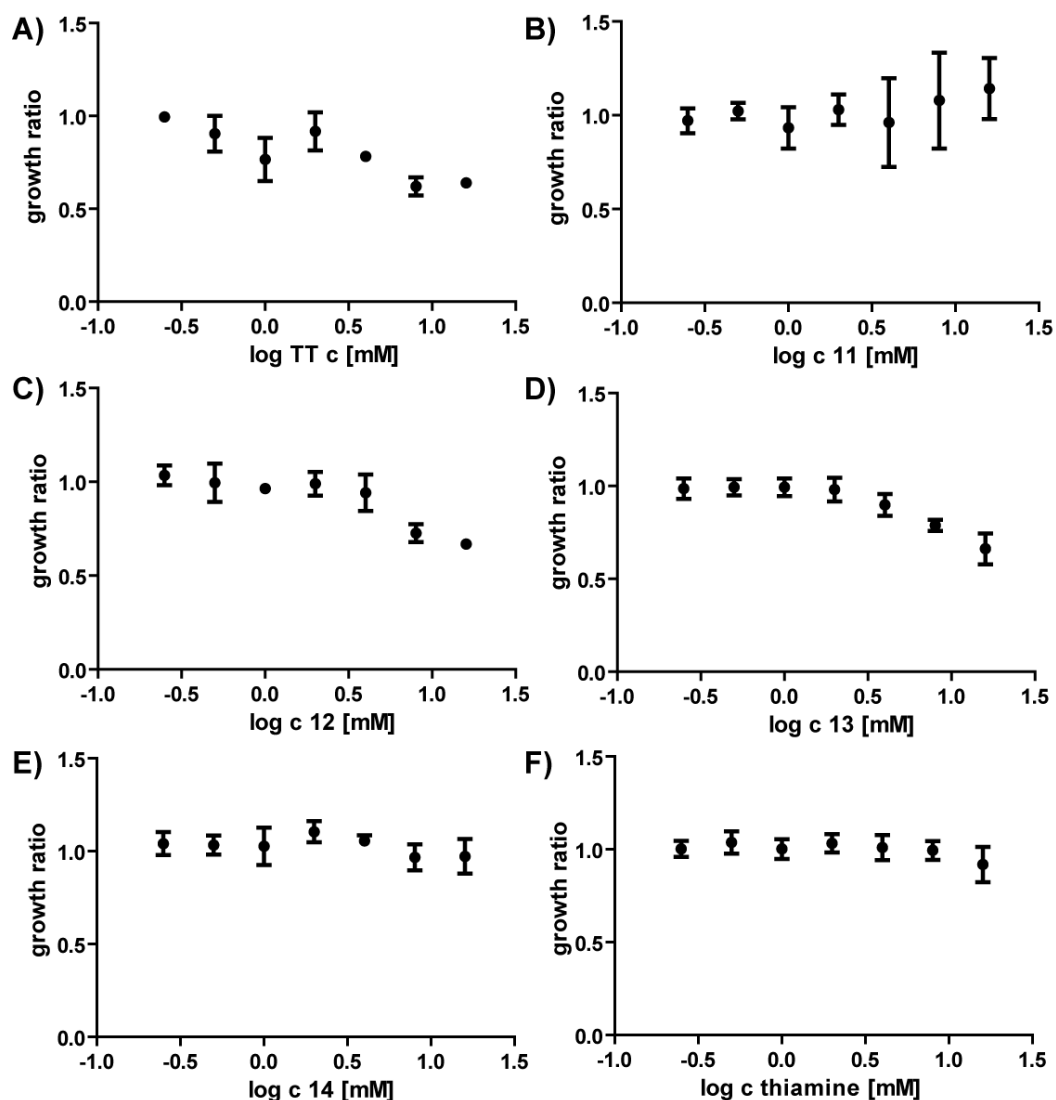
Figure 3.18: _E. coli_ DH5αZ1 growth in the presence of triazolethiamine compounds.
Bacterial growth is shown as ratio of growth in the presence of TT-compound versus growth
in the absence of any compound. Graphs A-E show assay results for indicated compound or
thiamine (F). Compound concentrations between $500\,\mu M$- $32\,mM$ at $495\,min$ are shown.

(Figure 3.18 C and D). The amine-compound (**14**) did not interfere with bacterial growth at
concentrations tested (Figure 3.18 E), which is surprising taking into account its strong effect
on riboswitch activation in the reportergene assay. Interestingly, the same effect was observed
for thiamine itself, which was expected to support growth in this thiamine auxotrophic strain
(Figure 3.18 F). However, it is possible that critical thiamine concentrations that would yield
to a concentration dependent growth are below the $500\,\mu M$ tested. _E. coli_ MG1655 cells
showed similar tendencies in triazole compound effects on bacterial growth, however they
were more subtle (Figure 8.13). This leads to the assumption that bacteria whose thiamine
biosynthesis is intact, somehow gain advantages in tolerating these thiamine analogs and
potentially even use parts of them as precursors for their own thiamine biosynthesis (Section
4.2.5).

PT did not show any effect on bacterial growth in DH5αZ1 cells (Figure 8.8), which is in line with its inability in activating the thiM riboswitch in the reporter gene assay (Figure 3.17). Most likely PT is degraded into thiamine precursors by a tenA activity (Sudarsan et al., 2005). However, in MG1655 cells, whose reporter gene expression could be downregulated by PT, this compound induces a decrease in bacterial growth (Figure 8.8).

Additionally, minimal inhibitory concentration determinations were conducted, that show a decrease in growth (displayed by smaller cell pellets) but no complete growth inhibition at concentrations up to 1 mM.

The Gram-negative bacterium *Haemophilus influenza* bears the thiM riboswitch upstream of an essential gene for thiamine biosynthesis. Thus, interfering with the riboswitch in regulating this gene, may cause severe effects on bacterial growth. Therefore, *H. influenza* was tested for TT-compound effects.

Normally, the fastidious *H. influenzae* are cultivated on bacitracin chocolate agar, made from red blood cells, which have been lysed by heating very slowly to 65 °C. Hence, it contains the required factor X (hemin) and factor V (NAD) for *Haemophilus* growth, but also undefined amounts of thiamine. The addition of bacitracin renders this medium selective for the *Haemophilus* genus (Kilian, 2001). It has been shown that *H. influenza*, whose shape ranges from cocobacilli to filamentous rods, grows better in humid atmosphere with added 5-10 % of CO_2 and temperatures between 33-37 °C (Kilian, 2001).

However, under minimal conditions the cultivation of these nonmotile, nonsporeforming, facultative anaerobes is rather demanding. No chemically defined media have been described before, that would allow sufficient testing in the presence of thiamine or TT-compounds under defined parameters. Similar to the chemically defined medium used for *Staphylococcus aureus* growth, a minimal *H. influenza* medium (CDM-HI) was created, which contains factor V and X, but no thiamine or glucose (Section 7). This allows the separate addition of the vitamin and sugar depending on the experimental set-up, i.e. vitamin deprived for TT-compound testing, sugar deprived for possible carba-sugar off-target tests.

However, growth tests in liquid culture were not successful. CDM-HI cultures containing glucose and thiamine, glucose but no thiamine, and neither glucose nor thiamine were inoculated with *Haemophilus influenzae* of an OD_{600} of 0.65 in a ratio of 1:100. Optical density was measured every day for a week, but did not indicate any growth. This could be due to the medium's nutrient content being insufficient or because cell growth is too slow to enable any OD_{600} detection after this incubation period. Yet, repetition of this set-up by inoculating the culture to a starting OD of 0.1 did not reveal any growth within seven days of monitoring either. This suggests that cultivation procedures are not yet optimal to support bacterial growth, either because essential components for *H. influenza* growth are absent from the minimal medium or that other conditions, such as incubation without shaking are deleterious.

As an alternative to cultivation in liquid culture, agar plates were prepared from CDM-HI containing glucose and thiamine, glucose but no thiamine, and neither glucose nor thiamine. After three days slight colony growth was visible on plates with glucose and thiamine. Minimal growth was also detected on the other plates on day five. Since this strain is not thiamine auxotrophic, it can compensate for the lack of thiamine in its surroundings by producing this vitamine from precursors. This may explain bacterial growth in CDM-HI without thiamine and also that growth takes longer (colonies appear only after five days). In order to verify

that the colonies are indeed *Haemophilus influenza* cells, single colonies were picked and restreaked on bacitracin chocolate agar. Subsequent tests of these cultures by Gram staining and microscopy as well as metabolic tests (see Section 6.3.4) confirmed them as *H. influenza*.

Since *Haemophilus influenza* growth was proven to occur under these conditions, agar diffusion tests were performed (see Section 6.3.3.3 for experimental details) using 128 mM or 12.8 mM of either TT, compound **14**, or thiamine on CDM-HI agar with glucose but without thiamine. Additionally, cells were also streaked on a plate with CDM-HI with glucose and with thiamine. After three days, very faint *H. influenza* growth was observed, however addition of thiamine or compound did not result in any quantifyable inhibition, even after incubation for up to 14 days. This could be due to uncertain stabilities of the compounds or any components in the growth agar.

3.2.2.3 Isolation thiamine derivatives from cell extract and tracing by HILIC/MS

TT activates the thiM riboswitch in a concentration dependent manner. However, it has been shown that the pyrimidine as well as the pyrophosphate helix of the aptamer domain need to be brought together by ligand binding to activate the riboswitch (Rentmeister et al., 2007). Therefore, it is likely that the TT compounds, like PT, are phosphorylated *in vivo*. To prove this, the isolation and detection of phosphorylated triazole thiamine from bacterial cell extracts was attempted using hydrophilic interaction liquid chromatography (HILIC) followed by mass spectrometry (MS). HILIC allows the separation of polar and hydrophilic compounds like amino acids, peptides, carbohydrates, plant extracts and various other polar compounds that usually have little or no retention in reverse phase liquid chromatography (RPLC) (Grumbach and Iraneta, 2004).

To analyze TT phosphorylation by HILIC/MS, bacterial cultures were grown in the presence or absence of thiamine or triazolethiamine and harvested after 24 h. After cell lysis, the lysate was cleared of proteins and nucleic acids by precipitation. The amount of thiamine species (thiamine, thiamine monophosphate (TMP) and thiamine pyrophosphate) was estimated by the thiochrome method (see Section 6.3.8 and 6.3.9 for experimental details).

All HILIC and HILIC/MS analysis were performed by Dr. Giorgia Greco in collaboration with Dr. Thomas Letzel from the Competence Pool Weihenstephan at the Technical University Munich.

First of all it had to be ensured that different thiamine species can be separated and detected by this method. Therefore, thiamine (T), TMP and TPP were analyzed separately (Figure 8.16) and as a mixture (Figure 8.17). To achieve this, standard solutions of thiamine and its derivatives were analyzed using a ZIC-HILIC column (see Section 6.3.10 for a detailed listing of the methods 6.19). The ZIC-HILIC stationary phase is attached to porous silica and is made of sulfobetaine, which has two permanently charged groups (Jandera, 2011). The separation of analytes is based on polar differences and is achieved by a hydrophilic partitioning mechanism superimposed on weak electrostatic interactions (Grumbach and Iraneta, 2004). The retention increases with polarity and hydrophobicity of the analyte. Hence, increasing the water content in the mobile phase will increase the affinity of the compound for the mobile phase as well, thus eluting the compound (Grumbach and Iraneta, 2004). Compounds like thiamine and TPP are more soluble in water due to their charges. All thiamine variants were detected individually, but also successfully separated and detected, when a compound mixture was used. Moreover, this experiment allowed an estimate on the expected retention times for thiamine (and variants) to be investigated in cleared cell lysates.

Sample number	Culture volume	500 µM T in o/n incubation	added to cell lysate	added post isolation	T detected	TPP detected
1	8 ml	-	-	-	-	-
2	8 ml	-	10 µM T	-	-	-
3	8 ml	-	100 µM T	-	+	-
4	8 ml	-	-	10 µM T	+	-
5	8 ml	-	-	100 µM T	+	-
6	8 ml	-	10 µM TPP	-	-	-
7	8 ml	-	100 µM TPP	-	-	+
8	8 ml	-	-	10 µM TPP	-	+
9	8 ml	-	-	100 µM TPP	-	+
10	8 ml	+	-	-	-	-
11	8 ml	+	10 µM T	-	-	-
12	8 ml	+	100 µM T	-	+	-
13	8 ml	+	-	10 µM T	+	-
14	8 ml	+	-	100 µM T	+	-
15	8 ml	+	10 µM TPP	-	-	-
16	8 ml	+	100 µM TPP	-	-	+
17	8 ml	+	-	10 µM TPP	-	+
18	8 ml	+	-	100 µM TPP	-	+
19	32 ml	-	-	-	n. a.	n. a.
20	32 ml	-	10 µM T	-	n. a.	n. a.
21	32 ml	-	100 µM T	-	n. a.	n. a.
22	32 ml	-	-	10 µM T	n. a.	n. a.
23	32 ml	-	-	100 µM T	n. a.	-
24	32 ml	-	10 µM TPP	-	n. a.	n. a.
25	32 ml	-	100 µM TPP	-	n. a.	n. a.
26	32 ml	-	-	10 µM TPP	n. a.	n. a.
27	32 ml	-	-	100 µM TPP	n. a.	+
28	32 ml	+	-	-	n. a.	-
29	32 ml	+	10 µM T	-	n. a.	n. a.
30	32 ml	+	100 µM T	-	n. a.	n. a.
31	32 ml	+	-	10 µM T	n. a.	n. a.
32	32 ml	+	-	100 µM T	n. a.	n. a.
33	32 ml	+	10 µM TPP	-	n. a.	n. a.
34	32 ml	+	100 µM TPP	-	n. a.	n. a.
35	32 ml	+	-	10 µM TPP	n. a.	n. a.
36	32 ml	+	-	100 µM TPP	n. a.	n. a.
37	80 ml	-	-	-	n. a.	+
38	80 ml	-	10 µM T	-	n. a.	n. a.
39	80 ml	-	100 µM T	-	n. a.	n. a.
40	80 ml	-	-	10 µM T	n. a.	n. a.
41	80 ml	-	-	100 µM T	n. a.	n. a.
42	80 ml	-	10 µM TPP	-	n. a.	+
43	80 ml	-	100 µM TPP	-	n. a.	+
44	80 ml	-	-	10 µM TPP	n. a.	n. a.
45	80 ml	-	-	100 µM TPP	n. a.	n. a.
46	80 ml	+	-	-	n. a.	+
47	80 ml	+	10 µM T	-	n. a.	n. a.
48	80 ml	+	100 µM T	-	n. a.	n. a.
49	80 ml	+	-	10 µM T	n. a.	n. a.
50	80 ml	+	-	100 µM T	n. a.	n. a.
51	80 ml	+	10 µM TPP	-	n. a.	n. a.
52	80 ml	+	100 µM TPP	-	n. a.	+
53	80 ml	+	-	10 µM TPP	n. a.	n. a.
54	80 ml	+	-	100 µM TPP	n. a.	+

Table 3.8: Cell extracts investigated by HILIC measurements and T or TPP detection results. n. a.= not applicable, where matrix background was too high for accurate detections.
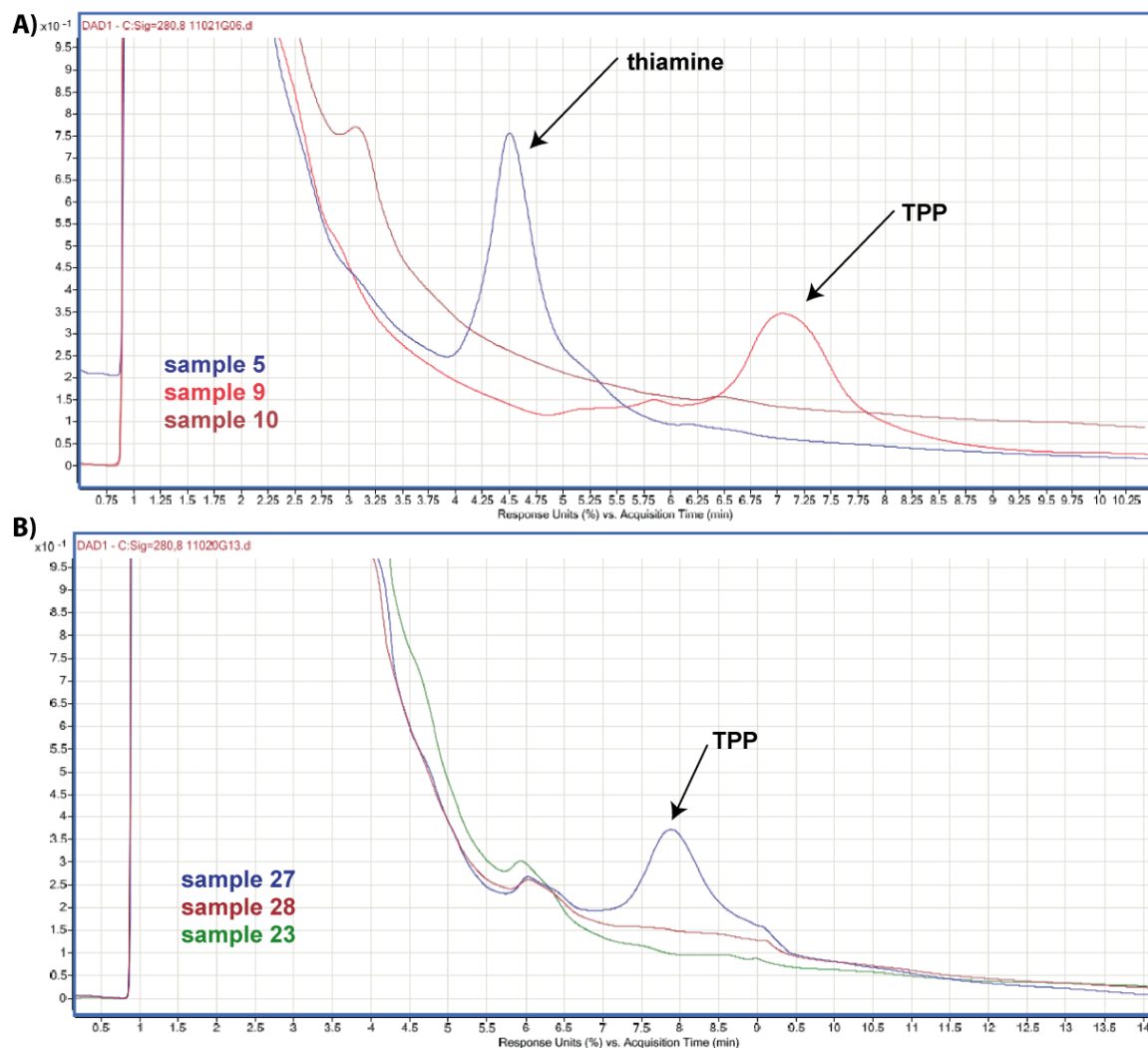
Figure 3.19: HILIC of 8 and 32 ml cultures. Detection of T and TPP in samples 5, 9 and 10 (8 ml culture volume, A) as well as samples 23, 27 and 28 (32 ml culture volume, B) using the UV-detector at 280 nm.

In order to identify optimal conditions for efficient detection of phosphorylated triazole compounds in cleared cell lysates, culturing and isolation procedures were optimized using thiamine. Not only different culture volumes, but also incubation of cells in the presence or absence of 500 μM thiamine were examined (Table 3.8). Additionally, cell lysates from these samples were supplemented to concentrations of 10 or 100 μM thiamine or TPP at two different points in the procedure: 1. immediately after cell lysis and 2. after the entire isolation protocol (Table 3.8 shows the array of samples analyzed).

In all 8 ml isolations, background matrix was so little that HILIC separation and MS detection was possible (Figure 3.19 A). Interestingly, T or TPP were only detected when spiked with 100 μM after cell lysis, or at least 10 μM after the isolation procedure (Figure 3.19 and Table 3.8). Thus, natural levels of thiamine conversion to TPP by mere addition
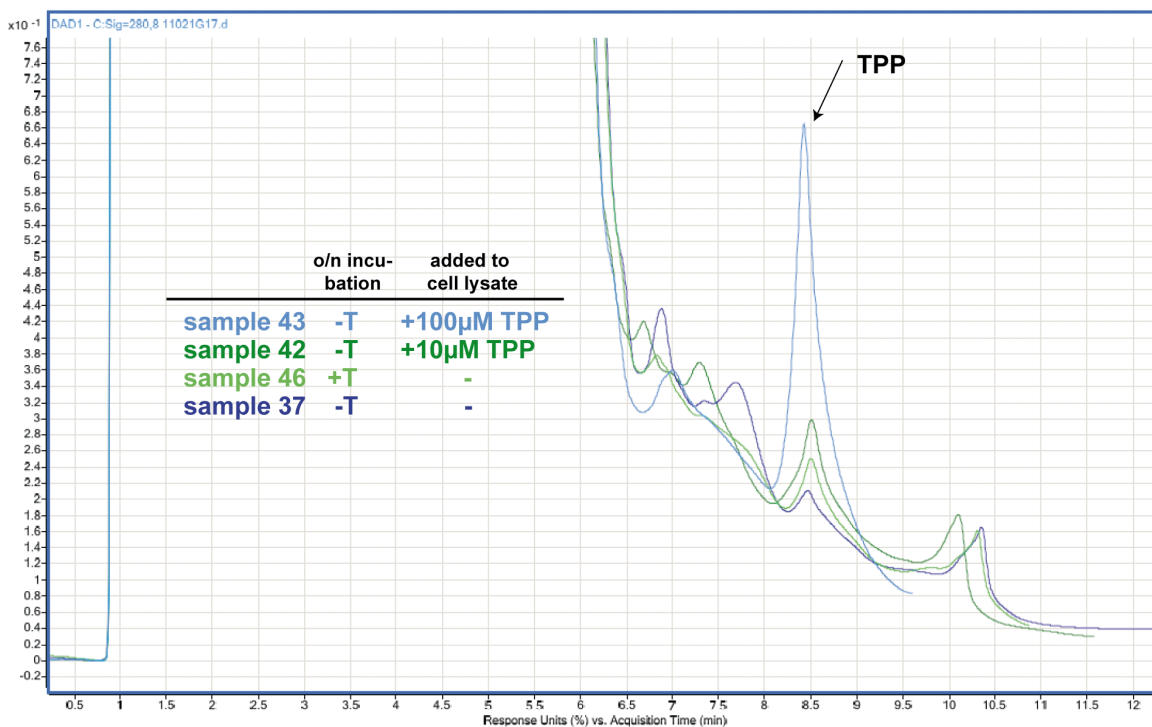
Figure 3.20: HILIC of 32 and 80 ml culture extracts. Detection of T and TPP in samples 37, 42, 43 and 46 using the UV-detector at 280 nm.

of thiamine to the culture medium were not detectable at this culture volume and by this detection method. Moreover, the fact that supplementation to 10 µM T or TPP to the cell lysate did not result in the detection of either substance later, implies the losses occuring during lysate clearance and the isolation protocol.

It would be interesting to estimate how much the difference is in T or TPP detected in sample 2 and 3 (or 6 and 7) as well as sample 2 and 11 or 3 and 12 (Table 3.8). Even though the comparison of normalized areas under the curve can only be considered a rough estimate of compound amounts present (personal communication Greco), such an analysis was undertaken for samples 52 and 54 (Figure 8.19) as well as 37 and 46 . These isolations are result of 80 ml cultures which in general showed higher matrix background that rendered the detection of thiamine impossible, as its peak is hidden in the matrix peak (Figure 3.20, Table 3.8 samples 37-54). Sample 37, which results from an incubation in the absence of thiamine and does not contain any supplementations added during the work-up procedure, contains 6 fold less TPP than sample 46, which only differs by its incubation in the presence of 500 µM thiamine over night (Figure 3.20). This indicates that the detection of naturally synthesized TPP from absorbed T is possible, when higher culture volumes are used for the isolation of thiamine derivatives (Table 3.8). However, this method detected only half the amount of TPP in a sample that was spiked with 100 µM TPP after the isolation protocol (sample 54) in comparison to a sample, to which TPP was added already to the cell lysate (sample 52, Supplementary Figure 8.19).

Matrix effects for samples 37-54 are very high and likely to interfere with the elution of TPP, which sometimes results in a double peak (personal communication Greco, Figure 8.20).

Comparing the double peaks of Figure 8.20 with the standards analyzed earlier, it also seems plausible that the double peak is due to degradation of added TPP to TMP (Figure 8.17), however this has to be investigated further.

Since HILIC analysis is very sensitive to pH, buffer conditions and salt concentrations, assay parameters were further optimized to contain as little additional ions as possible (refer to final isolation protocol Section 6.3.8 for exact conditions). Additionally, the chromatographic conditions were changed to be less retentive for ionic compounds, because so far thiamine and TPP were separated well, however the triazole compounds to be finally analyzed are
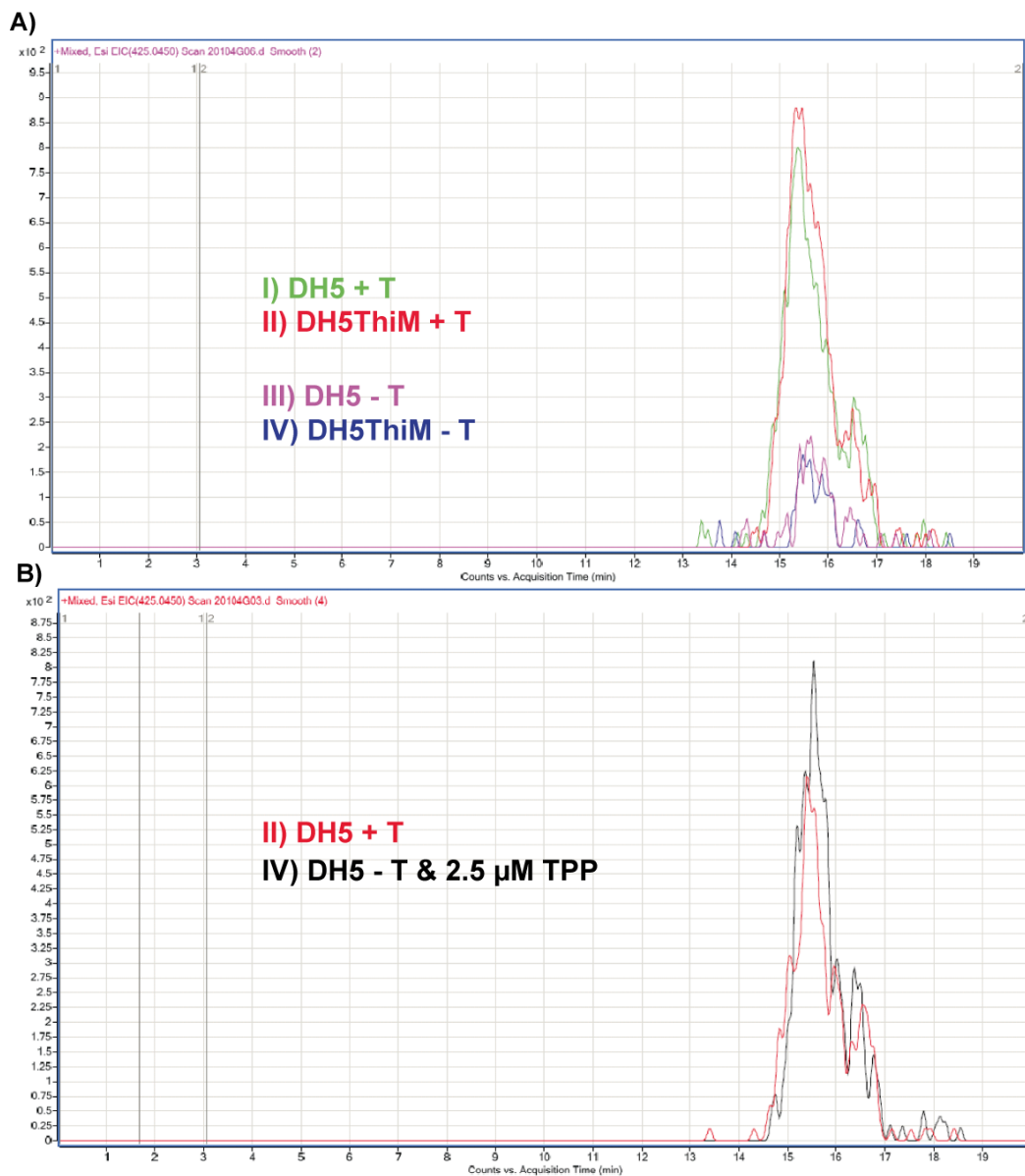
Figure 3.21: HILIC of low salt DH5αZ1 cell extracts. Analysis of DH5αZ1 cell with and without the pRS414 plasmid incubated in the presence and absence of thiamine (A). Estimation of TPP amounts in sample II by spiking sample IV with 2.5 µM TPP (B).

non-ionic (Greco, personal communication). Therefore, a YMC-Pack colum was used which has a diolic stationary phase with which retention depends on compound polarity (see Section 6.3.10 for a detailed listing of the methods 6.19). Accordingly, TPP is the most polar due to its charge (thiazole ring and pyrophosphate group), T is more polar than TT, because it is charged and therefore TT is eluted first. These alterations resulted in successful detection of low amounts of TPP in cells grown in the absence of thiamine (III and IV, refer to Figure 3.21 A) and a strong TPP-signal for cells incubated with thiamine over night (I and II, Figure 3.21 A). This indicates that even low TPP levels can be seen that most likely represent that portion of the vitamine previously engaged in its natural cofactor functions. Interestingly, no traces of thiamine were found (Figure 8.18), which could be due to the fact that thiamine is mostly converted to its phosphorylated forms intracellularly. To further prove that samples do not contain thiamine, sample B was spiked with different thiamine concentrations and thiamine could be detected easily at concentrations as low as 1 µM. Moreover, these spiking experiments allowed to check if thiamine ionization was affected by the matrix, which was not the case (Greco, personal communication). Moreover, no differences between sample III & IV and sample I & II were detected (Figure 3.21 A), indicating that the presence of the pRS414-thiM plasmid does not effect thiamine take-up or conversion to TPP. Assuming that sample IV and II have the same matrix, and further assuming that sample IV does not contain any TPP, then about 2.5 µM TPP is present in sample II (Figure 3.21 B).

After this optimization of assay, isolation and separation methods, the detection of *in vivo* phosphorylated triazolethiamine (TT) was attempted. Figure 3.22 shows the total ion current of a TT standard solution, detected in positive (red) and negative (blue) mode. In case of thiamine the positive mode was much more sensitive, because thiamine is already a positive ion and does not require addition of H^+. Rather than acquiring a H^+, TT loses one, so that the $[M-H]^-$ species is more easily detected (Greco, personal communication). No TT was detected in samples which had been incubated in the presence of 500 µM compound. However, analysis of DH5αZ1 cells incubated in the presence of 500 µM thiamine revealed TPP to be present, but no traces of thiamine were found, as observed in previous experiments (Figure 3.19). Taken together the hypothesis of intracellularly phosphorylated TTPP remains to be proven (Section 4.2.5 and 5.2).
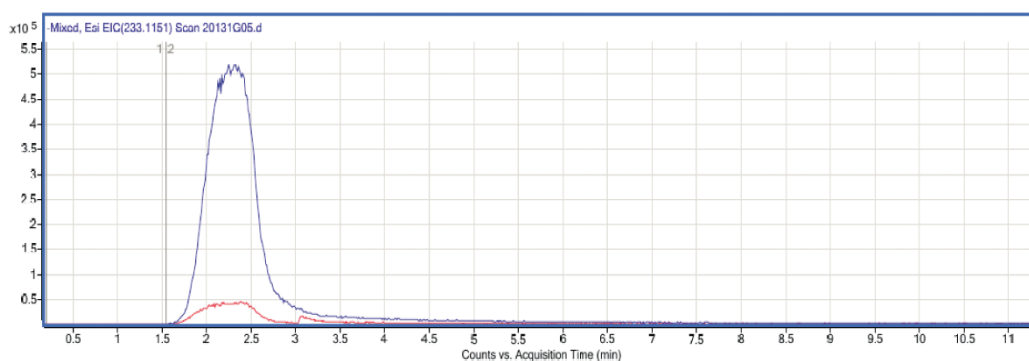
Figure 3.22: Ion chromatogram of triazolethiamine. Traces show TT (21 µM) detected in positive (red) and negative (blue) mode.

3.2.3 Investigation of triazole thiamine derivatives containing metal chelating groups as thiM riboswitch activators

In order to activate the thiM riboswitch, the recognition of two moieties by the aptamer domain is essential (Section 1.3.2). These are the pyrimidine moiety of TPP, which is recognized by the pyrimidine sensor helix, and the phosphate moiety recognized by the pyrophosphate sensor helix together with two Mg^{2+} ions and their coordinated water molecules (Edwards and Ferré-D'Amaré, 2006; Rentmeister et al., 2007). The TT compounds investigated in 3.2.2 contain the pyrimidine moieties and are thought to be pyrophosphorylated by the bacteria to receive the pyrophosphate group. In this section, the screening system introduced in 3.2.2 was used to investigate thiM riboswitch activation by TT compounds with alkyl-chain extensions capable of chelating up to two divalent metal ions. Therefore, these compounds do not rely on *in vivo* phosphorylation, because metal chelating groups are intended to mimic phosphate moieties. These compounds were divided into four different groups according to their structural similarity (Figures 3.23-3.26).

The first set of compounds comprise sulfones (**16**), sulfonamides (**17,18**), amide-linked pyruvate, malonate and salicylic acid moieties (**19-21**), a nitroalkene (**22**) and one compound that lacks a triazole ring and only contains a trimethoxybenzylmoiety linked by an amide bond to the pyrimidine ring that is common to all derivatives (Figure 3.23 A). These structures were investigated for thiM riboswitch activation in *E. coli* DH5αZ1 and MG1655 (Figure 3.23 B, C).

Generally, as observed in the previous screening (Section 3.2.2), compounds induce stronger β-galactosidase repression in MG1655 at 500 µM compared to the thiamine auxotrophic strain. In DH5αZ1, all compounds except **22** and **20** showed about 50 % reduction in reporter gene expression (Figure 3.23 B). However, in MG1655 the sulfone **16** leads to the strongest decrease in reporter gene expression (to about 10 %), closely followed by **18** (20 % reporter gene expression, Figure 3.23 C). The benzenesulfonamide **17** reveals only about 30 % reduction, possibly due to the bulky benzyl-ring (Figure 3.23 C). As these compounds all contain two S=O groups, they are most likely able to coordinate one metal ion. Similarly, the C=O groups in **19-21** can coordinate metal ions, however the pyruvate, malonate and salicylic acid moieties are the least active in the array of compounds tested. In addition, a relation between activity and bulkiness of the substitution can be supposed, as illustrated by the difference in reporter gene expression by **17** and **18** (Figure 3.23 A, C). However, the concentration dependent influence of these compounds will have to be investigated, so that IC$_{50}$-values can be used to relate differences in compound structure to differing thiM riboswitch activation. Interestingly, only for **17** and **21** β-galactosidase expression is comparable between the two *E. coli* strains (Figure 3.23 B, C). Compared to the reporter gene repression by **16**, the nitroalkene **22** shows a strong thiM riboswitch activation in MG1655 cells (Figure 3.23 C). Since the nitrogroup confers significant electron density, this moiety potentially interacts with a positively charged, divalent Mg^{2+} ion. Additionally, the difference in effect of compound **22** between MG1655 and DH5αZ1 is striking, and future experiments will have to reveal what causes this difference (Section 5.2).

Compound **23** is an exception to this group as it does not contain any ring structure in its center, but merely a planar amide bond (Figure 3.23 A). The oxygen of the methoxy groups imparts potential coordinating capability. The lack of a middle heterocyclic ring structure may not cause severe losses in binding affinity as it has been shown in *thi*-box riboswitch crystals to have only long distance electrostatic interactions with the RNA (Edwards and Ferré-D'Amaré,
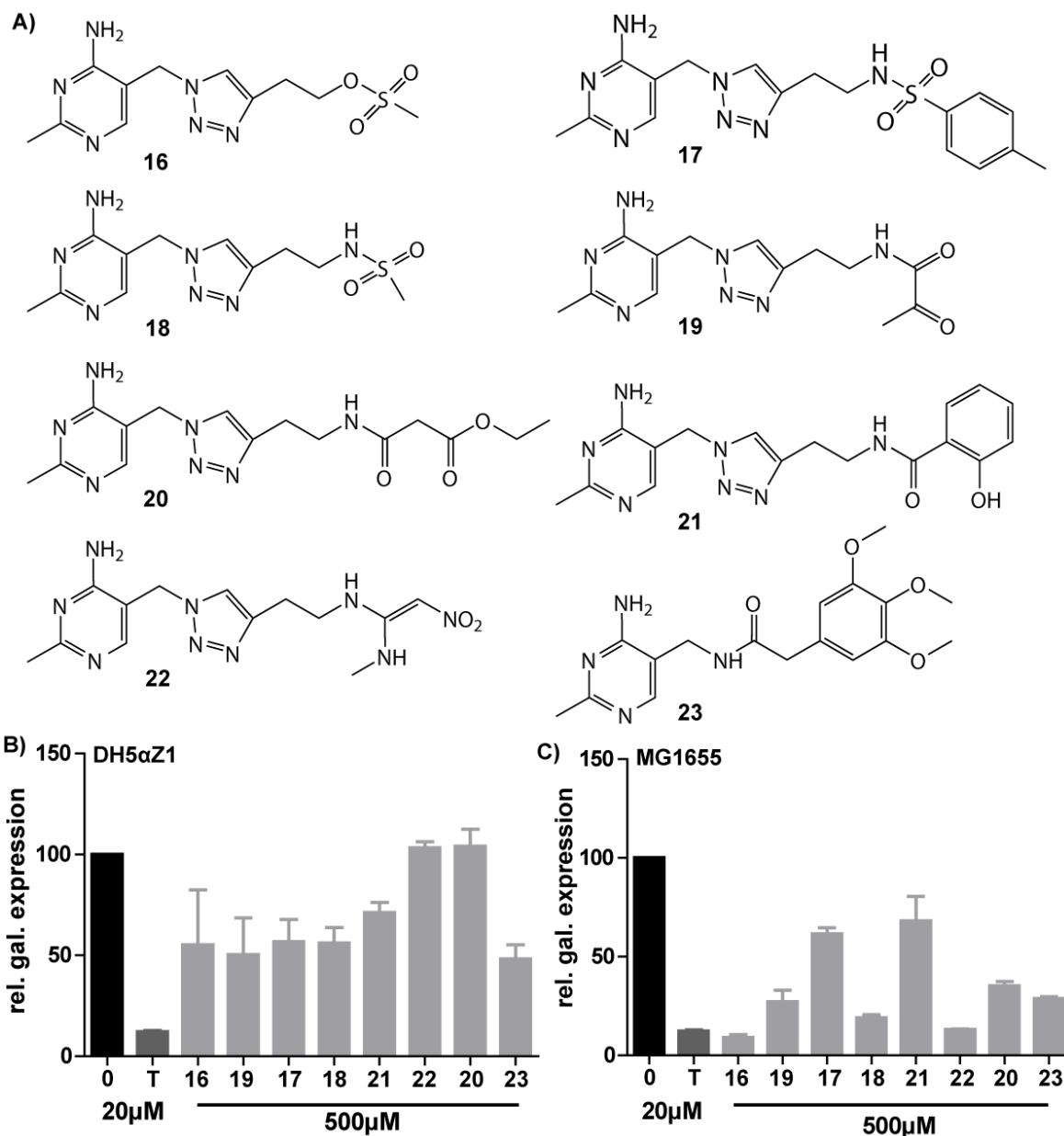
Figure 3.23: *In vivo* **screening of compound group I.** Chemical formulas of compounds **16** to **23** (A). ThiM riboswitch-dependent reporter gene expression in DH5αZ1 and MG1655 in the presence of thiamine analogs belonging to the compound group I (B).

2006; Thore et al., 2006). Compound **23** reduces thiM-dependent β-galactosidase expression to about 50 % in DH5αZ1 and to about 30 % in MG1655 (Figure 3.23 B, C).

The second group of triazolethiamine derivatives comprises sulfonamide (**24**) and the sulfone (**25**) connected to a benzyl group (Figure 3.24 A). These compounds only scarcely activate the thiM riboswitch in DH5αZ1 cells, especially the sulfonamide does not induce much reporter gene repression (Figure 3.24 B). In MG1655 cells, the effects are somewhat more pronounced, however reporter gene expression is only downregulated to about 50 % (Figure 3.24 C). Compound **17** which is fairly similar in structure, had a similar effect on
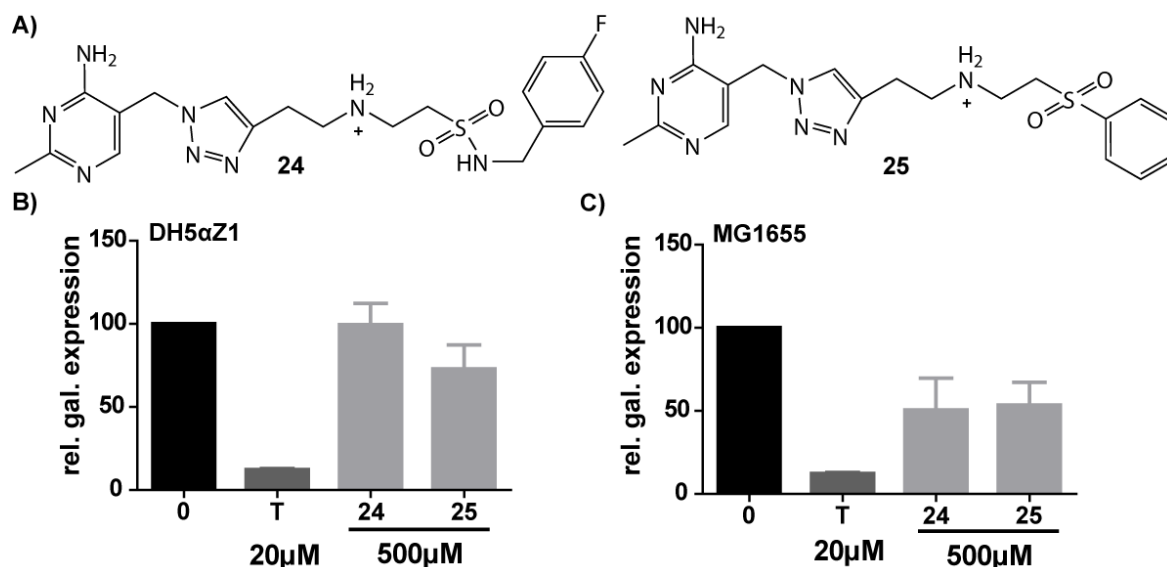
Figure 3.24: *In vivo* **screening of compound group II.** Chemical formulas of compounds **24** and **25** (A). ThiM riboswitch-dependent reporter gene expression in DH5αZ1 and MG1655 in the presence of thiamine analogs belonging to the compound group II (B).

thiM mediated reporter gene expression. Here again, it is conspicuous that compounds containing the planar benzol ring are not as active in thiM riboswitch activation, even though it is imaginable that this aromatic ring could tighten compound-riboswitch interaction by π-π-stacking with RNA nucleobases (Edwards and Ferré-D'Amaré, 2006; Thore et al., 2006).

The third group of triazolethiamine compounds are methotrexat- or folate-like (Figure 3.25 A). The carboxylate-ethyl-esters **26** are probably hydrolyzed by esterases when this compound is admitted into the cells resulting in **27**, which was also tested individually. Both compounds show significant reporter gene repression to less than 40 % in thiamine auxotrophic cells (Figure 3.25 B). In MG1655 cells, reporter gene expression is reduced to about 25 % (Figure 3.25 C). Reporter gene repression of **27** is slightly less prominent, which may be due to the fact that it is likely to be taken-up less efficiently due to its carboxy-moieties. As the assay is carried out over a time course of 24 hours in aqueous solutions, the hydrolyzation of esters is favored. This may explain the merely faint difference in reporter gene expression between compound **26** and **27**. Compounds of this group have enough flexibility to theoretically interact with two metal ions via the ester or carboxyl groups (personal communication Fraser Scott). Interestingly, these molecules activate the thiM riboswitch extensively, despite their relatively large size.

Finally, a fourth group of compounds was investigated, which is characterized by phosphonate groups (Figure 3.26 A). The carboxylate-ethyl-ester (**28**) is more likely to passively diffuse into the cells than compound **29** bearing the carboxyl-group. Phosphonate moieties are effective chelating agents and theoretically, should be able to coordinate two Mg^{2+}-ions. Interestingly, both substances show only slight thiM activation, which reaches even in MG1655 cells only 50 %. Maybe these compounds are not well absorbed by bacteria, or possibly the chelating effect the phosphonate group does not sufficiently mimic characteristics successfully employed by the naturally occuring pyrophosphate group.
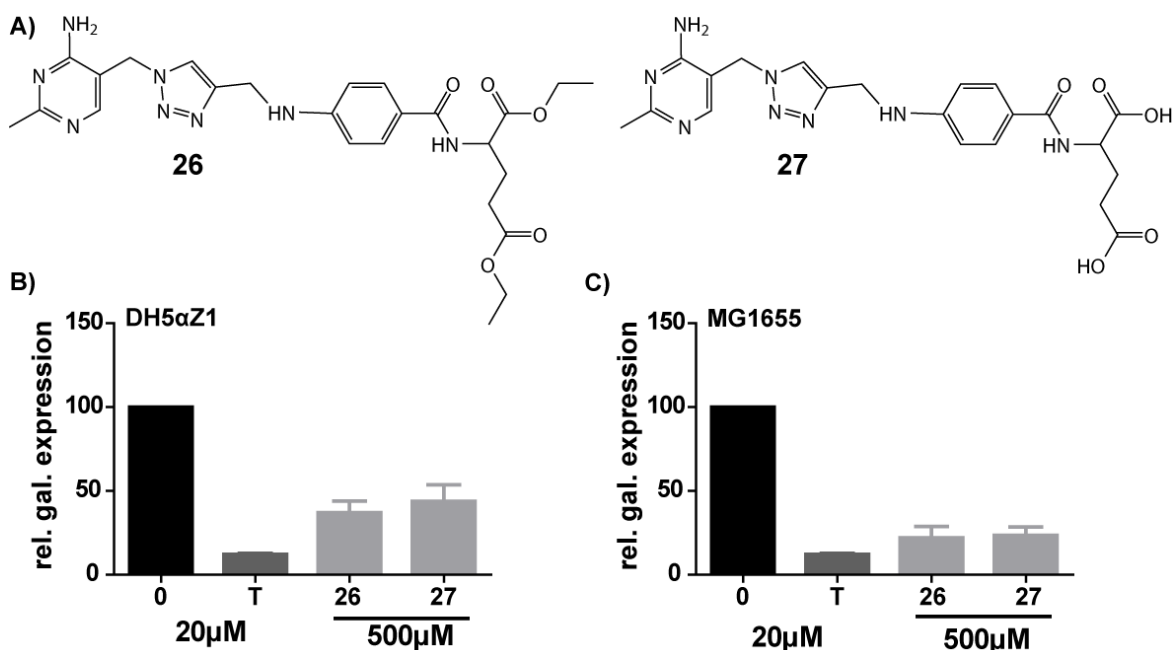
Figure 3.25: *In vivo* **screening of compound group III.** Chemical formulas of compounds **26** and **27** (A). ThiM riboswitch-dependent reporter gene expression in DH5αZ1 and MG1655 in the presence of thiamine analogs belonging to the compound group III (B).
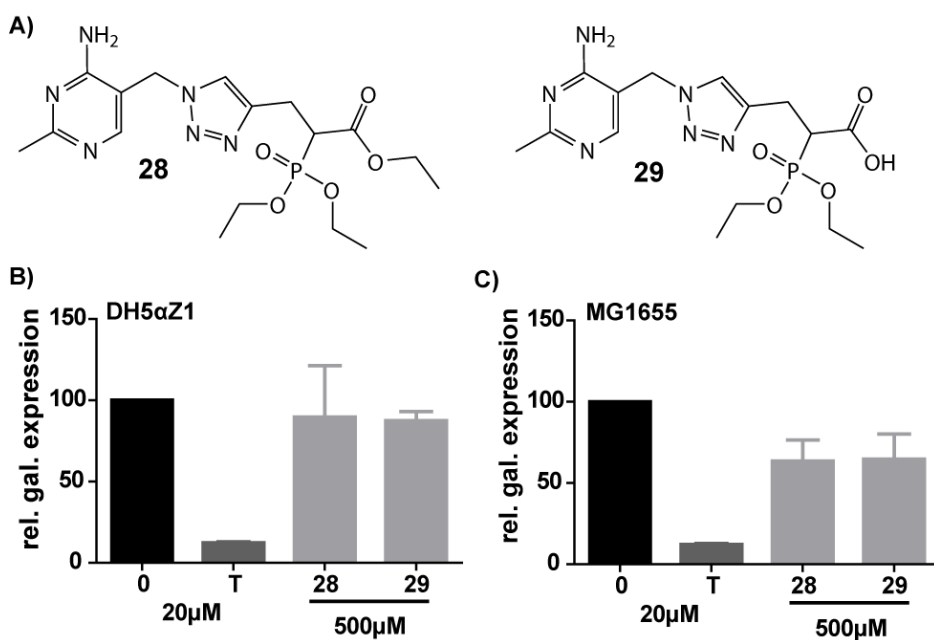
Figure 3.26: *In vivo* **screening of compound group IV.** Chemical formulas of compounds **28** and **29** (A). ThiM riboswitch-dependent reporter gene expression in DH5αZ1 and MG1655 in the presence of thiamine analogs belonging to the compound group IV (B).

In general, several compounds containing metal chelating moieties were identified that activate the thiM riboswitch in both bacterial strains and lead to a decrease in reporter gene expression of at least 50 %. These include compounds **16**, **18**, **19**, **23** as well as **26-29**, which should be further investigated, i. e. by determining IC_{50}-values from concentration dependent compound effects on riboswitch mediated gene expression (Section 4.2.6 and Section 5.2).

3.3 Screening set-up for identifying preQ$_1$ riboswitch modulators

Having employed the *in vivo* screening approach quite successfully for the identification of *thi*-box riboswitches, an analogous set-up was utilized to obtain a screening system for compounds that affect gene expression by the *Staphylococcus aureus* preQ$_1$ riboswitch. This class of riboswitches was first described in 2007 by Roth et al. in *Bacillus subtilis* (Section 3.3.1) and predicted to be present in at least 24 other bacterial species, among them also *S. aureus* (Supplementary material of Roth et al. (2007)). Hence, the aptamer domain or the entire intergenic region was cloned upstream of the lacZ gene to construct a preQ$_1$-dependent reporter gene assay, which is eventually to be used to screen a small library of preQ-analogs provided by Colin Sucklings group at the University of Strathclyde, Glasgow, UK.

3.3.1 PreQ riboswitch

The preQ riboswitch binds the queuosine precursor preQ$_1$ and contains the smallest aptamer domain known to date. Only 34 nt are necessary to recognize the ligand and discriminate it from preQ$_0$ with a five fold difference in affinity (Roth et al., 2007). The preQ$_1$ ligand forms hydrogen bonds that would be eliminated when its methylamine moiety is replaced by the cyano moiety of preQ$_0$ (compare structures in Figure 3.28). Two different aptamer classes, differing in structure, have been identified to recognize preQ$_1$ (Roth and Breaker, 2009; Meyer et al., 2008). The preQ$_1$-I class is more widely distributed as it was identified in firmicutes,
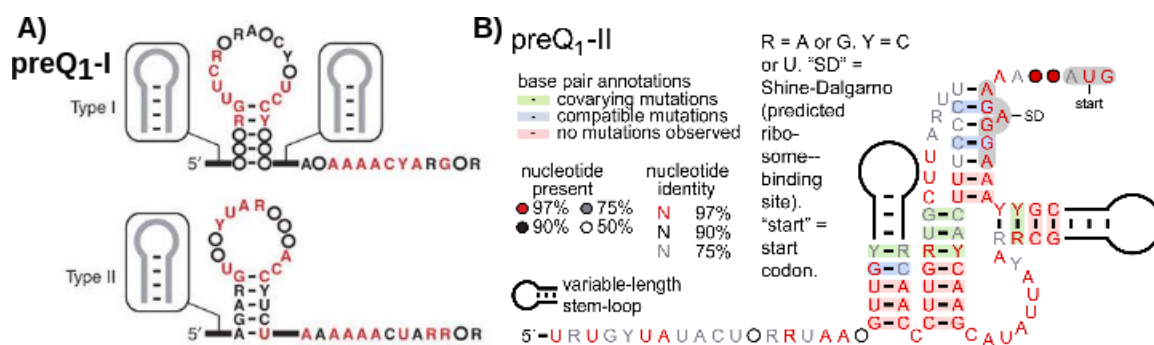
Figure 3.27: PreQ$_1$ riboswitch classes. Secondary structure consensus models of preQ$_1$ riboswitch classes I (A) and II (B). PreQ$_1$-I riboswitch class is taken from Roth et al. in 2007. Nucleotides in red and black are more than 95 % and 80 % conserved. Less conserved regions, which may vary slightly in the number of nucleotides, are represented by circles or heavy lines. Locations of less conserved, putative stem elements are indicated in gray (Roth et al., 2007). Conservation details for preQ$_1$-II riboswitch class are shown as inset in (B), which is taken from Meyer et al. 2008.

fusobacteria, and proteobacteria (Barrick and Breaker, 2007). It consists of a stem-loop and a short, adenosine-rich tail sequence. In-line probing analysis of wild-type and mutant $preQ_1$ riboswitches indicate that the specific $preQ_1$ contacts are made by a canonical Watson-Crick base pairing interaction with the ligand. The $preQ_1$-II class representatives are more confined in their distribution to the family of streptococcaceae. $PreQ_1$-II riboswitches adopt a pseudoknot structure and do not seem to bind their ligand by Watson-Crick interactions.

Both riboswitch classes regulate gene expression either by inhibition of translation initation or formation of a terminator stem loop structure that leads to premature transcription termination.

The aptamer domain folds into an H-type pseudoknot conformation where L1 and L3 are positioned in the major and minor grooves of co-axially stacked stems P2 and P1 (Kang et al., 2009; Spitale et al., 2009; Klein et al., 2009; Jenkins et al., 2011). $PreQ_1$ is almost completely encapsulated in the ligand-binding pocket by intercalating between the two helices where it forms a Watson-Crick base pair with C17. This helps to maintain continuous stacking of the two stems. Other parts of the molecule are specifically recognized by base and backbone residues within the aptamer structure (Klein et al., 2009). These interactions are facilitated by Ca^{2+} cations (Zhang et al., 2011).

3.3.1.1 PreQ biosynthesis and tRNA hypermodification

Prequeuosine (preQ) is a precursor of queuosine (Q), which is a hypermodified nucleoside found in most bacteria at the wobble position of GUN anticodons in tRNAs for tyrosine, asparagine, aspartate and histine (Harada, 1972). This queuosine modification is important for translational fidelity (Bienz, 1981; Meier, 1985). The biosynthesis of Q starts with GTP and proceeds through the intermediate $preQ_0$ (7-cyano-7-deazaguanine) and $preQ_1$ (7-aminomethyl-7-deazaguanine) by a series of reactions involving QueC and QueF (Iwata-Reuyl, 2003). In eubacteria, $preQ_1$ is then transferred to the appropriate tRNAs by a tRNA-guanine transglycosylase (TGT, Okada et al. (1979)), where it is further modified *in situ* by QueA to yield Q (Reuter et al., 1991) or its aminoacylated derivative (Roth et al., 2007; Salazar et al., 2004; Blaise et al., 2004).
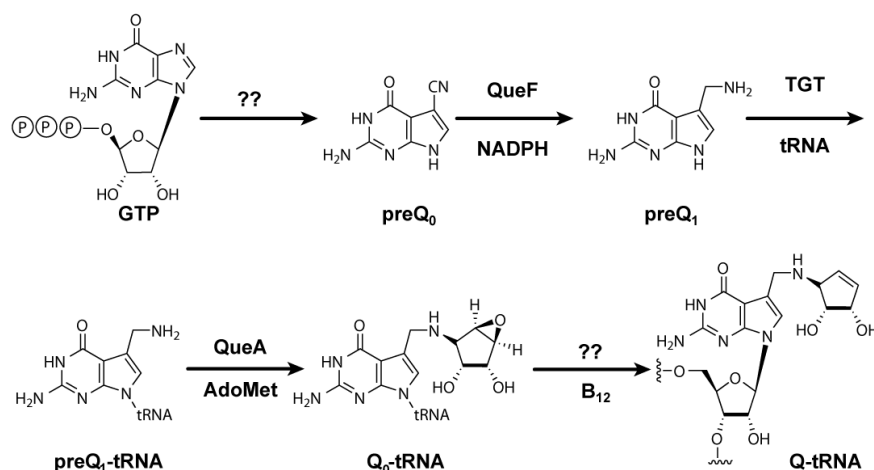
Figure 3.28: Schematic representation of the queuosine biosythesis pathway in bacteria. For detailed description refer to main text.

3.3.2 PreQ riboswitch reporter gene assay

Before initiating the actual screening, the reporter system was constructed. For this, the already mentioned pRS414 vector was used (Simons et al., 1987), and either the aptamer domain of the riboswitch or the entire intergenic region (IGR) located upstream of the *queEDC* operon was cloned in front of the lacZ reporter.

The secondary structure of the preQ$_1$ riboswitch of *Staphylococcus aureus* (Figure 3.29 A) consists of a 70 nt aptamer domain (blue), which forms two hairpin loops and a pseudoknot, and an expression domain (red) that inhabits a terminator stem (nucleotides 71-113). Upon preQ$_1$ binding (Figure 3.29 B), the terminator structure is formed. Consequently, the RNA polymerase halts and eventually falls off, thus downregulating transcription and reporter gene expression.
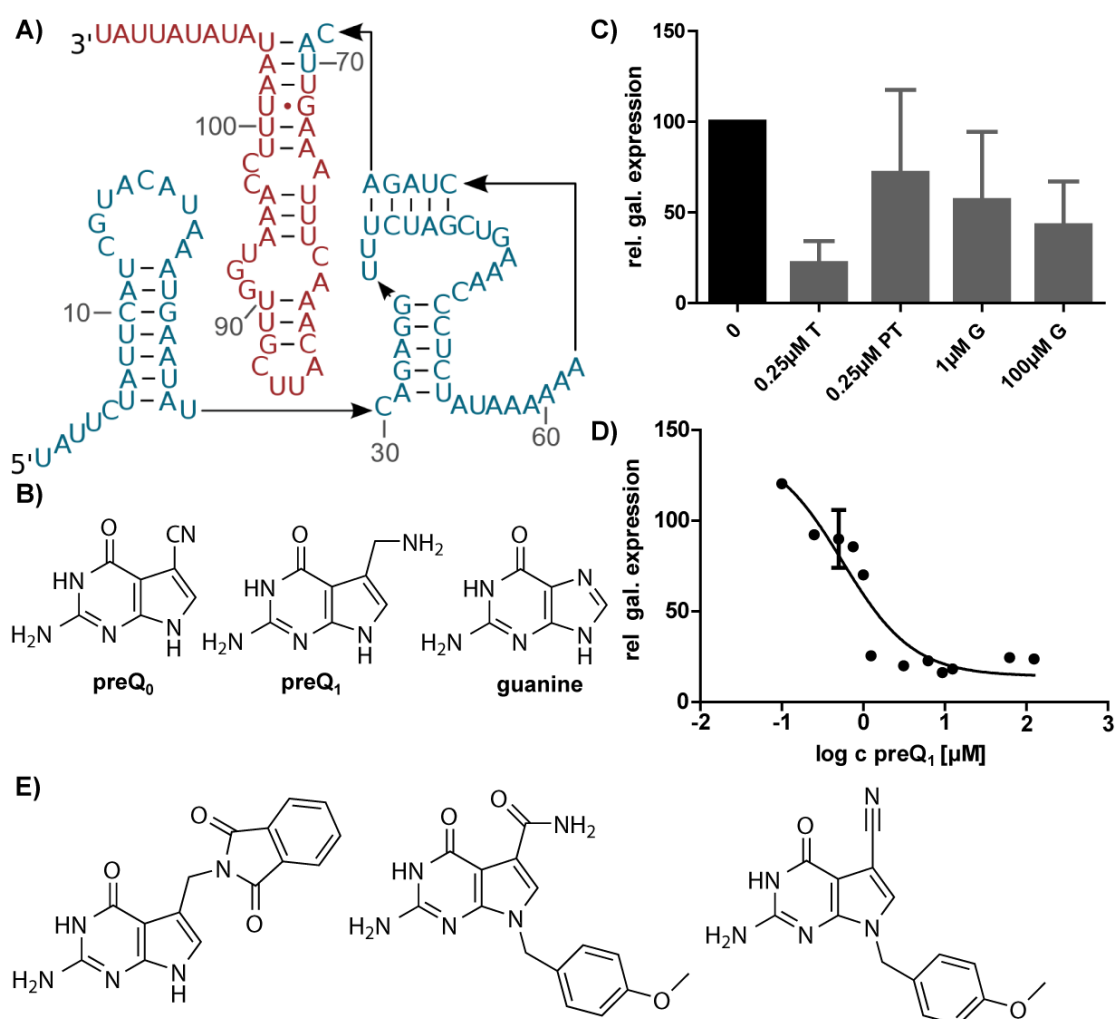
Figure 3.29: PreQ$_1$ riboswitch screening set-up. Secondary structure of *S. aureus* preQ$_1$ riboswitch illustrating the aptamer (blue) and expression platform (red, A). PreQ$_1$ and preQ$_0$ structures are shown in B. β-galactosidase assay of thiamine, guanine and the thiamine analogs triazolethiamine and pyrithiamine (C). Concentration dependent inhibition of reporter gene expression of *S. aureus* preQ$_1$ riboswitch (D). Examples of preQ$_1$ and preQ$_0$ analogs to be investigated for riboswitch modulation (E).

For want of prequeuosine, the influence of thiamine, guanine, and pyrithiamine on β-galactosidase expression was investigated using the aforementioned assay system (Figure 3.29 C). Guanine is known to be recognized by the preQ$_1$ riboswitch at elevated concentrations, whereas thiamine and PT do not share structural features with prequeuosine and were therefore used as negative controls. Unexpectedly, the addition of thiamine led to a downregulation of β-galactosidase expression (Figure 3.29 C). However, examining the metabolic network of *E. coli*, this effect could be caused by a cross-talk of the thiamine and guanine biosynthesis pathways. Pre-queuosine$_1$ is made from GTP, hence increasing the amount of precursors for GTP synthesis (like AIR or guanine), will lead to the production of more preQ$_1$. This may be the reason for the effects produced by thiamine, as it is converted via common precursors (AIR, Figure 3.28 and 1.12) into guanine or preQ$_1$, which could act on the riboswitch-mediated gene expression.

Guanine shows reporter gene downregulation at concentrations of up to 100 µM (Figure 3.29 B). Even though a similar biosynthetic cross-talk as for thiamine can be inferred for guanine leading to an increase in preQ$_1$ concentration, it is also possible that guanine itself causes the effective downregulation of β-galactosidase expression by binding to the riboswitch. Chemical features that distinguish preQ$_1$ from guanine, the aminomethyl group and carbon atom substitution at the 7 position, are molecular recognition determinants (Figure 3.29 B, Roth et al. (2007)). For *B. subtilis* preQ$_1$, a K$_d$ of about 20 nM was demonstrated by equilibrium dialysis (Roth et al., 2007) and is thereby only about 25-fold greater than for guanine (Roth et al., 2007). In this respect, 100 µM may seem quite high for demonstrating first effects, however it has to be pointed out, that guanine which is only barely soluble in aqueous solutions, was not used in these assays as a dilution in organic solvents such as DMSO. Hence, it is possible that the active concentration lies below the ones stated here.

Using 0.25 µM of the thiamine analog PT revealed a decrease of reporter gene expression to about 80 % (Figure 3.29 C). DH5αZ1 cells used for this experiment have been proven to be PT-insensitive before (Section 3.2.2.1). This resistance against PT is possibly due to the tenA gene, which codes for a thiaminase. This enzyme may accept PT as substrate and detoxify it directly by hydrolysis, hence contributing HMP to the salvage pathway for thiamine biosynthesis (Sudarsan et al., 2005). This in turn frees precursors for guanine and GTP biosynthesis, whose elevated concentrations may influence the reporter gene expression indirectly.

Finally, pre-queuosine$_1$ was tested and revealed reporter gene repression in a concentration dependent manner (Figure 3.29 D). This dose-response curve was fitted to obtain an IC$_{50}$-value of 0.56 µM. The preQ$_1$ was provided as trifluoroacetic acid (TFA) salt making it highly soluble in water. This assay system is now to be used for the *in vivo* screening of preQ analogs (Figure 3.29 E).

4 Discussion

In this study, riboswitches were investigated for their potential as new antibacterial targets. Two riboswitch representatives were used for the identification of new riboswitch modulating entities, namely the thiM riboswitch of *E. coli* and the glmS ribozyme of *S. aureus*. Riboswitch-targeting compounds were sought through screening *in silico* predicted, and rationally designed artifical compounds as well as classes of naturally occuring prospective riboswitch activators.

These attempts led to the identification of carba-sugars as novel activators of the glmS ribozyme, which were thoroughly characterized *in vitro* and were found to induce bacterial growth inhibition at a minimal inhibitory concentration of 625 µM. Furthermore, the natural nitrosourea analog of glucosamine, Streptozotocin, was identified as glmS ribozyme activator at millimolar concentrations *in vitro* and the investigation of aminoglycosides revealed Neomycin, Tobramycin, Paromomycin and Sisomycin as the most potent inhibitors of glmS ribozyme cleavage among the aminosugars tested. Triazolethiamine and its derivatives were identified as novel thiM riboswitch activators *in vivo*. They mimic the natural ligand TPP with their aminopyrimidine moiety and by either containing metal chelating groups imitating the pyrophosphate group or by being phosphorylated intracellulary by bacterial enzymes. The *in vivo* screening system for riboswitch modulators can be easily adapted to other riboswitch classes as shown for the preQ$_1$ riboswitch.

4.1 The glmS riboswitch of *S. aureus* Mu50

For the screening of potential natural as well as artifical ribowitch activators, the glmS ribozyme from *S. aureus* strain Mu50 was used, due to its clinical relevance for drug targeting. The predicted RNA sequence from Barrick et al. showed enzymatic activity dependent on the presence of GlcN6P and Mg^{2+}-ions *in vitro* (Section 3.1.1). The high structural conservation and wide phylogenetic distribution, which hypothesize glmS ribozymes in at least 463 Gram-positive and a few Gram-negative organisms (McCown et al., 2011), make an *in vivo* relevance of this ribozyme, as shown for *B. subtilis*, very likely (Collins et al., 2007). So far, there is only one other publication where the glmS ribozyme from *S. aureus* was used for a HTS set-up (*S. aureus* subsp. *aureus* Rosenbach, ATCC 35556, a methicillin-sensitive strain, Blount et al. (2006)). However, this study also focused on *in vitro* assays, presenting no *in vivo* proof of ribozyme activity. Nevertheless, definite proof of glmS ribozyme dependent GLMS expression in *S. aureus* remains to be given. Therefore, a reporter gene fusion would have to be designed, as has been done previously (Winkler et al., 2004; Collins et al., 2007) to prove *in vivo* use of this ribozyme-related regulatory mechanism.

It was suggested that the glmS mRNA might persist for extended periods of time in the cell without undergoing significant ribozyme cleavage, and then respond rapidly to rising concentrations of GlcN6P (Winkler et al., 2004). The *in vitro* characterization of the *S. aureus* glmS ribozyme revealed that it responds instantaneously to the addition of GlcN6P (Figure 3.8). This indicates that the RNA serves as a rapid switch that can form its active structure without the need for a forceful denaturation and annealing step (Lünse et al., 2011).

In *B. subtilis*, cobalt was shown to be able to substitute for magnesium and support RNA cleavage (Winkler et al., 2004). However, this was not the case for *S. aureus* glmS ribozyme. It is known that the specificity of a metal-ion binding pocket can result from a variety of factors, including the hardness of an ion, the identity of the coordinating ligands, the ionic radius, the preferred coordination geometry of the ion, and the metal's hydration number (Feig, 1999). Comparing these characteristics of divalent cobalt and magnesium ions demonstrates that they are quite similar (e. g. oxidation state: 2^+, hydration number: 6, ionic radius 0.75 vs. 0.72, etc., see Feig et al page 290f for extended list of metal ions and their properties). So why are cobalt ions not capable of replacing magnesium in the *S. aureus* ribozyme? One explanation could be given by the observation that larger RNAs tend to be more specific for certain metals than smaller ribozyme species. This is probably due to the more complicated overall fold, which creates greater opportunities for specific interactions and more tertiary contacts that must be maintained by these ions (Feig, 1999). Therefore, it should be investigated whether the elongated P1 stem of the staphylococcal glmS ribozyme (50 nt longer than that of *B. subtilis*) causes an increased specificity for magnesium ion interactions. Hence, this disparity in primary sequence and secondary structure may also account for the difference in optimal Mg^{2+} ion concentration needed for the cleavage reaction (Table 3.1).

4.2 Artificial riboswitch activators

In order to identify compounds that efficently target riboswitches and modulate their activity different routes can be followed. One of the approaches applied here includes the design of small libraries of chemically synthesized riboswitch ligand analogs. These were screened for riboswitch modulation either by an *in vitro* metabolite-induced self-cleavage assay in the case of the glmS ribozme or by an *in vivo* reporter gene assay for the thiM riboswitch. Additionally, a virtual screening method was employed for the identification of compounds mimicking GlcN6P in its 3D structure. Taken together these methods enabled the discovery of potent riboswitch activators, i. e. carba-sugars for glmS ribozyme activation and triazolethiamine as *thi*-box riboswitch activator.

4.2.1 Compounds mimicking the 3D-shape of GlcN6P

Screening a small library of compounds predicted by an *in silico* screening for chemical entities that mimic the three dimensional shape of glucosamine-6-phosphate (Section 3.1.3.1), led to the identification of a variety of compounds that were capable of either slightly inducing glmS ribozyme cleavage or of inhibiting its cleavage by GlcN6P.

In the initial screening for glmS ribozyme activators, performed at a final compound concentration of 2 mM, five compounds were identified which slightly activate the ribozyme (compounds **D4**, **D7**, **E5**, **E9**, and **F5**). Except **E9**, all of them were benzyl compounds with at least one amine moiety (anilines). The necessity of an amino-group for ribozyme cleavage has been known (Winkler et al., 2004) and now seems to be affirmed by the hit compound structures. However, the observed cleavages could also be due to an unspecific effect of RNA strand scissions that can be caused by anilines at abasic sites. Abasic sites are known to be spontaneously generated in RNA (Kazuya Nishikawa, 1982; Kochetkov and Budovskii, 1972) and could be present in the *in vitro* transcribed and purified RNA. An aniline-catalyzed strand cleavage proceeds via β-elimination to yield 3' fragments bearing 5'-phosphorylated termini (Figure 4.1). Cleavage is initiated by immonium ion formation, which renders the 2'-H

base-labile and the 3'-phosphate unit prone to β-elimination. The intermediate enol strongly prefers the keto tautomeric form which renders a δ-elimination, that could in principle be initiated via vinylogous deprotonation of 4'-H, slow (Küpfer and Leumann, 2007). Hence, amines like aniline can greatly accelerate strand cleavage near neutral pH in abasic RNA, whose spontaneous generation is slower than in DNA, but still observed (Kochetkov and Budovskii, 1972). This may also explain why compound **D4** increases glmS cleavage above percentages observed in the mere presence of GlcN6P (Figure 3.5).

Therefore, effects caused by these compounds should be further investigated, e.g. by cleavage-assay-independent experiments such as thermophoresis or isothermal titration calorimetry (ITC), where direct binding of the compounds could be monitored. Moreover, the analysis of cleaved glmS ribozyme on a high resolution sequencing gel should enable the detection of differences between the 2',3' cyclic phosphate and the 5' OH that is formed by a normal GlcN6P-mediated glmS cleavage reaction and the 5' phosphorylated terminus generated by the aniline-mediated scission.
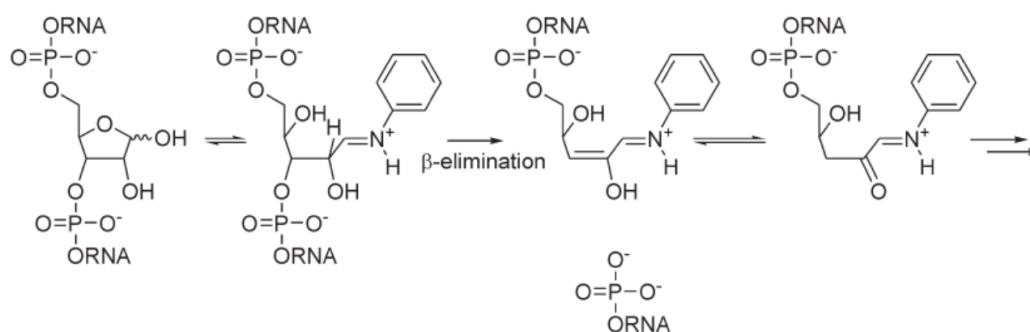
Figure 4.1: Intermediates in the aniline mediated strand scission at RNA abasic sites at slightly acidic pH.

In the second screening approach with more stringent assay determinants (500 µM compound in 0.5 % DMSO), several hits were identified that increased cleavage more than five fold over background cleavage. Especially compound **C11** and **D3** should be further investigated, preferably in a concentration dependent manner, as they induce cleavage to about 35 % at concentrations of 500 µM.

Interestingly, the strongest activators from the first screening, compounds **D7** and **E5**, were not confirmed under these screening conditions. They are close to the hit definition cut-off, but so are about 20 other compounds that were previously not able to activate glmS cleavage (Figure 3.4). The decrease in DMSO concentration under these assay conditions can have two effects that each may explain this differential outcome. On the one hand, decrease in DMSO concentration can change assay performance. Even though previous tests showed that DMSO concentrations up to 2 % did not have strong effects on glmS activation, cleavage was slightly pronounced in the presence of GlcN6P or GlcN with DMSO (Figure 8.3 E). The altered assay perfomance may be explained by the loss of RNA conformation structure due to the presence of DMSO (Gillchriest and Nelson, 1969). On the other hand, the decrease in DMSO concentration can influence compound solubility. Therefore, hits identified in the 2 mM, 2 % DMSO screening may not be as soluble as under the conditions in the 500 µM, 0.5 % DMSO screening. These two facts could individually or as a combination lead to the identification of different hits in the described screenings for glmS ribozyme activators.

In comparison to the natural activator GlcN6P all compounds identified by this *in silico* screening have much worse activities. Cleavage of compounds tested either at $2\,mM$ or $500\,\mu M$ never approached that of the $200\,\mu M$ GlcN6P, or even GlcN tested. Only compounds **C11** and **D3** showed at $500\,\mu M$ in $0.5\,\%$ DMSO a glmS activation close to $35\,\%$. This activation is more prominent than that conferred by the natural compound Streptozotocin ($20\,\%$ at $2\,mM$), but not nearly as promising as that of the synthetic CGlcN6P ($80\,\%$ at $200\,\mu M$). In contrast, the comparison of ribozyme inhibition by Reymond compounds and aminoglycosides demonstrates that here the natural compounds accomplish lower IC_{50}-values (e. g. $28.7\,\mu M$ for Neomycin vs. $488\,\mu M$ compound **D2**), hence more efficiently inhibit cleavage reactions. However, hits with low nanomolar potency are only rarely identified by virtual screening methods (Eckert, 2007).

Persistant blocking of glmS ribozyme action may also enable interference with GlmS regulation with detrimental outcome for glmS riboswitch containing bacteria. Hence, Reymond compounds were also investigated for their potential of interfering with proper ribozyme cleavage initiated by GlcN6P (Section 3.1.3.1 Figures 3.5). It remains to be proven whether these compounds specifically inhibit glmS ribozyme cleavage by competing with GlcN6P for its binding site or if more unspecific effects, like intercalation or binding to common RNA motifs (Thomas and Hergenrother, 2008), are the reason for these observations.

Virtual screenings are bound to identify lead structures instead of ready-to-use drugs, as they are usually used by industry or academia to support HTS-approaches (Schneider, 2010). Therefore, it is not surprising, that the virtual screening method used by Reymond did not lead to the identification of low micromolar glmS ribozyme activators. However, compounds were discovered which are capable of inhibiting ribozyme cleavage in the high micromolar range. These compounds can now be used as lead structures for refinded investigations.

4.2.2 Carba-sugars activate the glmS riboswitch of *S. aureus* and *B. subtilis* in vitro

The importance of GlcN6P functional groups for glmS ribozyme binding and activation has been investigated in several studies (Winkler et al., 2004; Lim et al., 2006; Klein and Ferré-D'Amaré, 2006; Cochrane et al., 2007). The phosphate group was shown to be critical for binding, as well as the closed ring conformation of the sugar with the first hydroxy-group in the α position (Lim et al., 2006). Crystal structures of the glmS ribozyme and GlcN6P show that the ring oxygen and the phosphate group are required for stabilization of the interaction of the glmS-riboswitch with GlcN6P rather than being involved in the catalysis reaction (Klein and Ferré-D'Amaré, 2006; Cochrane et al., 2007). Destabilization of these interactions as reflected by the carba-analog of GlcN6P is well tolerated, and is likely to account for the slight discrepancy in EC_{50}- and k_{obs}-values. However, more pronounced modifications, like as in compound **3**, lead to a significant loss of affinity and thus activity.

Moreover, crystallographic data underline that methylations at the anomeric C-atom hydroxyl (compounds **5-7**) render these molecules inactive, probably due to steric clashes and/or abolishment of hydrogen-bond interactions (Ferré-D'Amaré, 2010). Even though the 4-hydroxy group is critical for binding, the 3-hydroxy group might have only a modest impact on binding or otherwise might influence reactivity by means of an inductive effect on the 2-amine group (Lim et al., 2006). Indeed, compound **2**, which contains all functional groups minimally required for riboswitch recognition, is able to slightly induce ribozyme activation at elevated concentrations (Figure 8.3 D).

The observed rate constant for *B. subtilis* glmS riboswitch measured here is comparable to rate constants for this ribozyme in its *cis*-form observed by others (Winkler et al., 2004; Brooks and Hampel, 2009). However, the about ten fold slower rate of the *S. aureus* variant is remarkable. Brooks et al. found that *in vitro* folding of the glmS ribozyme into a native, catalytically active form is slow and rate-limiting. They determined the individual reaction rates specific to either Mg^{2+} dependent folding or ligand binding and catalysis (Brooks and Hampel, 2009). As described in Brooks et al., the glmS ribozyme was heated to 70 °C for 2 min and then allowed to cool to room temperature for 5 min which is concurrent to methods employed in the study at hand. However, their protocol proceeded by allowing prefolding in the presence of 15 mM Mg^{2+} for 90 min. Therefore, it is possible that the comparatively small observed rate constants are due to incomplete or unproper RNA folding. In future reactions prolonged prefolding incubations in the presence of appropriate divalent ions may be beneficial for assay performance. Considering the structural differences in *S. aureus* and *B. subtilis* as the former is known to comprise an extended P1 stem loop making its structure even more complex, glmS ribozyme mutants lacking this extended stem should be tested for their ribozyme speed after different folding procedures. Possibly this extension complicates folding in *S. aureus* compared to *B. subtilis*.

Furthermore, the comparatively small observed rate constants could be due to the lack of accessory proteins under *in vitro* conditions, that *S. aureus* needs for folding. Alternatively, it is possible that the P1 loop actually interacts with other important cofactors *in vivo*, i. e. another metabolite, ion or protein, which assists in more speedy cleavage.

In vitro results showed a slight decrease in cleavage activity of the natural ligand compared to its carba-analog. This may also be caused by the influences of RNA folding processes mentioned above, or by the increased EC_{50} values of an imperfect interaction partner which does not make as many specific contacts to the RNA (Section 3.1.4). In this regard, future work will attempt to restore the hydrogen bond which is lost in the carba-sugar compared to the natural ligand, i. e. by the addition of an aryl-residue at the carba-position (Section 5.1.4).

In summary, the spectrum and tolerance of GlcN6P modifications have now been addressed by biochemical ribozyme activity assays as well as crystallizations. The following interactions and characteristics are known to support ribozyme activation and should be kept in mind when designing or optimizing novel glmS ribozyme activating molecules (Section 5.1.4):

- a closed ring conformation (Lim et al., 2006; Lünse et al., 2011) with C-1 in the α-anomeric form

- the ring oxygen hydrogen bonds with a glmS nucleobase (Ferré-D'Amaré, 2010), loss of this group leads to a 2 fold reduction in EC_{50}-value (Lünse et al., 2011)

- C-6 position should contain a phosphate group, as loss of this moiety results in reduction in affinity (50 fold difference in EC_{50}-value, Winkler et al. (2004); Lim et al. (2006))

- presence of the amino-group at C-2 is essential for ribozyme activation (Winkler et al., 2004)

- C-3 and C-4 hydroxy groups interact with the RNA via hydrogen bonds (Lim et al., 2006; Klein and Ferré-D'Amaré, 2006).

4.2.3 Carba-GlcN inhibits growth of *S. aureus* Mu50

The minimal inhibitory concentration of CGlcN (625 μM or 133 μg/ml) may seem quite high in comparison to other antibiotics in use (e. g. MIC for vancomycin in Mu50 is $\geq$ 2.5 μM or $\geq$ 8 μg/ml). However, it is in the same range as MICs reported for other riboswitch-targeting compounds (Figure 1.5). For instance, L-4-oxalysine has a MIC of 4-140 μg/ml in *B. subtilis*, or the purine analogs reported by Blount et al. displayed MICs in the mg range (0.6-5 mg/ml, *S. aureus* MSSA). This indicates that targeting riboswitches needs elevated compound concentrations (Blount et al., 2007). Future experiments will have to reveal whether these elevated concentrations are caused in part by off-target effects (Section 5.1.3).

Mu50 cell count decreased with CGlcN concentrations increasing from 40 μM. However, it is yet unclear whether this is a result of bactericidal or bacteriostatic effects. Bacteriostatic antibiotics are those, which inhibit bacterial growth and cell division, but do not kill them. The killing effect of vancomycin, a bactericidal antibiotic, is evident from growth curve data, as bacterial growth only slightly elevates and then remains at the same absorption value (Figure 3.9 B). Chloramphenicol is a bacteriostatic and as VISA strains are known to be susceptible to chloramphenicol treatment under laboratory conditions, growth curves in the presence of this antibiotic in comparison to CGlcN should be performed. It is very likely that chloramphenicol curves look similar to growth curves obtained in the presence of CGlcN, where bacterial cell count increases to a certain level at which it remains. It is still under debate and investigation which of the effects, bactericidal or bacteriostatic, would be generally more beneficial in a clinical setting (Pankey and Sabath, 2004). Nevertheless, it is desirable to define their influence on carba-sugar activity, as each mechanism brings about its own advantages and contraindications. Bacteriostatic antibiotics for example, rely on the help of the immune system for clearance of the bacteria, whereas bactericidal antibiotics can cause immunogenic side effects by the quick release of bacterial toxins or antigens into the body.

Conclusive data on bacteriocidal versus bacteriostatic effect cannot be drawn from mere growth curve analysis. Due to the fact that only bactericidal antibiotics that also have bacteriolytic characteristics, meaning the ability of inducing bacterial cell rupture and lysis, would lead to decreasing or constantly low OD_{600} values, like observed for vancomycin. Therefore, growth curves in the presence of CGlcN, should be accompanied by a test for cell viability (such as the determination of colony forming units or minimal bactericidal concentrations (MBCs)).

There were several reasons for investigating synergistic effects of subinhibitory concentrations of vancomycin in combination with CGlcN on the VISA Mu50 strain. Vancomycin is an inhibitor of cell wall synthesis in *S. aureus* and other Gram-positive organisms. It binds to the C-terminal D-Ala-D-Ala residue of the peptidoglycan precursor and forms a stable, noncovalent complex, which prevents the use of the precursor for cell wall synthesis (Pootoolal et al., 2002). Therefore, trapping of vancomycin molecules in the cell wall peptidoglycan is believed to be one vancomycin resistance mechanism. The thicker the cell wall, the more vancomycin molecules would be trapped within the cell wall, thus allowing a decreased number of vancomycin molecules to reach the cytoplasmic membrane where its real functional targets are present (Breukink et al., 1999).

There are several Mu50 characteristics that are, at least in part, accounted responsible for this thickened cell wall. Mu50 shows increased GlmS activities compared to those reported for other control strains (Cui et al., 2000), which would secure the supply of UDP-GlcNAc

needed for enhanced peptidoglycan biosynthesis. Moreover, it was found that the uptake of GlcNAc is enhanced in Mu50 (Cui et al., 2003). More than 95 % of the absorbed GlcNAc is incorporated into the cell wall via UDP-GlcNAc, the central precursor metabolite of cell-wall peptidoglycan synthesis (Bearne, 1996; Ghosh et al., 1960; Wong et al., 1974).

The decreased bacterial growth in the presence of CGlcN and subinhibitory concentrations of vancomycin may present evidence for the interference of CGlcN with vancomycin resistance mechanisms. Increased GlcNAc import, and especially the increased peptidoglycan synthesis via elevated GlmS activities are likely to be counteracted by CGlcN action. After the observed tendencies have been confirmed, detailed future experiments will have to closely examine the influence of CGlcN on single vancomycin resistance factors (Section 5.1.5).

Carba-sugars were not only shown to be potent activators of the glmS ribozyme *in vitro*, but also abolished bacterial growth of a vancomycin intermediate resistant *S. aureus* strain at concentrations of 625 µM. This may mark the discovery of a new class of riboswitch modulating compounds that target glmS ribozymes. It will be interesting to further investigate the sole and combinatorial effects of CGlcN.

4.2.4 *thi*-box compound screening

Using a reporter gene-based assay system, a small library of triazolethiamine (TT) and derivatives was screened for thiM riboswitch activation in bacteria. TT was discovered as one of the most potent activators among the substances tested, and revealed IC_{50}-values in the low micromolar range for downregulation of β-galactosidase. Additionally, TT induced a decrease in bacterial growth with increasing concentrations (Sections 3.2.1, 3.2.2 and 3.2.2.2).

There have been other attempts to identify chemical scaffolds that act as *thi*-box riboswitch activators. In 2010, a fragment-based screening approach was published (Chen et al., 2010), that introduced low molecular weight compounds capable of competing with thiamine for binding to the aptamer domain of the thiM riboswitch. However, these compounds showed only affinities in the high micromolar to low millimolar range. Therefore, there was still potential for describing new modulators for this riboswitch class in addition to the already known *thi*-box riboswitch activator pyrithiamine.

The fragment-based screening approach presented by Chen et al. theoretically allows the discovery of structurally and chemically diverse ligands whose optimization can eventually lead to high affinity binders (Chen et al., 2010, 2012). However, results of the thiM-reporter gene assay indicate that compounds acting on riboswitches have to be carefully investigated *in vivo* while sole *in vitro* data may not be sufficient to predict compound behaviour. The differences in activation observed for the two tested bacterial strains suggests that an array of distinct strains with altering characteristics should always be investigated to confirm and underline observed *in vivo* effects.

The screening system introduced in this work is unique in that it allows the search for thiM riboswitch modulating compounds *in vivo*. Therefore, compounds that lead to downregulation of reporter gene expression are instantly known to be absorbed and metabolized by the bacteria in a way that is not detrimental to riboswitch activation. However, compound concentrations used in the growth medium do not reflect actual effective intracellular concentrations. Therefore, supporting *in vitro* assays will remain to be necessary for the characterization of riboswitch activators found by an *in vivo* screening. Additionally, it can be difficult to appraise which and how many metabolic conversions occurred to activate, or even deactivate,

promising compounds. However, elucidating these enzymatic reactions will oftentimes not only clarify compound mode of action, but may also reveal new, unresolved metabolic pathways and networks. Furthermore, this screening system is easily adaptable to other riboswitches controlling translation initiation, could be adjusted to transcription termination riboswitches and can be optimized for high-throughput screening by downscaling (see (Müller, 2011)).

4.2.5 Triazolethiamine compounds activate the TPP riboswitch

Thi-box riboswitches are interesting and attractive target structures for developing antibacterial compounds (Sudarsan et al., 2005; Blount and Breaker, 2006). Therefore, the thiM-reporter gene assay was used to screen a library of triazolethiamine and derivatives for riboswitch activation *in vivo*. Replacing the thiazole heterocycle of thiamine with 1,2,3 triazole appears to be a valuable strategy to generate thiamine analogs that interact with *thi*-box riboswitches and, thus, induce repression of gene expression *in vivo*, because this middle ring shares only long distance electrostatic interactions with the aptamer domain (Edwards and Ferré-D'Amaré, 2006).

Chen et al. showed that triazolethiamine pyrophosphate interacts with the thiM riboswitch *in vitro* with a similar affinity, as does thiamine pyrophosphate (Chen et al., 2012). Complimenting their *in vitro* studies, is the *in vivo* demonstration of triazolethiamine (TT) effects on repressing thiM-mediated reporter gene expression reported here. The advancement into the targeted organism, is a critical step that has to be taken, as drastic differences between *in vitro* and *in vivo* effects were observed. *In vitro* translation assays performed by Chen et al. indicated that TT and TTPP were able to induce conformational changes within the thiM riboswitch expression domain, however only to about 90 and 65 %, respectively (Chen et al., 2012). However, monitoring of reporter gene expression after overnight incubation in the presence of TT *in vivo*, indicated stronger repression to about 20 %. This alludes to an enhancement of gene regulation intracellularly that goes beyond mere binding and subsequent secondary structure changes followed *in vitro*. Maybe, yet unknown accessory cofactors, that are absent from the *in vitro* translation assay, support this signal amplification in bacteria.

Apart from that, it was observed that compound effects can differ drastically between bacterial strains. IC_{50}-values for TT compounds were found to vary 2-4 fold between DH5αZ1 and MG1655 cells, which is likely to be caused by the differences in genetic background between both strains. Half maximal inhibitory concentrations for TT-compounds were not as pronounced in MG1655 cells, which are thiamine prototroph, meaning capable of synthesizing thiamine from its precursors. Moreover, MG1655 cells bear a mutation in the pyrE gene, which codes for orotate phosphoribosyltransferase. This enzyme is responsible for the formation of orotidine 5'-monophosphate (OMP) from orotate and phosphoribosyl pyrophosphate (PRPP). As a result, levels of PRPP possibly increase, because it is not used for the synthesis of OMP anymore. This in turn may lead to enhanced purine and thiamine biosynthesis (Jensen, 1993) and also an increase in intracellular thiamine concentration that is usually between 0.25 µM and 4.5 µM (Schyns et al., 2005; Miranda-Ríos, 2007). Hence, the diminished compound effect could arise from the permanent intracellular presence of thiamine and its phosphorylated forms. These molecules are likely to compete with the compounds for binding to the riboswitch and especially for conversion of TT to TTPP by intracellular enzymes. In contrast, in DH5αZ1 cells available thiamine amounts can be controlled by addition of this vitamine to the culture medium, because these cells are thiamine auxotrophic. Therefore, it is likely that the amount of available thiamine or TPP for competition with compounds in riboswitch binding and

activation is less than in MG1655 cells.

Nevertheless, the differences in IC$_{50}$-values could not only arise from competing thiamine species, but also from differential TT-compound take-up or metabolism, which is certainly similar between these *E. coli* strains, but still distinct due to their discriminative genetic backround (Table 7.5). Influences by differing genetic backgrounds will have to be investigated in a continuative study (Section 5.2).

Additionally, there is another phenomenon that distinguishes reporter gene assay outcome between both strains. In *E. coli* cells, absolute β-galactosidase expression for compounds **11-15** is usually more pronounced than in DH5αZ1. This may be due to another prominent difference in the genetic background of these strains, namely their natural copy of the lacZ gene. In DH5αZ1 cells this gene is inactivated (Simons et al., 1987; Hanahan, 1985), whereas in MG1655 *E. coli* cells it is still present and active (Blattner et al., 1997). A simple point mutation at amino acid position 202 changing aspartic acid to phenylalanine (D $\rightarrow$ F) obliterates all binding and catalysis of the endogenous β-galactosidase (Xu et al., 2004). Furthermore, DH5αZ1 cells bear a thi^{-1} mutation, which renders them dependent on thiamine supplementation (Table 7.5). This genetic alteration is a deletion of a single nucleotide in the sequence of thiG leading to a frameshift and thereby an inability of autonomously synthesizing thiamine precursors (Kay, 1972). Although thiG itself has not been directly assigned to thiamine phosphorylation *in vivo* (Jurgenson et al., 2009), its mutation may lead to imbalances in the thiamine biosynthesis cascade that account for the lack of activity of some compounds in this strain, i. e. compound **13**.

HILIC has been found to allow enrichment and the targeted analysis of post-translational modifications (PTMs) such as glycosylation (Hägglund et al., 2004), N-acetylation (Boersema et al., 2007) and phosphorylation (McNulty and Annan, 2008) in proteomics applications (Boersema et al., 2008). HILIC measurements of triazolethiamine-treated cell lysates are intended to illuminate compound fate *in vivo* and prove phosphorylation of TT to TTPP in *E. coli*. Even though the isolation procedure could be significantly optimized to reliably detect TPP in *E. coli* cell lysates, matrix backgrounds were too high and amounts of phosphorylated triazolethiamine to low to detect any TTPP (Section 6.3.10). Future directions involve the spiking of untreated cell lysate with chemically synthesized TTPP. This would allow to further optimize HILIC parameters and to note TTPP retention times. Moreover, cells could be engineered to overexpress separate proteins of the TPP biosynthesis pathway, so that, if TTPP is also generated by these enzymes, its levels would increase and be more readily detected (Section 5.2).

The influence of compounds **11-14** on bacterial growth was evaluated. The distinct efficiencies in gene repression and inhibition of bacterial growth point at possible secondary effects of the metabolite-analogs. These side effects may be due to interactions with enzymes involved in TPP metabolic pathways. The contradictory effects observed for compound **13**, being ineffective in regulation of *thi*-box controlled gene expression, but inhibiting bacterial growth, may point in this direction. Indeed, it has been shown that triazole-derivatives of TPP inhibit enzymes involved in the biosynthesis of TPP (Erixon et al., 2007; Chen et al., 2010; Kay, 1972). However, *thi*-box riboswitches have been shown to bind their ligand in an extended conformation (Serganov et al., 2006), which contrasts the V-conformation in which TPP is known to be bound in enzymes (Muller et al., 1993). This may enable a precise refinement of compound characteristics, so that only the thiM riboswitch is bound.

Investigation of compound effects on *Haemophilus influenza* growth should be further optimized, maybe by preparing the chemical defined medium and the agar plates afresh for every experiment and avoid any storage at 4 °C. Additionally, other strains containing *thi*-box riboswitches that control essential genes should be investigated in growth assays, e. g. *Brucella melitensis* (Blount and Breaker, 2006).

4.2.6 Triazolethiamine compounds with metal-chelating groups activate the TPP riboswitch *in vivo*

Crystallographic and biochemical studies of the TPP riboswitch bound to TPP analogs reveal that the riboswitch is less sensitive to variations at the pyrophosphate end of the molecule than within the aminopyrimidine moiety (Edwards and Ferré-D'Amaré, 2006; Sudarsan et al., 2005). This suggests that the pyrimidine acceptor loop (J2/3) is somewhat preorganized and consequently unable to adapt to alterations in the composition of the aminopyrimidine moiety, whereas the pyrophosphate acceptor loop is more disordered and flexible (Rentmeister et al., 2007; Montange and Batey, 2008; Edwards and Ferré-D'Amaré, 2006). This is why triazole compounds were synthesized that should function directly without further enzymatic modification. These compounds contain groups capable of chelating at least one divalent metal ion, and thereby possibly mimic a phosphate or pyrophosphate group.

Compounds **16-19** which can coordinate a metal ion via their sulfonyl or pyruvate-like diketone groups, showed less successful reporter gene repression with larger substituents. This indicated a tendency towards less tolerance of the riboswitch toward more bulky substituents (e. g. compound **17**).

The benzyl, phenyl, or aryl fluoride rings added to several compounds (**17**, **21**, **24**, **25**) were intended to form additional RNA interactions, possibly through stacking. However, it appears that the linker distances used were not optimal to allow such an interaction, since all compounds containing such a moiety showed only modest thiM riboswitch activation.

Sulfone and sulfonamide compounds have long been known for their antibacterial action (Domagk, 1940). Therefore, similar sulfur containing compounds, such as **16-18**, should be tested for antibacterial effects unrelated to thiM riboswitch activation, i. e. in bacterial strains that do not use *thi*-box riboswitches for gene regulation.

The methotrexate-like and folate-like compounds **26** and **27** belong to those molecules investigated here, which are theoretically capable of chelating two divalent ions. This would make their metal-complexing characteristics very much like TPP and in fact these compounds revealed quite strong influences on reporter gene expression in both strains. Surprisingly, the difference between the ester and carboxylic acid form of the otherwise identical compound is not significant. It would be expected that compounds whose charged carboxylic acid groups are "masked" via esterification, would enter the cell more easily. Yet, it has to be kept in mind, that for the reporter gene assay the cells are incubated in the presence of compound for 24 hours in aqueous solution. In this milieu it is very likely that esterifications are already hydrolyzed before **26** can be taken-up. Maybe shorter incubation times will enable the investigation of differential effects of **26** and **27** as actual ester or carboxylic acid. The same considerations can be applied to the phosphonate-compounds **28** and **29** and their carbon acid moiety. Surprisingly, the otherwise observed tendency of larger substituents leading to a general decrease in thiM activation, does not prove true for **26** and **27**. *In vitro* binding studies will have to reveal the influence of the kind of metal chelating moiety on riboswitch

binding. The phosphonates **28** and **29** are very soluble in water, which can be very beneficial, especially when compared to compounds with non-polar moieties (**17**, **24**, **25**), that are less easily dissolved. However, these compounds show only slight effects on thiM riboswitch activation despite their ability to theoretically coordinate two metal ions and no differences can be observed between the carboxylic acid and ester form.

Compound **23**, which represents an exception from the triazoles tested, revealed intriguing effects on thiM riboswitch activation in DH5αZ1 and MG1655 cells- an effect previously only so drastically observed for TT itself. In **23**, the pyrimidine ring is linked via a peptide bond to a trimethoxybenzyl moiety (Figure 4.2). As the central thiazole ring of TPP is known to only form long distance interactions with the binding pocket, it is not surprising that the triazole ring can be omitted. Additionally, another structual feature of compound **23** raised curiosity: taking together the pyrimidine ring and the trimethoxybenzyl moiety, this compound looks very similar to trimethoprim (Figure 4.2). Trimethoprim is known to have antibacterial features and to date they are accounted to the inhibition of proteins within the bacterial tetrahydrofolate biosynthesis pathway. However, these results indicate that trimethoprim may be able to interact with *thi*-box riboswitches. *Haemophilus influenza* and *E. coli* are known to be especially susceptible to trimethoprim treatment. It is intriguing that at least for the former, essential genes are regulated by *thi*-box riboswitches and in the latter at least three of these riboswitches control a total of 11 genes (Blount and Breaker, 2006). Therefore, the effect of trimethoprim on thiM riboswitch activation should be investigated using the β-galactosidase reporter gene assay.
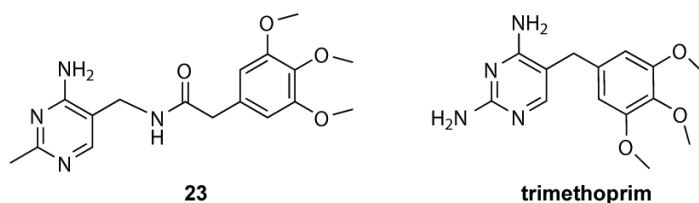
Figure 4.2: Chemical formulas for compound 23 and trimethoprim.

Moreover, it would be worthwhile to further investigate the influence of the absent triazole ring in compound **23** on reporter gene modulation. The synthesis of a trimethoxybenzyl containing triazole thiamine derivative would allow such an evaluation.

Future experiments, such as thermophoresis, will have to reveal, how tightly these metal chelating triazolethiamine derivatives (**16-29**) bind to the riboswitch *in vitro* (Section 5.2). However, mere *in vitro* data is not sufficient to interpret compound effects on riboswitches, as not only binding to the aptamer domain, but also the induction of rather global structural changes within the expression domain are necessary to confer gene regulatory function. Therefore, the β-galactosidase assay should be used to determine IC_{50}-values for the most active compounds, e.g. **16**, **18**, **22**, **23**, **25** and **26**. Furthermore, the mutated thiM variant should be used to investigate specificity of compound effects, as has been done for TT derivatives lacking any metal chelating groups.

4.3 Natural riboswitch activators

If riboswitches are indeed valuable antibacterial targets, microorganisms will have evolved substances that address these RNA elements. Roseoflavin, an FMN analog produced by *S. davawensis*, is a prominent example of a natural riboswitch activator (Lee et al., 2009). Therefore, apart from the methods of ribowitch modulator identification by investigating "artificial" chemical entities, there are numerous routes conceivable in order to find " natural" riboswitch modulators. Examples include the screening of natural product libraries, like the one at the Max-Planck-Institute for Molecular Physiology in Dortmund, using similar or even identical assay systems as employed for searching through small molecule libraries. Additionally, assaying crude extracts or culture supernatants for substances causing a riboswitch-related phenotype may present a route of investigation.

Here, already known RNA targeting molecules, aminoglycosides, were explored for their effect on glmS ribozyme cleavage. As observed for other ribozymes, aminoglycosides also inhibit glmS ribozyme cleavage reactions. Furthermore, Streptozotocin, which shares high structural similarity to the natural glmS ribozyme cofactor GlcN6P, was found to activate the glmS ribozyme.

Finally, when exploring the mode of action of novel or known natural products, riboswitches should be considered as targets.

4.3.1 Aminoglycosides as glmS ribozyme inhibitors

Aminoglycosides were tested for their ability to modulate glmS ribozyme activation for several reasons. Apart from some structural analogy, aminoglycosides are known to bind to and interact with RNA. Their primary mode of action for conferring antibiotic activity is supposed to be their interaction with the A-site of the ribosome (Green and Noller, 1997; Pape et al., 1999). However, in the 1990s they have been shown to be potent inhibitors of ribozymes. Group I intron self-splicing (von Ahsen et al., 1991), self-cleavage of the hammerhead (Stage et al., 1995) and human hepatitis delta virus (HDV) ribozymes (Rogers et al., 1996; Chia et al., 1997), the magnesium-induced self-cleavage reaction of the hairpin ribozyme (Earnshaw and Gait, 1998) and the tRNA processing activity of RNase P RNA (Mikkelsen et al., 1999) are all inhibited by the same aminoglycosides, most prominently by Neomycin B and Tobramycin (Schroeder et al., 2000). Binding of aminoglycosides to nonribosomal RNAs is now acknowledged to possibly contribute to their potential therapeutic applications but also to the side effects that are observed for this class of compounds (Walter et al., 1999).

Here, Neomycin B was also identified as the most potent inhibitor of glmS ribozyme cleavage. Literature suggests that this effect is not caused by a specific competition of the aminoglycoside with GlcN6P on its binding site, but the rather unspecific binding interactions that aminoglycosides are known to form with structured RNA (Famulok and Hüttenhofer, 1996; Tor, 2003). This is supported by the finding that a group I intron inhibited by Neomycin B was shown to bind more than one antibiotic molecule (von Ahsen and Noller, 1993) and multiple binding sites for aminoglycosides on RNA molecules are likely to coexist (Hendrix et al., 1997; Michael K, 1999). There have been attempts to modify aminoglycosides to make them more specific for a certain target (Blount and Tor, 2006). These strategies could also be used to improve aminoglycoside-glmS ribozyme binding. Future experiments, such as thermophoresis may allow to investigate glmS ribozyme-Neomycin B interactions and establish whether binding occurs in a 1:1 ratio or how the change of certain moieties (Neomycin vs.

Tobramycin, Kanamycin A vs. Kanamycin B) affects binding constants.

Changing an amino group in Kanamycin B to a hydroxy group in Kanamycin A practically abolishes inhibitory activity in the self-splicing (von Ahsen et al., 1991) and Rev-RRE assays (Zapp et al., 1993) and a similar trend was observed for Neomycin B versus Paromomycin in these studies. Analogous to these reports are the observations for glmS ribozyme cleavage inhibition that takes place in the presence of Kanamycin B, but is not detectable, when Kanamycin A is used. In the same way, Paromomycin is not as potent as Neomycin B in hindering glmS ribozyme cleavage.

Hence, the mere change of an amino group can have great effects on aminoglycoside activity. This accentuates the fact that electrostatic interactions are a major contributor to aminoglycoside-RNA affinity. Therefore, altering the basicity of the amino groups by the removal of their neighboring hydroxy group affects the overall charge of the modified analogs and their RNA binding capability (Wang, 1997). Thus, the appropriately deoxygenated aminoglycoside derivatives possess a higher overall positive charge at a given pH value relative to their parent natural product. Hence, the hydroxy groups also influence RNA affinity. Kanamycin B, for example, is twenty-fold less active than Tobramycin (its 3'-deoxy derivative) in inhibiting self-splicing of group I introns, and the trend holds also for other RNA targets (Tor, 2003) including the glmS ribozyme as investigated here. Generally however, it remains difficult to estimate the influence of additional or lacking amino- or hydroxyl groups, as in some cases already slight structural differences cause a prominent effect on glmS ribozyme cleavage inhibition, for example for Neomycin and Paromomycin, whereas in other cases, e. g. Tobramycin and Kanamycin B, small structual variations did not have such a great effect.

In addition, there are several reports in which aminoglycosides enhance RNA cleavage. Examples include Neomycin B which hydrolyses the phosphate ester bonds in a di-ribonucleoside monophosphate (ApA) (Tor et al., 1998) and the tRNA^{Phe} which was found to be susceptible to aminoglycoside-mediated cleavage (Kirk and Tor, 1999; Belousoff et al., 2009). This is due to the remarkable ability of aminoglycosides to flexibly remodel themselves to fit into multiple RNA folds. This makes them to promiscous RNA binders (Tor, 2003), as they often occupy several binding sites on the RNA molecules and rigidify the RNA by these interactions. Even though direct interactions of the aminoglycoside in RNA cleavage reactions cannot be excluded, this aminoglycoside-mediated increase in rigidity is also held responsible for contributing to aminoglycoside-mediated RNA hydrolysis (Tor, 2003). These observations prompted the investigation of glmS ribozyme activation by aminoglycosides, however without identifying any amino-cyclitiols capable of inducing specific RNA scission.

RNA aptamers binding to aminoglycosides with high affinity (in the nanomolar range) have also been selected by *in vitro* methods (Wallis et al., 1995; Famulok and Hüttenhofer, 1996). Interestingly, all aptamers have a similar architectural fold but little sequence homology. In order to investigate, which structures are recognized by the aminoglycosides, truncated versions of the glmS ribozyme, comprising interesting structural architectures, could be tested *in vitro* for aminoglycoside binding.

4.3.2 Streptozotocin as glmS ribozyme activator

The nitrosourea glycoside Streptozotocin has been investigated for its potential activation of the glmS ribozyme. Even though ribozyme specific cleavage was induced at high millimolar concentrations *in vitro*, the question remains whether these effects are relevant *in vivo*. Streptozotocin is taken-up by PTS transporters which phosphorylate it at its C-6 position.

This may lead to a significant increase in ribozyme activation potential, which will have to be evaluated *in vitro* by the testing of a synthesized phosphorylated Streptozotocin variant for glmS ribozyme cleavage.

Additional evidence for the potential ability of Streptozotocin binding to the glmS riboswitch can be conferred from data presented by Lim et al. In their study, compound **9** is almost as active as GlcN6P and only bears an additional methylation at the amino group. This indicates that there is some tolerance at this group in ribozyme activation (Lim et al., 2006).

Definite proof of Streptozotocin influence on glmS ribozyme activation *in vivo*, however, can only be obtained by the concerted investigation of ribozyme-reporter gene fusions and quantitative real-time PCR of the glmS mRNA (Section 5.1.6). These experiments will allow the quantification of glmS mRNA levels under Streptozotocin influence compared to untreated cells. If this compound acts on the glmS ribozyme, mRNA levels are expected to drop.

Finally, it has to be ruled out that cleavage intensities observed are only due to a contamination of Streptozotocin with GlcN, that is still present in the purified product at about 2 %. Detailed investigations indicate that the ribozyme cleavage observed cannot be accounted to the mere presence of up to 2 % GlcN (Schüller, 2012).

The minimal inhibitory concentration data obtained for Streptozotocin in different media suggests that richer medium decreases Streptozotocin uptake. This indicates that decreasing concentrations of amino-sugars in the medium will lead to enforced Streptozotocin take-up, which is conferred by PTS mediated transport. Furthermore, it was surprising to find that the vancomycin-resistant Mu50 strain has lower MICs than the sensitive SG511 strain, which is known to be very susceptible to cell wall targeting antibiotics. This observation for Mu50 cells can be due to different scenarios. As this VISA strain is known to have increased GlmS-mediated production of cell wall precursors, lower MICs may stem from more pronounced effects of Streptozotocin on GlmS protein repression via the glmS ribozyme action proposed here. Alternatively, merely the enhanced take-up of GlcNAc (Cui et al., 2003) results in increased incorporation of Streptozotocin.

Lastly the synthesis of a Streptozotocin analog that is not capable of alkylating DNA is needed to understand how much of the observed antibacterial effect is due to the prospective action on the riboswitch or due to the mere DNA alkylating character of this nitrosourea compound.

4.4 The promise of riboswitches as antibacterial drug targets

RNA is known to be a suitable drug target (Section 3.1.7.1) and many antibacterial drugs address rRNA structures (Schroeder et al., 2000). However, these interactions are often found to be due to rather fortuitous and not due to natural actions of the RNA, which can cause a lack of selectivity (Hermann and Tor, 2005). Riboswitches however, evolved to bind low molecular weight ligands in a defined binding pocket with high affinity and specificity (Blount and Breaker, 2006). As such, this should allow the design of highly selective riboswitch-targeting compounds that do not bind to other cellular targets (Blount and Breaker, 2006). Because of the characteristic recognition of ligands, the screening of small molecule libraries containing ligand analogs proved to be a very successful strategy for the identification of riboswitch modulators (Sections 3.1.3.2, 3.2.2 and 3.2.3). Carba-sugars as well as triazolethiamine and its derivatives descend from those screening approaches.

As many different riboswitch classes have been described that bind a variety of metabolites, this would allow targeting of different metabolic pathways in bacteria. Therefore, existing analog libraries for a broad spectrum of metabolites, usually previously employed for the identification protein inhibitors, are oftentimes readily available for the application in riboswitch-modulator screenings (i.e. the TT compound library, or the adenine analog library used for the screening by Alexander Müller, Müller (2011)).

Many genes regulated by riboswitches are often essential and therefore important for survival or virulence (Zhang et al., 2004). Especially compounds targeting these essential genes should have lethal effects, provided that the mimic cannot functionally replace the natural metabolite (Blount and Breaker, 2006). This underlines the prospect of the glmS ribozyme being a valid target for the identification of antibacterial substances, as Donald et al. proved the glmS gene to be essential in *S. aureus* by chemical genomics, based on 245 *Staphylococcus aureus* antisense RNA strains (Donald et al., 2009). This corroborates the observed ability of CGlcN to effectively interfere with bacterial growth of *S. aureus* Mu50 (Section 3.1.5). In addition to this, riboswitches sometimes regulate a collection of genes, which in themselves may not be essential, but the interference with proper expression of this assembly may have detrimental effects on bacterial growth (Blount and Breaker, 2006; Mandal et al., 2003). The decreased growth of *E. coli* in the presence of TT is a good example of this phenomenon. In these bacteria, eleven TPP-metabolism-related genes are controled by three riboswitches and possibly the collective attack of regulatory components within this metabolic pathway by TT causes the observed loss in viability (Section 3.2.2.2).

Depending on their phylogenetic distribution, riboswitches could be used as broad spectrum antibiotic targets (e.g. *thi*-box riboswitches, which are the most widely distributed riboswitch class), or the only sparsly distributed ribsowitches are targets for selective drugs, e.g. glmS ribozymes are mostly found in Gram-positive organisms and only few examples are predicted to exist in Gram-negatives (McCown et al., 2011). This implies completely different, prospective application patterns for TT compounds or carba-sugars as antibacterials.

Furthermore, an array of riboswitch targeting compounds, that display either long known antibacterial effects, or are newly rationally designed or found as natural products, proves these RNA elements to be addressable structures. Several riboswitch-activating compounds, like guanine analogs (Kim et al., 2009; Gilbert et al., 2006) and others, were identified by rational design according to available 3D structures and biochemical data. A similar approach was used in designing the GlcN6P-analog library screened here (Section 3.1.3.2 A). However, the virtual screening described in Section 3.1.3.1 takes the use of 3D information for the identification of riboswitch targeting compounds one step further. Subsequent *in vitro* analysis of the appointed potential 57 glmS ribozyme modulators suggests activities in the micromolar range regarding their ability to inhibit ribozyme cleavage (Section 3.1.3.1). Hence, with increased availablility of riboswitch-ligand crystals more artificial riboswitch activators can be designed for yet untargeted riboswitch classes either by hand or with computer-aided methods. In combination with the applicability of riboswitch activity tests for high-throughput screening approaches (Mayer and Famulok, 2006; Blount et al., 2006), the concerted use of rational/*in silico* methods and brute force attempts pave the way for the successful identification of riboswitch modulators from comparatively large, but ligand-optimized libraries.

The fact that antibacterial compounds with previously unidentified mode of action affect riboswitches, supports the arguement for these RNA structures as suitable antibacterial targets. Most prominent examples of such compounds with previously unidentified MoA include pyrithiamine (PT) which was found to target *thi*-box riboswitches (Woolley and White,

1943) and L-aminoethylcysteine (AEC) and DL-4-oxalysine (Shiota et al., 1958; McCord, 1957) which act on lysine riboswitches (Figure 1.5). Future investigations will show, if the natural GlcN analog Streptozotocin owes part of its antibacterial effect to the action on the glmS ribozyme rather than only causing cell death by DNA methylation (Section 3.1.7.2). Similarly, effects of compound **23** on thiM riboswitch activation encurage the investigation of the long used antibiotic trimethoprim for side effects on *thi*-box riboswitches.

Ultimate proof of riboswitches being valid antibacterial targets is presented by organisms which produce vindicative substances acting on riboswitches. Roseoflavin, a riboflavin analog, is synthesized by *Streptomyces davawensis* and inhibits the growth of several Gram-positive bacteria by repression riboflavin biosynthesis through activation of the FMN riboswitch. Furthermore, Streptozotocin may turn out to be a second example of such a natural defense mechanism, in this case employed by *Streptomyces achromogenes* (Section 3.1.7.2).

In summary, riboswitches make great targets for antibacterial research for all the above mentioned reasons. However, there are some important challenges that need to be met. It will be crucial to identify those riboswitches that can repress the expression of a relevant gene below a level that is required for survival (Blount and Breaker, 2006). And even when gene expression is completely abolished, bacterial salvage pathways may allow compensation of the lack of important metabolites, as seen for PT, which is detoxified by some bacteria via TenA activity. Moreover, it is crucial to choose riboswitch targets that regulate the biosynthesis of metabolites that cannot be readily available from mammalian host tissue (Blount and Breaker, 2006). The Streptozotocin growth curves presented here underline the importance of this fact, as it was observed that already in bacterial cell culture richer growth media led to increased MICs. This suggests that Streptozotocin uptake is diminished when other sugar species compete for absoption by PTS transporters. Of course, in human tissue other sugar species are also going to be present. In addition, even though riboswitches have not been identified in humans or any other higher eukaryotic organism yet, it is important to consider toxic effects that could arise from riboswitch targeting compounds that mimic ligands also present in humans, e.g. we may not have a TPP riboswitch, but TPP is also used by our enzymes as cofactor. Therefore, riboswitch targeting compounds need to be optimized to exclusively and specifically address their target and not human proteins, which may be possible considering the fact that riboswitches recognize their ligand differently than proteins (Blount and Breaker, 2006). TPP for example is bound by proteins in a V-conformation, however by the TPP riboswitch in an extended conformation. Nevertheless, TT identified as thiM riboswitch activator here is already known as pyruvate decarboxylase (PDC) inhibitor in *Zymomonas mobilis* (Erixon et al., 2007), depending on protein homologies this may also be true for the human PDC. Also, a CGlcN analog, 2-acetamido-1,2,5-trideoxy-1,5-imino-D glucitol has been shown to inhibit a human enzyme, namely N-acetyl-β-hexosaminidase (Ho et al., 2010). These two examples indicate, how challenging it can be to identify compounds that target only riboswitches.

5 Outlook

In this study, mainly the glmS ribozyme of *S. aureus* and the thiM riboswitch of *E. coli* were addressed as new antibacterial targets. For both riboswitch classes, activators were sought through a variety of different means, such as evaluation of compounds predicted by a virtual screening, screening of rationally designed metabolite analog libraries as well as investigation of natural products. Compound screenings were undertaken either by *in vitro* or direct *in vivo* approaches. Through these efforts, carba-sugars were discovered as novel glmS ribozyme activators, that cofactor cleavage of the glmS ribozyme in *S. aureus* almost as efficiently as the natural metabolite GlcN6P. Moreover, CGlcN revealed reduced bacterial growth of a VISA strain with a MIC of 625 μM. In addition to carba-sugars, triazolethiamine (TT) was discovered as another class of riboswitch targeting compounds. TT is likely to be taken-up by the bacteria and phosphorylated *in vivo*. The newly formed TTPP acts on the thiM riboswitch, as shown by a reporter gene assay as well as underlined by *in vitro* ITC interaction measurements by Chen et al. (Chen et al., 2012). Taken together these findings pose exciting new questions to be solved and open up new research possibilities.

5.1 The glmS ribozyme of *S. aureus* Mu50

It was sought to identify modulators of the glmS ribozyme of the vancomycin intermediate resistant *Staphylococcus aureus* strain Mu50. Natural and chemical compound collections and candidates were investigated for their influence on ribozyme cleavage using a metabolite-induced self-cleavage assay. However, initially, the glmS ribozyme had to be amplified from genomic DNA and enzymatic activity verified, since it had only been *in silico* predicted to exist in *S. aureus* (Barrick et al., 2004). This characterization revealed some discrepancies between the *S. aureus* and the *B. subtilis* glmS ribozyme. The *B. subtilis* glmS ribozyme not only accepts Co^{2+} as divalent ion for the cleavage reaction and needs lower Mg^{2+} concentrations for efficient RNA scission, it also cleaves $10\times$ faster than its *S. aureus* homolog (Winkler et al., 2004; Lünse et al., 2011).

Hence, future investigations should try to illuminate the reason for these differences. Considering the ribozyme secondary structure, one distinction is obvious: the P1 stem of the *S. aureus* is 50 nucleotides longer than the one in *B. subtilis*. Therfore, it is imaginable that differences in observed rate constants might originate from distinct functions of this structural feature. Ribozyme variants should be designed to investigate this. For example, parts of the P1 stem of the *S. aureus* glmS should be deleted or transferred onto the *B. subtilis* P1 stem. These modified constructs could be used in cleavage assays to define changes in observed rate constants. Additionally, cleavage deficient mutants could be used for thermophoresis measurements to evaluate changes in affinity for the ribozyme's cofactor, or chemical and enzymatic probing studies may be employed to define important secondary structural motifs necessary for glmS ribozyme activity. Finally, these variants should also be tested for their metal ion requirements and the influences metal ion variations have on cleavage.

Taken together these investigations may provide conclusive explanations for differences in ribozyme cleavage speeds and metal preferences.

5.1.1 Refinement of *in silico* prediction of compounds mimicking the 3D shape of GlcN6P

The *in silico* screening by the Reymond group identified 57 compounds with high similarity in their 3D shape to GlcN6P, which were subsequently tested for glmS ribozyme activation or inhibition. All compounds tested revealed activities in the high micromolar to millimolar range, which is often the case for compounds identified via virtual screenings (Eckert, 2007). However, these compounds may serve as starting point for lead optimizations to yield substances that have affinities in the low micromolar to nanomolar range (Tudor I. Oprea and Leeson, 2001). Therefore, hit structures identified in this initial screening could be used to refine database searches by looking for compounds that are structurally similar to them. Perhaps, the new structures show identical or even enhanced effects in ribozyme activation.

Furthermore, it has been shown that in ligand based virtual screenings combinations of 2D and 3D approaches predominantly identify hits with affinities in the low micromolar range (< 1 µM, Ripphausen et al. (2010)). Therefore, the combination of the already applied 3D method with 2D approaches, and possibly machine learning methods, may allow the identification of stronger binders (Ripphausen et al., 2010).

Additionally, other computational methods should be considered. Given that there are several crystal structures of the glmS ribozyme available, computer-assisted *de novo* design of bioactive compounds with drug-like properties could be tried. *De novo* design is the creation of bioactive compounds by incremental construction of a ligand model within a model of the receptor, the structure of which is known from X-ray or NMR data (Schneider, 2010; Schneider and Fechner, 2005). Thereby, novel molecular structures are produced from scratch with desired pharmacological properties (Schneider and Fechner, 2005). Together with rational refinements, i. e. ensuring the presence of an amino-group or equivalent for ribozyme activation, this may lead to interesting chemical structures, that are not necessarily GlcN6P analogs. This may in turn solve specificity concerns arising with respect to drug applications in humans, that do not have riboswitches but GlcN6P catabolizing enzymes.

Finally, it may also be expedient to search more data bases for possible hit structures and possibly expand the searches towards natural products that are available.

5.1.2 Detailed investigation of hit compounds screened from current Reymond prediction

The hit structures identified as glmS ribozyme activators (**C1**, **C11**, **D1**, **D3**, **D4**, **D7**, **E5**, **E9**, **F2**, **F5**) or inhibitors (**B7**, **C3**, **C8**, **C9**, **D2**, **D6**, **D9**, **E6**, **E8**, **F6**, **F7**, **F8**) should be investigated for concentration dependent modulation of ribozyme activity, if this has not been done already. For most promising hits cleavage rate constants should also be determined to allow comparison with GlcN6P and CGlcN6P. Furthermore, the already created glmS cleavage mutant (Figure 8.3 B) should be used, to descry binding and affinity of these compounds, for example by thermophoresis measurements. For this, the uncleavable glmS riboswitch mutant is GMPS transcribed and fluorescein labelled at its 5' end and subsequently used to determine dissociation constants (Section 5.1.7).

5.1.3 Define the mode of action of carba-sugars

Carba-sugars have been discovered as glmS ribozyme activators by screening a small, rationally designed GlcN6P analog library (Section 3.1.3.2 and 3.1.4). Furthermore, CGlcN was shown to inhibit bacterial growth with increasing concentrations. Of course, although *in vitro* data suggests that this is due to direct action on the glmS ribozyme, this has to be proven *in vivo*. For this, the total RNA content of *S. aureus* will be isolated from cells incubated in the presence and absence of CGlcN. After reverse transcription of the RNA to cDNA using random hexamer primers it is subjected to quantitative real-time PCR amplifications. This will define the relative amounts of glmS RNA originally present in untreated vs. treated cells. This experiment should allow to conclude whether CGlcN confers at least part of its detrimental effects due to constitutive activation of the glmS ribozyme and hence enforced degradation of the glmS mRNA by RNases. However, since CGlcN is an analog of GlcN and GlcN6P it is also possible that some of its effect is derived from interference with naturally occuring protein actions. Therefore, in a broader study, enzymes which convert GlcN, GlcN6P or close derivatives thereof should be investigated *in vitro* for their ability to recognize and potentially be inhibited by carba-sugars.

Another important question that will have to be addressed is how carba-sugars enter the bacterial cell. For CGlcN6P, it is very unlikely that passive diffusion through the cell membrane is taking place. In addition, it is questionable whether there are transporters that would transmit this charged molecule through the bacterial barriers. Therefore, masking of the phosphate group may allow passive diffusion of CGlcN6P (McGuigan et al., 2008).

For the unphosphorylated CGlcN however, it is very likely that this cyclitiol is taken-up via endogenous sugar transporters. The phosphoenolpyruvate:sugar phosphotransferase system (PTS) allows bacteria to specifically transport sugars across the cell membrane and phosphorylate them in the process. PTS are multi-protein transporters that are composed of two general energy coupling proteins, Enzyme I (EI) and a histidine-containing phosphoprotein (HPr) and several sugar-specific Enzymes II (EII). In *S. aureus* ptsG codes for EII recognizing glucose, glcA for an EII for glucoseamine and ptaA for N-acetyl-glucoseamine-EII module. Hence, constructing genomic deletion mutants of each of these PTS transporters or combinations thereof, would allow the investigation of CGlcN take-up. If staphylococci really absorb this compound via active transportation using one or a mixture of these PTS, minimal inhibitory concentrations are expected to rise in according mutant strains. Moreover, strains which contain a mutation in two, possibly all three PTS transporters would allow to estimate how much CGlcN or even CGlcN6P could passively diffuse into the cell. The construction of genomic deletion mutants is already described for staphylococci (McNamara, 2008) and directed mutagenesis by allelic replacement is now the most commonly used technique to alter the *S. aureus* genome. It involves the design of an appropriate insert for a deletion plasmid that contains a fusion of the 5' and 3' ends of the gene to be deleted. The plasmid can be amplified in *E. coli* and then brought into RN4220. This *S. aureus* strain can accept plasmid DNA isolated from *E. coli* as it is restriction endonuclease deficient. Finally, plasmids isolated from this strain can be tranferred into *S. aureus* Mu50 cells (Arnaud et al., 2004).

If CGlcN really is to be taken-up via PTS transporters it would imply that the compound will be phosphorylated to yield CGlcN6P, which was proven to be even more effective in glmS ribozyme activation *in vitro*. This bioactivation phenomenon of the prodrug CGlcN by PTS to the drug CGlcN6P should also be further investigated by isolating the phosphorylated cyclitiol variant from bacterial cell lysate. Methods like HILIC (introduced and discussed

in Sections 3.2.2.3 and 6.3.10) and metabolome analysis may be suitable for this. The latter enables the identification and quantification of primary metabolites in bacterial cells, which may provide insight into the fate of CGlcN. The characterization of the intracellular metabolism has been vastly investigated by Lalk and coworkers, who have established suitable methods for the investigation of the intracellular *Staphylococcus aureus* metabolome (Meyer et al., 2010). Established methods include HPLC-MS (high pressure liquid chromatography-mass spectrometry), GC-MS (gas chromatography-mass spectrometry) and NMR approaches (Meyer et al., 2010).

Since carba-sugars or other riboswitch-targeting compounds could be useful as new antibacterial drugs, it should be assessed early on whether these metabolite analogs have any adverse effects in *in vivo* models. The primary objectives of early *in vivo* preclinical toxicity testing of drug candidates is to characterize potential adverse effects, and to provide initial estimates of safety margins to determine if a compound is likely to be safe for use in humans, or whether to eliminate such molecules from further development (Fielden and Kolaja, 2008). Since there have been no riboswitches identified in higher eukaryotes yet, compounds aiming at these structures should not have any effect. But riboswitch modulators known to date are all metabolite analogs with relatively high similarity to the natural riboswitch ligand, ligands that are present in eukaryotes: TPP, adenine, guanine, FMN, GlcN6P. Therefore, it has to be investigated whether these analogs disturb processes in the host. Therefore, some preliminary testing could be performed by assaying riboswitch targeting compounds for toxic effect on human cell culture cells.

Another specificity test of riboswitch-modulator-mediated effects is the investigation of bacterial species that do not regulate their genes via the explored riboswitch. Therefore, carba-sugars should be tested on other Gram-positive organisms, which do not contain the glmS riboswitch. If bacterial growth is impeded here as well, this observation may provide a first hint at some off-target phenomena. Gram-positive organisms that do not control GlcN6P metabolism via the glmS ribozyme are *Streptococcus pneumoniae* and *Mycobacterium tuberculosis* (Blount and Breaker, 2006).

Gram-negative strains only seldomly carry the glmS ribozyme. Hence, pathogenic strains like *Yersinia pestis*, *Vibrio cholera*, *Helicobacter pylori*, *Haemophilus influenza*, *Escherichia coli*, *Francisella tularensis*, *Acinetobacter baumannii*, *Brucella melitensis* or *Salmonella enterica* could be used for these assays (Blount and Breaker, 2006). Gram-negative organisms may already pose another complication to specificity testing, as it may be possible that the compound is hindered in getting to its actual target by another barrier - the outer membrane.

Apart from investigating off-target effects on bacteria that do not contain the glmS ribozyme, it will also be of utmost interest to define the spectrum of organisms affected by carba-sugar action. There are several other pathogenic bacteria which are predicted to carry the glmS riboswitch, e. g. *Listeria monocytogenes*, *Enterococcus fecalis* or *Bacillus anthracis* (Blount and Breaker, 2006). Therefore, it would be interesting to subject these and other organisms to minimal inhibitory concentration (MIC) measurements, assess changes in growth curves, or determine minimal bactericidal concentrations (MBC) to define carba-sugar mediated effects on bacterial survival.

5.1.4 Second generation carba-sugars

Even though CGlcN6P binds to and activates the glmS ribozyme almost as efficiently as its natural metabolite GlcN6P, there is still room for improvement. The exchange of the ring

oxygen in the carba-compounds for a CH_2-group abolishes one hydrogen bond interaction between ligand and RNA according to crystal structures (Figure 5.1 A, Klein and Ferré-D'Amaré (2006)). Therefore, the synthesis of second generation of carba-sugars which reach better affinites, e. g. by restoring this hydrogen bond, is indicated.

One strategy for creating high affinity glmS ribozyme binders by rational design involves the modification of R to simple methyl, ethyl or propyl extensions, an aryl moiety or other heterocycles like imidazole (Figure 5.1 B). Depending on the linker length, the aryl-ring may possibly get involved in stacking interactions with the nucleobase G65 (Figure 1.7). Moreover, the placement of an alkine or acylester via a linker at R would allow to modify the carba-sugar at this position with a variety of azide-compounds by "click-chemistry", or carbonic acid fragments by a transesterification reaction (Figure 5.1 C and D).

5.1.5 Combination of vancomycin and CGlcN

Vancomycin is often combined with other antibiotics like gentamicin and rifampin, for the treatment of serious methicillin-resistant *S. aureus* infections (Deresinski, 2009). These combinations are desirable to overcome some shortcomings of this glycopeptide antibiotic, like poor tissue and intracellular penetration, lack of activity against organisms growing in biofilm, slow bactericidal effect, lack of interference with toxin production and lack of activity against some *S. aureus* isolates, including hVISA and VISA strains (Deresinski, 2007a,b).

Even though the role of CGlcN in aiding to overcome the first four deficits is unclear, it may present a novel means of rendering vancomycin-resistant staphylococcal strains susceptable again for this glycopeptide antibiotic. If CGlcN, which hampers GlmS-enzyme fidelity indirectly by targeting the glmS ribozyme, is used in combination with vancomycin it may convert vancomycin resistant strains back to being more vancomycin susceptable by antagonizing some of the resistant phenotype characteristics. Likewise, increased uptake of GlcNAc in Mu50 would aid CGlcN action, because it is likely that this carba-sugar is also taken-up by this PTS transporter.

Therefore, investigations as performed in Section 3.1.6 should be intensified and underlined by additional experiments, e. g. electron micrograph imaging which would allow an evaluation of changes in cell wall thickness upon treatment with CGlcN (Howden et al., 2010).

5.1.6 Synthesis and investigation of phosphorylated Streptozotocin *in vitro*

As Streptozotocin is known to be taken-up via PTS transporters, it is also evident that it will be phosphorylated *in vivo* (Lengeler, 1980). Hence, its active form is the C-6 phosphorylated variant inside bacteria.

In the *in vitro* studies of Streptozotocin-induced glmS ribozyme self-cleavage revealed induction of RNA scission at millimolar concentrations. It has been discussed previously (Section 3.1.7.2 and 4.3.2) that the lack of the phosphate group at C-6 of Streptozotocin very likely causes a significant decrease in EC_{50}-values (Table 3.2) for glmS ribozyme cleavage. This suggests that the phosphorylated variant of Streptozotocin may be even more potent in activating the glmS ribozyme *in vitro*. Therefore, phosphorylated Streptozotocin should be synthesized.
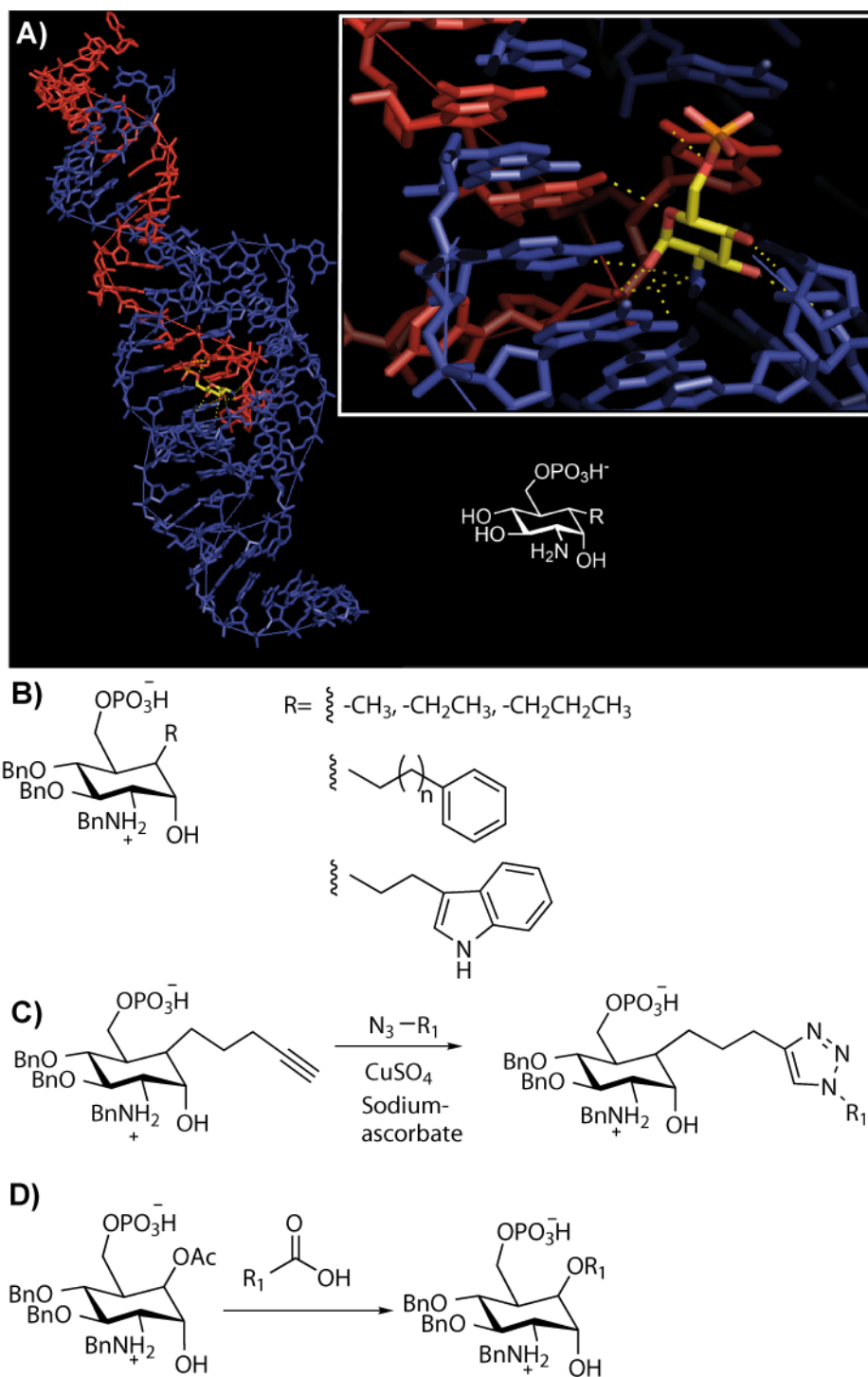
Figure 5.1: Second generation carba-sugars. Crystal structure of glmS ribozyme with GlcN6P. The inset zoomes in on the metabolite binding site of the glmS aptamer domain with GlcN6P bound and illustrates the hydrogen bond interaction the oxygen forms normally with adjacent nucleobases (A, Figure by Prof. Dr. Günter Mayer). Modifications of protected CGlcN6P at R for ethyl, methyl, propyl, aryl, or imidazole moieties (n=1-7, B). The insertion of an alkine linker allows modification of CGlcN6P with a library of azides via "click-chemistry" (C). The insertion of an acetylester linker allows modification of CGlcN6P with a library of carbonic acid molecules via a transesterification reaction (D).

5.1.7 Determination of binding constants of streptozotocin and CGlcN to glmS RNA via thermophoresis

Microscale thermophoresis is a novel technique that allows the determination of different interaction parameters, such as dissociation constants or binding kinetics based on the movement of molecules along a temperature gradient (Wienken et al., 2010; Duhr and Braun, 2006). To be able to monitor the movement of molecules, they have to be fluorescently labelled, or intrinsic fluorescence, such as tryptophan fluorescence in proteins, can be used. In the case of the glmS ribozyme, the RNA can be generated with a guanosine monophosphate thioate at its 5' end that will allow coupling to fluorescein (Section 6.4.1.1 and 6.4.1.3). For this, the cleavage deficient glmS mutant should be used to facilitate the mere investigation of affinities and no enzymatic activities, which already has been sufficiently analyzed using the metabolite-induced self-cleavage assay.

Once this assay has been tested for its validity with molecules known to interact with the ribozyme (like GlcN6P, Glc6P, GlcN etc., Klein and Ferré-D'Amaré (2006); Klein et al. (2007a)), it can be employed to investigate CGlcN, Streptozotocin, aminoglycosides and Reymond compounds for their interactions with this RNA. This may shed more light on structure activity relationships, or allow the identification of moieties tolerated in cofactor binding, but that are, in comparison with the metabolite-induced self-cleavage assay, not capable of ribozyme activation.

5.2 The thiM riboswitch of *E. coli*

Triazolethiamine (TT) and some of its derivatives were discovered as *thi*-box riboswitch activators *in vivo*. This section will briefly summarize how TT and its derivatives should be further characterized regarding their binding to *thi*-box riboswitches , their influence on bacterial metabolism or viability.

Even though affinity of TTPP has been determined via equilibrium dialysis and ITC (Chen et al., 2012), analogous information needs to be obtained for compounds that mimic TPP through metal chelating moieties. Aforementioned microscale thermophoresis measurements are in analogy also suitable to measure interactions between triazolethiamine compounds and the thiM riboswitch. In addition to the wild-type thiM RNA construct, the aptamer domain mutant used in Section 3.2.2, and other riboswitch classes distinct from TPP riboswitches should be used to exclude unspecific small molecule-RNA interactions.

Moreover, concentration dependent effects of metal chelating compounds **16** to **29** on thiM riboswitch activation should be tested using the reporter gene assay. These compounds enable thiM riboswitch activation independent from *in vivo* phosphorylation.

Together, these data will highlight structure activity relationships (SARs) and facilitate the design of triazolethiamine analogs with improved properties with respect to RNA binding and thiM riboswitch activation. Of course, these investigations can always be extended towards TPP riboswitches from other model organisms or clinically relevant pathogens.

The attempts of proving triazolethiamine phosphorylation *in vivo* using HILIC should be continued. Even though amounts of TTPP generated *in vivo* are not detectable against background, it may be possible to improve this signal-to-noise ratio by feeding TT to bacterial cells engineered to have increased thiamine metabolism. This could be achieved by a concommitant overexpression of proteins that are very likely using TT as substrate for phosphorylation, such as ThiK (Figure 1.12).

Possibly, also stable isotope labelling of TT-compounds may allow tracing and MS detection.

The impact of triazolethiamine compounds on β-galactosidase repression has been shown to be dependent on the bacterial strain used. Because TT and its non-metal-chelating derivatives need to be phosphorylated by bacterial enzymes before they can bind to and activate the thiM riboswitch, the genetic background of the bacterial strain can have a significant influence on thiM-mediated reporter gene expression.

These differences in genetic background should be addressed in future studies to learn not only about TT-compound metabolism, but also to illuminate the fates of other *thi*-box riboswitch activators, such as PT or oxythiamine. Therefore, MG1655 mutants should be constructed that contain the same thiG point mutation that renders DH5αZ1 cells thiamine auxotrophic (thi^{-1}, (Kay, 1972)). If this deletion causes MG1655-thi^{-1} cells to behave like DH5αZ1 cells in response to PT or TT compounds in their β-galactosidase repression, genes within the thiCEFGH cluster should be more closely investigated, since thiG itself has not directly been assigned to thiamine phosphorylation *in vivo* yet. The separate expression of these and other proteins involved in thiamine biosynthesis may enable an *in vitro* reconstitution of this metabolic pathway. This could be used to investigate compound alterations catalyzed by Thi-proteins in an extracellular context as an extension of what may happen *in vivo*.

Apart from this, MG1655 cells bear a mutation in the pyrE gene, which codes for orotate phosphoribosyltransferase responsible for metabolizing phosphoribosyl-pyrophosphate (PRPP) into orotidine-5-phosphate. As a result, levels of PRPP possibly increase, which may lead to enhanced purine and thiamine biosynthesis and, thus, probably higher levels of enzymes that phosphorylate thiamine and consequently the compounds described in Section 3.2.2 (Jensen, 1993). Therefore, a similar mutation may be brought into DH5αZ1 cells for comparison with MG1655 performance in the reporter gene assay.

Finally, a genetic variant of MG1655 cells in which the natural lacZ gene is deleted should be studied. Even though the presence of endogenous levels of β-galactosidase do not abolish TT-compound effects, maybe the enzyme is responsible for having faster ONPG-conversions in comparison to DH5αZ1 cells. This strain can be obtained from the Coli Genetic Stock Center (CGSC) at Yale University, USA.

Additionally, the use of fragments identified by Cressina et al. in 2011 for crystallization in complex with the thiM riboswitch revealed interesting abilities of the aptamer domain to interact with small molecules deficient in a pyrophosphate (-like) moiety. A nucleobase was observed to flip into the binding pocket allowing enhanced interaction with groups of the ligand otherwise not engaged (personal communication Katie Deigan). Therefore, the thiM riboswitch should be crystallized in the presence of TT and its metal-chelating derivatives. It would be interesting to investigate whether similar mechanisms are employed in their recognition. Especially compound **14**, whose *in vivo* phosphorylation is enigmatic, could bind and activate the thiM riboswitch through a similar interaction.

5.2.1 Investigation of antibacterial effects on *H. influenza* and other bacterial species

Haemophilus influenza, which is known to control essential genes via *thi*-box riboswitches, has been used to monitor antibacterial effects of TT compounds. However, since this strain is fairly difficult to cultivate under minimal conditions, other bacterial species should be considered for the investigation of antibacterial effects.

The decrease in bacterial growth in *E. coli* indicates that even when compounds interfere

with thiM riboswitches that do not control essential genes, a phenotypic effect can be observed. Therefore, growth curves, agar diffusion tests or minimal inhibitory concentration tests may be performed for other bacterial species, like *Staphylococcus aureus* for example that do not regulate essential genes via *thi*-box riboswitches.

Another interesting organism for the investigation of antibacterial effects is *Mycobacterium tuberculosis* due to its thiamine prototrophy. As these cells refrain from thiamine take-up and depend entirely on their own thiamine biosynthesis (Du et al., 2011). Inhibiting this metabolic pathway may have detrimental effects on the bacterium. The thiamine biosynthetic genes thiC, thiD, thiS, thiF, iscS, thiG, thiO and thiL are essential for *M. tuberculosis* (Sassetti et al., 2003). Of them thiO and thiL are under riboswitch control. Therefore, if TT compounds are able to passively diffuse into the cells or enter them via thiamine carrier independent mechanisms, they may have effects on this recalcitrant bacterium.

Additionally, the filarial endobacterium *Wolbachia* was found to contain a *thi*-box riboswitch, which controls the expression of a putative membrane protein (personal communication Alexander Müller). Therefore, the impact of TT compounds on *Wolbachia* growth should be assayed.

5.3 Identification of modulating compounds for other riboswitch classes

The variety of screening approaches discussed earlier in this work for the glmS ribozyme as well as for the preQ$_1$ and *thi*-box riboswitches (Sections 3.1.1, 3.2.1 and 3.3.2) can easily be transferred to other riboswitch classes or to the same riboswitch class from different organisms. A reporter gene assay in analogy to the preQ$_1$- or the thiM system has been employed already to screen for adenine riboswitch modulators (refer to Alexander Müller's thesis for details, Müller (2011)). Additionally, the preQ$_1$ screening system can be used for the screening of prequeuosine analogs (Section 3.3.2).

So far, only five different classes of riboswitches are addressed by artifical ligands, including lysine, FMN, TPP and purine riboswitches as well as the glmS ribozyme (Figure 1.5). Therefore, there is a variety of undrugged riboswitches left (see Section on riboswitch classes, 1.1.1) to be addressed. Screening of small, rationally designed libraries has proven to be a very promising approach for riboswitch modulator identification. However, future experiments and evaluations will have to reveal, if metabolite analogs survive the tough assessment of off-target effects in toxicology and *in vivo* testing, as they are, as of now, very likely, to interact with proteins also.

6 Methods

This chapter describes the standard methods used for all experiments whose data is referred to in the results or which are discussed throughout this work. The main experimental areas include working with nucleic acids (Section 6.1 and Section 6.2) and working with bacteria (Section 6.3). Techniques employed in these two fields are often prerequisites of methods used for the interaction analysis (Section 6.4).

6.1 Working with nucleic acids

Investigating RNA elements like riboswitches demands the use of a fairly broad spectrum of methods dealing with nucleic acids. In the following sections protocols for the amplification of DNA, the *in vitro* generation of RNA, the labelling, enrichment, purification, modification and analysis of nucleic acids are given.

6.1.1 Preparation of DEPC water

In order to prepare RNase free water diethylopyrocarbonate (DEPC) was added to ddH_2O in a ratio of 1:500 (v/v). After vigorous mixing, the solution was incubated over night at room temperature (RT) in a fume hood. Then, the solution was autoclaved at $121\,°C$ for $60\,min$ for sterilization and to destroy unreacted DEPC (Wiener et al., 1972).

6.1.2 Agarose gel electrophoresis

Agarose gels were used to check the yield of PCR reactions or integrity of RNA. These gels have a wide range of separation, but a relatively low resolving capacity. Varying the concentration of agarose, nucleic acid fragments from about 20 to 50,000 bp can be separated. $2.5\,\%$ (w/v) gels have been used to separate up to $\sim 1000\,nt$ long PCR products from shorter primers. $1\,\%$ (w/v) gels were used to separate longer sequences, e. g. plasmids.

The agarose powder was suspended in $0.5\times$ TBE, melted and kept at $65\,°C$. $0.5\times$ TBE was used as gel running buffer as well. Agarose solution ($40\,ml$) was mixed with $4\,µl$ ethidium bromide and poured into the gel cast. Before loading, samples were mixed 1:1 with $2\times$ gel loading buffer (7.1). The gel was run at $140\,V$ for $15\text{-}25\,min$. The bands were visualized in a UV transilluminator (BioRad) and evaluated by comparison with the DNA or RNA ladder (7.6).

6.1.3 Polymerase chain reaction

PCR was used to exponentially amplify defined DNA sequences by *in vitro* enzymatic replication. When the dsDNA template is heated to $94\,°C$ it is separated into single strands that do not reanneal when rapidly cooled to $60\,°C$. The primers added are complementary to the 3' and 5' ends of the DNA template and are now able to bind to their target sites.

This allows the DNA polymerase to start the amplification at 72 °C. Since Kary Mullis introduced the use of a thermostable DNA polymerase to this concept, several PCR cycles can be performed in a row without having to add new enzyme after each heating to 94 °C (Saiki et al., 1988). Here two different thermostable polymerases where used whose specific characteristics were of advantage.

6.1.3.1 Taq PCR

To amplify DNA templates larger than 600 nt a Taq PCR was performed. The Taq polymerase derives from the thermophilic bacterium *Thermus aquaticus* (Chien et al., 1976), which survives high temperatures during the PCR reaction. Even though it can replicate a 1000 bp strand in less than 10 s at 72 °C it has no 3'-5' exonuclease activity. Due to this lack of proof-reading a single base substitution error of about 1 in 9000 nt has been measured by (Tindall and Kunkel, 1988).

Reagent	Amount	Stock	Resultant
Taq PCR buffer (Promega) with MgCl$_2$	10 µl	10×	1×
5' Primer	1 µl	100 µM	1 µM
3' Primer	1 µl	100 µM	1 µM
dNTP Mix	0.8 µl	25 mM	0.2 mM
DNA template	1 µl		1-10 nM
Taq DNA Polymerase	0.5 µl	5 U/µl	
water	85.7 µl		
total volume	100 µl		

Table 6.1: Pipetting scheme for Taq polymerase chain reaction

Standard PCR conditions		
Denaturing	94 °C	60 s
Annealing	60 °C	60 s
Extension	72 °C	90 s
Heated Lid	110 °C	

Table 6.2: Standard reaction conditions for PCR

6.1.3.2 Pfu PCR

DNA sequences below 1000 nt were amplified using Pfu PCR (homemade). The Pfu DNA polymerase, isolated from *Pyrococcus furiosus*, comprises a 3'-5' exonuclease and thus proof-reading activity. Although not as fast as the Taq, only 1 in 1.6×10^6 mismatches occur (Lundberg et al., 1991). This makes the Pfu DNA polymerase a desirable tool for exact DNA amplification. For this PCR same standard conditions were used as for Taq PCR reactions. Whenever exact amplification of DNA sequences longer than 1000 nt was necessary, a commercially available Pfu polymerase was used (7.3).

Reagent	Amount	Stock	Resultant
Pfu PCR buffer	10 µl	10 ×	1 ×
MgCl$_2$	8 µl	25 mM	2 mM
5'Primer	1 µl	100 µM	1 µM
3'Primer	1 µl	100 µM	1 µM
dNTP Mix	0.8 µl	25 mM	0.2 mM
DNA template	1 µl		1-10 nM
Pfu DNA polymerase	1 µl	2.5 mM	
water	77.2 µl		
total volume	100 µl		

Table 6.3: Pipetting scheme for Pfu polymerase chain reaction

6.1.3.3 Site-directed mutagenesis

Site-directed mutagenesis, first described by Hutchison et al. (1978), was performed to obtain
e. g. the glmS ribozyme cleavage mutant or the thiM riboswitch mutant variant. The
mutagenic primers (7.10) were 30-32 nt in length centering the changed nucleotide(s).
Both mutagenic primers must contain the desired mutation and anneal to the same sequence
on opposite strands of the plasmid. Primers should be 25 to 45 bp in length and contain
app. 10 to 15 bp of the correct sequence up- and downstream of the mutation. The melting
temperature T$_m$ should be over or equal to 78 °C and can be calculated according to formula

$$T_m = 81.5 + (0.41(\%GC)) - \frac{675}{N - \%mismatch} \tag{6.1}$$

or formula

$$T_m = 81.5 + 0.41(\%GC) - \frac{675}{N}, \tag{6.2}$$

where N is the primer length in basepairs, *% GC* and *% mismatch* are integers.
   The GC-content should be over 40 % and primers should start with a G or C nucleobase.
It is important to keep the primer concentration in excess. Stratagene suggests varying the
amount of template while keeping the concentration of the primer constantly in excess.

Reagent	Stock	Volume [µl]	Resultant
reaction buffer	10 ×	5	1×
Vector		x	80 ng
5' Primer		1.25	12.5 pmol
3' Primer		1.25	12.5 pmol
dNTP mix (provided)		1	
Quik sol. Reagent		1.5	
water	ad 50 µl		

Table 6.4: Pipetting scheme for site-directed mutagenesis using a QuikChange Lightning Kit
from Stratagene.

80 ng of vector containing the insert to be mutated, 12.5 pmol of primer (see 7.10 for
designed primers) and other components were mixed as indicated in Table 6.4. After mixing,

1 µl of QuikChange Lightning Enzyme was added. For the negative control the reaction mix was also prepared as shown above, only primer volumes were substituted by water. The PCR reaction was run under the parameters stated in Table 6.5. 5 min were chosen to secure complete elongation, although elongation time for the plasmid was calculated to be shorter.

	Cycles	Temperature	Time
Initial Denaturation	1	95 °C	2 min
Denaturation	2-18	95 °C	20 s
Annealing		60 °C	10 s
Elongation		68 °C	30 s/kb of plasmid
Final Elongation		68 °C	5 min

Table 6.5: PCR parameters of site-directed mutagenesis.

The PCR samples were purified using the Nucleospin Extract II kit (Macherey Nagel, 6.1.4.2). Provided instructions were followed, except for the elution step, where 2× 15 µl water were used. Hereafter, a DpnI digest was performed by addition of 2 µl enzyme (provided with Stratagene kit) to each sample and incubation at 37 °C for 30 min. The Dpn I endonuclease is specific for methylated and hemimethylated DNA and is used to digest the parental DNA template and thus to select the mutation-containing DNA. Another Nucleospin purification protocol was followed, including changes mentioned above, before the whole eluate was used for a transformation into 100 µl XL10 GOLD cells (6.3.1.2). All of the transformation mix was plated on an agar plate containing the appropriate antibiotic.

This site-directed mutagenesis protocol should be performed for vector without any mutagenic primers, to check for DpnI enzyme function by estimating the background of unmutated plasmids still present after transformation into XL10 GOLD cells.

6.1.3.4 Quantitative real-time PCR

Quantitative real-time PCR (qPCR) is a method to quantitatively evaluate the amount of target DNA molecules and to either define an absolute number of copies or to get a relative estimate compared to a standard condition. In this study, the qPCR $\Delta\Delta C_T$ method was used (Livak and Schmittgen, 2001), which enabled an estimate of relative mRNA levels compared to control conditions.

For this a mastermix according to Table 6.6 is assembled in a PCR-template free environment. Primers and all solutions used for the mastermix were opened before cDNA vial was, to avoid any DNA contamination. Once the mastermix was prepared, the enzyme was added last and the mix was put in the PCR stripes (19 µl per well). Then 1 µl sample was added and every row was sealed with a lid-stripe immediately afterwards. Before actual PCR reaction, the stripes were shortly centrifuged to collect reaction in the bottom of the well.

Reagent	Amount	Stock	Resultant
Rox	0.5 µl	1:10	
PCR buffer	2 µl	10×	1×
MgCl$_2$	1.6 µl	25 mM	2 mM
SYBR green	0.2 µl	100×	1×
5' primer	1 µl	10 µM	0.5 µM
3' primer	1 µl	10 µM	0.5 µM
dNTPs	0.025 µl	100 mM	125 µM
Taq Genaxxon	0.4 µl	5 U	1.25 U
ddH$_2$O ad 19 µl			

Table 6.6: Pipetting scheme for qPCR.

	Cycles	Temperature	Time
Initial Denaturation	1	95 °C	30 s
Denaturation	2-40	95 °C	10 s
Annealing		55 °C	10 s
Elongation		72 °C	30 s
Melting curve		95 °C to 25 °C	

Table 6.7: qPCR parameters.

Samples were usually run in triplicates and at least three non template controls (NTC) were also included into the assay. After the PCR reaction samples were run on an agarose gel to evaluate them for unspecific amplifications such as primer dimers.

6.1.4 DNA and RNA purification

After enzymatic reactions nucleic acids had to be purified to separate them from proteins or to desalt before further enzymatic treatment. There were two options for purification, namely phenol-chloroform extraction followed by precipitation (6.1.4.1) and the use of a commercially available kit (6.1.4.2).

6.1.4.1 Phenol-chloroform extraction and precipitation of nucleic acids

Phenol-chloroform extraction is used to isolate DNA or RNA from proteins. To one volume of sample one volume of phenol was added, vortexed well and centrifuged at maximum speed for 3 min. The aqueous phase was transferred into a new microcentrifuge tube and two volumes of chloroform were added, followed by vortexing and centrifuging (see above). Again the upper phase was separated, 1/10 volume 3 M NaOAc, 1 µl glycogen and three volumes of EtOH abs. were added, gently mixed and incubated at -80 °C for 30 min. Now the samples were centrifuged at maximum speed (Eppendorf tabletop centrifuge 5417C, 20817 rcf) for 20-30 min at 4 °C. Afterwards, the supernatant was removed, the pellet was washed with 100 µl 70 % EtOH, centrifuged for 5 min and air-dried after the supernatant had been removed. The RNA or DNA was taken up in (DEPC) water (1/10 of the starting volume) and kept at -20 °C until use.

6.1.4.2 Nucleospin columns

The NucleoSpin Extract II kit from Macherey-Nagel was used for purifications of DNA after PCR or restriction digests, DNA extractions from agarose gels, as well as desalting or elimination of shorter DNA fragments (i.e. primer dimers).

The procedures stated in the manufacturers manual were closely followed, except for elution steps. Here, elution was done with $2\times$ $20\,\mu$l of either elution buffer NE or ddH$_2$O/DEPC H$_2$O.

6.1.5 *In vitro* transcription

The transcription of DNA into RNA can be accomplished *in vitro* by designing the template to contain a T7 promotor at its 5' end (usually introduced by PCR). The first 2-3 nucleotides to be transcribed should be guanines, because the T7 RNA polymerase affinity for this purine is higher compared to that of other nucleotides. This puts a more efficient transcription into favor.

To prevent inhibitory effects of accumulating pyrophosphate, which is released when a nucleoside triphosphate is incorporated into the growing chain, inorganic pyrophosphatase (IPP) is added. It catalyzes the hydrolysis of inorganic pyrophosphate to form orthophosphate. Transcription of dsDNA containing a T7 RNA polymerase promoter was performed at standard conditions (Table 6.8). The reaction was incubated at 37 °C over night. To body-label RNA, $1\,\mu$l α ^{32}P-GTP was added.

Reagent	Amount	Stock	Resultant
Tris pH 7.9	$20\,\mu$l	$200\,$mM	$40\,$mM
MgCl$_2$	$25\,\mu$l	$100\,$mM	$25\,$mM
DTT	$5\,\mu$l	$100\,$mM	$5\,$mM
NTP Mix	$10\,\mu$l	$25\,$mM	$2.5\,$mM
α ^{32}P-GTP	$1\,\mu$l	$10\,\mu$Ci/μl	$10\,\mu$Ci
RNasin	$1.24\,\mu$l	$40\,$U/μl	$0.5\,$U/μl
Inorganic pyrophosphatase	$0.2\,\mu$l	$2\,$U/μl	$0.02\,$U/μl
dsDNA template	$10\,\mu$l	150-300 pmol	1.5-3 μl
T7 RNA polymerase	$5\,\mu$l	$50\,$U/μl	$0.5\,$Uμl
water	$22.56\,\mu$l		
total volume	$100\,\mu$l		

Table 6.8: Pipetting scheme for *in vitro* transcription.

6.1.6 Polyacrylamide gel electrophoresis

Polyacrylamide gel electrophoresis was used to separate DNA or RNA samples either for preparative or analytical purposes (Chrambach and Rodbard, 1971). Glass plates were washed with soap and water, rinsed with deionized water, thereafter with 80 % ethanol, dried with paper towels. Spacers and combs are washed and dried like glass plates. Those glass plates without pocket are put on a pipet-tip-box under the hood. Since three spacers are needed per gel, one on each side, one on the bottom, they were aligned to glass plate edges. The glass plate with pocket was put on top of this assembly and spacers and glass plates are

adjusted, so that everything was level and so that there was no room between spacers. To fix this construction, clamps were used (one at the bottom, two on each side). Now the PA gel solution was prepared by mixing solution C, D and B (see 7.1) in appropriate ratios in an Erlenmeyer flask to obtain wanted thickness and number of gels (refer to 6.9). APS (10 %) and TEMED were added in stated amounts. Erlenmeyer flask was swirled once to mix components and gel was quickly poured into prepared glass chamber, the comb was added last. Finally the gel solidified dependent on PA percentage for 15-30 min (polymerization control was used as guide). After polymerization comb and bottom spacer were removed and wells were rinsed with water. Gel was placed into the running chamber and buffer tanks were filled with 1× TBE buffer. Gel was pre-run for 30 min. Before samples were loaded (70 µl for thick gels, 15 µl for thin gels), pockets were rinsed again with buffer.

Gel Percentage	Solution	Amount	in ml		
		100	70	50	30
4 %	C	16	11.2	8	4.8
	D	74	51.8	37	22.2
	B	10	7	5	3
5 %	C	20	14	10	6
	D	70	49	35	21
	B	10	7	5	3
6 %	C	24	16.8	12	7.2
	D	66	46.2	33	19.8
	B	10	7	5	3
8 %	C	32	22.4	16	9.6
	D	58	40.6	29	17.4
	B	10	7	5	3
10 %	C	40	28	20	12
	D	50	35	25	15
	B	10	7	5	3
12 %	C	48	33.6	24	14.4
	D	42	29.4	21	12.6
	B	10	7	5	3
15 %	C	60	42	30	18
	D	30	21	15	9
	B	10	7	5	3
17 %	C	68	47.6	34	20.4
	D	22	15.4	11	6.6
	B	10	7	5	3
20 %	C	80	56	40	24
	D	10	7	5	3
	B	10	7	5	3
	APS 10 %	0.8	0.56	0.4	0.24
	TEMED	0.04	0.028	0.02	0.012

Table 6.9: PA-gel recipe Shown are the ratios of solutions B, C and D for gels ranging from 4-20 %. 30 ml are enough for one thin gel, 50 ml for one thick gel.

Gel Percentage	Position bromophenol	Position xylenecyanol
5	35 nt	130 nt
6	26 nt	106 nt
8	19 nt	70-80 nt
10	12 nt	50 nt
20	8 nt	28 nt

Table 6.10: Migration of DNA fragments with dyes in denaturing polyacrylamide gels.

6.1.7 RNA work-up

After *in vitro* transcription the samples (100 µl) were treated with 0.5 µl of DNaseI (5 U/µl) for 10-20 min at 37°C and purified by polyacrylamide gel electrophoresis. For this, samples were mixed with 2× sucrose loading buffer and 50 µl were loaded in each pocket of a thick PA-gel of needed percentage. The gel was pre-run for 15-30 min. The gel was run at a constant power of 20 W and approximately 360 V. Once the RNA to be separated was in the middle of the gel (for orientation xylenecyanol and bromphenol blue, see Table 6.10, were used), the glass plates were removed and gel is wrapped in saran wrap. Placing the gel on a fluor-coated silica plate allowed UV shadowing at 254 nm. The right sized bands were cut out with a sterile scalpel blade, crushed with a 1 ml plastic tip, suspended in 500 µl 0.3 M NaOAc (pH 5.4) and incubated at 65 °C for 90 min under vigorous shaking. Afterwards gel suspension was passed through a 5 ml syringe packed with silanized glass wool followed by 2-5 washings with 100 µl 0.3 M NaOAc solution. For short oligos or small amounts of RNA 1 µl of glycogen was added to make even small pellets visible. The RNA was precipitated with three volumes of EtOH abs., incubated for 20 min at -80 °C and centrifuged at 4 °C for 30 min. The supernatant was taken off and a washing with 100 µl 70 % EtOH was performed. After another spin for 5 min at RT and removal of the supernatant the pellets were air-dried and redissolved in DEPC water (usually 10 µl).

6.1.8 Concentration measurements

There were two devices used to determine nucleic acid concentration (dsDNA, ssDNA, RNA). Either the concentration of nucleic acid solutions was determined using a UV-spectrophotometer which measured the absorption at a wavelength of 260 nm (Abs 260) in a quartz cuvette (path length 1 cm). The concentration c was calculated using the Lambert-Beer law

$$c = Abs_{260} \cdot d \cdot \varepsilon \quad , \tag{6.3}$$

where d is the dilution factor and ε the absorption coefficient (depending on the nucleic acids to be measured: dsDNA= 50 µg/ml, ssDNA= 30 µg/ml, ssRNA= 40 µg/ml).

Or nucleic acid concentration was measured using the NanoQuant infinite 200 (Tecan). Here, 2 µl of samples were applied to previously blanked spots and measured using the correct parameters (ssDNA/dsDNA/RNA) on the NanoQuant plate (up to 16 samples).

6.1.9 5' Phosphorylation

Phosphorylation as needed for 5' end labelling of glmS ribozyme was performed by using the T4 polynucleotide kinase (PNK, (Berkner and Folk, 1977) and (van de Sande et al., 1973)). This enzyme originating from the T4 bacteriophage, catalyzes the transfer of the γ-phosphate of ATP to the 5' end of DNA or RNA. Synthetically synthesized oligonucleotides (e. g. needed for chemical probing analysis) which do not contain a phosphate at their 5' end, were used without any further treatment, whereas digested plasmid fragments or *in vitro* transcribed RNA had to be dephosphorylated using calf intestine alkaline phosphatase (CIAP, 6.1.10). The reaction mixture as shown in Table 6.11 was prepared on ice, before an incubation at 37 °C for 30-60 min took place. The product was desalted and excess γ-ATP removed by passing through a G25 column (6.1.11.1).

Reagent	Amount	Stock	Resultant
T4 PNK buffer	2 µl	10×	1×
CIAP DNA/RNA	45 pmol/ 3 µl	0.5 µM	
P-ATP	2 µl	20 µCi	10 µCi/µl
T4 PNK (NEB)	2 µl	10 U/µl	20 U
RNasin	0.3 µl	40 U/µl	12 U
water (DEPC)	9.7 µl		
total volume	20 µl		

Table 6.11: Pipetting scheme for 5' phosphorylation.

6.1.10 5' Dephosphorylation

Calf intestinal alkaline phosphatase (CIAP, Fosset et al. (1974); Chappelet-Tordo et al. (1974)) catalyzes the hydrolysis of 5' phosphate groups from DNA, RNA, and ribo- and deoxyribonucleoside triphosphates. This enzyme is used to prevent recircularization and religation of linearized cloning vector DNA by removing phosphate groups from both 5'-termini and may also be used for the dephosphorylation of 5' phosphorylated ends of DNA or RNA for subsequent labeling with $\gamma\,{}^{32}$P-ATP and T4 polynucleotide kinase (Section 6.1.9). CIAP is active on 5' overhangs, 5' recessed and blunt ends.

Reagent	Stock	Amount	Resultant
CIAP buffer	10×	5 µl	1×
BSA	10×	5 µl	1×
RNA/DNA template		1.5 µM/75 pmol	
CIAP	20 U/µl	0.85 µl	17 U
RNasin	40 U/µl	0.5 µl	20 U
DEPC water	ad 50 µl		
Total volume	50 µl		

Table 6.12: Pipetting scheme for 5' dephosphorylation.

All components stated in Table 6.12 were mixed and the enzymes RNasin and CIAP were added last. The first incubation took place at 37 °C for 15 min, after which 0.5 µl of CIAP (20 U/µl stock) were added, followed by the second incubation step of 15 min at 55 °C, after which 0.5 µl 0.5 M EDTA were added. Hereafter, the enzyme was inactivated by incubation

at 75 °C for 10 min. The subsequent addition of 150 µl DEPC water was followed by a phenol-chloroform extraction and sodiumacetate precipitation (Section 6.1.4.1). The pellet was dissolved in 5 µl DEPC water of which 3 µl were used for subsequent phosphorylation reactions and the remaining 2 µl were run on an agarose gel to check for integrity.

6.1.11 Gel filtration

Gel filtration separates molecules according to their size as they pass through a gel filtration medium packed in a column. This method was used to separate nucleic acids from unincorporated nucleotides, to desalt or rebuffer samples. Since the molecules do not bind to the filtration medium, the buffer conditions do not affect resolution. Therefore, a convenient buffer for following experiments or one suitable to the preservation of sensitive molecules can be used for elution. The gel filtration medium is a porous matrix of spherical particles that are inert as well as chemically and physically stable. As the buffer passes through the column, molecules that are larger than the pores of the matrix are unable to diffuse into the pores and pass through the column. Smaller molecules diffuse into the pores and are delayed in their passage down the column (Healthcare, 2008). There were two different gel filtration devices used (see Sections 6.1.11.1 and 6.1.11.2).

6.1.11.1 G25 columns

According to the GE booklet (Healthcare, 2008), the MicroSpin G25 columns, which contain a Sephadex resin, are designed for the rapid purification of DNA for applications, including desalting, buffer exchange, and removal of unincorporated nucleotides from end-labelled oligonucleotides. They can be used for any DNA greater than 10 bases in length. For all applications the instructions provided by the manufacturer were followed. Radioactive phosphorylation reactions were usually passed through the column after it had been washed with 100 µl DEPC water.

6.1.11.2 NAP-10 columns

NAP-10 columns follow the same principle as G25 columns (Sephadex resin), but require only gravity to run and no microcentrifuge steps. They were used to purify GMPS transcribed RNA samples from excess GMPS-nucleotide before being used for biotin- or fluorescein-labelling (Sections 6.4.1.1). After cap and bottom of NAP-10 colum were removed, columns were washed with 15 ml DEPC water. After a maximum of 1 ml sample was applied to the dry column, elution followed adding 1.5 ml DEPC water. Drops were collected in approximately 200 µl aliquots for sodiumacetate precipitation.

6.2 RNA analysis

6.2.1 Secondary RNA structure analysis

The function of RNA molecules *in vitro* and *in vivo* often depends on their secondary and tertiary structure, as well as on the information encoded in their Watson-Crick base-pairing potential. Therefore, chemical probing can be used to elucidate the secondary structure of the ribozymes and riboswitches bound to their ligand or in their apo-state.

6.2.1.1 Chemical Probing

In chemical probing, those positions in the RNA structure that are single stranded are sensitive to chemical modifications. Three different chemicals, all attacking different nucleobases, were used.

Dimethylsulfate (DMS) alkylates the Watson-Crick positions of adenosines (N1) and cytidines (N3) not involved in base pairing or tertiary-structure hydrogen bonding. Therefore, four reaction tubes containing the reaction mixture (Table 6.13) with HEPES (0.5 M stock pH 7.8, final concentration 50 mM) as probing buffer were prepared. Just prior to use, the DMS was diluted (1 µl of 10.56 M DMS stock in 16.6 µl of 100 % ethanol to result in 600 mM). Further dilution to 300, 150 and 75 mM occurred. 1 µl of the different DMS dilutions was added to each tube. The final reaction concentrations were then 60, 30, 15 and 7.5 mM (Rentmeister et al., 2008; Ziehler, 2000).

Kethoxal alkylates the N1 and 2-NH_2 Watson-Crick positions of guanosines not involved in base-pairing or tertiary structure hydrogen bonding. The procedure and probing buffer for the four reaction tubes was the same as for DMS, except prior to use a 4.27 M stock of kethoxal was diluted (1 µl of 4.27 M kethoxal stock in 20.35 µl DEPC water results in 200 mM). Further dilution to 100, 50 and 25 mM was performed and 1 µl of each added to a tube. The final reaction concentrations were thus 20, 10, 5 and 2.3 mM (Rentmeister et al., 2008; Ziehler, 2000).

Reagent	Amount	Resultant
RNA	1 µl	0.9 µg/ 20 pmol/ 2 µM
probing buffer	1 µl	1 ×
100 mM MgCl$_2$	0.5 µl	5 mM
1 M KCl	0.5 µl	0.5 M
DEPC water	ad 9 µl	

Table 6.13: Pipetting scheme for chemical probing reactions.

CMCT (1-Cyclohexyl-3-(2-morpholinoethyl)carbodiimide metho-*p*-toluenesulfonate) alkylates the N3 Watson-Crick position of uridines which are not involved in base pairing or tertiary structure hydrogen bonding. Different reagents are mixed according to Table 6.13. As probing buffer potassiumborate (0.5 M stock; 50 mM final) was used. Prior to use, CMCT was heated to 37 °C and vortexed well to ensure complete solubilization of reagent. 0.5 M CMCT is immediately diluted to 250 mM and 125 mM. Final concentrations in the probing reactions were 50, 25 and 12.5 mM (Rentmeister et al., 2008; Ziehler, 2000).

To achieve final concentrations stated above, 1 µl of the chemical was added to the prepared mix (Table 6.13). One tube, where DEPC water was added instead of the chemical, was used as negative control. The reactions were incubated at RT for 20 min and stopped by addition of 2 µl of 3 M NaOAc and 30 µl ethanol abs. Upon precipitation at -80 °C (20 min), samples were centrifuged at 20817 g, 4 °C for 30 min. The air-dried pellet was redissolved in 40 µl RNase-free water. For the primer extension that followed, 4 µl were used.

6.2.1.2 Reverse Transcription for chemical probing

Reverse transcription was performed after the reaction of different alkylating reagents with the RNA as mentioned in Section 6.2.1.1. The reverse transcriptase will stop upon encountering alkylated Watson-Crick determinants, thus revealing which nucleotides in the RNA sequence

are paired and which are single stranded. Strong secondary structure, such as hairpin loops within the RNA, can cause the enzyme to pause, creating a prematurely terminated product. Therefore, it is essential to perform a reaction on an unmodified RNA as negative control.

Reagent	Amount	Resultant
5× first strand buffer	4 µl	1×
0.1 M DTT	2 µl	0.01 M
Chemically modified RNA	4 µl	
5' Kinased RT Primer	1 µl	
25 mM dNTP mix	0.4 µl	
DEPC water	7.6 µl	
total volume	19 µl	

Table 6.14: Pipetting scheme for reverse transcription using Superscript II enzyme.

The reverse transcription was carried out using the Superscript II enzyme (Invitrogen). Different components of the reaction were mixed as indicated in Table 6.14, incubated for 10 min at 65 °C followed by a cool down to 0 °C for 1 min. Upon addition of 1 µl of Superscript II enzyme, a 50 min elongation step at 42 °C and an inactivation at 70 °C for 15 min occurred. RNase H (1 µl) was used to digest the RNA strand of the DNA-RNA duplex in 20 min at 37 °C. These reactions were followed by sodium acetate precipitation using 2 µl and 66 µl ethanol abs. (cool for 15 min at -80 °C). Supernatant was removed and the dry pellet was resuspended in 30 µl 1× sucrose loading buffer.

The location of primer-extension terminations is determined by comparison to didesoxynucleotide sequencing reactions using the same primer and template as the RNA being examined (Ziehler, 2000).

6.2.1.3 Sequencing ladder

A sequencing reaction of a DNA template of RNA used for the chemical probing should be carried out in order to serve as standard. The 5' end labelled 3' primer already prepared for the reverse transcription is used here as well. 5 pmol (in 5 µl) of the PCR product were treated with 1 µl exonuclease I (10 U/µl) and 1 µl shrimp alkaline phosphatase (SAP, 2 U/µl), supplied with the Sequenase Version 2.0 PCR product sequencing kit, USB.

The exonuclease I removes residual single-stranded primers and any other single-stranded DNA produced by PCR, whereas the SAP removes the remaining dNTPs from the PCR mixture. After an incubation at 37 °C for 15 min both enzymes were inactivated at 80 °C (15 min).

Then the 5' end labelled primer (5-10 pmol) was annealed to the pre-treated DNA (6 µl) and the volume adjusted with water to 10 µl. This was incubated at 100 °C for 2-3 min, quickly placed on ice afterwards and kept there until needed for the next step.

Reagent	Amount
Termination mix (ddA, ddC, ...)	2.5 µl
Sequenase 10× buffer	0.6 µl
Annealed DNA mixture	2.0 µl
DTT 0.1 M	0.2 µl
Sequenase	0.7 µl
total volume	6.0 µl

Table 6.15: Pipetting scheme for termination reactions of the sequenase sequencing.

Finally, the termination reactions (four tubes, one for each didesoxynucleotide) were prepared as shown in Table 6.15 and incubated for 10 min at 37 °C. The reaction was stopped by addition of 1 µl 3 M NaOAc, 30 µl EtOH abs. and the DNA was precipitated (-80 °C, 15 min, centrifuged 30 min at 20817 g). Once supernatant was taken off, the pellet was resuspended in 6 µl 1× sucrose loading buffer. The samples were heated to 75 °C for 2 min immediately before loading and 2-3 µl were applied to the gel in the order GATCGTAC.

6.2.1.4 Sequencing Gels

Sequencing gels were run in chemical probing experiments or for separation of nucleic acids with only a small difference in the number of nucleotides.

To prepare a sequencing gel, glass plates were thoroughly washed with a sponge and soap to remove gel pieces. Then plates were rinsed with deionized water and finally with 80 % ethanol. Each washing step was followed by careful drying. Glass plates were silanized with 5 % dimethylsilylchloride in dichloromethane. The gel chamber was assembled by putting spacers along the long sides of that glass plate attached to the buffer chamber, the other silanized glass plate was put on top, clamps were clipped to the sides of the glass plate sandwich and aligned with the glass-plate-spacer assembly at the bottom. When the bottom clamp had been tightened, the comb was sled into the upper space between the plates and secured by small clamps. 100 ml of an e. g. 8 % urea PA-gel were prepared in an Erlenmeyer flask (6.1.6), APS and TEMED are added and the mixture is drawn into a 60 ml syringe with a short flexible tube ending in a tip. All air bubbles were removed and the syringe was used to slowly pump gel between the glass plates. Gel polymerized for at least 1 h or over night, bottom clamp was removed and gel placed in buffer chamber. Before sample loading, the sequencing gel is pre-run at 1800 V for 1 h. 1× TBE was used as running buffer. 3 µl the sample, sequencing ladder or 1× sucrose loading buffer were loaded. The sequencing gel was run at increasing voltages (1800-2200 V, changed about every 45 min) until the sample was nicely separated (about 3-4 h). After the run, the gel was disassembled by removing the buffer and the side clamps and it was placed on pipet-tip-boxes - the buffer chamber facing up. Thereafter, the glass plates were carefully separated from each other, the upper glass plate slowly and carefully removed, the gel wet with ddH$_2$O using a spraying device. A thin Whatman paper was slightly and homogeneously wet with ddH$_2$O, thoroughly placed onto gel. Then the wet paper with gel sticking to it was bent, thereby slowly removing the gel from the lower glass plate. Bubbles close to the edge were removed and the gel was covered with saran wrap and a phosphorimager screen followed by incubation at -80 °C over night.

6.2.2 mRNA isolation from Gram-positive bacteria

For isolation of complete bacterial RNA, 5 ml precultures were incubated to an OD_{600} of about 1.0. Then, 2 volumes of prewarmed (37 °C) RNA protect Bacteria reagent are pipetted into a 15 ml falcon tube (10 ml) and one volume (5 ml) of bacteria suspension are added, followed by immediate vortexting for 5 s. After incubation at RT for 5 min, the sample was centrifuged for 10 min at 5.000 g. The supernatant was decanted and residual liquid was removed by gently dabbing the inverted tube once onto a paper towel (the remaining supernatant did not exceed about 80 µl per 100 µl Hepes in the lysis step). At this point pellets can be stored at -20 °C for up to 2 weeks or at -80 °C for up to 4 weeks. For subsequent RNA purification pellets are thawed at room temperature.

For the actual RNA isolation the PrestoSpin R Bug-Kit (Molzym) was used. The pellet was thawed at RT, resuspended in 500 µl Hepes-EDTA (Hepes 10 mM, EDTA 1 mM, pH8) and 32 µl Lysostaphin (5 mg/ml, Sigma-Aldrich) were added. This mixture was incubated for 2 h at 37 °C in a waterbath.

The RNA preparation was performed according to the manual provided with the PrestoSpin kit, starting at step 3 with the addition of 250 µl buffer CH and immediate vortexing for 5 s. When necessary, the suspension was stirred with the pipet tip for homogenization and stood until visible lysis had occurred (at least 5 min). Once the suspension became clear and viscous, hence complete lysis had taken place, 200 µl of buffer AB were added. After vortexing for 5 s, the solution was transferred to a spin column by pipetting, and centrifuged for 30 s at 12.100 g. The flow through was discarded and 400 µl of buffer DB2 were added into the spin column. After centrifugation for 30 s, flow through was discarded and this washing step with DB2 repeated. For DNA degradation, buffer DB2-DNase I mix (preparation: 4 µl=40 U DNase I were mixed with 110 µl DB2 in a sterile, RNase-free tube, vortexed and placed on ice until use) was added to the sample and incubated at RT for 20 min with closed tube lid. Subsequently, 400 µl of buffer WB were added to the spin column, which was thereafter centrifuged at 12.100 g for 30 s and the flow through was discarded. Finally, the column was washed with 400 µl 70 % ethanol by centrifugation at 12.100 g for 3 min. Here, it is strictly avoided to contaminate the column with ethanol. Now, the column was carefully transferred into a new 1.5 ml reaction tube and 80 µl DEPC H_2O preheated to 70 °C were used to elute the RNA by placing the liquid in the center of the column, closing the lid and incubating for 1 min. Subsequent centrifugation at 12.100 g for 1 min eluted RNA solution, whose concentration was then determined as described under Section 6.1.8.

Finally, before total RNA can be used for reverse transcription it had to be purified and concentrated. This was done with the help of the RNeasy Min Elute Clean-up Kit by Qiagen. The sample volumes were adjusted to 100 µl by addition of DEPC H_2O. Then, 350 µl buffer RLT were added and the solutions mixed well. Thereupon, 250 µl of 96-100 % ethanol were added to the diluted RNA and mixed by pipetting. Without centrifugation, the sample (700 µl) was transferred to an RNeasy Min Elute spin column that had been placed in a 2 ml collection tube. After the lid was closed gently, centrifugation followed at 8.000 g for 15 s. The flow through was discarded and the spin column put into a new 2 ml collection tube. After addition of 500 µl buffer RPE, centrifugation for 15 s at 8.000 g washed the spin column membrane. Flow through was discarded again and 500 µl of 80 % ethanol were added to the column. Centrifugation with the lid closed for 2 min at 8. 000 g washed the spin column membrane. Again, the flow through was discarded, however this time it was assured that no ethanol was carried over. For this, the column was placed in yet another 2 ml tube and

centrifuged with an open lid for 5 min at full speed. Thereafter, the collection tube was discarded and the column was placed into a 1.5 ml tube for final elution. For this, 14 µl RNase free water, preheated to 70 °C, was added directly to the center of the membrane, the lid was closed gently and the sample was centrifuged at full speed for 1 min to elute RNA (dead volume of the spin column is 2 µl, therefore resulting in 12 µl final volume).

This protocol was followed by RNA concentration measurement (concentrations were between 800-1500 ng/µl).

6.2.3 Reverse transcription for quantitative real-time PCR

Before reverse transcription for quantitative real-time PCR took place, RNA integrity was checked by running it on an agarose gel of appropriate percentage. If no RNase degradation took place, two distinct bands (around 1500 nt and 2900 nt) were observed representing bacterial rRNA.

Reagent	Resultant	Amount	Stock
step 1			
RNA	3 µg	x	
Random hexamer primers	0.3 µg	1.5 µl	0.2 µg/µl
DEPC H$_2$O ad 12 µl			
step 2			
Reaction buffer	1×	4 µl	5×
dNTPs		1 µl	10 mM
RNasin		1 µl	
DEPC H$_2$O		1.75 µl	
step 3			
BioScript		0.5 µl	200 U/µl

Table 6.16: Pipetting scheme of RT for qPCR.

For reverse transcription, RNA and primers were mixed according to Table 6.16 step 1 and incubated for 5 min at 70 °C followed by cooling to RT/4 °C. Then, components as stated in step 2 (Table 6.16) were added, followed by an incubation for 10 min at 25 °C. Finally, the BioScript reverse transcriptase was added (step 3, Table 6.16) and the mixture incubated for 30 min at 60 °C, another 0.5 µl BioScript were added followed by another incubation for 30 min at 60 °C. The reaction was stopped by adding 2.5 µl EDTA (0.5 mM pH 8) and 5 µl NaOH (1 M), incubation for 15 min at 65 °C. Finally, the mixture was neutralized by adding 12.5 µl Tris (pH 7.5, 1 M).

Reverse transcription protocol was followed by purification of cDNA using the Fermentas PCR purification kit according to the manufacturer's protocol. For cDNA elution, 40 µl elution buffer were used.

6.2.4 Metabolite induced self-cleavage assay

The metabolite-induced self-cleavage assay (as described in (Winkler et al., 2004; Lünse et al., 2011)) was used not only to investigate different glmS ribozyme characteristics, such as k$_{obs}$ and EC$_{50}$ values, but also to screen for glmS riboswitch modulators. This makes this assay an integral part of the glmS ribozyme research presented in this work.

6.2.4.1 RNA preparation for metabolite-induced self-cleavage assay

To investigate the glmS ribozyme by the metabolite-induced self-cleavage assay, radioactively labeled glmS RNA had to be prepared. For this, a T7 RNAP transcription from the PCR template was performed according to Section 6.1.5. However, whenever working with glmS RNA, Tris buffer has to be avoided. Therefore, Hepes buffer was used for all glmS ribozyme containing reactions. *In vitro* tanscription was followed by PA-gel purification (Section 6.1.6 and Section 6.1.7). RNA was dissolved in 10 µl DEPC H_2O and used for the 5' dephosphorylation and phosphorylation with $\gamma\,^{32}$P-ATP (Sections 6.1.10 and 6.1.9). The phosphorylation reaction is purified by employing a G25 column. Subsequent PAGE and RNA work-up led to RNA pellets that were dissolved in 10-20 µl DEPC H_2O.

Before actual experiments were performed, a cleavage assay test was done to control glmS ribozyme cleavage in the presence of 200 µM GlcN6P or GlcN and 10 mM $MgCl_2$. Moreover, these tests were used as an estimate on how much the stock RNA can be diluted for further experiments (usually 1:10-1:20)

For the cleavage assay test a thin 17 % PA-gel is poured (according to Section 6.1.6). Then 1.5 ml tubes are prepared by appropriate labelling. For every experiment a positive control (addition of 200 µM GlcN or GlcN6P), an RNase control (no addition of $MgCl_2$) and a negative control (no addition of metabolite) was performed. Reaction contained components according to Table 6.17. The cleavage buffer, $MgCl_2$, DEPC water and metabolite were mixed in prepared 1.5 ml tube. The final reaction volume was 10 µl.

GlmS RNA has to be prefolded before its use in the cleavage assay. For this, the RNA was heated to 90 °C for 1 min. It has to be assured that the RNA solution does not contain divalent ions like Mg^{2+} as they would cause disintegration of RNA, when heating. After a short spin, the RNA was allowed to adjust to room temperature by incubation at 23 °C for 5 min so that RNA can fold into its active conformation.

Now the radioactively labeled glmS RNA was added to the cleavage reaction mix thereby initating it. Therefore, incubation at 37 °C for 30 min was started immediately.

Reagent	Stock	Volume	Resultant
Cleavage buffer	10×	1 µl	1×
$MgCl_2$	100 mM	1 µl	10 mM
RNA		0.5 µl	
Metabolite	1 mM	2 µl	200 µl
DEPC H_2O ad 10 µl			

Table 6.17: Pipetting scheme for metabolite-induced self-cleavage assay.

The cleavage reaction was stopped by the addition of 2× sucrose-loading buffer (5 µl) and a short spin to collect the entire sample in vial bottom for proper mixing. In the mean time, a PA-gel was pre-run, then samples were loaded and run at 450-600 V for 2-3 h. Subsequently, the gel chamber was disassembled, the gel wrapped in saran wrap and exposed to a phosphorimager screen over night at -80 °C. The screen was read and band intensities evaluated using AIDA software.

Thereupon, RNA stocks were diluted as stated above and used for either endpoint determinations (Section 6.2.4.2) or kinetics (Section 6.2.4.3) depending on the scientific hypothesis under investigation.

6.2.4.2 Endpoint determinations

Endpoint determinations of the metabolite-induced self-cleavage assay were used to monitor concentration dependent effects of compounds or metabolites on glmS cleavage, as well as for the screenings of Reymond compounds, the GlcN6P analog library and the natural activators, namely aminoglycosides and Streptozotocin. These measurements were stopped after a certain time interval had passed, usually 30 minutes, by addition of 5 µl 2× sucrose PAGE loading buffer. Subsequently, the samples were loaded on a pre-run, analytical PA-gel (17 %) until full length glmS ribozyme band and cleavage fragment were well separated (usually 2-3 h, at 400-600 V).

Reymond screenings were performed with stated compound and DMSO concentrations. For example, for the screening in the presence of 2 mM compound in 2 % DMSO, compound stocks (usually 100 mM in 100 % DMSO) were diluted to 10 mM in 10 % DMSO with DEPC water. Finally, 2 µl of this screening stock solution were used per reaction. Assay buffer contained a final concentration of 50 mM Hepes, pH 7.5, 200 mM KCl and 10 mM $MgCl_2$, 200 µM GlcN or GlcN6P in controls or 2 mM compound in 2 % DMSO in a final reaction volume of 10 µl. The cleavage reaction took place at 37 °C for 30 min until it was stopped by addition of 2× sucrose PAGE loading buffer.

EC_{50} value determinations increasing concentrations of activator (i. e. GlcN6P, CGlcN6P, GlcN6S etc.) were assayed. To evaluate half maximal glmS cleavage, the ratio of glmS cleaved was plotted against the logarithm of metabolite concentration used in the cleavage reaction, leading to a sigmoidal dose-response curve (Figure 8.1). This curve was fitted using the equation $Y = (Bottom) + (Top - Bottom)/1 + 10^{LogEC_{50}-X}$, which yielded EC_{50} values shown in Table 3.2. R^2 values were referred to as indicators for goodness of fit.

IC_{50} values were calculated from dose-response curves of tested cleavage inhibitor and fitted using the equation $Y = (Bottom) + (Top - Bottom)/1 + 10^{LogIC_{50}-X}$. For this, varying concentrations of potential inhibitors were tested in competition with constant GlcN6P concentration (usually 200 µM).

6.2.4.3 Kinetics

For kinetic measurements samples were withdrawn from a larger stock at different time intervals (0, 1, 3, 5, 7, 10, 15, 30, 60 minutes). The 10 µl taken were put in prepared microcentrifuge tubes that already contain 5 µl 2× sucrose-loading buffer to immediately stop the reaction. These kinetic measurements were mainly used for the determination of k_{obs} values which were obtained by fitting the curve of cleavage rate/time to the equation $Y = YMAX * (1 - e^{-K-X})$. This equation describes the pseudo-first order association kinetics of the interaction between a substrate and an enzyme. Y is in this case enzyme activity. X is time. Y starts out equal to zero and increases to a maximum plateau (at equilibrium) equal to YMAX. When X equals 0.6932/K, Y equals 0.5*YMAX (Turner, 1997).

6.3 Working with bacteria

Bacteria are not only the key player in antibacterial research for evaluating drug effects on bacterial growth (Section 6.3.6) and viability (Section 6.3.5), but they are also important laboratory tools for the amplification (Section 6.3.12) and manipulation of DNA (Sections 6.3.15, 6.3.15.2). The following sections provide insight into laboratory techniques used

for handling and investigating bacteria such as *Staphylococcus aureus*, *Escherichia coli* and *Haemophilus influenza*.

6.3.1 Cultivation of *Escherichia coli*

Initial inoculations of *E. coli* bacteria from frozen glyci cultures as well as *E. coli* used for the amplification of DNA plasmids were cultivated in LB-medium (7.1) at 37 °C under vigorous shaking (130–150 rpm). For experiments in which the influence of thiamine analogs on bacterial growth or on β-galactosidase expression was tested, minimal medium was used (7.1).

Several *E. coli* strains were used in this study. XL10 Gold were utilized for standard plasmid transformations. For β-galactosidase assays two different strains were chosen: The laboratory K12 strain MG1655 that has only few mutations in its genome (Table 7.5, Blattner et al. (1997)), and DH5αZ1, carrying, in addition to DH5α inherent genomic alterations (Table 7.5), at its attB locus two copies of Lac and Tet repressor encoding genes driven by the constitutive promoters P_{laciq} and P_{N25}, integrated according to Lutz and Bujard (1997); Diederich L (1992).

6.3.1.1 LB media and plates

For about twenty 10 cm dishes 7.5 g agarose and 10 g LB media were mixed and deionized water was added to 500 ml. This was autoclaved for 15 min at 121 °C. Hereafter, the LB agar had to cool until handwarm before the appropriate antibiotic (stock: Ampicillin 100 mg/ml, Kanamycin 50 mg/ml) was added 1:1000. After proper mixing, LB agar plates were poured and solidified under sterile conditions. Plates were kept at 4 °C.

6.3.1.2 Transformation of XL10 GOLD

XL10 GOLD ultracompetent cells were gently thawed on ice. For each reaction 45 µl of cells were aliquoted into a pre-chilled 2 ml tube and 2 µl β-mercaptoethanol were added. Cells were kept on ice constantly. After a gentle swirl, the entire ligation reaction (up to 20 µl) was added and the cells were incubated for 30 min on ice after gentle mixing. In the meantime SOC medium was pre-warmed to 37 °C. Cells were heat-shocked at 42 °C (in a waterbath) for 30 s, followed by a short incubation on ice for 2 min. Then 500 µl SOC medium were added and the cells were incubated at 37 °C for 1 h shaking at 225-250 rpm. This incubation time varies depending on the antibiotic resistance that needs to be produced by the cell. Prior to plating, cell suspension was centrifuged at 1000 rpm for 3 min and the supernatant was decanted. Cells were resuspended in remaining medium and spread on an LB-agar plate containing the appropriate antibiotic using a Drigalski applicator followed by incubation at 37 °C over night.

6.3.2 Cultivation of *Staphylococcus aureus* strains

The Gram-positive *S. aureus* grows optimally at temperatures between 35 and 37 °C. From a mixed population of bacteria, selective or differential media, such as mannitol salt agar or Baird-Parker-Agar are used (McNamara, 2008). For routine cultivation however, Brain Heart Infusion (BHI), Tryptic Soy, Columbia, Mueller-Hinton or Penassay broth can be used. Chemically defined media, as published by Charles and Rawal (1976); Laue and Macdonald (1968); Wu and Bergdoll (1971) can be used to cultivate Staphylococci under controled growth

conditions. For freezing of bacteria at -80 °C the media should contain 30 % v/v glycerol (low passage organisms should always be chosen).

6.3.2.1 Mueller-Hinton (MH), 0.5×MH and chemically defined medium (CDM)

In this study, *S. aureus* was mainly cultivated either in chemically defined medium (for components and preparation refer to 7.4) or in Mueller-Hinton (MH) or 0.5×MH broth. Mueller-Hinton media was developed for the cultivation of pathogenic neisseriae and other fastidious microorganisms. It consists of 2 g/l beef infusion, 1.5 g/l corn starch, 17.5 g/l acid casein peptone (H) (pH of 7.4). Mueller-Hinton Broth was used because it is a rich medium however without any monosaccharides such as glucose readily available. Furthermore, MH agar can be used to carry out sensitivity testing of a great number of antimicrobial agents.

The chemically defined medium (CDM) was used as a 2× solution and did not contain any sugar equivalent, however higher aminoacid concentrations. Aminoacids are used by bacteria to synthesize glucose. This medium supports *S. aureus* growth, however, because glucose has to be synthesized from aminoacids, bacterial growth is slower compared to rich medium such as BHI or MH. Components for this medium were weighed and dissolved in appropriate solutions according to Table 7.4. The different groups were mixed by adding the groups to group V. Sterile water was added to about 400 ml and the pH was set to 7.0 using HCl. Once all components are mixed the medium is sterilized by filtration.

6.3.3 Cultivation of *Haemophilus influenza* and *parainfluenza*

Haemophilus influenza is a Gram-negative, non-acid fast, nonmotile, nonsporeforming bacterium whose shape ranges from cocobacilli to filamentous rods. This bacterium is a facultative anaerobic and requires factor X (hemin) and factor V (NAD). Both Haemophilus strains were grown in humid atmosphere with added 5-10 % of CO_2 and temperatures ranging from 33-37 °C. *H. influenza* is usually grown on plates that contain either so-called Haemophilus-test agar (HT), chocolate agar (boiled blood agar) or blood agar with a hemolytic strain as nurse.

6.3.3.1 Chocolate agar, bacitracin chocolate agar, blood agar with nurse, Haemophilus test agar

Chocolate agar is a non-selective, enriched growth medium consisting of 10 % fresh sheep blood that was slowly heated to 80 °C. Lysed red blood cells provide the essential growth factors NAD and hemin for *Haemophilus influenzae*. Chocolate agar alone is non-selective, however with the addition of bacitracin the medium becomes selective, most critically, for the genus Haemophilus.

Blood agar contains mammalian blood (usually sheep or horse), typically at a concentration of 5–10 % and in addition meat extract, tryptone, sodium chloride, and agar. Blood agar is usually used to isolate fastidious organisms and detect hemolytic activity. However, these plates were used here to observe *H. infl.* growth in the hemolytic zone of a *S. aureus.* Hemolysis frees factor V and X as nutrients for the *Haemophilus.*

Extensive studies performed by Jorgensen and colleagues led to the development of Haemophilus Test Medium (HTM, Jorgensen et al. (1987, 1990)). This medium is Mueller Hinton agar or broth supplemented with X factor, V factor and yeast extract (beef extract 2 g/l, yeast extract 5 g/l, acid hydrolysate of casein 17.5 g/l, hematin 15 mg/l, starch 1.5 g/l, nicotinamide adenine dinucleotide 15 mg/l, agar 17 g/l).

6.3.3.2 Chemically defined medium for *H. influenza* for growth in liquid culture or on agar plates

Chemically defined medium for *Haemophilus influenza* (CDM-HI) was prepared according to the protocol stated for 2× CDM for *S. aureus* with the following alterations: in the preparation of CDM-HI not only glucose was omitted, but also the vitamin thiamine was not added. Appropriate glucose and thiamine sterile stock solutions were prepared to be added separately after the medium was prepared and steril-filtered. Additionally, an NAD and heme solution (also sterile) were prepared and added to the normal CDM medium preparation protocol. For this, heme was dissolved in sterile water/2 N NaOH mix (1:1) to a final concentration of 7.5 mg/ml. This solution was used to supplement the sterile 2×CDM-HI to a final heme concentration of 30 mg/l. Moreover, 15 mg NAD were dissolved in 6 ml water/NaOH mix (1:1, sterile) and added to the medium.

Furthermore, the medium was used as 1× whenever it was used for growth assays in liquid culture, however, when agar plates were prepared the 2× stock solution was mixed 1:1 with agarose (which was dissolved in sterile water also to a 2× concentration, i. e. 2 %). This resulted in a 1 % 1× CDM-HI agarose, that was poured into 3 cm dishes for growth tests on agar.

6.3.3.3 Agar diffusion test

Triazolethiamine compounds were investigated for their effect on *H. influenza* growth by so-called agar diffusion tests. Here, a cell suspension was made by collecting several colonies from a chocolate agar plate and inoculating a NaCl solution with them. This suspension was vortexed until all cell lumps were dissolved. Subsequently OD_{600} was measured and cells with an OD of 0.7 were streaked on the appropriate agar plate (e. g. HI-CDM). Holes were punched in the center of the agar plate using the front of a sterile blue pipet tip. The holes were filled with the appropriate compound dilution (i. e. 128 mM or 12.8 mM of TT compounds). Cells were incubated at 37 °C for several days until colonies were visible. Normally, the size of the zone of inhibition is used as a measure of the compound's effectiveness. However, with faint *Haemophilus* growth this was not possible.

6.3.4 *H. influenza* tests

In order to determine whether colonies grown on HI-CDM medium were *H. influenza*, different tests as suggested by the "Manual of clinical microbiology" (Kilian, 2001) were performed.

6.3.4.1 Gram-staining

For the Gram-staining (Gram, 1884; Gephart and Phillips., 1981), bacteria were streaked onto a cover slip which was prepared with a drop of NaCl solution. Cover slips were air-dried for about 10 min, and then drawn through a bunsen burner flame 3 times to fix cells on the cover slip. Now, crystal violet solution (see below for solution preparation) was added for 2 min, followed by washing step with Lugol solution for 1 min. Cover slip was washed using acetone decolorizer (acetone, 50 ml, ethanol (95 %), 50 ml) and rinsed under ddH$_2$O. This procedure was followed by the counterstaining with Safranin (Stock solution: 2.5 g Safranin O, 100 ml 95 % ethanol; Working solution: 10 ml stock solution, 90 ml ddH$_2$O). Cover slip was dried in filter paper.

Subsequent microscopy was performed using a Laica DMLB with an N-plan $10\times/0.25$ or $100\times/1.25$ lens.

Crystal violet staining reagent is prepared as solution A which contains 2 g Crystal violet (certified 90 % dye content) in 20 ml ethanol, 95 % (v/v), and solution B which contains 0.8 g ammonium oxalate in 80 ml ddH$_2$O. Solutions A and B were mixed to obtain crystal violet staining reagent, which was stored for 24 h and filtered through paper prior to use.

6.3.4.2 Catalase and oxidase test

The majority of *H. influenza* are oxidase and catalase positive (Kilian, 2001). For catalase test, a colony was streaked on a cover slip and H$_2$O$_2$ was added dropwise. If bubbles were observed, the catalase test was declared positive.

The oxidase test uses disks impregnated with a reagent such as N,N,N',N'-tetramethyl-p-phenylenediamine (TMPD) or N,N-dimethyl-p-phenylenediamine (DMPD), which is also a redox indicator. The reagent becomes a dark-blue to maroon color when oxidized, and colorless when reduced. Oxidase-positive bacteria possess cytochrome c oxidase or indophenol oxidase which result in a color change to pink, through maroon and into black, within 10–30 seconds.

6.3.4.3 Fermentation tests

H. influenza use only glucose for fermentation (Kilian, 2001). To prove this, vials (2 ml) containing the appropriate medium (supplemented with factor V and X) with according sugar (glucose, sucrose, mannose, lactose and xylose) and bromokresol purple as indicator were inoculated with *Haemophilus influenza*. Upon fermentation of the sugar the indicator will turn yellow.

However, even for the positive control, no change in color could be observed. Probably the liquid cultivation medium is not sufficient for proper growth of this fastidious bacterial strain.

6.3.5 Determination of minimal inhibitory concentrations

For minimal inhibitory concentration determinations 5 ml precultures were incubated over night under appropriate conditions from a picked colony. In the morning this preculture was used to inoculate a new culture, i. e. to an OD$_{600}$ of 0.2, and grown till an optical density of 1 (approximately 1×10^{-9} cells per ml) was reached. This bacterial suspension was then diluted 1:10.000 to approximately 1×10^{-5} cells per ml, e. g. by adding 50 µl bacterial suspension to 5 ml medium and then using this to further dilute 20 µl in 20 ml.

A sterile 96-well plate (clear, round-bottom, clear lid) was used to prepare compound concentrations to be tested. Total volume of 200 µl or, to save precious compounds, a total volume of 100 µl was used. However, row A and H as well as column 1 and 12 were not used for data point collection, but rather filled with 200 µl medium, as were all other wells not used for the experiment.

For a final total volume of 100 µl, 50 µl of growth medium were put in each well. A stock solution of the compound to be tested was prepared, that is 4 fold concentrated, e. g. if the highest concentration in the assay was supposed to be 600 µM, the stock solution was 2.4 mM. Then a dilution row was made in the well plate by adding 50 µl of the compound stock to first well. After mixing by pipetting, 50 µl are transferred from the first to the second well. This was carried on to the lowest compound concentration to be tested. From this last well,

50 µl are taken and discarded. Finally, 50 µl of bacterial suspension (prepared as described above) were added to each well. Mixing occurred by pipetting.

A medium contamination control as well as a compound contamination control were also pipetted and evaluated.

The plate is mixed for 10 min on a shaking plate and then transferred to a 37 °C incubator. After 24 h, or 48 h if no growth is visible after first time interval, the plate was read and all wells were marked where no obvious bacterial growth was seen. The minimal concentration for which no growth was observed is noted as MIC.

6.3.6 Measurement of growth curves in a Tecan plate reader

Bacterial growth in the presence of compounds was monitored in a sterile 96-well plate (clear round-bottom) with a clear lid. For this, either a total volume of 200 µl or, to save precious compounds, a total volume of 100 µl was used. However, row A and H as well as column 1 and 12 were not used for data point collection, but rather filled with 200 µl medium, as were all other wells not used for the experiment.

For a final total volume of 100 µl, 50 µl of growth medium are put in each well. A stock solution of the compound to be tested is prepared, that is 4 fold concentrated, e. g. if the highest concentration in the assay is supposed to be 600 µM, the stock solution was 2.4 mM. Then a dilution row is made in the well plate by adding 50 µl of the compound stock to first well. After mixing by pipetting, 50 µl are transferred from the first to the second well. This is carried on to the lowest compound concentration to be tested. From this last well, 50 µl are taken and discarded. Finally, 50 µl of bacterial suspension were added to each well. Mixing occurred by pipetting.

A medium contamination control as well as a compound contamination control were also pipetted and evaluated.

The bacteria are prepared for this assay by picking a colony from an approprate culture plate and incubating a 5 ml preculture over night under optimal growth conditions. Next day, OD_{600} was determined and cells were diluted in a new 5 ml preculture to an OD_{600} of 0.1. Now, cells were incubated till an OD_{600} of 0.2, which was then added to the prepared 96-well plate, leading to a final OD of 0.1 in each well.

Even though an OD_{600} of 0.1 is quite high, it is necessary to enable immediate Tecan measurements. Tecan plate reader Sunrise was used for these growth curve recordings, usually measuring OD_{600} every 15 min for 24 h under vigorous shaking every 2 min for 1 min.

6.3.7 β-galactosidase assay

On day one, 5 ml precultures of *E. coli* cells (either DH5αZ1 or MG1655) containing the reporter gene plasmid pRS414.2 thiM were prepared in LB medium. These cultures were incubated over night at 37 °C and 155 rpm.

The following day, 8 ml precultures of *E. coli* [pRS414.2 thiM] were prepared in minimal medium with and without 20 µM thiamine and with increasing AHT concentrations (if pNYL MCS11 N25 aptamer plasmids were used as well) according to Table 6.18. These cultures were inoculated with the LB culture (OD_{600}= 0.5) 1:500 and incubated for 24 h at 37 °C, 150 rpm.

Reagent	Stock	Volume
M9 Medium	5×	1600 µl
MgSO$_4$	1 M	40 µl
Glucose	20 %	80 µl
Casamino Acids	20 µg/µl	75 µl
Ampicillin	100 mg/ml	8 µl
depending on reporter	construct and other	plasmids add:
Kanamycin	50 mg/ml	8 µl
Thiamine	20 mM	8 µl
AHT	2mg/ml	0.4-3.2 µl depending on assay
ddH$_2$O ad 8 ml		

Table 6.18: Pipetting scheme for β-galactosidase assay.

After the incubation time had passed (day three), the OD$_{600}$ was measured by mixing the cell suspension well and transferring 195 µl of it into a 96-well plate (flat bottom, F profil, Roth) and subsequent measurement in the Tecan NanoQuant reader. The rest of the cell suspension was centrifuged at 5000 g for 3 min, the supernatant was discarded and cells were washed twice with 800 µl ice cold 1× PBS. Washed cells were transferred into a 1.5 ml reaction tube before the last washing step, centrifuged at 5000 g for 3 min, the supernatant discarded. The cell pellet was resuspended in 200 µl lysis buffer (promega, a 5× buffer diluted to 1× before addition) and incubated for 15 min at RT. During the incubation time, reaction tubes (1.5 ml) were prepared for each sample in duplicate and 75 µl of 2× assay buffer added. After the incubation time, cells were pelleted by centrifugation at 5000 g for 3 min and 75 µl cell lysate were added to the 2× assay buffer. Then tubes were incubated in a thermomixer of appropriate size at 37 °C until conversion to a yellow colored suspension was obvious. The incubation time was noted and 250 µl 1 M Na$_2$CO$_3$ solution was added to stop the reaction. Finally, absorbance was measured at 420 nm in the Tecan NanoQuant plate reader.

The same assay conditions were used for preQ$_1$ riboswitch reporter gene assays, here however thiamine was exchanged for appropriate preQ$_1$ concentrations. When DH5αZ1 cells were used that contained the thiM reporter gene plasmid as well as AHT-dependent hairpin expressing plasmid pNYL MCS11, kanamycin and also appropriate AHT concentrations had to be added to the medium (see Table 6.18).

This assay set-up was also down-scaled for the screening of TT-compounds by using only 4 ml as final volume.

6.3.8 Thiamine, TMP and TPP extraction for HILIC

Sample preparation for HILIC starts with the same procedure as setting up a β-galactosidase assay (final volume of 8 ml, refer to Section 6.3.7). After the 24 h incubation step, OD$_{600}$ is measured in a 96-well plate. Then suspension was centrifuged at 5000 g for 15 min, supernatant was discarded and the cell pellet resuspended in 200 µl ddH$_2$O and transferred into a 1.5 ml tube. Sample was centrifuged for 1 min at 21.000 g and supernatant taken-off. Again 200 µl H$_2$O were added and cells incubated for 15 min at RT. Hereafter, samples were snap frozen in liquid nitrogen, thawed and sonicated for 20 s. This freeze-thaw cycle was repeated once before OD$_{600}$ of the sample was determined to calculate lysis efficiency (percent lysis = (1-(A600 sonicated/A600 suspension))*100). Usually lysis efficiencies between 60 and 70 %

were reached.

Now, samples were centrifuged for 20 min at 20.000 g, transferred into a new 1.5 ml tube and 600 µl acetonitrile were added for protein and nucleic acid precipitation. The sample was incubated at -80 °C for 20 min, centrifuged at 4 °C for 30 min at 20.000 g. The supernatant was again transferred into a new tube and acetonitrile was evaporated in the speed vac for approximately 2 h to a remaining volume of 150-200 µM. In order to eliminate phospholipids from the extraction, a phenol chloroform extraction was performed according to Section 6.1.4.1. This was followed by estimation of thiamine and thiamine derivatives in the sample by using the thiochrome method.

Samples are immediately snap frozen and stored at -20 °C before they were sent for HILIC analysis on dry ice.

6.3.9 Thiochrome assay

The thiochrome assay was first proposed by Jansen in 1936 (Fujiwara and Matsui, 1953) and is a method based on the oxidation of thiamine by potassium ferricyanide in an alkaline medium, extraction of the thiochrome formed by isobutanol and estimation of the intensity of the violet-blue fluorescence in ultraviolet light (Hennessy and Cerecedo, 1939). Other phosphoric esters of thiamine (TMP and TPP) behave similarly in the thiochrome assay and cocarboxylase activity can be determined to distinguish the different species (Haugen, 1961; Bhagvat and Devi, 1946). Triazolethiamine and derivatives cannot be converted to a thiochrome-like compound, pyrithiamine however can be converted to "pyrichrome" (Airth and Foerster, 1962).

In order to estimate the amounts of thiamine species successfully isolated from bacteria, the thiochrome method was used. For this, a 2× concentrated thiamine standard solution was prepared ranging from 1 mM to 25 µM (final concentration; testing eight concentrations: 1000, 750, 500, 250, 100, 75, 50, 25 µl and also no thiamine). A black 96-well plate (flat bottom, Greiner) was used for these measurements. The wells were pepared by adding the 100 µl of the thiamine concentration row and samples to be measured. Each standard or sample was measured as triplicate. Then 100 µl of 2× thiochrome reagent (2 mM $K_3Fe(CN)_6$ and 2 M NaOH, always prepared freshly) are quickly added by using a multi-pipet.

Samples were measured immediately using the VarioSkan (Thermo). The program consisted of a 1-minute shaking followed by a kinetic measurement for 30 min every 30 s at ex375/em450.

Standard row was plotted (logarithm of thiamine concentration against RFU) and the equation for the linear slope was used to calculate sample thiamine concentrations.

6.3.10 HILIC

HILIC measurements were performed by Dr. Giorgia Greco from the technical University Munich. For samples shown in Table 3.8 and Figures 3.19, 3.20 and 3.21 analysis parameters according to method 1 (see Table 6.19) were used. For the analysis of the triazole, method 2 was established (Table 6.19). In both methods UV-detection was done at 220, 254 and 280 nm and MS-detection was performed in scan mode ranging from 100-3200 m/z, positive and negative polarity.

Method I	
Column	ZIC-HILIC from Merck Sequant, Umea, Sweden (150x2.1, 3.5 µm, 200 Å)
Eluent A	acetonitrile (ACN) 100 %
Eluent B	NH$_4$OAc 10 mM/ACN 90/10 v/v
Flow	0.4 ml/min
Gradient (time [min]/% B)	0/30
	7/30
	20/45
	21/30
Method II	
Column	YMC-pack diol (150x2.1, 5 µm)
Eluent A	acetonitrile (ACN) 100 %
Eluent B	NH$_4$OAc 10 mM/ACN 90/10 v/v
Flow	0.4 ml/min
Gradient (time [min]/% B)	0/15
	5/15
	15/50
	16/15
	20/15

Table 6.19: Methods used for HILIC preparation of cell extracts.

6.3.11 Glycerol stocks

To store transformed cells for prolonged periods at -80 °C, glycerol stocks were made by adding 500 µl of cell culture to 500 µl of sterile glycerin medium (Section 7.1). Glycerinstocks were prepared in 2 ml cryo-vials.

6.3.12 Plasmid preparation from *E. coli*

For plasmid preparation in different scales, the appropriate plamid prep kit (Macherey Nagel, 7.6) was used. Instructions were followed as stated in the manufacturers protocol, except that either deionized water was used for elution or, when very large DNA plasmids were prepared elution proceeded by incubation with 25 µl provided elution buffer and incubation for three minutes before centrifugation. This procedure was repeated to obtain 50 µl of prepared plasmid for further experimentation such as sequencing (Section 6.3.14) or cloning (Section 6.3.15).

6.3.13 Isolation of genomic DNA from *S. aureus* Mu50

The isolation of *S. aureus* genomic DNA was performed using the PrestoSpin D Bug kit from Molzym. At day 1, a 5 ml culture of MH broth was inoculated with a colony of *S. aureus* Mu50 and incubated at 37 °C over night under vigorous shaking. The following day, the stationary culture was centrifuged (1-4 ml liquid culture) in a microcentrifuge at 13.000 rpm for 2 min. After the supernatant was removed completely, the cell pellet was resuspended in 50 µl buffer RS including 5 µl Lysostaphin (10 mg/ml stock), which attacks the pentapeptide chain interconnecting the disaccharide. Lysozyme is inefficient against *S. aureus*, because

these bacteria have acetylated muramic acids which are not recognized for cleavage by this enzyme anymore. This suspension was mixed until homogeneous and incubated for at least 30 min at 37 °C until the solution is viscous. Then 250 µl of buffer CH were added and the solution immediately vortexed for 5 s. If necessary this suspension was also stirred with the pipet tip for homogenization. Now, samples were incubated for at least 5 min or until visible lysis. This was followed by the addition of 200 µl buffer AB, thorough vortexing for 5 s and transfer of the supernatant to a spin column (provided with the kit). The solution occasionally became turbid as a result of protein precipitation. The loaded column was centrifuged at 13.000 rpm for 30 s, nucleic acids bind to the matrix and flow through was discarded. For RNA degradation, 200 µl buffer including RNase A was pipetted into the spin column, which was then incubated for 5-10 min with a closed lid. Then 400 µl buffer WB were added to the spin column and centrifuged at 13.000 rpm for 30 s. Once the flow through was discarded, the column was washed with 400 µl of 70 % ethanol by centrifugation at 13.000 rpm for 3 min. Again the flow through was discarded and the column was transferred to a 1.5 ml tube. For elution, 80 µl of preheated (70 °C) ddH$_2$O were pipetted in the center of the column. After incubation for 1 min with closed lid, centrifugation for 1 min at 13.000 rpm took place. The eluate was used again for the same procedure. Finally, the concentration of DNA samples was determined as stated above (Section 6.1.8).

6.3.14 Sequencing

For sequencing, samples were sent to the GATC biotech AG. Appropriate primers were either chosen from the freely available ones listed on the GATC-website or designed and then synthesized by GATC. A list of designed primers that are now available at GATC can be found in Table 7.8.

6.3.15 Cloning

6.3.15.1 Restriction digests

For restriction digests fast digest enzymes by Fermentas were used and a mastermix was prepared according to Table 6.20.

Reagent	Amount	Resultant
Digest Buffer	2 µl	1×
DNA	x	200 ng
Digest Enzyme	1 µl	
ddH$_2$O ad 30 µl		

Table 6.20: Pipetting scheme for restriction digests.

Incubation of digest reaction took place at 37 °C for 20 min and the digested product was purified using the NucleoSpin kit (Section 6.1.4.2). Concentrations were measured and part of the sample was run on an agarose gel to check for correct product length.

6.3.15.2 Ligation of DNA fragments

To ligate DNA, two restricted fragments were mixed to a final amount of 150 ng (in equimolar concentration) together with 2 µl DNA ligase and 2× ligation buffer (to yield a final 1×) in a

total volume of 50 µl. The sample was incubated for 5 min at room temperature and was then ready for transformation.

6.4 Interaction analysis

6.4.1 Microscale thermophoresis

Microscale thermophoresis (MST) is a new method that enables the quantitative analysis of molecular interactions in solution at the microliter scale. This method was used to determine interactions between compounds or metabolites and riboswitches. For this the RNA was labeled at its 5' end using *in vitro* GMPS transcription and subsequent fluorescein labelling (Sections 6.4.1.1 and 6.4.1.3). All measurements were performed on the Monolith NT.115 (NanoTemper Instruments).

For every round of measurements 16 glass capillaries were prepared that contained 10 µl of sample solution. This sample solution consisted of a final labeled RNA concentration of 20 nm (RNA was properly folded before addition to the mix), assay buffer (same as used in i.e. glmS *in vitro* cleavage assays) and finally 1 µl of appropriate compound was added to obtain the wanted final concentration. These components were mixed in 0.5 ml tubes and incubated for about 5 min at RT till equilibrium was formed. Then capillaries are loaded and optionally closed with putty at each side.

For fluorescein labeled RNA the blue LED laser was used (Laser on time: 40 s, Laserpower: 70 %). For more detailed methods descriptions refer to the Bachelor thesis of Jens Hör (Hör, 2011).

6.4.1.1 GMPS-transcription

This transcription method allows the incorporation of a modified guanosine nucleotide at the 5' end of the RNA. The guanosine monophosphate thioate can later react with iodoacetyl-moiety of labelling molecule like biotin or fluorescein by a nucleophilic substitution.

Reagent	Amount	Stock	Resultant
Tris pH 7.9 (or Hepes for glmS ribozyme)	20 µl	200 mM	40 mM
MgCl$_2$	25 µl	100 mM	25 mM
DTT	5 µl	100 mM	5 mM
NTP Mix	10 µl	25 mM	2.5 mM
RNasin	1.24 µl	40 U/µl	0.5 U/µl
Inorganic pyrophosphatase	0.2 µl	2 U/µl	0.02 U/µl
dsDNA template	10 µl	150-300 pmol	1.5-3 µl
T7 RNA polymerase	5 µl	50 U/µl	0.5 Uµl
GMPS	6.7 µl	150 mM	10 mM
water	11.86 µl		
total volume	100 µl		

Table 6.21: Pipetting scheme for GMPS-transcription

Reaction mix was composed as shown in Table 6.21. A positive control, approximately 100-200 nt long was transcribed as well to ensure activity of enzymes, proper salt and buffer conditions. The transcription was run over night. Before samples were phenol-chloroform extracted and precipitated according to Section 6.1.4.1, yield was checked running an agarose

gel. The pellet was resuspended in 100 µl DEPC water and passed through G25 columns (6.1.11.1) twice.

6.4.1.2 Biotinylation of RNA

Before the biotinylation was started RNAs were checked for integrity on an agarose gel. For the labeling reaction the components listed in Table 6.22 were mixed and added to the GMPS transcribed RNA. Whenever the glmS ribozyme was used in this protocol, Tris buffer was substituted by Hepes buffer, since Tris increases the self-cleavage reaction of this riboswitch. Since the pH can vary dramatically with different amounts of RNA being added, the pH was measured. It was only preceded when the pH lay around 8 or after it had been adjusted to 8. The mix was heated to 80 °C for 1 min and immediately put on ice for 5 min. In the meantime a crumb of EZ-link PEO-iodoacetyl biotin (by Thermo Scientific) was dissolved in 100 µl DMF. 40 µl of biotin solution were added to the 360 µl of labelling mix at RT and then incubated at 40 °C for 2 h, 300 rpm.

Reagent	Amount	Stock
TE (Tris 800 mM, EDTA 500 mM) pH 8	40 µl	10×
Urea	100 µl	8.3 M
RNasin	4 µl	40 U/µl
GMPS transcription	100 µl	
DEPC water	116 µl	
total volume	360 µl	

Table 6.22: Composition of RNA labelling mixture

6.4.1.3 Fluorescein-labelling of RNA

For successful fluorescein-labelling reactions, the same protocol and procedure as stated under Section 6.4.1.2 was followed, except for the use of iodoacetamido-fluorescein (4 mM final) dissolved in DMF as labelling substrate.

6.4.1.4 Ammonium acetate precipitation

Samples were split into 2× 200 µl and 1 µl of DNaseI was added. Incubation for 20 min at 37 °C allowed the digest of remaining DNA templates. 100 µl 6 M NH_4OAc and 900 µl of EtOH abs. were added. The tube was inverted to mix and frozen at -80 °C for 10 min, spun at 4 °C for 20 min at 20817 rcf. The pellet was washed using 70 % EtOH, centrifuged for 5 min and air-dried, then dissolved in 50 µl 1× sucrose PAGE loading buffer. Finally, the protocol for RNA work-up was followed (Section 6.1.7), fluorescein-labelled RNA was run in the dark. The resulting biotinylated or fluorescein-labelled RNA pellet was taken up in 20 µl DEPC water. Whereas the yield and quality of biotinylated RNA was checked by gel shift assay (Section 6.4.1.5), fluorescein-labelled RNA was run on an agarose gel and evaluated using the fluorescence reading options of the phosphorimager or by simple absorption measurements at 494 nm and 260 nm.

6.4.1.5 Gel shift assay

Biotinylated RNA was mixed in equimolar concentrations with streptavidin (SA-stock: 150 mM) and incubated at RT for 15-25 min before 2× RNA agarose loading buffer was added. Samples were immediately loaded on an agarose gel of convenient percentage (Section 6.1.2). Positive and negative controls as well as unbiotinylated RNA were run for orientation.

7 Materials

7.1 Solutions

Solution	Ingredient	
Agarose loading buffer 2× pH 8.0	Tris/HCl	50 mM
	EDTA	50 mM
	Glycerine	50 % (v/v)
Assay buffer 2×	sodium phosphate buffer, pH 7.3	200 mM
	$MgCl_2$	2 mM
	β-mercaptoethanol	100 mM
	o-nitrophenyl-β-D-galactopyranosid	1.33 mg/ml
Cleavage Buffer 10×	Hepes pH 7.5	500 mM
	KCl	2 M
DEPC water	DEPC	1:500 (2 ml for 1 l water)
LB media	NaCl	5 g/l
	yeast extract	5 g/l
	tryptone	10 g/l
	water	ad 1 l
M9 medium 5×	KH_2PO_4	15 g
	NH_4Cl	5 g
	NaCl	2.5 g
	Na_2PO_4	30 g
	ddH_2O	ad 1 l
PBS 10×, pH 7.4	NaCl	1.37 M
	KCl	27 mM
	Na_2HPO_4	65 mM
	NaH_2PO_4	14.7 mM
Pfu PCR buffer 10×	Tris/HCl pH 8.8	200 mM
	KCl	100 mM
	Triton X-100	1 %(v/v)
	$(NH_4)_2SO_4$	100 mM
	BSA	1 mg/ml
RNA loading buffer 2× pH 8.0	Formamide	9.5 ml
	SDS 10 %	25 µl
	EDTA 0.5 M	10 µl
	bromophenol blue	crumb
	water	0.5 ml
Solution B	Urea 8.3 M in 10× TBE	

Solution	Ingredient	
Solution C	Rotiphorese Sequenziergel Konzentrat	
Solution D	Urea 8.3 M	
Sucrose Loading buffer 2×	Tris/HCl	45 mM
	Boric Acid	45 mM
	Urea	4 M
	Sucrose	10 %
	SDS	0.05 %
	EDTA	2 mM
Sucrose Loading buffer 1×	Tris/HCl	45 mM
	Boric Acid	45 mM
	Urea	4 M
	Sucrose	10 %
	SDS	0.05 %
	EDTA	100 mM
SOC media	Trypton	2 % (w/v)
	Yeast extract	0.5 % (w/v)
	NaCl	0.2 % (w/v)
	$MgCl_2$	10 mM
	$MgSO_4$	10 mM
	Glucose	20 mM
TBE 10×	Tris/HCl	890 mM
	Boric Acid	890 mM
	EDTA pH 8.0	20 mM
Taq PCR buffer 10×	Tris/HCl pH 9.0	100 mM
	KCl	500 mM
	Triton X-100	1 % (v/v)

7.2 Equipment

Equipment	Manufacturer
-80°C freezers, -20°C freezers, refrigerators	AEG, Heraeus
96 well plates, half area, flat, black, medium binding	Greiner Bio One
96 well plates, flat, black, medium binding	Greiner Bio One
96 well plates, flat, clear	Roth
Agarose gel camera	BioRad
Agarose gel and equipment	in house construction
Analytical balance	Sartorius
Autoclave	Systec
Balance	Chyo
Beaker	Schott
BioMate 3 photometer	Thermo Spectronic
Centrifuges	Eppendorf and Beckmann
Clamps	Mauy
Counter for radioactivity	Berthold
Cryo-vials	Greiner Bio One

Equipment	Manufacturer
Cylinder	Faust
Disposable cuvettes	Roth
Drigalski applicator	In-house construction
Electrophoresis apparatus and chambers	BioRad and Fischer Scientific
Eppi racks	Roth
Eppendorf concentrator 5301	Eppendorf
Eppendorf tabletop centrifuge 5417C	Eppendorf
Erlenmeyer flask	Schott
Fluorescence spectrometer	Perkin Elmer
G25 columns	GE Healthcare
Gel dryer	BioRad
Glass plates for PAGE	Baack
Glass bottles	Schott
Glassplate with buffer chamber	BioRad
Glassplate (sequencing gels)	BioRad
Glasspipet tips (25 ml, 10 ml, 5 ml)	Hirschmann
Glasswool silanized	Serva
Gloves	Peske
Head-top-tumbler	Heidolph
Heating blocks	Bachofer
Hollow needles	Roth
Hood (bacteria)	Antares
Incubator shaker	Innova
Incubator (37 °C-90 °C)	WTC binder
Magnetic stirrer	IKA
Membrane filters 45 µm, 25 mm	Sigma-Adrich
Microwave	Bosch
Multichannel pipette	Eppendorf
Multipette	Eppendorf
NanoQuant infinite 200	Tecan
NAP5 columns	GE Healthcare
NAP10 columns	GE Healthcare
Parafilm	Faust
PCR Thermocycler	Biometra
Peristaltic pump	LKB Bromma
Petridishes for LB-agar plates	Faust
pH-meter	Inolab
pH paper	Macherey-Nagel
Phosphorimager screens & cassettes	Fuji
Phosphorimager FLA-3000	Fujifilm
Pipets	Eppendorf
Pipet tips	Sarstedt
Pipetboy Acu-jet pro	Brand
Power supply for PAGE	Consort
Radioactivity protection gear (goggles, shields etc.)	Sigma
Reaction tubes (2 ml, 1.5 ml, 0.5 ml)	Eppendorf/Sarstedt

Equipment	Manufacturer
Saran wrap	Roth
Sequencing gel chamber & equipment	BioRad
Serological pipettes	Faust
Scalpel blades	Labomedic
Shaker	GFL
Sonification manifold	Bandelin
Spacers/ Comb, thin (0.5 mm)	BioRad
SPR Biacore	GE Healthcare Life Science
Sterile filters (syringe filter / bottle top)	Merck Millipore
Sunrise plate reader	Tecan
Syringe (60 ml)	Henke/Sass/Wolf
Tips for multipette; Combitips plus	Eppendorf
Thermomixer Eppendorf	Eppendorf
UV Transilluminator	BioRad
VarioSkan	Thermo
Vortex mixer	Neolab
Water bath	GFL
Water purification system	Werner
Tecan Ultra reader	Tecan

7.3 Chemicals

Chemical	Manufacturer
Acetic acid (99,8%)	Merck
Acetonitrile (ACN)	Fluka
N-Acetyl-muramic acid (MurNAc)	Sigma
N-Acetyl-α-D-Glucosamine-1-phosphate (GlcNAc1P) 95 %	Sigma
N-Acetyl-D-Glucosamine-6-phosphate disodium salt (GlcNAc6P)	Sigma
N-Acetyl-D-Glucosamine (GlcNAc) 99 %	Sigma
Adenine	Sigma
Agar	Invitrogen
Agarose	Merck
Ampicillin sodium salt	AppliChem
Ammoniumacetate	Grüssing
Ammoniumchloride (NH_4Cl)	ChemSolute
Ammomiumperoxodisulfate (APS) > 98 % reinst	Roth
Bis-Acrylamid, Rotiphorese	Roth
Biotin	Sigma-Aldrich
Boric acid	Grüssing
Bovine Serum Albumin (BSA, nuclease and protease free)	Calbiochem
Bradford-reagent	BioRad
Bromphenol blue	Merck
Calf intestine alkaline phosphatase (CIAP)	Promega

Chemical	Manufacturer
CIAP Buffer	Promega
Casamino Acids Vitamin assay	Becton Dickinson
Chloroform	Merck
Coenzyme B_{12}	Sigma
Coomassie Brilliant Blue G250	Merck
Dichlormethane	Merck
Dichlorodimethylsilane	Acros organics
Dimethylformamide (DMF)	Fischer Scientific
Diethylopyrocarbonate (DEPC)	Sigma
Dimethylsulfoxide (DMSO)	AppliChem
1,4-Dithiothreitol (DTT)	Roth
di-Sodiumhydrogenphosphate-dihydrate	Merck
DNase	Roche
Ethanol abs.	Merck
Ethidium bromide	Roth
Ethylendiamintetraacetic acid (EDTA) p.A.	AppliChem
EZ-link PEO-iodoacetyl biotin	Thermo Scientific
Formaldehyde (36%)	Fluka
D-Fructose-6-phosphate dipotassium salt	Sigma
D-(+)-Glucose (Glc)	Sigma
α-D-Glucose-1-phosphate dipotassium salt dihydrate (Glc1P)	Fluka
D-Glucose-6-phosphate (Glc6P)	Sigma
D-Glucosamine-1-phosphate (GlcN1P)	Sigma
D-Glucosamine-6-phosphate (GlcN6P)	Sigma
D(+)-Glucosamine-hydrochloride (GlcN) min 99 %	Sigma
L-Glutamine	Merck
Glycerin	Roth
Glycine	Roth
Guanine	Fluka
Guanosine-5'-thiophosphate disodium salt	emp biotec
Hepes Pufferan 99,5 % p.a.	Roth
Hemin	Sigma
Hydrochloric acid (HCl)	Roth
Hyoxanthine 99 %	Sigma
Imidazole	Roth
Iodacetamido-fluorescein	Sigma
Iodacetamido-biotin (EZ-link PEG_2)	Thermo Scientific
Isoamyl alcohol	Roth
Isopropanol	Merck
Kanamycin sulfate	Sigma
Lennox L Broth (LB)	Sigma
Lysis Buffer 5×	Promega
Lysostaphin	Sigma-Aldrich
Magnesiumchloride-hexahydrate($MgCl_2$-6×H_2O) 99 % p.a.	ACROS organics
Magnesiumsulfate ($MgSO_4$×7H_2O)	Merck
Methanol	VWR

Chemical	Manufacturer
β-Mercaptoethanol 98 %	Rad
Agarose gel and equipment	in house construction
Analytical balance	Sartorius
Autoclave	Systec
Balance	Chyo
Sigma	
Monopotassiumphosphate (KH_2PO_4)	Sigma-Aldrich
o-Nitrophenyl-β-D-galactopyranosid (ONPG)	Roth
Phenol	Roth
Potassium chloride (KCl) 99,5 % p.a.	Grüssing
Potassiumdihydrogenphosphate	Riedel de Haen
Pyrithiamine hydrobromide	Sigma-Aldrich
Pyridoxamine dihydrochloride	Fluka
Pyridoxal hydrochloride	Sigma
RNasin	Promega
Rnase H	Promega
RNA protect Bacteria reagent	Qiagen
Rotiphorese Sequenziergel Konzentrat	Roth
Salt optimized carbon medium (SOC)	Sigma
Sodium Acetate	Grüssing
Sodium carbonate Na_2CO_3 p. a.	Riedel de Haen
Sodium chloride p. A.	ChemSolute
Sodium dodecylsulfate (SDS)	Roth
Sodium hydrogenphosphate Na_2HPO_4 ×$2H_2O$ p.a.	Sigma Aldrich
Sodium hydroxide (NaOH)	Grüssing
Sodium orthovanadate	AppliChem
Sodium pyrophosphate	AppliChem
Sodium trifluoroacetate 98 %	Alfa Aesar
Spermidine trihydrochlorid 98 %	Sigma
Streptavidin	Sigma
Streptozotocin	Sigma
Superscript Reverse Transcriptase II	Invitrogen
T4 Polynucleotide kinase (PNK)	NEB
T4 PNK buffer	NEB
Tetrabutylammonium chloride	Fluka
Tetracyclinehydrochloride 95 %	Roth
N,N,N',N' -Tetramethylethylendiamide (TEMED)	Roth
Thiamine hydrochloride	Sigma
Thiamine monophosphate chloride dihydrate	Sigma
Thiamine pyrophosphate	Sigma
Tris Ultra Quality 99.9 %	Roth
Triton X-100	Merck
Tween-20	Calbiochem
Urea	AppliChem
XL10 Gold ultracompetent cells	Stratagene

7.4 Chemically defined media

Component	Amount in mg
Group I	
$FeSO_4 \times 7H_2O$	5
$Fe(NO_3)_3 \times 9H_2O$	1
$MnSO_4$	5
dissolve in 1 ml H_2O	
Group II A	
L-tryptophan	100
L-cystein	50
dissolve in 1 ml 2 N HCl at 55 °C	
Group II B	
L-leucin	100
DL-alanin	100
L-isoleucin	100
L-methionine	100
L-threonine	200
L-arginine	100
DL-histidine	100
L-valine	100
L-lysine	100
L-glutamine	100
dissolve in 10 ml H_2O	
Group II C	
L-asparagine	100
L-phenylalanine	100
L-serine	100
L-proline	100
L-hydroxyproline	100
L-glutamic acid	100
glycine	100
L-tyrosine	100
dissolve each amino acid in 1 ml 2.5 N NaOH at 55 °C	
Group III	
p-aminobenzoic acid	0.2
biotin	0.2
folic acid	0.8
nicotinamid	1
α-NAD	2.5
D-panthoic acid	2
pyridoxal HCl	1
pyrodoxamin-di-HCl	1
riboflavin	2
thiamine HCl	1
cobalamine	0.1
dissolve components in 10 ml H_2O and dropwise addition of	
2.5 N NaOH until the solution becomes clear	

Group IV	
adenine	20
guanine HCl	20
uracil	20
dissolve in 3 ml 2 N HCl at 90 °C	
Group V	
K_2HPO_4	200
KH_2PO_4	1000
$MgSO_4 \times H_2O$	700
$CaCl_2 2 \times H_2O$	7
NaOAc $3 \times H_2O$	4500
$NaHCO_3$	2500
D-glucose	1000
HEPES	13,000
dissolve components in 300 ml H_2O	
H_2O ad 500 ml	

7.5 Bacterial strains

Organism	Mutations
E. coli MG1655	F^-, lambda$^-$, rph^{-1}
E. coli DH5αZ1	laci^q, PN25-tetR, Sp^r, deoR, supE44, Delta(lacZYA-argFV169), Phi80 lacZDeltaM15, recA1, hsdR17(rK- mK+), endA1, gyrA96, thi-1, relA1
E. coli XL10 GOLD	endA1, glnV44, recA1, thi-1, gyrA96, relA1, lac, Hte, Δ(mcrA)183, Δ(mcrCB-hsdSMR-mrr)173 tetR, F'[proAB lacIqZΔM15 Tn10(TetR Amy CmR)]
H. influenza DSMZ 11121	Rd [KW20] (Fleischmann et al., 1995)
S. aureus SG511-Berlin	VSSA
S. aureus Mu50	VISA

Table 7.5: Microorganisms and their genetic background. deoR: Allows uptake of large plasmids; regulatory gene mutation allowing constitutive expression of genes for deoxyribose synthesis; endA1: Abolishes non-specific endonuclease I activity; improves quality of plasmid DNA isolations; gyrA96: Resistance to nalidixic acid; DNA gyrase mutation; hsdR17(rK- mK+): Restriction minus, modification positive; transformed DNA will not be cleaved by endogeneous restriction endonucleases; laci^q: lac promoter up-mutation; constitutive overproduction of Lac repressor; DeltaM15: Allows α-complementation of β-galactosidase activity, partial deletion of β-D-galactosidase gene; PN25-tetR: constitutive production of Tet repressor; recA1: Prevents recombination between introduced DNA and host DNA; confers UV-light sensitivity; relA1: Allows RNA synthesis in the absence of protein synthesis; rph-1: a 1 bp deletion that results in frameshift over last 15 codons and has polar effects on pyrE, leading to suboptimal pyrimidine levels on minimal medium; Sp^r: resistance to Spectinomycin; supE44: Suppresses amber (UAG) mutations; thi-1: Requires thiamine for growth on minimal media; Hte phenotype allows high transformation with large plasmid inserts.

7.6 Kits

Kit	Manufacturer
NucleoSpin Extract II	Macherey-Nagel
NucleoSpin Plasmid kit	Macherey-Nagel
NucleoSpin Xtra Midi & Maxi kits	Macherey-Nagel
QuikChange Lightning	Agilent Technologies Inc. (Stratagene)
PCR purification kit	Fermentas
PrestoSpin D Bug	Molzym
PrestoSpin R Bug	Molzym
RNeasy Min Elute Clean-up	Qiagen
Sequenase Version 2.0 PCR product sequencing	USB

7.7 Standards, nucleotides and synthetic oligos

Type	Length	Manufacturer
DNA ladder	100-10,000 bp	PeqLab
	100-1,000 bp	PeqLab
RNA ladder	low range	Fermentas
	high range	Fermentas

Table 7.6: DNA and protein ladders

Nucleotides/ radiochemicals	Manufacturer
dNTP-Set	Roche
NTP-Set	Roche
α ^{32}P-GTP P-ATP, 10 mCi/ml	NEN, Zaventem, Belgium
γ ^{32}P-ATP P-GTP, 10 mCi/ml	NEN, Zaventem, Belgium

Table 7.7: Nucleotides and radiochemicals

Name	Sequence (5' to 3')
GATC-pRS414.2 empty-555953	CTG CCA GGA ATT GGG GAT CG
GATC-5' pRS414.2 Insert B-342112	GAA GCA ACG GCC CGG AGG

Table 7.8: Sequencing primers at GATC

Name	Sequence (5' to 3')
N25.47	AAT GCT AAT ACG ACT CAC TAT AGG GAG AGA GAG ACA GTC TAC GTA TT
N25.21	TGT ACC TAC GTC TGC AGT GAA
Oligo1	AAT ACG TAG ACT GTC TCT CTC TCC C
5' TPP+T7	TCG TAA TAC GAC TCA CTA TAG GAA CCA AAC GAC TCG
3' TPP	TTG CGC TGG ATC CAG CAG GTC GA
5' Sau glmS+T7	GATT AAT ACG ACT CAC TAT AGG GCA GTT AAA GCG CCT GTG CAA ATA
5'+T7 glmS Sau long (5'Sau glmS rbzm long)	TCG TAA TAC GAC TCA CTA TAG GTA ATG ATT AAT GGA AAG GGG G
3' Sau glmS neu	ATC TTA TTA ACT TTG TCC ATT AAG TCA CCC
N25.1 mut1F	AAT TCG CGC GGC ATA CCT GCT GCT CTG TGC CGC GCG
N25.1 mut R	GAT CCG CGC GGC ACA GAG CAG CAG GTA TGC CGC GCG
N25.1 mut2 F	AAT TCG CGC GGC ATA CCT CCT GCT CTG TGC CGC GCG
N25.1 mut2R	GAT CCG CGC GGC ACA GAG CAG GAG GTA TGC CGC GCG
5' glmS clvsite mut gg-mittellang	GCA CAG GCG GGA ACT GTA CTG CCG
3' glmS clvsite mut gg-mittellang	CGG CAG TAC AGT TAA CCC GCC TGT GC
Aptamer 7	AGA GAG AGA CAG TCT ACG TAT TCC TAC CCG ACA CAA TTC TAA TCT ACT TCA CTG CAG ACG TAG GTA CA
5'primiR 18a19a+bdgsite+T7	AAT GCT AAT ACG ACT CAC TAT AGG AGT GCT TTT TGT TCT AAG GTG C
3' primiR 18a19a+bdgsite	GGA GTG CTA CAG AAG CTG TCA CAT CA
5' primiR 19a+bdgsite+T7	AAT GCT AAT ACG ACT CAC TAT AGG AAG TTA TGT ATT CAT CC
3' primirR19a+bdgsite	GGA AGC TGT CAC ATC AGA TAG ACC
3' primiR19a+mut bdgsite	GGA AGC TGT CAC ATC AGA TAG ACC AGG CAG ATT CTA CAT CAC TCC AAT AAA AGT ACA CAA AAT T
5' mutATG 1	GTT GAC GAG GAT TGA GGT TAT CG
3' mutATG 1	GCA TAA CCT CAA TCC TCG TCA AC
5' mutATG 2	GAA TTT TCG GCG GGT GCC TCC CGG
3' mutATG 2	CCG GGA GGC ACC CGC CGA AAA TTC

Name	Sequence (5' to 3')
5' mutATG 3	GAG AAA TCA CGT GAT CTT CC
3' mutATG 3	GGA AGA TCA CGT GAT TTC TC
5' mutATG 4	CCA AAA AAC GTG TAG GAA GGG GAC AC
3' mutATG 4	GTG TCC CCT TCC TAC ACG TTT TTT GG
5' mutATG 4LV	CGT GAT CTT CCA AAA AAC GTG TAG GAA GGG GAC
3' mutATG 4LV	GTC CCC TTC CTA CAC GTT TTT TGG AAG ATC ACG
5' glmS clvmut gg	TAT TTA TTT GCA CAG GCG GGT TAA CTG TAC TGC CGA AC
3' glmS clvmut gg	GTT CGG CAG TAC AGT TAA CCC GCC TGT GCA AAT AAA TA
N25.1 LS FP (+T7)	TCG TAA TAC GAC TCA CTA TAG GCG CGG CAT ACC TGG TGC TCT GGTG CCG CGC
N25.1 LS RP (+T7)	GCG CGG CAC AGA GCA CCA GGT ATG CCG CGC CTA TAG TGA GTC GTA TTA CGA
5' pNYL insert	TCG TAA TAC GAC TCA CTA TAG GAT CAG CAG GCA CTG ACC G
3' pNYL insert	AAC AGA TAA AAC GAA AGG CCC AGT CTT TCG ACT GAG CC
N25.3 Apt FP (T7)	TCG TAA TAC GAC TCA CTA TAG ACA CTT CGA GCG GGT ACG AGT GTC
N25.3 Apt.RP	GAC ACT CGT ACC CGC TCG AAG TGT CTA TAG TGA GTC GTA TTA CGA
T7.glmSEGFP	TCT AAT ACG ACT CAC TAT AGG GTC AGA TCC GCT AGC GCT ACC
glmSEGFP	GCT TTA TTT GTA ACC ATT ATA AGC TGC
N25.1AptFP+T7	TCG TAA TAC GAC TCA CTA TAG GCA TAC CTG GTG CTC TGT GCC
N25.1AptRP	GGC ACA GAG CAC CAG GTA TGC CTA TAG TGA GTC GTA TTA CGA
N25.3LS RP+T7	CGG ACA CTC GTA CCC GCT CGA AGT GTC CGC TAT AGT GAG TCG TAT TAC GA
N25.3LS FP	TCG TAA TAC GAC TCA CTA TAG CGG ACA CTT CGA GCG GGT ACG AGT GTC CG
5' pNYLins w/o T7	ATC AGC AGG ACG CAC TGA CCG
chempro3'SauglmSlo	CAC TAT CCT CCT CGT CTA C
5' BamHI pSil Apt7	ATT GAA CGG ATC CGA TAC GTA GAC TGT CTC TCT CTC CCG TAA
3' HindIII pSil Apt7	CAA GTT AAA GCT TTT CCA AAA AAT CAC TGC AGA CGT AGG TAC ATT
5' T7 Apt7w/ODN	AAT GCT AAT ACG ACT CAC TAT AGA TAC GTA GAC TGT CTC TCT CTC CCG TAA
3' Apt7w/ODN	CAT TAC ATG GAT GCA GAC GTC ACT AA
Apt7 DNAw/ODN	GAT ACG TAG ACT GTC TCT CTC CCG TAA GGA GAG AGA GAC AGT CTA CGT ATC CTA CCC GAC ACA ATT CTA ATC TAC TCA CTG CAG ACG TAG GTA CAG TAA TGT ACC TAC GTC TGC AGT GAT TTT TTG GAA
3' pNYLins 27	CAA CAG ATA AAA CGA AAG GCC CAG TC

Name	Sequence (5' to 3')
FP 16S rRNA	ATT AGA TAC CCT GGT AGT CCA CGC C
RP 16S rRNA	CGT CAT CCC CAC CTT CCT CC
N25.1m1 AptFP+T7	TCG TAA TAC GAC TCA CTA TAG GCA TAC CTG CTG CTC TGT GCC
N25.1m1 AptRP	GGC ACA GAG CAG CAG GTA TGC CTA TAG TGA GTC GTA TTA CGA
N25.1m1LS FP+T7	TCG TAA TAC GAC TCA CTA TAG GCG CGG CAT ACC TGC TGC TCT GTG CCG CGC
N25.1m1LS RP	GCG CGG CAC AGA GCA GCA GGT ATG CCG CGC CTA TAG TGA GTC GTA TTA CGA
N25.1m2 AptFP+T7	TCG TAA TAG GAC TCA CTA TAG GCA TAC CTC CTG CTC TGT GCC
N25.1m2 AptRP	GGC ACA GAG CAG GAG GTA TGC CTA TAG TGA GTC GTA TTA CGA
N25.1m2LS FP+T7	TCG TAA TAC GAC TGA CTA TAG GCG CGG CAT ACC TCC TGC TCT GTG CCG CGC
N25.1m2LS RP	GCG CGG CAC AGA GCA GGA GGT ATG CCG CGC CTA TAG TGA GTA GTA TTA CGA
T7+preQlong	VAAT GCT AAT ACG ACT CAC TAT AGG TTG TAT ACT CCG TTC TAA ATG TG
5' preQlngßgal	CAC TAT AGG GAA TTC TTG TAT ACT CCG TTC TAA ATG TG
3' preQ1 Mu50	TTT TGT AAT TGC TCC TAT CA
3' preQ1 Mu50ßGal	CGG GCA TGG ATC CAG GTC GAC TTG CAT AGT TTG CTC CTT TTT GTA ATT GCT CCT ATC
5' preQSauEcoRI	CAC TAT AGG GAA TTC TAT TCA TCG TAC
Sau preQ1 AD	TAT TCT ATT CAT CGT ACA TAA ATG AAT ATC AGA GGT TTC TAG CTG AAA CCC TCT ATA AAA AAC TAG ACA TT
5' preQSau+T7	AAT GCT AAT ACG ACT CAC TAT AGG GTA TTC TAT TCA TCG TAC
3' preQ1	AAT GTC TAG TTT TTT ATA GAG GG
3' preQ1 βGal rep	CGG GCA TGG ATC CAG GTC GAC TTG CAT AGT TTG CTC CTA ATG TCT AGT TTT TTA TAG AGG G
5' pNYLins +T7NEW	TCG TAA TAC GAC TCA CTA TAG GAT CAG CAG GAC GCA C
pNYL ins NEW	AAC AGA TAA AAC GAA AGG CCC AGT CTT TCG ACT G
5' NheI glmS ATG1234	ATT GAA CGC TAG CTC TTG TTC TTA TTT TCT C
3' BglIII glmS ATG1234	ATT GAA CTC TAG AGT CCC CTT CCT ACA CGT TTT TTG GA
5' KpnI glmS ATG 1234	ATT GAA CGG TAC CTC TTG TTC TTA TTT TCT C
3' BamHI glmS ATG1234	ATT GAA CCC TAG GGT CCC CTT CCT ACA CGT TTT TTG GA
5' Ad.RS	TCG TAA TAC GAC TCA CTA TAG GGA AAT AGC TAT TAT CAC TT
3' Ad. RS	AAA AAA AAT CCT GAT TAC AAA AAA TGT C

Name	Sequence (5' to 3')
5' TTPHHaz	TAA TAC GAC TCA CTA TAG GGA GTC TCC TTC GGT ACA TCC AGC TGA TGA GTC CCA AAT AGG ACG
3' TTPHHaz 1.20	TCT CCT TCG TGG AAT CCA GGA ATA ATC CCT ACG CTG GCA TTA TCC AGA TCA GGT GAT ACG GGT ATT TCT CAG CC
blck strand	ATT TGG GAC TCA TCA GCT GG
3' TTPHHaz2.5	TCT CCT TCG TGG AAT CCA GGA TCC ATC CCT ACG CTG GCA TTA TCC AGA TCA GGT GAT ACG GGT ATT TCT CAG CC
5' Ad.RS-xtd	ATG AAC GGG AAT TCT CGT AAT ACG ACT CAC
3' Ad. RS-xtd	CTT GGC ATG GAT CCA GGT TTA CTT GCA TAT TTT GCT CCT AAA AAA
3' tpp.91	CGT GAC TTC CCT ACG CTG GCA T
5' T7 shp Apt 7	AAT GCT AAT ACG ACT CAC TAT AGG GAT ACG TAG TAA TAC GTA TCC TAC C
3' shp Apt 7	AAT CAC TGC AGA TTC ATC TGC AGT GAG TAG
3' Ad.RSxtd 1st	AGG TTT ACT TGC ATA TGT TGC TCC TAA AAA AAA TCC TGA TTA CAA AAA ATG
3' Ad.RSxtd 2nd	CTT GGC ATG GAT CCA GGT TTA CTT GCA TAT GTT GCT C
pRS414.2 fw	AGG AGC AAA CUA UGC AAG UCG
pRS414.2 rv	GAA TTC CGA TCC CCA ATT
pRS414.2 empty fw	CCG GGC AGG CCA T
5' GLMS nt1	ATG TGT GGA ATT GTT GGT TAT ATT GGC
3' GLMS nt916	CTG CAT GGT AGC TTG TAC CTG
5' qPCR GLMS	GCT GAT AGT AGC GAT TTT GAT GG
3' qPCR GLMS	GCA TAT GAA CCA TGT AAT AAT GAC AC
5' glcA fmt1 BamHI	ATT GAA CGG ATC CAC CAA CGT GTT ACT AAG TAA GAT TAG GC
3' glcA fmt1 KpnI	ATT GAA CGG TAC CCG ATT GCG ACA CCT AAT GCG
5' glcA fmt 2 KpnI	ATT GAA CGG TAC CAT GTT GAG GAA GGT CAA GAA G
3' glcA fmt2 NcoI	ATT GAA CCC ATG GAT AGC CTC GAA TAC AGT G
5' ptsG fmt1 BamHI	ATT GAA CGG ATC CAC TTG CGT GTT ACT GGT A
3' ptsG fmtI XhoI	ATT GAA CCT CGA GCT GCT GCT TCC ATG ACC G
5' ptsG fmt2 XhoI	ATT GAA CCT CGA GAA ACT GAA TGG TGA AGG ATT CG
3' ptsG fmt2 NcoI	ATT GAA CCC ATG GCT CGC TAC TTC GCA TAC GC
5' ptaA fmt1 BamHI	ATT GAA CGG ATC CGC CTA GGT GAC TAT AAC GGA G

Name	Sequence (5' to 3')
3' ptaA fmt1 KpnI	ATT GAA CGG TAC CTA TAG CTA CAC CAA TTG C
5' ptaA fmt2 KpnI	ATT GAA CGG TAC CGA ATA CGA TTG GTA GAG GTG
3' ptaA fmt2 NcoI	ATT GAA CCC ATG GTT AGA TTT GCG CTT TAG CTG
gyrB-297	TTA GTG TGG GAA ATT GTC GAT AAT
gyrB-547	AGT CTT GTG ACA ATG CGT TTA CA

Table 7.10: Synthetic oligonucleotides

8 Appendix

8.1 Supplementary Material

Activator	EC$_{50}$ *S. aureus*	R^2	EC$_{50}$ *B. subtilis*	R^2
GlcN6P	3.6 µM	0.98		
GlcN	189 µM	0.98		
CGlcN6P	6.2 µM	0.98	2.1 µM	0.93
GlcN6S	160 µM	0.98		

Table 8.1: EC$_{50}$ values for glmS activating metabolites. To obtain these values, percent glmS cleavage was plotted against the logarithm of metabolite concentration used in the cleavage reaction. This sigmoidal dose-response curve was fitted as mentioned in Methods Section 6.2.4.2. Goodness of fit is indicated by R^2 values.
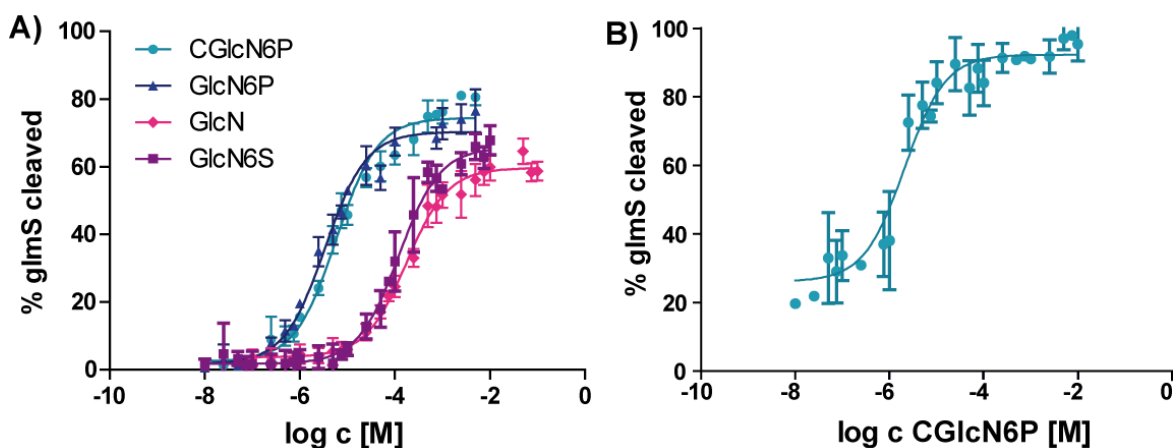
Figure 8.1: Dose-response curves for EC$_{50}$ determinations. (A) Dose-response curve used for EC$_{50}$ determination of *S. aureus* glmS ribozyme cleavage in the presence of increasing GlcN6P (dark blue), GlcN (magenta), CGlcN6P (light blue) or GlcN6S (purple) concentrations. Error bars indicate standard deviation of at least three independent experiments. (B) Dose-response curve used for EC$_{50}$ determination of *B. subtilis* glmS ribozyme cleavage in the presence of increasing CGlcN6P concentrations. Error bars indicate standard deviation of at least three independent experiments.
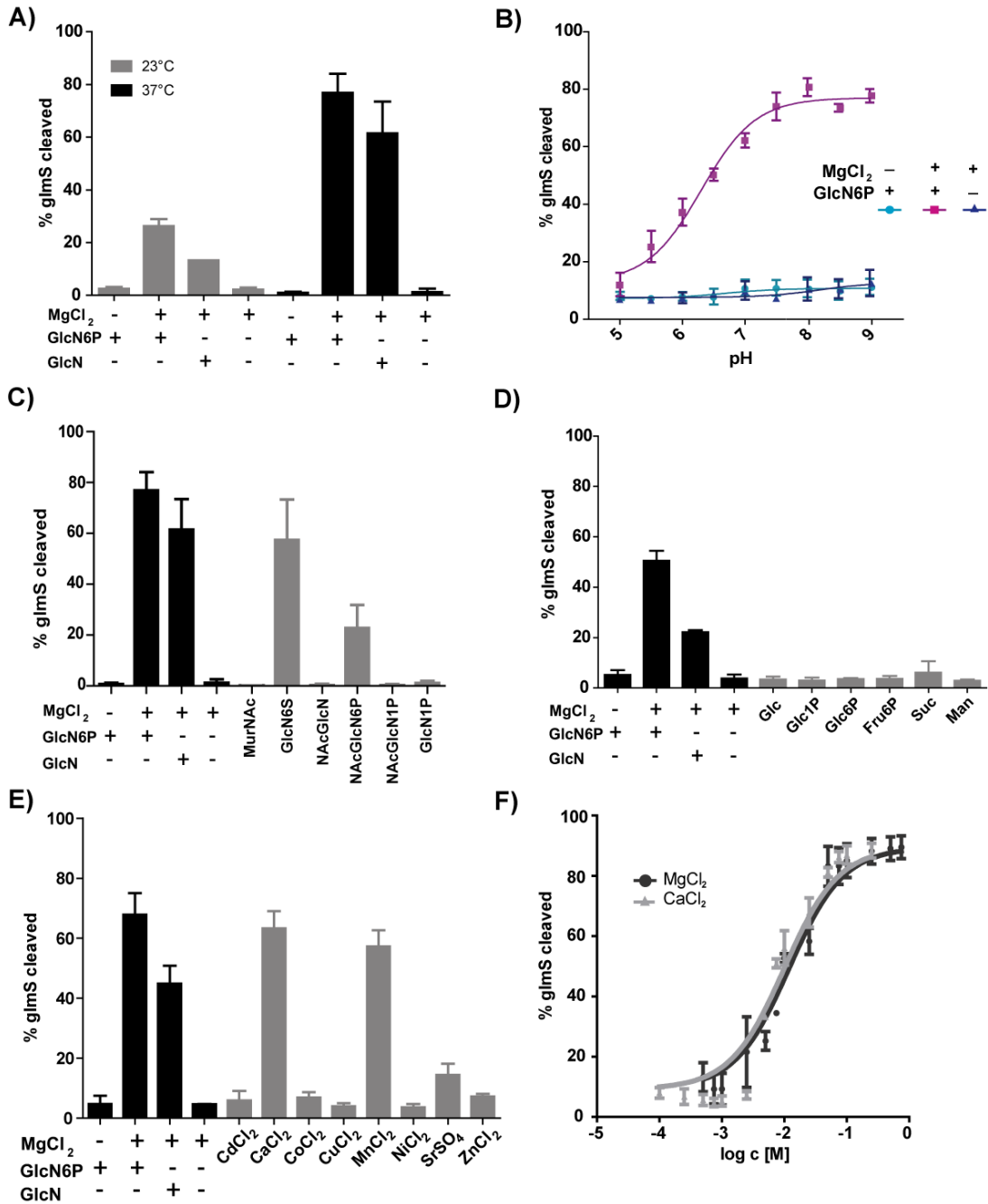
Figure 8.2: *S. aureus* **glmS ribozyme characteristics.** (A) Temperature dependency of glmS self-cleavage. At physiological temperatures of 37 °C (black bars) cleavage is more prominent than at RT (23 °C, gray bars). (B) pH dependency of glmS self-cleavage. With increasing pH the ratio of cleaved glmS increases reaching a cleavage maximum at pH of about 7.5. (C) Metabolite-induced cleavage assay using different sugar metabolites or a chemical analog of GlcN6P, namely GlcN6S, as substrate. (D) Metabolite-induced cleavage assay using different mono- and disaccharides (Glc= D-glucose, Glc1P= glucose-1-phosphate, Glc6P= glucose-6-phosphate, Fru6P= fructose-6-phosphate, Suc= Sucrose, Man= Mannose) at a final concentration of 2 mM. (E) Salts were tested at 10 mM final concentration. (F) Concentration dependent analysis of $MgCl_2$ and $CaCl_2$ aided glmS cleavage.
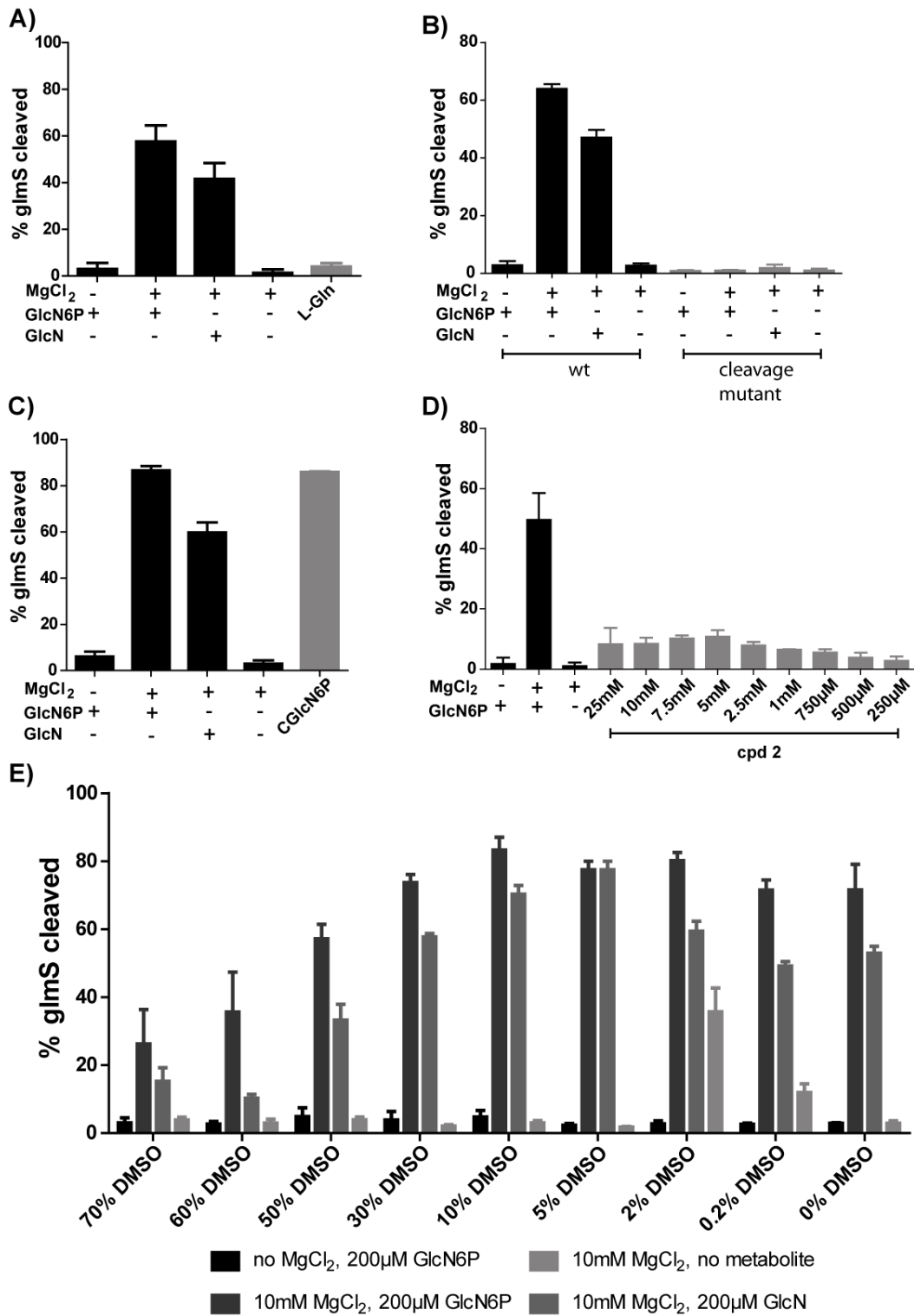
Figure 8.3: Metabolite induced self-cleavage assay of glmS ribozyme of *S. aureus* and *B. subtilis*. (A) Metabolite induced self-cleavage of *S. aureus* glmS ribozyme upon addition of L-glutamin (L-Gln, 200 μM) (B) Metabolite induced self-cleavage of the wildtype (wt) glmS ribozyme of *S. aureus* in comparison to the cleavage mutant, which does not show any self-cleavage upon addition of GlcN6P or GlcN. (C) Metabolite induced self-cleavage of *B. subtilis* glmS ribozyme upon addition of CGlcN6P (200 μM). (D) Concentration dependent effect of compound **2** on *S. aureus* glmS ribozyme cleavage. (E) Influence of increasing DMSO concentrations on metabolite induced self-cleavage assay.
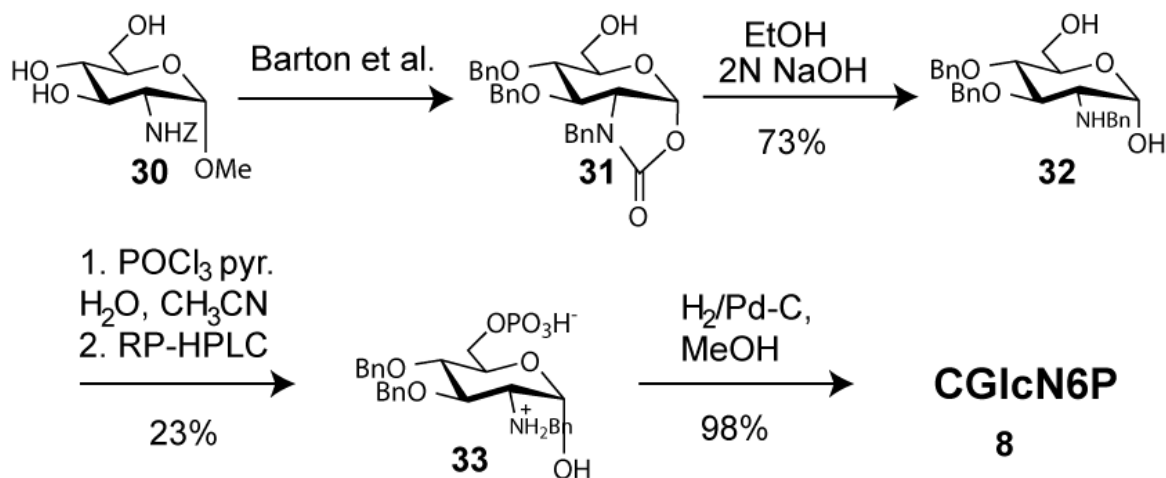
Figure 8.4: Synthesis scheme of carba-glucosamine-6-phosphate. Methyl glycoside **30** was converted to carba-cycle **31** as described by Barton et al. (1990). Basic cleavage of the cyclic carbamate gave diol **32** that could be selectively phosphorylated at the primary hydroxyl group to yield **33**. Catalytic hydrogenation gave carba-sugar **8**.
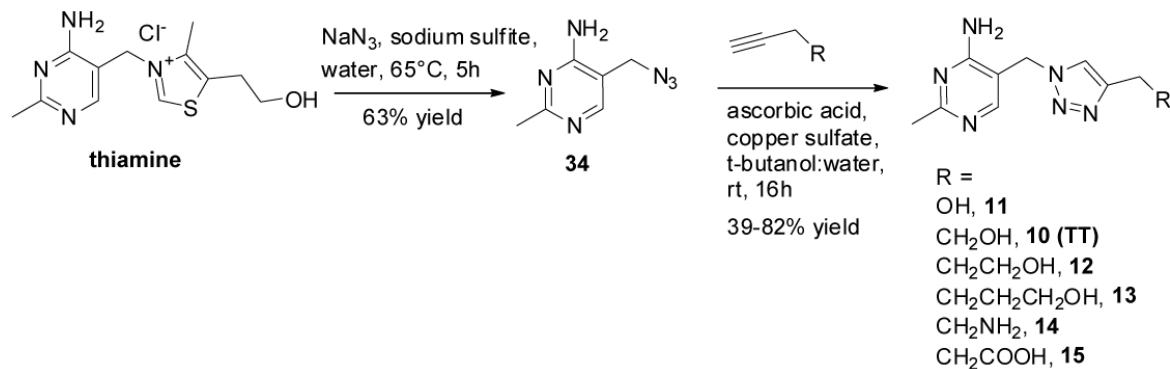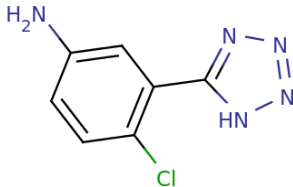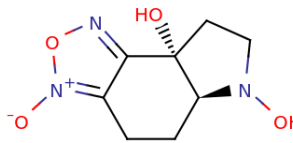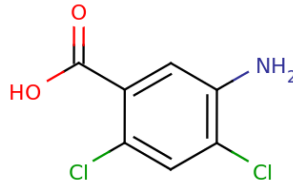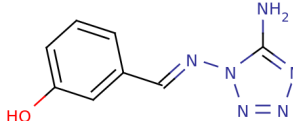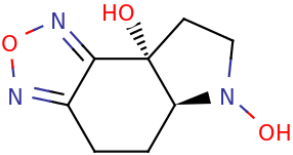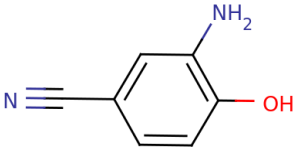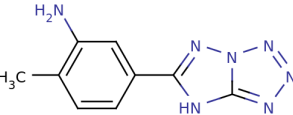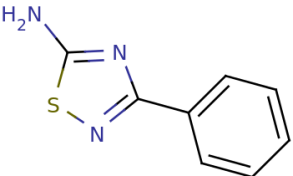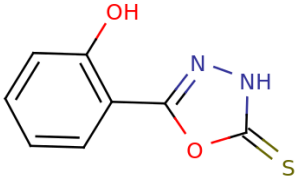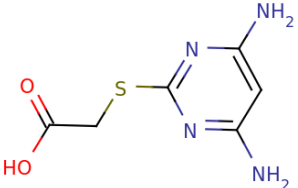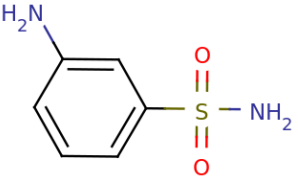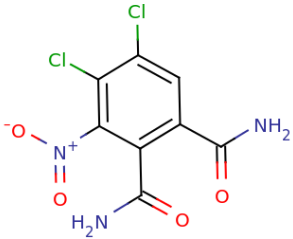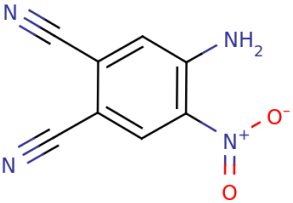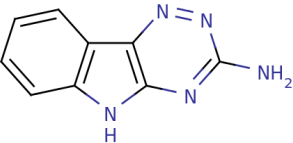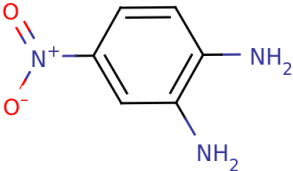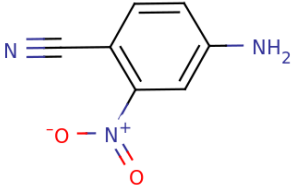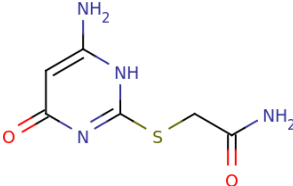
Figure 8.5: Synthesis scheme of compounds 11-15. Synthesis of compounds **11-15** was achieved using a "click" chemistry approach utilizing a common azide intermediate, **34**. This was obtained from thiamine itself in a substitution reaction with sodium azide which has been previously reported by Erixon et al. (Erixon et al., 2008). Compound **34** was then reacted with the appropriate substituted alkyne to generate the small library of six thiamine derivatives.
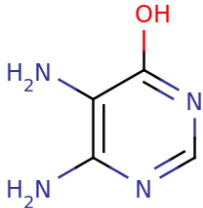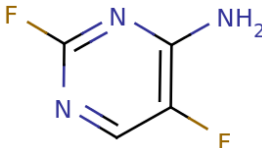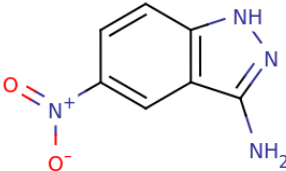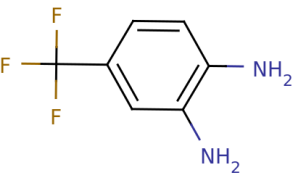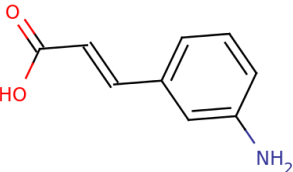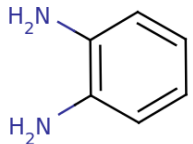
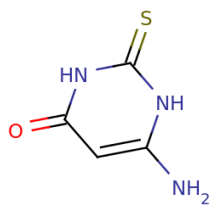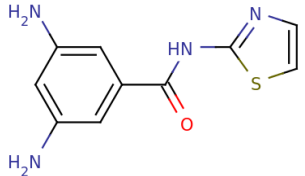| Screening plate coordinate	Library name	Library stock conc. in 100 %DMSO	Chemical formula	Screening 2 mM cpd in 2 % DMSO	Screening competition w/ 200 µM GlcN6P & 2 mM cpd in 2 %DMSO	Screening 500 µM cpd in 0.5 % DMSO	Concentration dependency
B1	OSSL 147279	100 mM		-	-	-	-
B2	OSSK 327912	100 mM		-	-	-	-
B3	OSSK 976609	100 mM		-	-	-	-
B4	OSSK 762475	100 mM		-	-	-	-
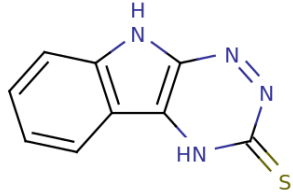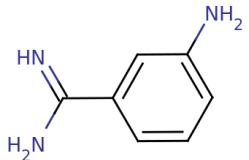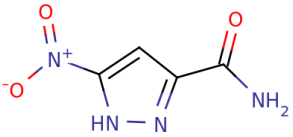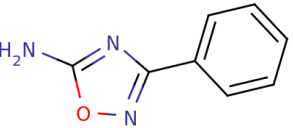
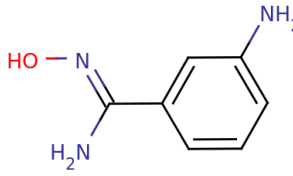| Screening plate coordinate	Library name	Library stock conc. in 100 %DMSO	Chemical formula	Screening 2 mM cpd in 2 % DMSO	Screening competition w/ 200 µM GlcN6P & 2 mM cpd in 2 %DMSO	Screening 500 µM cpd in 0.5 % DMSO	Concentration dependency
B5	OSSK 388924	100 mM		-	-	-	-
B6	OSSL 312478	100 mM		-	-	-	-
B7	OSSK 804294	100 mM		-	X	-	X
B8	OSSK 685964	100 mM		-	-	-	-
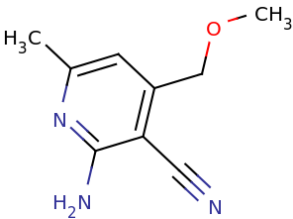
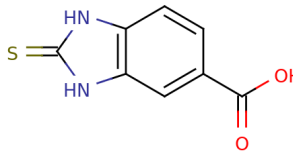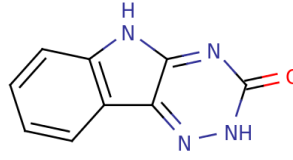| Screening plate coordinate	Library name	Library stock conc. in 100 %DMSO	Chemical formula	Screening 2 mM cpd in 2 % DMSO	Screening competition w/ 200 µM GlcN6P & 2 mM cpd in 2 %DMSO	Screening 500 µM cpd in 0.5 % DMSO	Concentration dependency
B9	OSSK 383494	100 mM		-	-	-	-
B10	OSSL 120981	100 mM		-	-	-	-
B11	OSSK 695929	100 mM		-	-	-	-

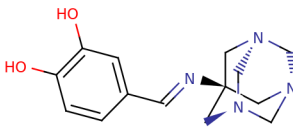| Screening plate coordinate	Library name	Library stock conc. in 100 %DMSO	Chemical formula	Screening 2 mM cpd in 2 % DMSO	Screening competition w/ 200 μM GlcN6P & 2 mM cpd in 2 %DMSO	Screening 500 μM cpd in 0.5 % DMSO	Concentration dependency
B12	OSSL 047840	100 mM		-	-	-	-
C1	OSSL 142441	100 mM		-	-	X	-
C2	OSSK 732300	100 mM		-	-	(X)	-

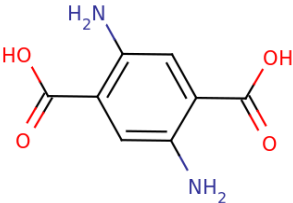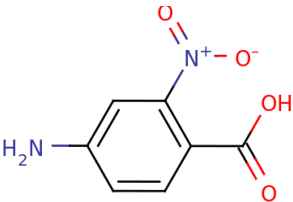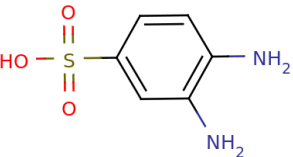| Screening plate coordinate	Library name	Library stock conc. in 100 %DMSO	Chemical formula	Screening 2 mM cpd in 2 % DMSO	Screening competition w/ 200 µM GlcN6P & 2 mM cpd in 2 %DMSO	Screening 500 µM cpd in 0.5 % DMSO	Concentration dependency
C3	OSSL 029294	100 mM		-	X	-	X
C4	OSSL 003990	100 mM		-	-	(X)	-
C5	OSSL 121122	100 mM		-	-	-	-

Screening plate coordinate	Library name	Library stock conc. in 100 %DMSO	Chemical formula	Screening 2 mM cpd in 2 % DMSO	Screening competition w/ 200 µM GlcN6P & 2 mM cpd in 2 %DMSO	Screening 500 µM cpd in 0.5 % DMSO	Concentration dependency
C6	OSSL 130094	100 mM		X*	X*	-	-
C7	OSSL 131038	100 mM		-	-	-	-
C8	OSSK 982966	100 mM		-	X	-	X

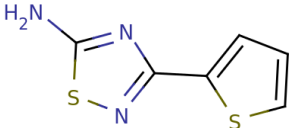| Screening plate coordinate	Library name	Library stock conc. in 100 %DMSO	Chemical formula	Screening 2 mM cpd in 2 % DMSO	Screening competition w/ 200 µM GlcN6P & 2 mM cpd in 2 %DMSO	Screening 500 µM cpd in 0.5 % DMSO	Concentration dependency
C9	OSSK 144325	100 mM		-	X	(X)	-
C10	OSSL 123765	100 mM		-	(X)	-	-
C11	OSSL 255027	100 mM		-	-	X	-
C12	OSSK 735072	100 mM		-	-	(X)	-

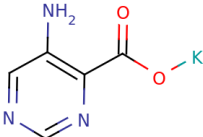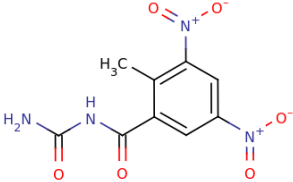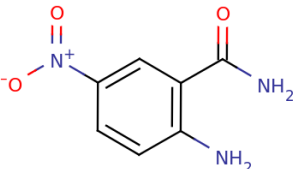| Screening plate coordinate	Library name	Library stock conc. in 100 %DMSO	Chemical formula	Screening 2 mM cpd in 2 % DMSO	Screening competition w/ 200 µM GlcN6P & 2 mM cpd in 2 %DMSO	Screening 500 µM cpd in 0.5 % DMSO	Concentration dependency
D1	OSSL 119073	100 mM		-	-	(X)	-
D2	OSSL 312386	100 mM		-	X	(X)	X
D3	OSSK 712512	100 mM		-	-	-	-

Screening plate coordinate	Library name	Library stock conc. in 100 %DMSO	Chemical formula	Screening 2 mM cpd in 2 % DMSO	Screening competition w/ 200 µM GlcN6P & 2 mM cpd in 2 %DMSO	Screening 500 µM cpd in 0.5 % DMSO	Concentration dependency
D4	OSSL 015052	100 mM		X	X**	-	-
D5	OSSK 199931	100 mM		-	-	-	-
D6	OSSL 013876	100 mM		-	X	-	-

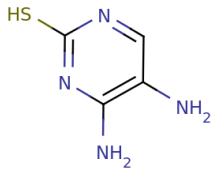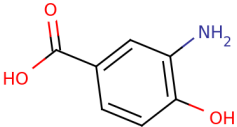| Screening plate coordinate	Library name	Library stock conc. in 100 %DMSO	Chemical formula	Screening 2 mM cpd in 2 % DMSO	Screening competition w/ 200 μM GlcN6P & 2 mM cpd in 2 %DMSO	Screening 500 μM cpd in 0.5 % DMSO	Concentration dependency
D7	OSSL 116374	100 mM		X	-	-	-
D8	OSSK 762394	100 mM		-	X*	-	-
D9	OSSK 633341	100 mM		-	X	-	-
D10	OSSL 148421	100 mM		-	-	-	-

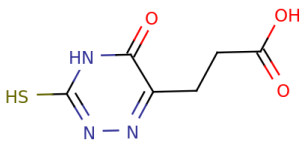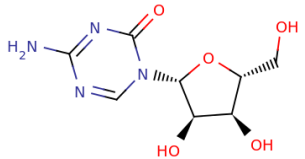| Screening plate coordinate	Library name	Library stock conc. in 100 %DMSO	Chemical formula	Screening 2 mM cpd in 2 % DMSO	Screening competition w/ 200 µM GlcN6P & 2 mM cpd in 2 %DMSO	Screening 500 µM cpd in 0.5 % DMSO	Concentration dependency
D11	OSSK 338580	10 mM		-	-	-	-
D12	OSSL 141603	100 mM		-	-	-	-
E1	OSSL 122658	100 mM		-	-	-	-

Screening plate coordinate	Library name	Library stock conc. in 100 %DMSO	Chemical formula	Screening 2 mM cpd in 2 % DMSO	Screening competition w/ 200 µM GlcN6P & 2 mM cpd in 2 %DMSO	Screening 500 µM cpd in 0.5 % DMSO	Concentration dependency
E2	OSSK 692937	100 mM		-	-	-	-
E3	OSSK 813669	100 mM		-	-	-	-
E4	OSSL 132498	100 mM		-	-	-	-
E5	OSSL 121704	100 mM		X	-	-	-

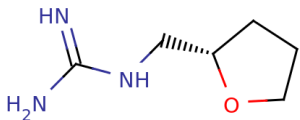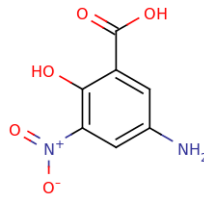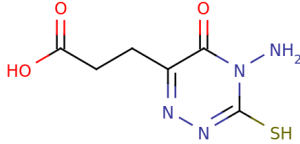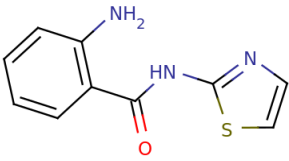| Screening plate coordinate	Library name	Library stock conc. in 100 % DMSO	Chemical formula	Screening 2 mM cpd in 2 % DMSO	Screening competition w/ 200 µM GlcN6P & 2 mM cpd in 2 %DMSO	Screening 500 µM cpd in 0.5 % DMSO	Concentration dependency
E6	OSSK 813667	100 mM		X*	X*	-	-
E7	OSSL 312281	100 mM		-	-	-	-
E8	OSSK 698044	100 mM		-	X	-	-
E9	OSSL 297340	100 mM		X	-	-	-

Screening plate coordinate	Library name	Library stock conc. in 100 %DMSO	Chemical formula	Screening 2 mM cpd in 2 % DMSO	Screening competition w/ 200 µM GlcN6P & 2 mM cpd in 2 %DMSO	Screening 500 µM cpd in 0.5 % DMSO	Concentration dependency
E10	OSSK 676877	100 mM		-	-	-	-
E11	OSSL 312293	100 mM		-	-	-	-
E12	OSSK 002497	100 mM		-	-	-	-
F1	OSSK 529154	100 mM		-	-	-	-

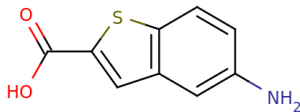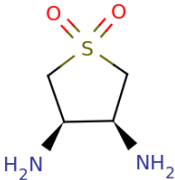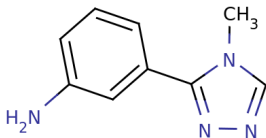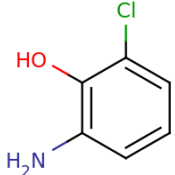| Screening plate coordinate	Library name	Library stock conc. in 100 %DMSO	Chemical formula	Screening 2 mM cpd in 2 % DMSO	Screening competition w/ 200 µM GlcN6P & 2 mM cpd in 2 %DMSO	Screening 500 µM cpd in 0.5 % DMSO	Concentration dependency
F2	OSSL 313057	100 mM		-	-	-	-
F3	OSSL 299430	10 mM		-	-	-	-
F4	OSSK 531676	100 mM		-	-	-	-
F5	OSSL 312911	100 mM		X	-	-	-
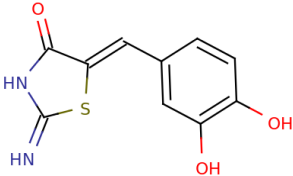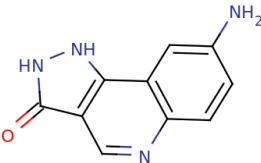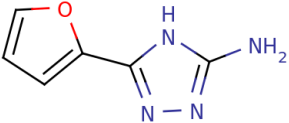
Screening plate coordinate	Library name	Library stock conc. in 100 %DMSO	Chemical formula	Screening 2 mM cpd in 2 % DMSO	Screening competition w/ 200 µM GlcN6P & 2 mM cpd in 2 %DMSO	Screening 500 µM cpd in 0.5 % DMSO	Concentration dependency
F6	OSSL 279020	100 mM		-	X	-	-
F7	OSSL 160624	100 mM		-	X	-	-
F8	OSSK 647579	100 mM		-	X	-	-

Table 8.3: **Reymond compounds and results of different screening approaches.** If compounds appeared as hits in a screening approach they are marked with an X. X* indicate compounds that appeared as hits from the band quantification data, but turned out to be artifacts, when primary PA-gel appearance was considered. (X) indicate compounds that could be counted as hits, because they are very close to the hit cut-off-line. X** marks compounds with unexpected effects on screening outcome, such as D4, which did not only show glmS cleavage activation in the first screening, but also revealed increased glmS activation in the GlcN6P competition screening.
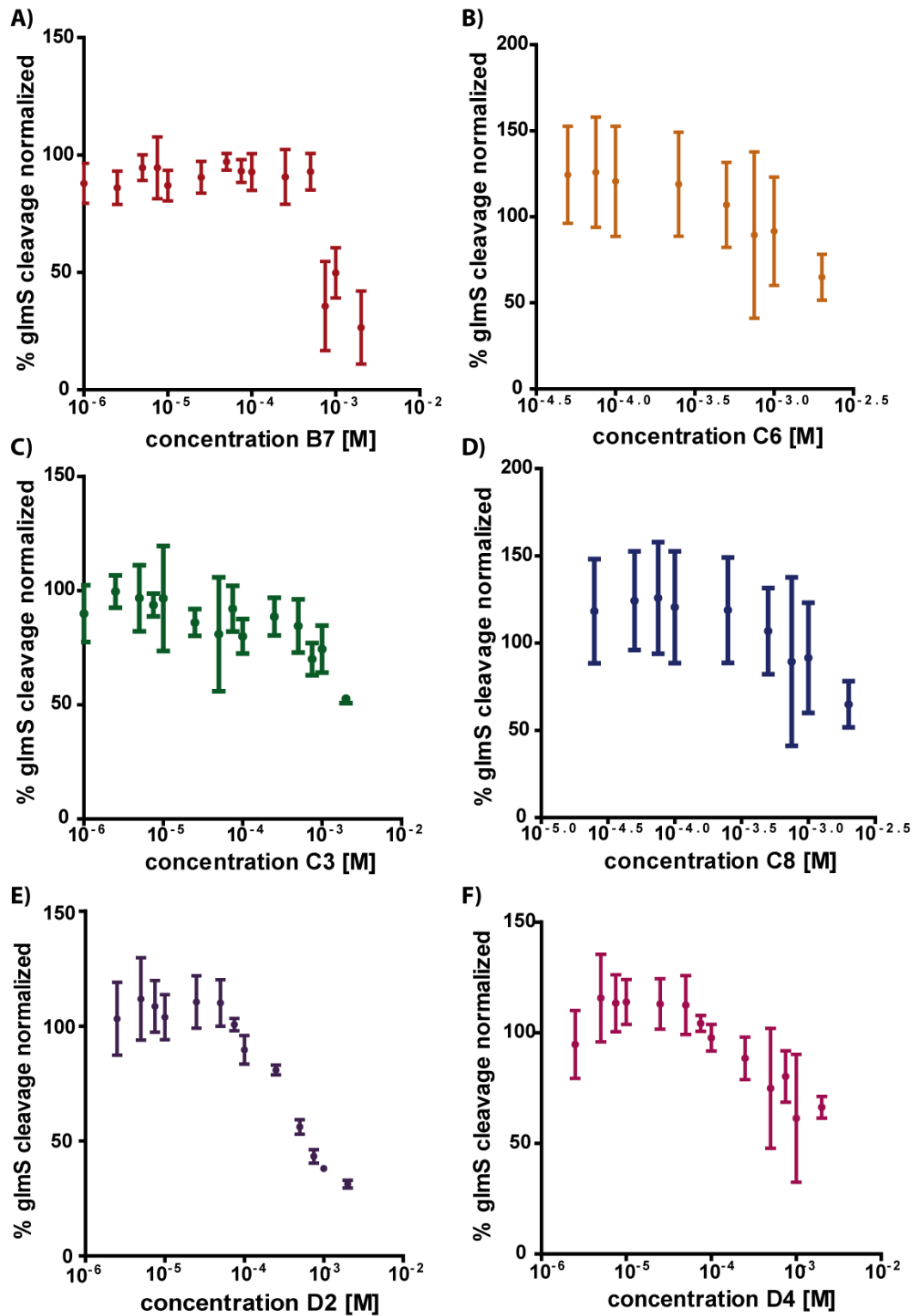
Figure 8.6: Reymond compounds with concentration dependent inhibition of glmS ribozyme cleavage. Graphs show metabolite-induced self-cleavage assays carried out in the presence of 200 μM GlcN6P and increasing concentrations of Reymond compound **B7** (A), **C6** (B), **C3** (C), **C8** (D), **D2** (E) and **D4** (F). Compound concentrations ranging from 1 μM-2 mM were not sufficient to inhibit cleavage completely.
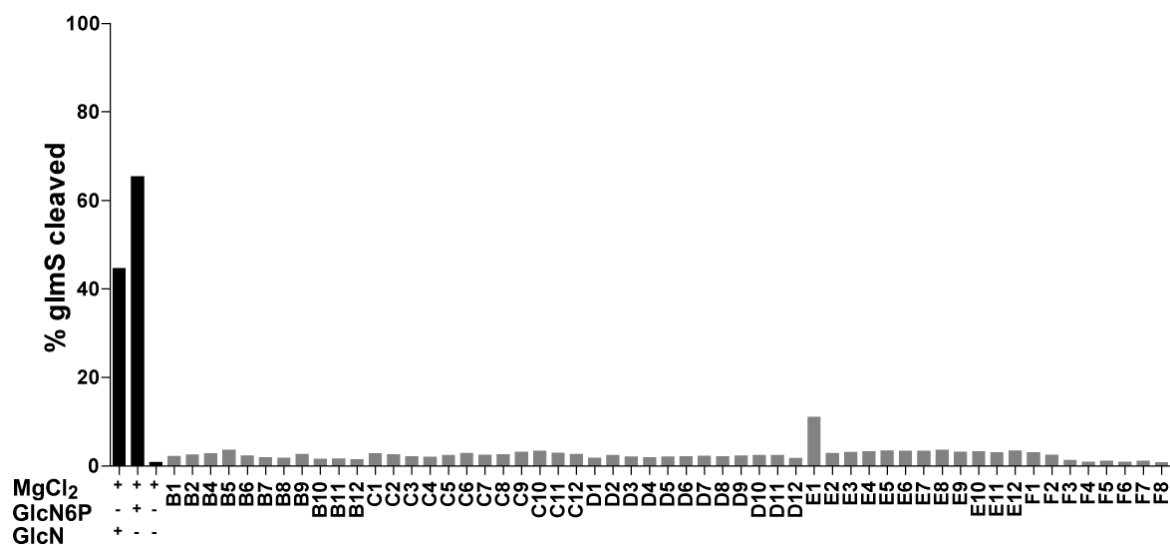
Figure 8.7: Screening of Reymond compounds for activation of glmS ribozyme. For this screening the glmS ribozyme was incubated with the Reymond compound library at a final compound concentration of $20\,\mu M$ in $2\,\%$ DMSO. None of the compounds increased the cleavage above background levels. Increase in glmS activation for compound **E1** is due to unspecific RNA degradation most likely due to an RNase contamination.
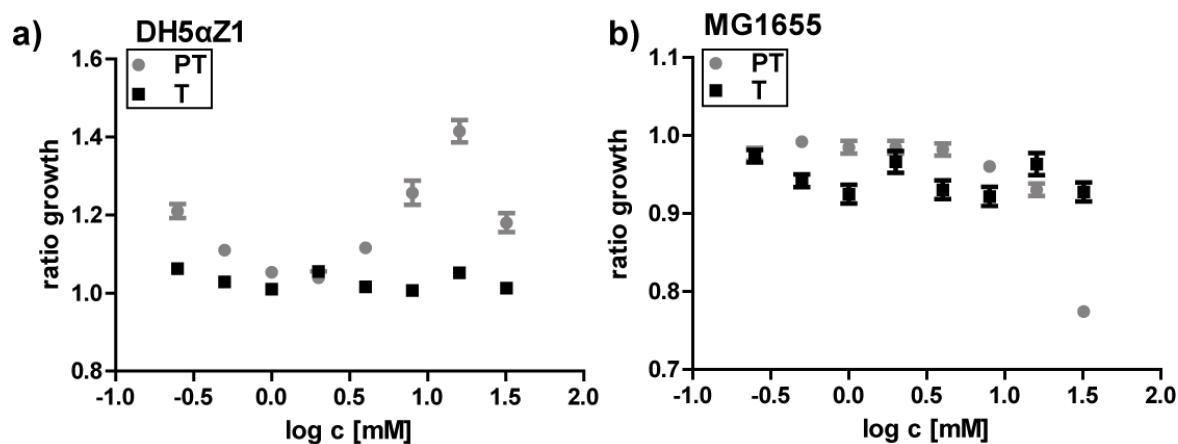
Figure 8.8: Growth curves of DH5αZ1 and MG1655 in M9 minimal medium in the presence of PT and T. A) DH5αZ1 cells do not show diminished growth upon increasing pyrithiamine concentrations, whereas OD_{600} of MG1655 cells decreases at concentrations higher than $8\,mM$ (B). Graphs show bacterial growth at t=495 min in the presence of PT or T in relation to growth in the absence of any compound. Bacterial growth was determined by measurement of OD_{600} over 15 minutes for 24 h (see Section 6.3.6 for details).
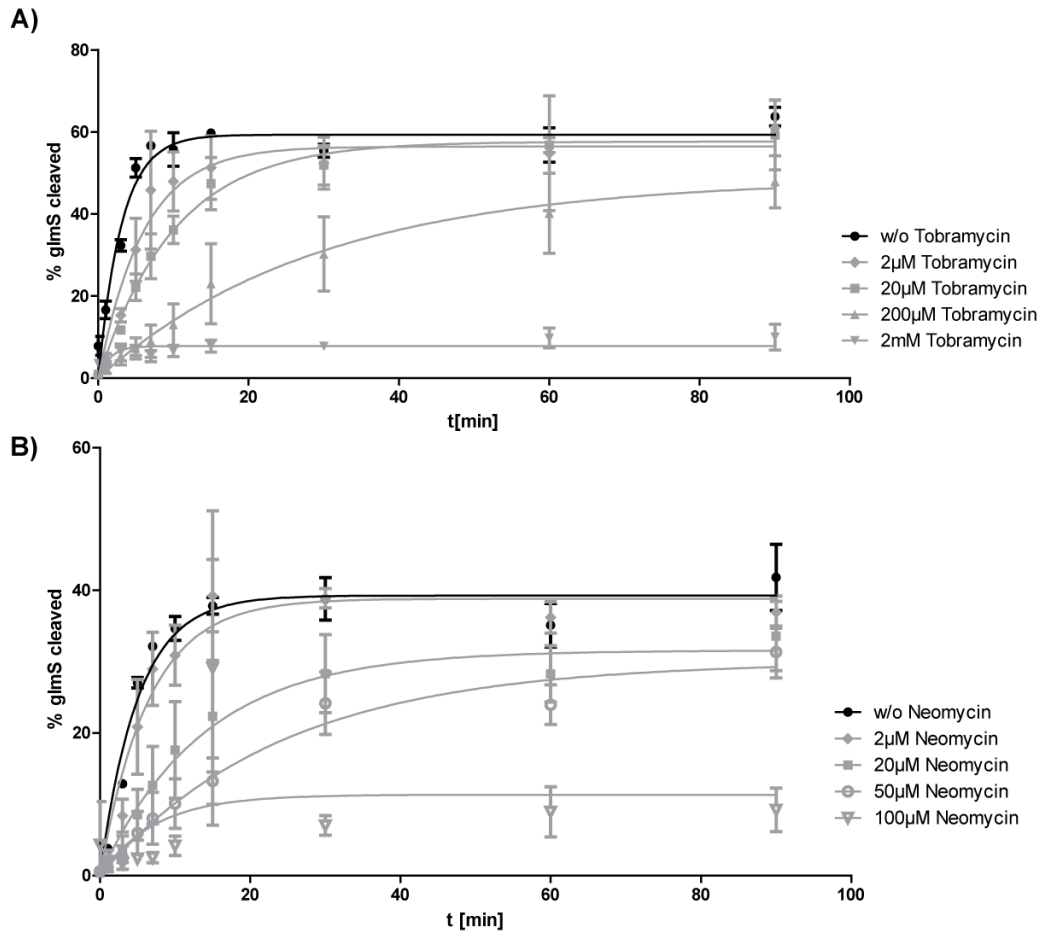
Figure 8.9: k$_{obs}$ determinations for *S. aureus* glmS cleavage inhibition by aminogly-cosides. Metabolite-induced self-cleavage of *S. aureus* glmS in the presence of $200\,\mu$M GlcN6P and indicated concentrations of Tobramycin (A) and Neomycin (B). These k$_{obs}$ determinations were performed by Anna Schüller.
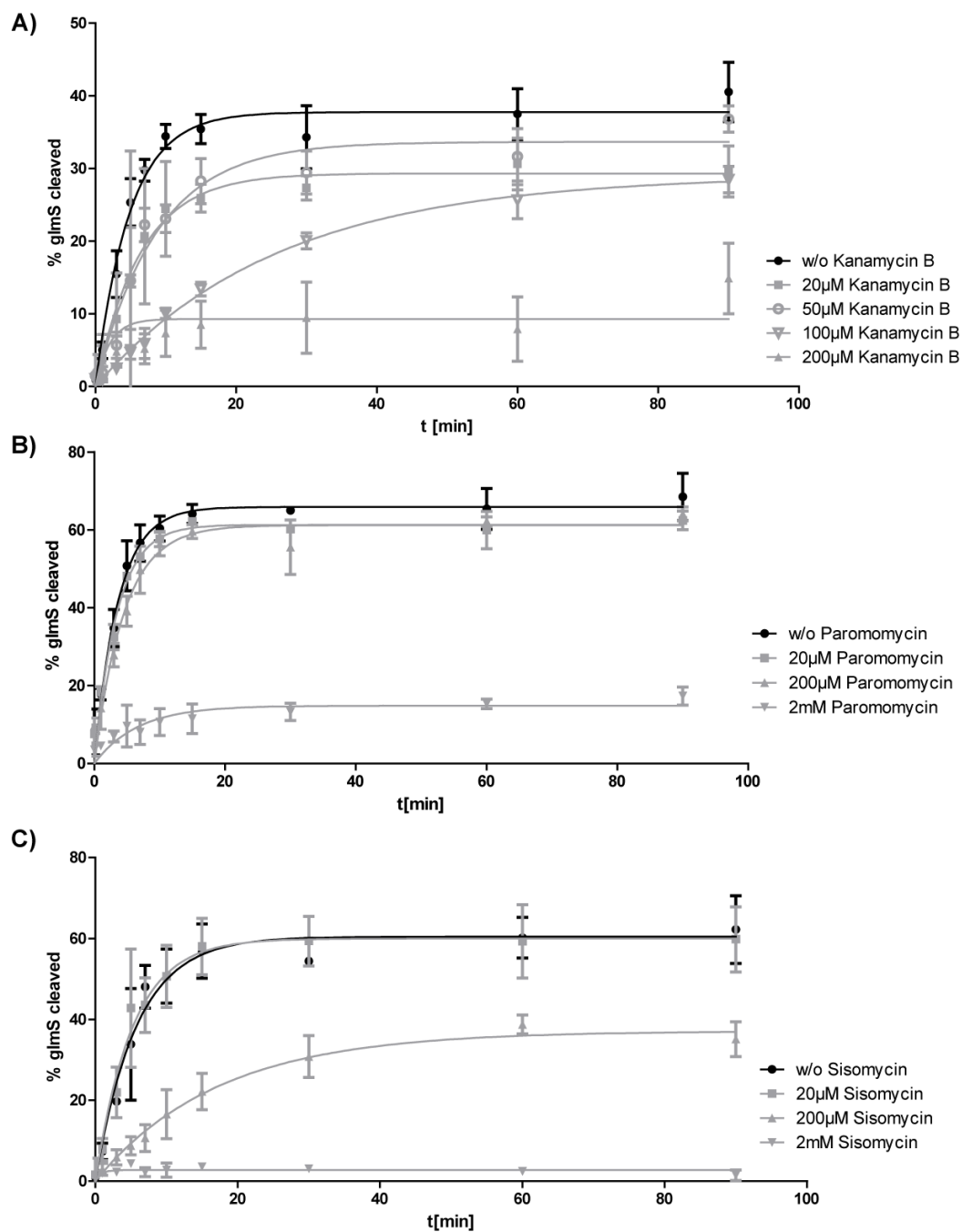
Figure 8.10: k$_{obs}$ determinations for *S. aureus* glmS cleavage inhibition by aminogly-cosides. Metabolite-induced self-cleavage of *S. aureus* glmS in the presence of 200 µM GlcN6P and indicated concentrations of Kanamycin B (A), Paromomycin (B) and Sisomycin (C). These k$_{obs}$ determinations were performed by Anna Schüller.
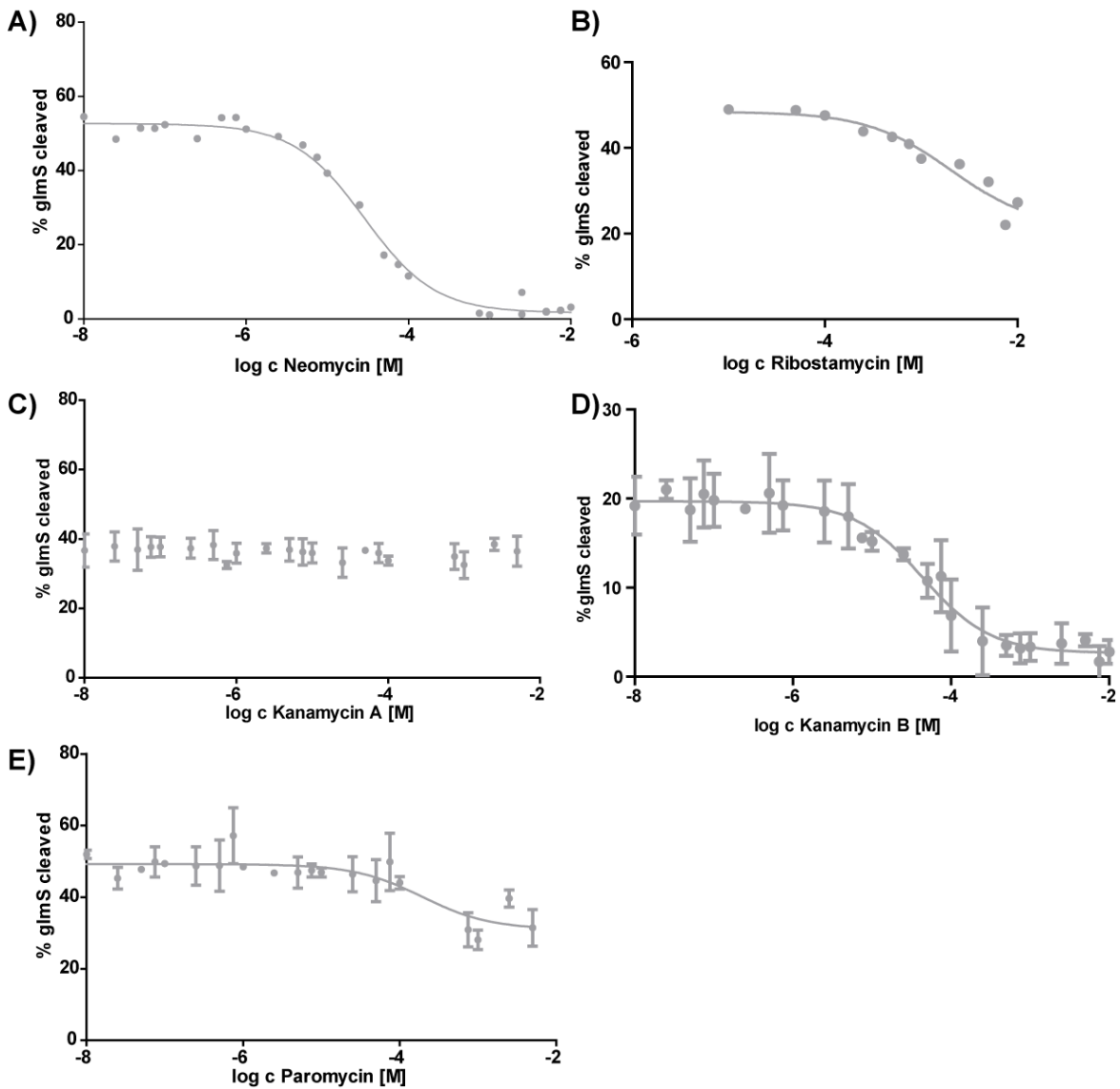
Figure 8.11: IC$_{50}$ value determination for inhibition of glmS ribozyme cleavage by aminoglycosides. Concentration dependent effect of Neomycin (A), Ribostamycin (B), Kanamycin A (C), Kanamycin B (D) and Paromomycin (E) was investigated in the presence of 200 µM GlcN6P after incubation at 37 °C for 30 min. Aminoglycoside concentrations ranging from 10 nM to 10 mM were used. Concentration dependent inhibition by Kanamycin B was monitored by Anna Schüller.
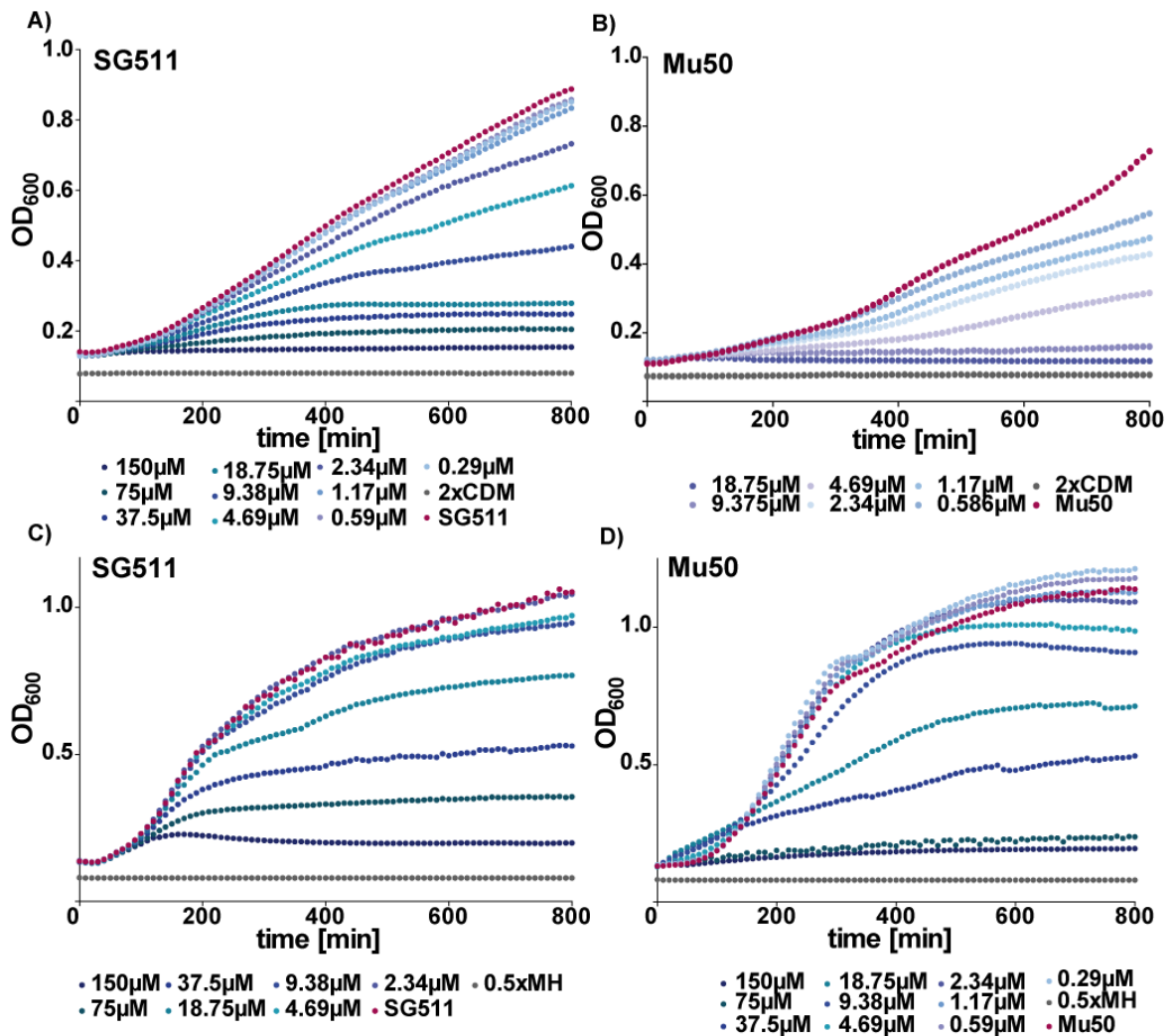
Figure 8.12: Growth of *S. aureus* Mu50 and SG511 in the presence of increasing Streptozotocin concentrations in 2×CDM and 0.5×MH. Graphs show optical density measured at 600 nm plotted against the time. Bacterial growth without Streptozotocin added is shown in magenta and contamination controls of medium alone are depicted in gray.
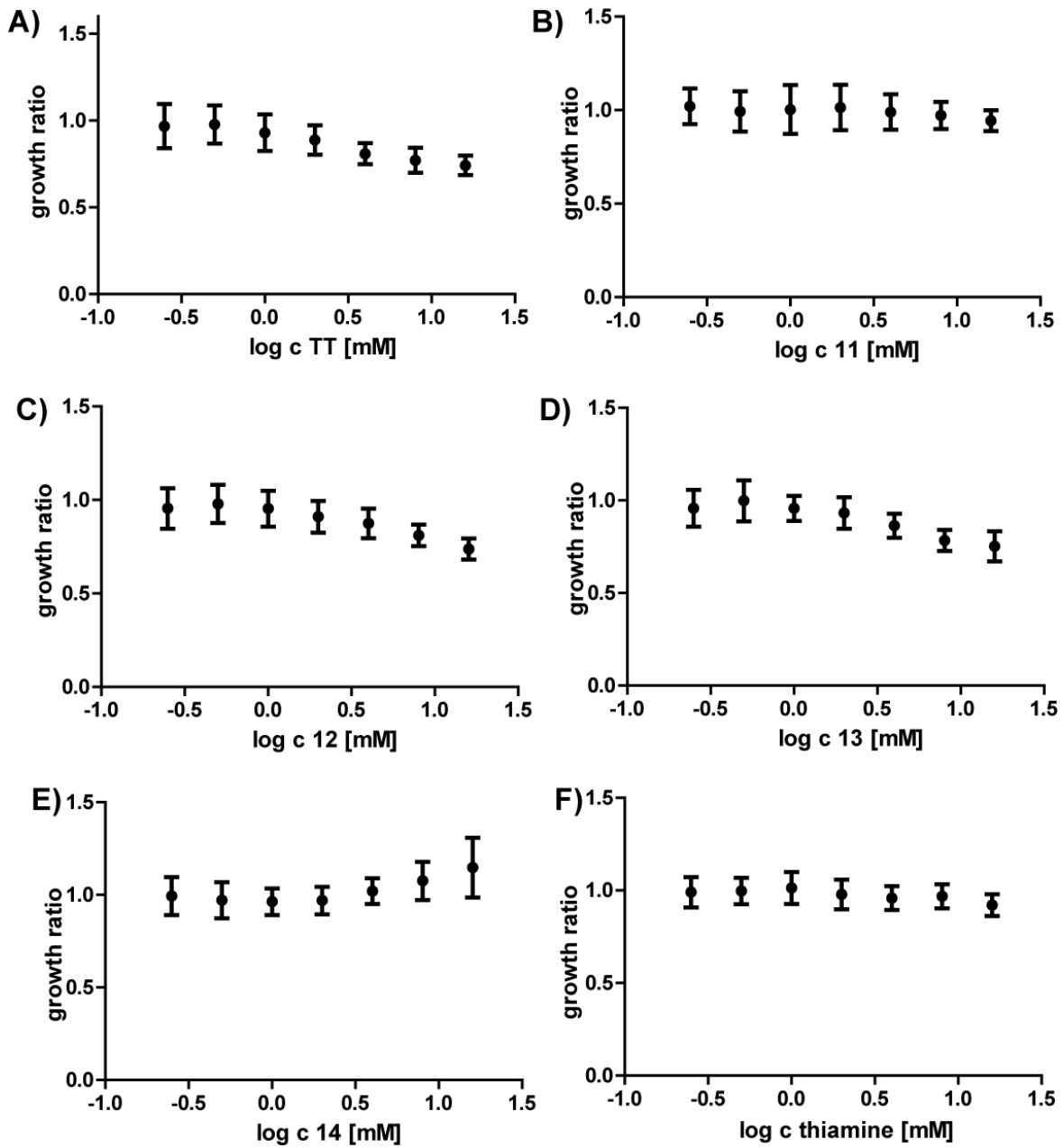
Figure 8.13: Growth ratio of MG1655 in M9 minimal medium with compound versus no compound added. Bacterial growth is shown as ratio of growth in the presence of TT-compound versus growth in the absence of any compound. Graphs show assay results for indicated compound (A-E) or thiamine (F). Compound concentrations between $500\,\mu M$- $32\,mM$ at $495\,min$ are shown.
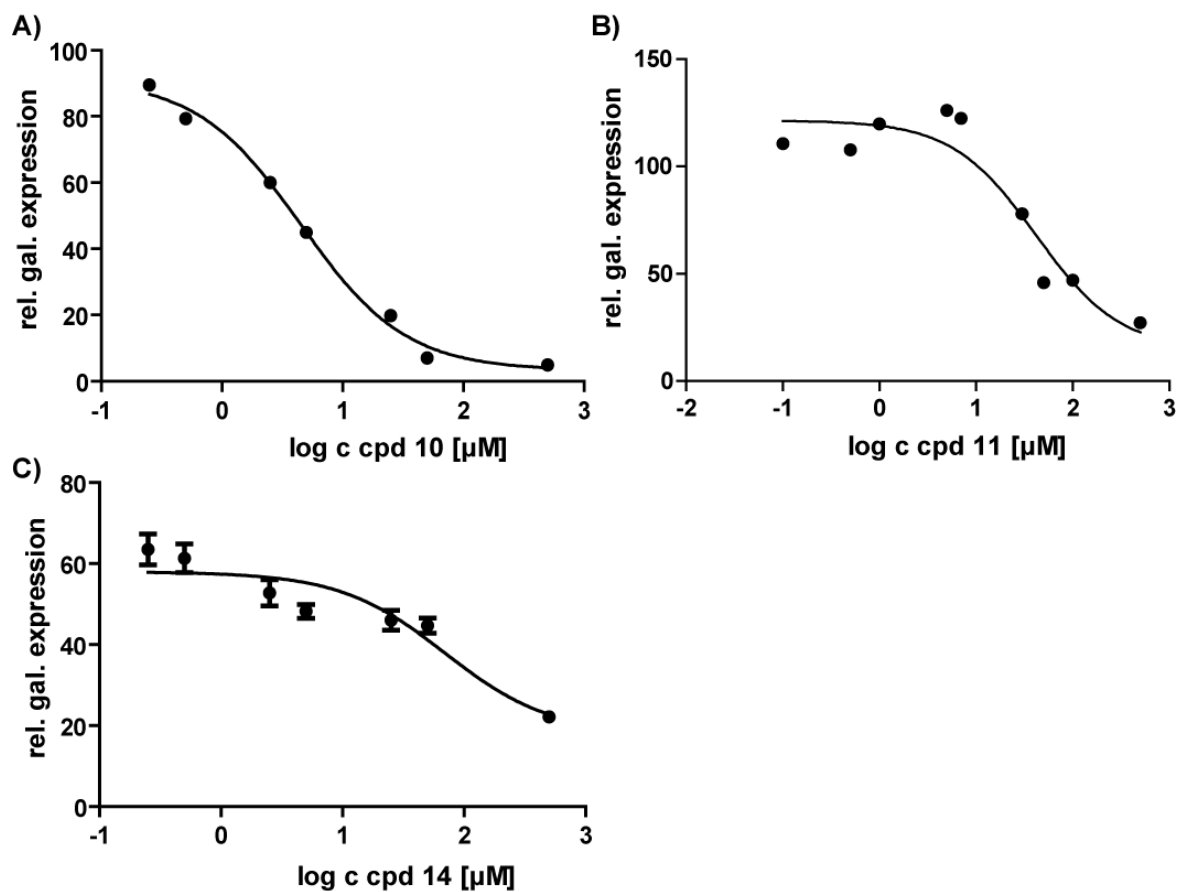
Figure 8.14: Concentration dependent effect of TT compounds on β-galactosidase expression in DH5αZ1 cells. Dose-response curves obtained by monitoring β-galactosidase expression in DH5αZ1 cells with increasing compound concentrations (0.01-500 µM) for compound 10 (A), 11 (B) and 14 (C). Each experiment, of which one exemplary curve is depicted here, was measured in duplicates and repeated at least two times. Mean and standard deviations of these measurements are shown in Table 3.7.
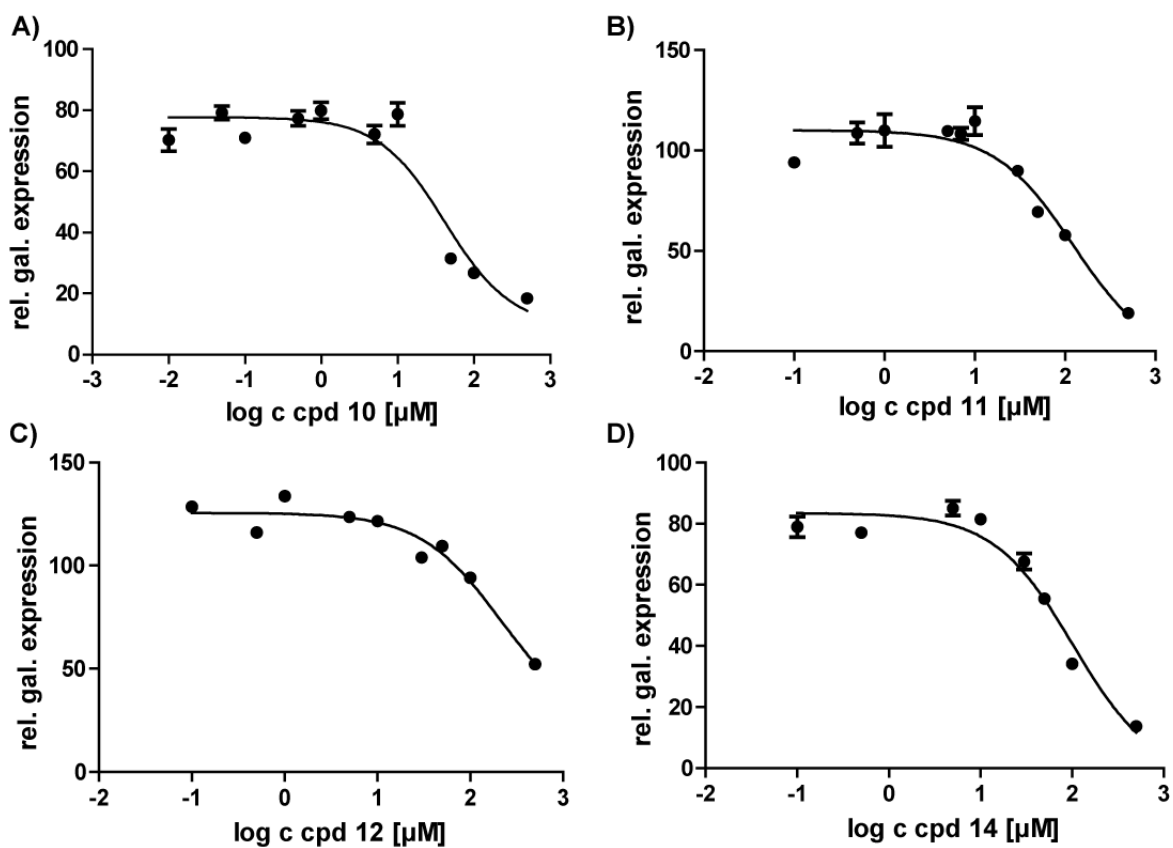
Figure 8.15: Concentration dependent effect of TT compounds on β-galactosidase expression in MG1655 cells. Dose-response curves obtained by monitoring β-galactosidase expression in MG1655 cells with increasing compound concentrations (0.01-500 µM) for compound 10 (A), 11 (B),12 (C) and 14 (D). Each experiment, of which one exemplary curve is depicted here, was measured in duplicates and repeated at least two times. Mean and standard deviations of these measurements are shown in Table 3.7.
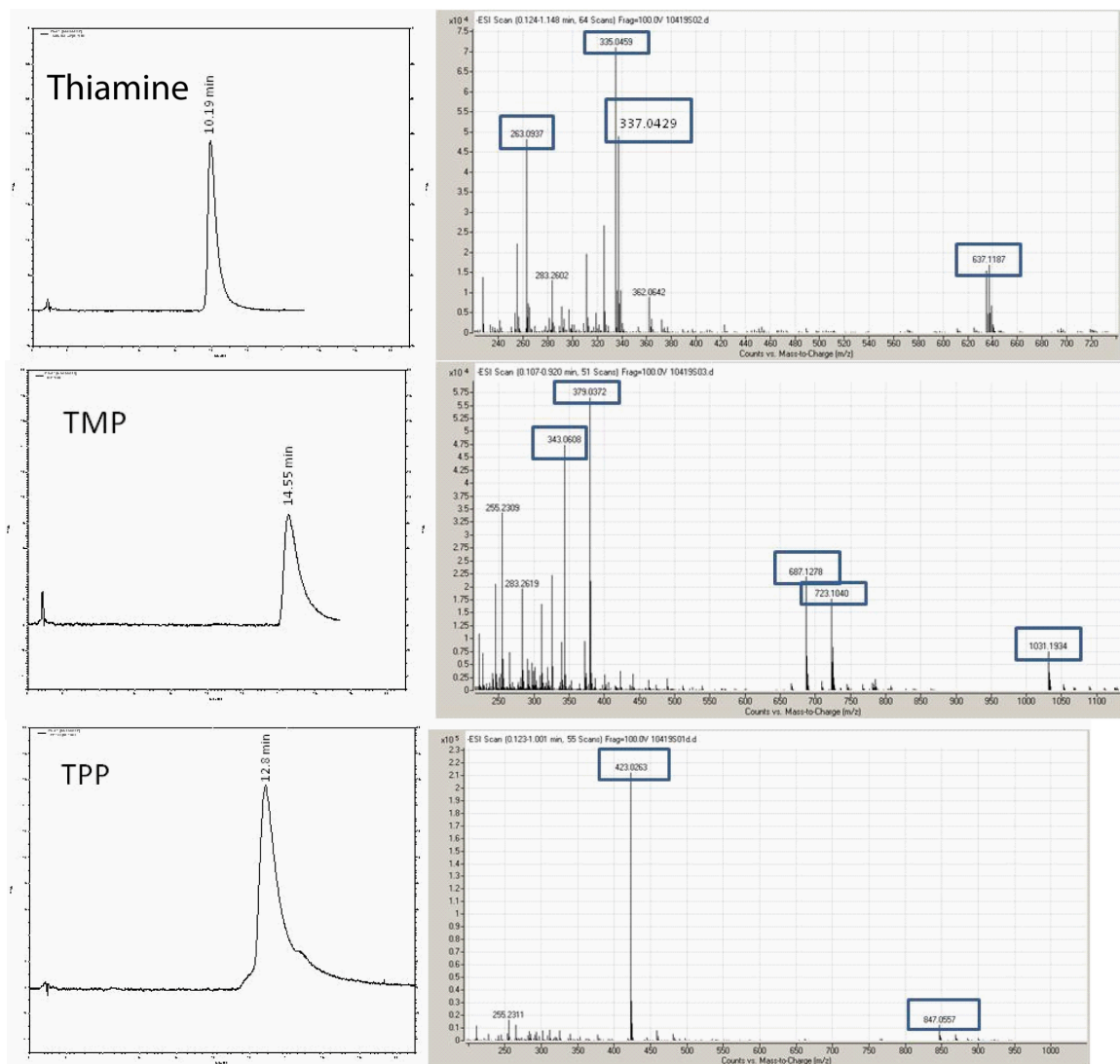
Figure 8.16: Individual HILIC/MS measurements of thiamine, thiamine monophosphate and thiamine pyrophosphate. Thiamine, thiamine monophosphate and thiamine pyrophosphate can be separated using HILIC and analyzed and identified by MS/MS.
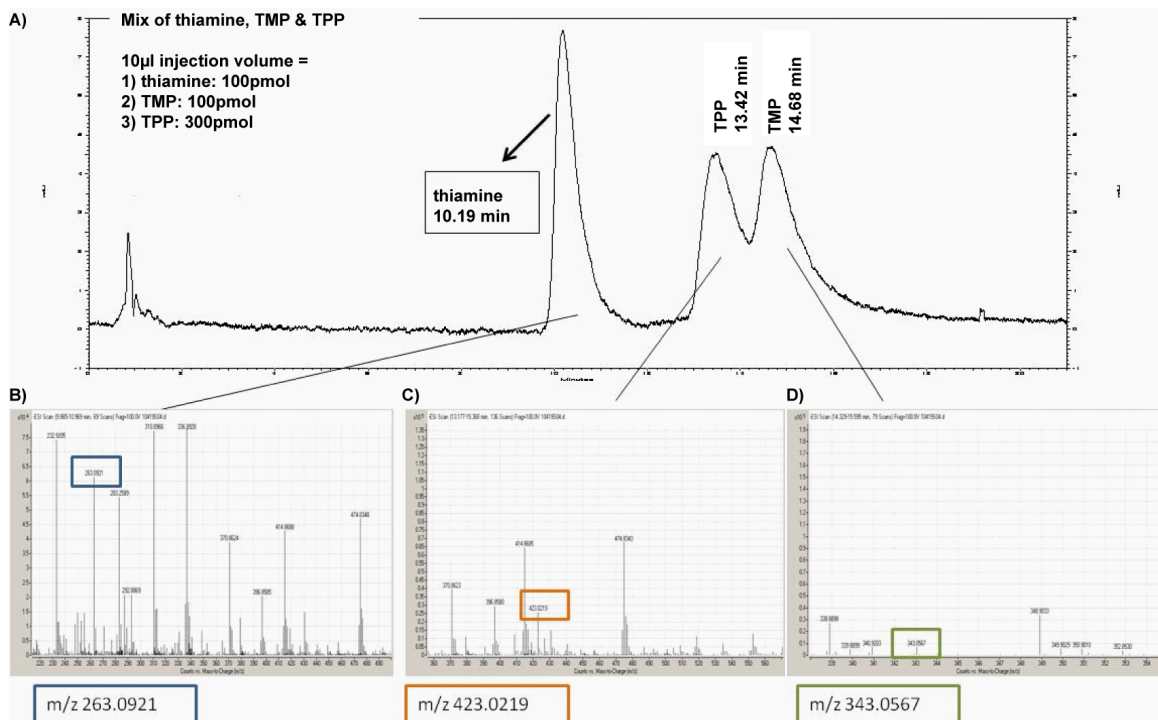
Figure 8.17: HILIC/MS measurements of thiamine, thiamine monophosphate and thiamine pyrophosphate mixture. Thiamine, thiamine monophosphate and thiamine pyrophosphate can be properly separated using HILIC and analyzed and identified by MS/MS.
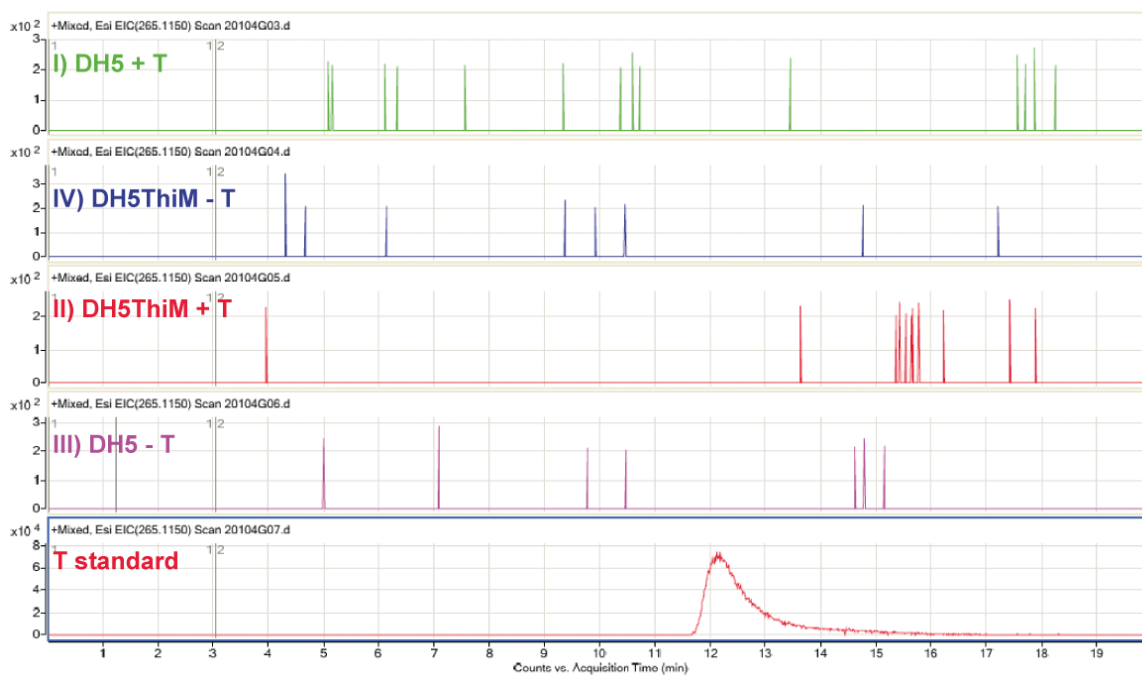
Figure 8.18: HILIC/MS measurements of samples 46, 51-54. All samples stem from 80 ml compound isolations and a TPP double peak was detected in all samples.
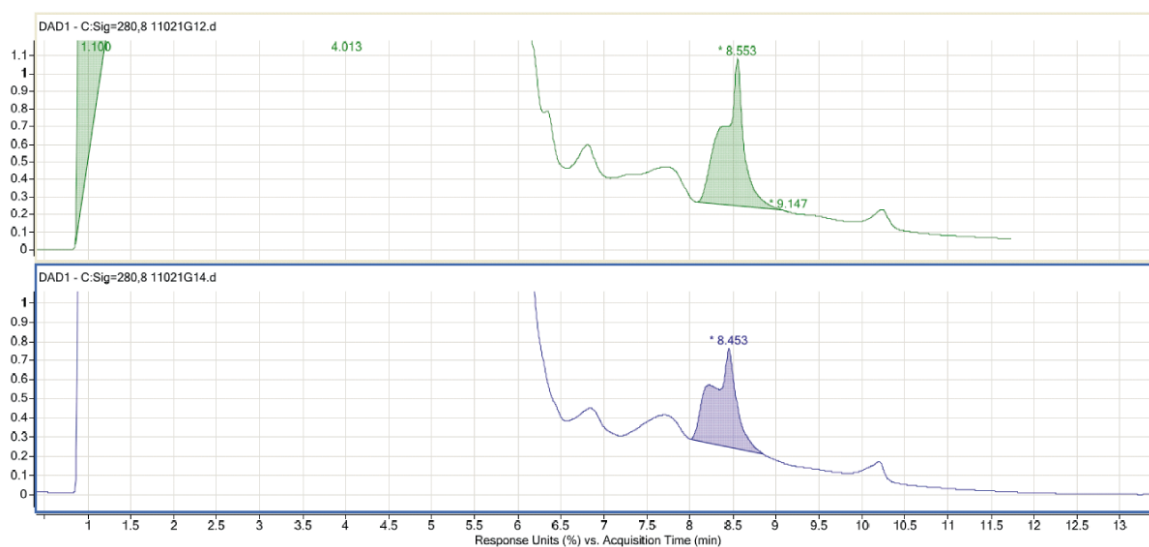
Figure 8.19: Rough quantification of samples 52 and 54 by HILIC. HILIC curves of sample 52 (green) and sample 54 (blue) are shown. Refer to Table 3.8 for sample conditions. The area under the curve is determined (see shaded region) as 405 (sample 52) vs. 280 (sample 54) and can be considered a rough estimate of TPP amounts in these samples (personal communication Giorgia Greco).
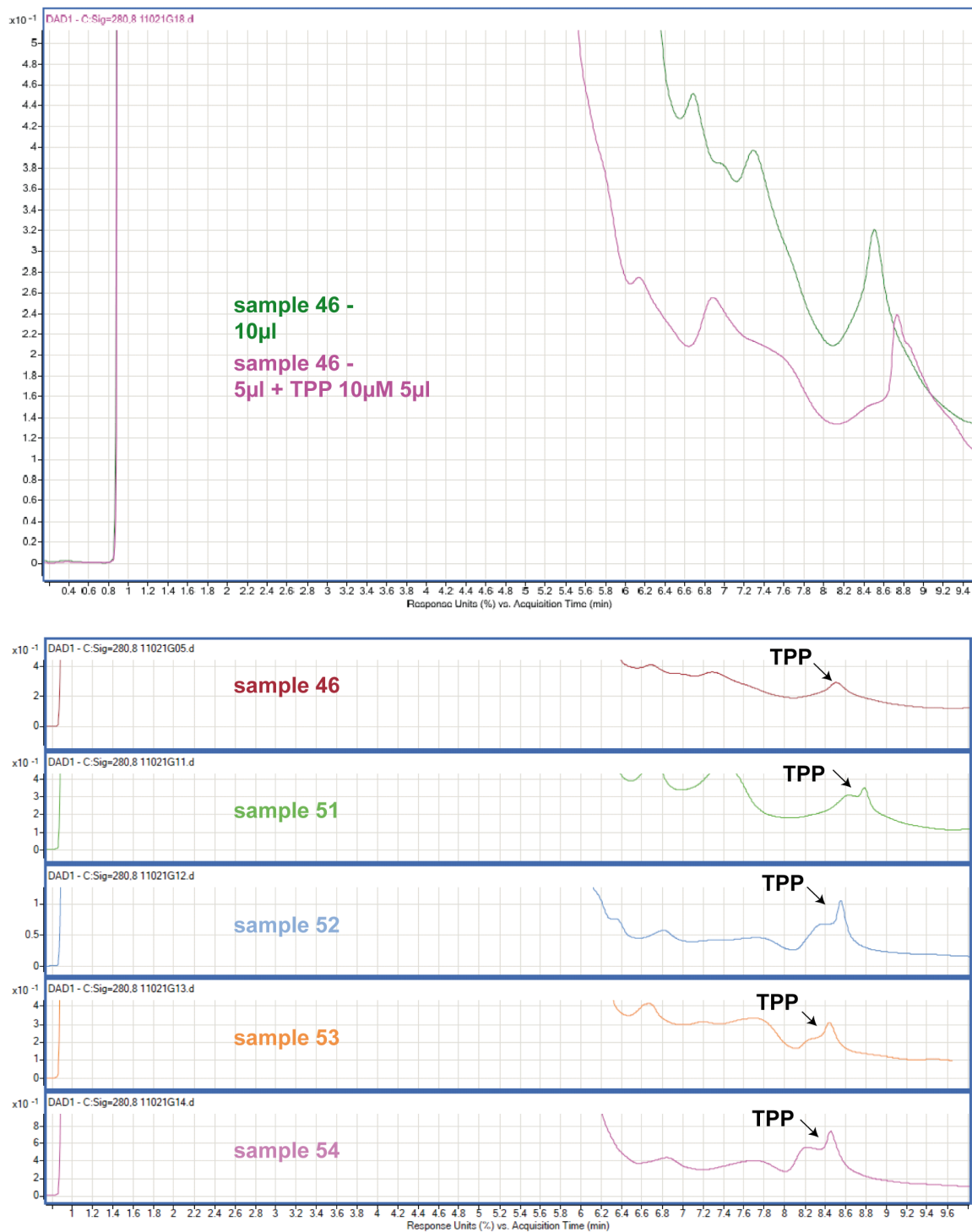
Figure 8.20: HILIC measurements for TPP detection. HILIC measurement of sample 46 (green) and sample 46 spiked with $10\,\mu M$ TPP (red) (A). Comparison of HILIC measurements for samples 46 (red), 51 (green), 52 (blue), 53 (yellow) and 54 (pink) (B). The double peak is TPP, which runs as double peak due to matrix effects or possibly the left peak resembles hydrolyzed TPP species such as TMP.

Bibliography

(2008), 2008, WHO. *URL:* `http://www.who.int/mediacentre/factsheets/fs310/en/index.html`.

Aalberts, D. P. and Hodas, N. O. (2005). Asymmetry in RNA pseudoknots: observation and theory. *Nucleic Acids Res*, 33 No. 7:2210–2214, 2005. doi: 10.1093/nar/gki508. *URL:* `http://dx.doi.org/10.1093/nar/gki508`.

Airth, R. L. and Foerster, G. E. (1962). Simultaneous determination of thiamine and pyrithiamine. *Anal Biochem*, 3:383–395, May 1962.

Alvarez-Lerma, F., Alvarez, B., Luque, P., Ruiz, F., Dominguez-Roldan, J.-M., Quintana, E., Sanz-Rodriguez, C., and Group, A. D. A. N. N. S. (2006). Empiric broad-spectrum antibiotic therapy of nosocomial pneumonia in the intensive care unit: a prospective observational study. *Crit Care*, 10 No. 3:R78, 2006.

Ames, T. and Breaker, R. (2010). *Bacterial riboswitch discovery and analysis. In The Chemical Biology of Nucleic Acids.* John Wiley and Sons, 2010.

Ames, T. D. and Breaker, R. R. (2011). Bacterial aptamers that selectively bind glutamine. *RNA Biol*, 8 No. 1:82–89, 2011.

Ammer, J., Brennenstuhl, M., Schindler, P., Höltje, J. V., and Zähner, H. (1979). Phosphorylation of streptozotocin during uptake via the phosphoenolpyruvate: sugar phosphotransferase system in Escherichia coli. *Antimicrob Agents Chemother*, 16 No. 6: 801–807, Dec 1979.

André, G., Even, S., Putzer, H., Burguière, P., Croux, C., Danchin, A., Martin-Verstraete, I., and Soutourina, O. (2008). S-box and T-box riboswitches and antisense RNA control a sulfur metabolic operon of Clostridium acetobutylicum. *Nucleic Acids Res*, 36 No. 18:5955–5969, Oct 2008. doi: 10.1093/nar/gkn601. *URL:* `http://dx.doi.org/10.1093/nar/gkn601`.

Arias, C. A. and Murray, B. E. (2008). Emergence and management of drug-resistant enterococcal infections. *Expert Rev Anti Infect Ther*, 6 No. 5:637–655, Oct 2008. doi: 10.1586/14787210.6.5.637. *URL:* `http://dx.doi.org/10.1586/14787210.6.5.637`.

Arnaud, M., Chastanet, A., and Débarbouillé, M. (2004). New vector for efficient allelic replacement in naturally nontransformable, low-GC-content, gram-positive bacteria. *Appl Environ Microbiol*, 70 No. 11:6887–6891, Nov 2004. doi: 10.1128/AEM.70.11.6887-6891.2004. *URL:* `http://dx.doi.org/10.1128/AEM.70.11.6887-6891.2004`.

Ataide, S. F., Wilson, S. N., Dang, S., Rogers, T. E., Roy, B., Banerjee, R., Henkin, T. M., and Ibba, M. (2007). Mechanisms of resistance to an amino acid

antibiotic that targets translation. *ACS Chem Biol*, 2 No. 12:819–827, Dec 2007. doi: 10.1021/cb7002253. *URL:* http://dx.doi.org/10.1021/cb7002253.

Babitzke, P. and Romeo, T. (2007). CsrB sRNA family: sequestration of RNA-binding regulatory proteins. *Curr Opin Microbiol*, 10 No. 2:156–163, Apr 2007. doi: 10.1016/j.mib. 2007.03.007. *URL:* http://dx.doi.org/10.1016/j.mib.2007.03.007.

Badet, B., Vermoote, P., Haumont, P. Y., Lederer, F., and LeGoffic, F. (1987). Glucosamine synthetase from Escherichia coli: purification, properties, and glutamine-utilizing site location. *Biochemistry*, 26 No. 7:1940–1948, Apr 1987.

Baker, J. L., Sudarsan, N., Weinberg, Z., Roth, A., Stockbridge, R. B., and Breaker, R. R. (2012). Widespread genetic switches and toxicity resistance proteins for fluoride. *Science*, 335 No. 6065:233–235, Jan 2012. doi: 10.1126/science.1215063. *URL:* http://dx.doi.org/10.1126/science.1215063.

Barrick, J. E. and Breaker, R. R. (2007). The distributions, mechanisms, and structures of metabolite-binding riboswitches. *Genome Biol*, 8 No. 11:R239, 2007. doi: 10.1186/ gb-2007-8-11-r239. *URL:* http://dx.doi.org/10.1186/gb-2007-8-11-r239.

Barrick, J. E., Corbino, K. A., Winkler, W. C., Nahvi, A., Mandal, M., Collins, J., Lee, M., Roth, A., Sudarsan, N., Jona, I., Wickiser, J. K., and Breaker, R. R. (2004). New RNA motifs suggest an expanded scope for riboswitches in bacterial genetic control. *Proc Natl Acad Sci U S A*, 101 No. 17:6421–6426, Apr 2004. doi: 10.1073/ pnas.0308014101. *URL:* http://dx.doi.org/10.1073/pnas.0308014101.

Barton, D. H., Augy-Dorey, S., Camara, J., Dalko, P., Delaumény, J. M., Géro, S. D., Quiclet-Sire, B., and Stütz, P. (1990). Synthetic methods for the preparation of basic D- and L-pseudo-sugars. Synthesis of carbocyclic analogues of N-acetyl-muramyl-L-alanyl-D-iso-glutamine (MDP). *Tetrahedron*, 46:215–230, 1990.

Batey, R. T., Gilbert, S. D., and Montange, R. K. (2004). Structure of a natural guanine-responsive riboswitch complexed with the metabolite hypoxanthine. *Nature*, 432 No. 7015:411–415, Nov 2004. doi: 10.1038/nature03037. *URL:* http://dx.doi.org/10.1038/nature03037.

Bearne, S. L. (1996). Active site-directed inactivation of Escherichia coli glucosamine-6-phosphate synthase. Determination of the fructose 6-phosphate binding constant using a carbohydrate-based inactivator. *J Biol Chem*, 271 No. 6:3052–3057, Feb 1996.

Begley, T. P., Downs, D. M., Ealick, S. E., McLafferty, F. W., Loon, A. P. V., Taylor, S., Campobasso, N., Chiu, H. J., Kinsland, C., Reddick, J. J., and Xi, J. (1999). Thiamin biosynthesis in prokaryotes. *Arch Microbiol*, 171 No. 5:293–300, Apr 1999.

Belousoff, M. J., Graham, B., Spiccia, L., and Tor, Y. (2009). Cleavage of RNA oligonucleotides by aminoglycosides. *Org Biomol Chem*, 7 No. 1:30–33, Jan 2009. doi: 10.1039/b813252f. *URL:* http://dx.doi.org/10.1039/b813252f.

Berkner, K. L. and Folk, W. R. (1977). Polynucleotide kinase exchange reaction: quantitave assay for restriction endonuclease-generated 5'-phosphoroyl termini in DNA. *J Biol Chem*, 252 No. 10:3176–3184, May 1977.

Bhagvat, K. and Devi, P. (1946). Interference by certain substances in the estimation of thiamine by the thiochrome method. *Curr Sci*, 15 No. 11:312, Nov 1946.

Bienz, M. & Kubli, E. (1981). Wild type tRNATyr reads the TMV RNA stop codon, but Q basemodified tRNATyr does not. *Nature*, 294:188–190, 1981.

Blaise, M., Becker, H. D., Keith, G., Cambillau, C., Lapointe, J., Giegé, R., and Kern, D. (2004). A minimalist glutamyl-tRNA synthetase dedicated to aminoacylation of the tRNAAsp QUC anticodon. *Nucleic Acids Res*, 32 No. 9:2768–2775, 2004. doi: 10.1093/nar/gkh608. *URL:* http://dx.doi.org/10.1093/nar/gkh608.

Blattner, F. R., Plunkett, G., Bloch, C. A., Perna, N. T., Burland, V., Riley, M., Collado-Vides, J., Glasner, J. D., Rode, C. K., Mayhew, G. F., Gregor, J., Davis, N. W., Kirkpatrick, H. A., Goeden, M. A., Rose, D. J., Mau, B., and Shao, Y. (1997). The complete genome sequence of Escherichia coli K-12. *Science*, 277 No. 5331:1453–1462, Sep 1997.

Blount, K., Puskarz, I., Penchovsky, R., and Breaker, R. (2006). Development and application of a high-throughput assay for glmS riboswitch activators. *RNA Biol*, 3 No. 2: 77–81, Apr 2006.

Blount, K. F. and Breaker, R. R. (2006). Riboswitches as antibacterial drug targets. *Nat Biotechnol*, 24 No. 12:1558–1564, Dec 2006. doi: 10.1038/nbt1268. *URL:* http://dx.doi.org/10.1038/nbt1268.

Blount, K. F. and Tor, Y. (2006). A tale of two targets: differential RNA selectivity of nucleobase-aminoglycoside conjugates. *Chembiochem*, 7 No. 10:1612–1621, Oct 2006. doi: 10.1002/cbic.200600109. *URL:* http://dx.doi.org/10.1002/cbic.200600109.

Blount, K. F., Wang, J. X., Lim, J., Sudarsan, N., and Breaker, R. R. (2007). Antibacterial lysine analogs that target lysine riboswitches. *Nat Chem Biol*, 3 No. 1:44–49, Jan 2007. doi: 10.1038/nchembio842. *URL:* http://dx.doi.org/10.1038/nchembio842.

Boersema, P. J., Divecha, N., Heck, A. J. R., and Mohammed, S. (2007). Evaluation and optimization of ZIC-HILIC-RP as an alternative MudPIT strategy. *J Proteome Res*, 6 No. 3:937–946, Mar 2007. doi: 10.1021/pr060589m. *URL:* http://dx.doi.org/10.1021/pr060589m.

Boersema, P. J., Mohammed, S., and Heck, A. J. R. (2008). Hydrophilic interaction liquid chromatography (HILIC) in proteomics. *Anal Bioanal Chem*, 391 No. 1: 151–159, May 2008. doi: 10.1007/s00216-008-1865-7. *URL:* http://dx.doi.org/10.1007/s00216-008-1865-7.

Boyle-Vavra, S., Labischinski, H., Ebert, C. C., Ehlert, K., and Daum, R. S. (2001). A spectrum of changes occurs in peptidoglycan composition of glycopeptide-intermediate clinical Staphylococcus aureus isolates. *Antimicrob Agents Chemother*, 45 No. 1:280–287, Jan 2001. doi: 10.1128/AAC.45.1.280-287.2001. *URL:* http://dx.doi.org/10.1128/AAC.45.1.280-287.2001.

Boyle-Vavra, S., Challapalli, M., and Daum, R. S. (2003). Resistance to autolysis in vancomycin-selected Staphylococcus aureus isolates precedes vancomycin-intermediate resistance. *Antimicrob Agents Chemother*, 47 No. 6:2036–2039, Jun 2003.

Bibliography

Breaker, Ronald R (2008). Complex riboswitches. *Science*, 319 No. 5871:1795–1797, Mar 2008. doi: 10.1126/science.1152621. *URL:* `http://dx.doi.org/10.1126/science.1152621`.

Breaker, Ronald R (2010). Riboswitches and the RNA World. *Cold Spring Harb Perspect Biol*, Nov 2010. doi: 10.1101/cshperspect.a003566. *URL:* `http://dx.doi.org/10.1101/cshperspect.a003566`.

Breaker, Ronald R (2011). Prospects for riboswitch discovery and analysis. *Mol Cell*, 43 No. 6:867–879, Sep 2011. doi: 10.1016/j.molcel.2011.08.024. *URL:* `http://dx.doi.org/10.1016/j.molcel.2011.08.024`.

Breukink, E., Wiedemann, I., van Kraaij, C., Kuipers, O. P., Sahl, H., and de Kruijff, B. (1999). Use of the cell wall precursor lipid II by a pore-forming peptide antibiotic. *Science*, 286 No. 5448:2361–2364, Dec 1999.

Brink, M. F., Brink, G., Verbeet, M. P., and de Boer, H. A. (1994). Spectinomycin interacts specifically with the residues G1064 and C1192 in 16S rRNA, thereby potentially freezing this molecule into an inactive conformation. *Nucleic Acids Res*, 22 No. 3:325–331, Feb 1994.

Brooks, K. M. and Hampel, K. J. (2009). A rate-limiting conformational step in the catalytic pathway of the glmS ribozyme. *Biochemistry*, 48 No. 24:5669–5678, Jun 2009. doi: 10.1021/bi900183r. *URL:* `http://dx.doi.org/10.1021/bi900183r`.

C. Lewis, A.R. Barbiers (1959/1960). Streptozotocin, a new antibiotic. In vitro and in vivo evaluation. *Antibiot. Ann.*, 7:247–254, 1959/1960.

Chambers, H. F. (1997). Methicillin resistance in staphylococci: molecular and biochemical basis and clinical implications. *Clin Microbiol Rev*, 10 No. 4:781–791, Oct 1997.

Chambers, H. F. (2001). The changing epidemiology of Staphylococcus aureus? *Emerg Infect Dis*, 7 No. 2:178–182, 2001.

Chappelet-Tordo, D., Fosset, M., Iwatsubo, M., Gache, C., and Lazdunski, M. (1974). Intestinal alkaline phosphatase. Catalytic properties and half of the sites reactivity. *Biochemistry*, 13 No. 9:1788–1795, Apr 1974.

Charles, B. G. and Rawal, B. D. (1976). Cultivation of Staphylococcus aureus in a synthetic medium of low ultraviolet absorptivity. *Antimicrob Agents Chemother*, 10 No. 6: 915–917, Dec 1976.

Cheah, M. T., Wachter, A., Sudarsan, N., and Breaker, R. R. (2007). Control of alternative RNA splicing and gene expression by eukaryotic riboswitches. *Nature*, 447 No. 7143:497–500, May 2007. doi: 10.1038/nature05769. *URL:* `http://dx.doi.org/10.1038/nature05769`.

Chen, L., Cressina, E., Leeper, F. J., Smith, A. G., and Abell, C. (2010). A Fragment-Based Approach to Identifying Ligands for Riboswitches. *ACS Chem Biol*, Feb 2010. doi: 10.1021/cb9003139. *URL:* `http://dx.doi.org/10.1021/cb9003139`.

Chen, L., Cressina, E., Dixon, N., Erixon, K., Agyei-Owusu, K., Micklefield, J., Smith, A. G., Abell, C., and Leeper, F. J. (2012). Probing riboswitch-ligand interactions using thiamine pyrophosphate analogues. *Org Biomol Chem*, 10 No. 30: 5924–5931, Aug 2012. doi: 10.1039/c2ob07116a. *URL:* http://dx.doi.org/10.1039/c2ob07116a.

Chesneau, O., Morvan, A., and Solh, N. E. (2000). Retrospective screening for heterogeneous vancomycin resistance in diverse Staphylococcus aureus clones disseminated in French hospitals. *J Antimicrob Chemother*, 45 No. 6:887–890, Jun 2000.

Chia, J.-S., Wu, H.-L., Wang, H.-W., Chen, D.-S., and Chen, P.-J. (1997). Inhibition of Hepatitis Delta Virus Genomic Ribozyme Self-Cleavage by Aminoglycosides. *J Biomed Sci*, 4 No. 5:208–216, 1997.

Chien, A., Edgar, D. B., and Trela, J. M. (1976). Deoxyribonucleic acid polymerase from the extreme thermophile Thermus aquaticus. *J Bacteriol*, 127 No. 3:1550–1557, Sep 1976.

Chrambach, A. and Rodbard, D. (1971). Polyacrylamide gel electrophoresis. *Science*, 172 No. 982:440–451, Apr 1971.

Chuard, C., Vaudaux, P. E., Proctor, R. A., and Lew, D. P. (1997). Decreased susceptibility to antibiotic killing of a stable small colony variant of Staphylococcus aureus in fluid phase and on fibronectin-coated surfaces. *J Antimicrob Chemother*, 39 No. 5: 603–608, May 1997.

Ciampi, M. Sofia (2006). Rho-dependent terminators and transcription termination. *Microbiology*, 152 No. Pt 9:2515–2528, Sep 2006. doi: 10.1099/mic.0.28982-0. *URL:* http://dx.doi.org/10.1099/mic.0.28982-0.

Cochrane, J. C., Lipchock, S. V., and Strobel, S. A. (2007). Structural investigation of the GlmS ribozyme bound to Its catalytic cofactor. *Chem Biol*, 14 No. 1:97–105, Jan 2007. doi: 10.1016/j.chembiol.2006.12.005. *URL:* http://dx.doi.org/10.1016/j.chembiol.2006.12.005.

Cochrane, J. C., Lipchock, S. V., Smith, K. D., and Strobel, S. A. (2009). Structural and chemical basis for glucosamine 6-phosphate binding and activation of the glmS ribozyme. *Biochemistry*, 48 No. 15:3239–3246, Apr 2009. doi: 10.1021/bi802069p. *URL:* http://dx.doi.org/10.1021/bi802069p.

Collins, J. A., Irnov, I., Baker, S., and Winkler, W. C. (2007). Mechanism of mRNA destabilization by the glmS ribozyme. *Genes Dev*, 21 No. 24:3356–3368, Dec 2007. doi: 10.1101/gad.1605307. *URL:* http://dx.doi.org/10.1101/gad.1605307.

Corbino, K. A., Barrick, J. E., Lim, J., Welz, R., Tucker, B. J., Puskarz, I., Mandal, M., Rudnick, N. D., and Breaker, R. R. (2005). Evidence for a second class of S-adenosylmethionine riboswitches and other regulatory RNA motifs in alpha-proteobacteria. *Genome Biol*, 6 No. 8:R70, 2005. doi: 10.1186/gb-2005-6-8-r70. *URL:* http://dx.doi.org/10.1186/gb-2005-6-8-r70.

Bibliography

Croft, M. T., Moulin, M., Webb, M. E., and Smith, A. G. (2007). Thiamine biosynthesis in algae is regulated by riboswitches. *Proc Natl Acad Sci U S A*, 104 No. 52: 20770–20775, Dec 2007. doi: 10.1073/pnas.0705786105. *URL:* http://dx.doi.org/10.1073/pnas.0705786105.

Cui, L., Murakami, H., Kuwahara-Arai, K., Hanaki, H., and Hiramatsu, K. (2000). Contribution of a thickened cell wall and its glutamine nonamidated component to the vancomycin resistance expressed by Staphylococcus aureus Mu50. *Antimicrob Agents Chemother*, 44 No. 9:2276–2285, Sep 2000.

Cui, L., Ma, X., Sato, K., Okuma, K., Tenover, F. C., Mamizuka, E. M., Gemmell, C. G., Kim, M.-N., Ploy, M.-C., El-Solh, N., Ferraz, V., and Hiramatsu, K. (2003). Cell wall thickening is a common feature of vancomycin resistance in Staphylococcus aureus. *J Clin Microbiol*, 41 No. 1:5–14, Jan 2003.

Cui, L., Iwamoto, A., Lian, J.-Q., min Neoh, H., Maruyama, T., Horikawa, Y., and Hiramatsu, K. (2006). Novel mechanism of antibiotic resistance originating in vancomycin-intermediate Staphylococcus aureus. *Antimicrob Agents Chemother*, 50 No. 2: 428–438, Feb 2006. doi: 10.1128/AAC.50.2.428-438.2006. *URL:* http://dx.doi.org/10.1128/AAC.50.2.428-438.2006.

Dambach, M. D. and Winkler, W. C. (2009). Expanding roles for metabolite-sensing regulatory RNAs. *Curr Opin Microbiol*, 12 No. 2:161–169, Apr 2009. doi: 10.1016/j.mib.2009.01.012. *URL:* http://dx.doi.org/10.1016/j.mib.2009.01.012.

Daum, R. S., Gupta, S., Sabbagh, R., and Milewski, W. M. (1992). Characterization of Staphylococcus aureus isolates with decreased susceptibility to vancomycin and teicoplanin: isolation and purification of a constitutively produced protein associated with decreased susceptibility. *J Infect Dis*, 166 No. 5:1066–1072, Nov 1992.

Davies, J., Gilbert, W., and Gorini, L. (1964). Streptomycin, suppression, and the code. *Proc Natl Acad Sci U S A*, 51:883–890, May 1964.

Davies, J., Anderson, P., and Davis, B. D. (1965). Inhibition of protein synthesis by spectinomycin. *Science*, 149 No. 3688:1096–1098, Sep 1965.

Deresinski, Stan (2007a). Counterpoint: Vancomycin and Staphylococcus aureus–an antibiotic enters obsolescence. *Clin Infect Dis*, 44 No. 12:1543–1548, Jun 2007. doi: 10.1086/518452. *URL:* http://dx.doi.org/10.1086/518452.

Deresinski, Stan (2007b). Vancomycin: does it still have a role as an antistaphylococcal agent? *Expert Rev Anti Infect Ther*, 5 No. 3:393–401, Jun 2007. doi: 10.1586/14787210.5.3.393. *URL:* http://dx.doi.org/10.1586/14787210.5.3.393.

Deresinski, Stan (2009). Vancomycin in combination with other antibiotics for the treatment of serious methicillin-resistant Staphylococcus aureus infections. *Clin Infect Dis*, 49 No. 7:1072–1079, Oct 2009. doi: 10.1086/605572. *URL:* http://dx.doi.org/10.1086/605572.

Diederich L, Rasmussen LJ, Messer W. (1992). New cloning vectors for integration in the lambda attachment site attB of the Escherichia coli chromosome. *Plasmid*, 28 No. 1: 14–24, Jul 1992.

Domagk, G. (1940). Zu den experimentellen Grundlagen der Chemotherapie der bakteriellen Infektion mit den Sulfonamiden und ihren Derivaten. *Dtsch. med. Wschr.*, 66:203, 1940.

Donald, R. G. K., Skwish, S., Forsyth, R. A., Anderson, J. W., Zhong, T., Burns, C., Lee, S., Meng, X., LoCastro, L., Jarantow, L. W., Martin, J., Lee, S. H., Taylor, I., Robbins, D., Malone, C., Wang, L., Zamudio, C. S., Youngman, P. J., and Phillips, J. W. (2009). A Staphylococcus aureus fitness test platform for mechanism-based profiling of antibacterial compounds. *Chem Biol*, 16 No. 8:826–836, Aug 2009. doi: 10.1016/j.chembiol.2009.07.004. *URL:* http://dx.doi.org/10.1016/j.chembiol.2009.07.004.

Dorrestein, P. C., Zhai, H., Taylor, S. V., McLafferty, F. W., and Begley, T. P. (2004). The biosynthesis of the thiazole phosphate moiety of thiamin (vitamin B1): the early steps catalyzed by thiazole synthase. *J Am Chem Soc*, 126 No. 10:3091–3096, Mar 2004. doi: 10.1021/ja039616p. *URL:* http://dx.doi.org/10.1021/ja039616p.

Du, Q., Wang, H., and Xie, J. (2011). Thiamin (vitamin b1) biosynthesis and regulation: a rich source of antimicrobial drug targets? *Int J Biol Sci*, 7 No. 1:41–52, 2011.

Duhr, S. and Braun, D. (2006). Why molecules move along a temperature gradient. *Proc Natl Acad Sci U S A*, 103 No. 52:19678–19682, Dec 2006. doi: 10.1073/pnas.0603873103. *URL:* http://dx.doi.org/10.1073/pnas.0603873103.

Earnshaw, D. J. and Gait, M. J. (1998). Hairpin ribozyme cleavage catalyzed by aminoglycoside antibiotics and the polyamine spermine in the absence of metal ions. *Nucleic Acids Res*, 26 No. 24:5551–5561, Dec 1998.

Eckert, H.; Bajorath, J. (2007). Molecular similarity analysis in virtual screening: foundations, limitations and novel approaches. *Drug Discovery Today*, 12:225–233, 2007.

Edwards, T. E. and Ferré-D'Amaré, A. R. (2006). Crystal structures of the thi-box riboswitch bound to thiamine pyrophosphate analogs reveal adaptive RNA-small molecule recognition. *Structure*, 14 No. 9:1459–1468, Sep 2006. doi: 10.1016/j.str.2006.07.008. *URL:* http://dx.doi.org/10.1016/j.str.2006.07.008.

Erixon, K. M., Dabalos, C. L., and Leeper, F. J. (2007). Inhibition of pyruvate decarboxylase from Z. mobilis by novel analogues of thiamine pyrophosphate: investigating pyrophosphate mimics. *Chem Commun (Camb)*, No. 9:960–962, Mar 2007. doi: 10.1039/b615861g. *URL:* http://dx.doi.org/10.1039/b615861g.

Erixon, K. M., Dabalos, C. L., and Leeper, F. J. (2008). Synthesis and biological evaluation of pyrophosphate mimics of thiamine pyrophosphate based on a triazole scaffold. *Org Biomol Chem*, 6 No. 19:3561–3572, Oct 2008. doi: 10.1039/b806580b. *URL:* http://dx.doi.org/10.1039/b806580b.

Famulok, M. and Hüttenhofer, A. (1996). In vitro selection analysis of neomycin binding RNAs with a mutagenized pool of variants of the 16S rRNA decoding region. *Biochemistry*, 35 No. 14:4265–4270, Apr 1996. doi: 10.1021/bi952479r. *URL:* http://dx.doi.org/10.1021/bi952479r.

Bibliography

Feig, AL, Uhlenbeck-OC (1999). *The role of metal ions in RNA biochemistry In: The RNA world.* Cold Spring Harbor, New York: Cold Spring Harbor Laboratory Press, 1999.

Ferraz, V., Dusé, A. G., Kassel, M., Black, A. D., Ito, T., and Hiramatsu, K. (2000). Vancomycin-resistant Staphylococcus aureus occurs in South Africa. *S Afr Med J*, 90 No. 11:1113, Nov 2000.

Ferré-D'Amaré, Adrian R (2010). The glmS ribozyme: use of a small molecule coenzyme by a gene-regulatory RNA. *Q Rev Biophys*, 43 No. 4:423–447, Nov 2010. doi: 10.1017/ S0033583510000144. *URL:* `http://dx.doi.org/10.1017/S0033583510000144`.

Fielden, M. R. and Kolaja, K. L. (2008). The role of early in vivo toxicity testing in drug discovery toxicology. *Expert Opin Drug Saf*, 7 No. 2:107–110, Mar 2008. doi: 10.1517/14740338.7.2.107. *URL:* `http://dx.doi.org/10.1517/14740338.7.2.107`.

Fleischmann, R. D., Adams, M. D., White, O., Clayton, R. A., Kirkness, E. F., Kerlavage, A. R., Bult, C. J., Tomb, J. F., Dougherty, B. A., and Merrick, J. M. (1995). Whole-genome random sequencing and assembly of Haemophilus influenzae Rd. *Science*, 269 No. 5223:496–512, Jul 1995.

Fosset, M., Chappelet-Tordo, D., and Lazdunski, M. (1974). Intestinal alkaline phosphatase. Physical properties and quaternary structure. *Biochemistry*, 13 No. 9:1783– 1788, Apr 1974.

Fourmy, D., Recht, M. I., Blanchard, S. C., and Puglisi, J. D. (1996). Structure of the A site of Escherichia coli 16S ribosomal RNA complexed with an aminoglycoside antibiotic. *Science*, 274 No. 5291:1367–1371, Nov 1996.

Fourmy, D., Y.-S. and Puglisi, J. (1998). Paromomycin binding induces a local conformational change in the A-site of 16S rRNA. *J. Mol. Biol.*, 277:333–345., 1998.

Fuchs, R. T., Grundy, F. J., and Henkin, T. M. (2006). The S(MK) box is a new SAM-binding RNA for translational regulation of SAM synthetase. *Nat Struct Mol Biol*, 13 No. 3:226–233, Mar 2006. doi: 10.1038/nsmb1059. *URL:* `http://dx.doi.org/10.1038/ nsmb1059`.

Fujiwara, M. and Matsui, K. (1953). Determination of thiamine by the thiochrome reaction. *Analytical Chemistry*, 25:810–812, 1953.

Gephart, P., R. E. M. R. N. E. N. W. W. N. K. and Phillips., G. B. (1981). *Manual of Methods for General Bacteriology.* ASM Press, Washington D.C., 1981.

Ghosh, S., Blumenthal, H. J., Davidson, E., and Roseman, S. (1960). Glucosamine metabolism. V. Enzymatic synthesis of glucosamine 6-phosphate. *J Biol Chem*, 235: 1265–1273, May 1960.

Gilbert, S. D., Mediatore, S. J., and Batey, R. T. (2006). Modified pyrimidines specifically bind the purine riboswitch. *J Am Chem Soc*, 128 No. 44:14214–14215, Nov 2006. doi: 10.1021/ja063645t. *URL:* `http://dx.doi.org/10.1021/ja063645t`.

Gillchriest, W. C. and Nelson, P. L. (1969). Protein synthesis in bacterial and mammalian cells. *Biophys. J.*, 9:A–133, 1969.

Girolamo, M. D., Girolamo, A. D., Cini, C., Coccia, R., and Marco, C. D. (1986). Thialysine utilization for protein synthesis by CHO cells. *Physiol Chem Phys Med NMR*, 18 No. 3:159–164, 1986.

Gram, H.C. (1884). Ueber die isolirte Färbung der Schizomyceten in Schnitt- und Trockenpräparaten. *Fortschitte der Medicin*, 2:185–189, 1884.

Green, R. and Noller, H. F. (1997). Ribosomes and translation. *Annu Rev Biochem*, 66:679–716, 1997. doi: 10.1146/annurev.biochem.66.1.679. *URL:* `http://dx.doi.org/10.1146/annurev.biochem.66.1.679`.

Grumbach, Eric S., W.-D. D. M. M. J. R. A. B. and Iraneta, P. C. (2004). Hydrophilic Interaction Chromatography Using Silica Columns for the Retention of Polar Analytes and Enhanced ESI-MS Sensitivity. *LCGC Magazine*, 22 No. 10:1010–1023, 2004.

Grundy, F. J. and Henkin, T. M. (1998). The S box regulon: a new global transcription termination control system for methionine and cysteine biosynthesis genes in gram-positive bacteria. *Mol Microbiol*, 30 No. 4:737–749, Nov 1998.

Görke, B. and Vogel, J. (2008). Noncoding RNA control of the making and breaking of sugars. *Genes Dev*, 22 No. 21:2914–2925, Nov 2008. doi: 10.1101/gad.1717808. *URL:* `http://dx.doi.org/10.1101/gad.1717808`.

Hanahan, D. (1985). *DNA Cloning: A Practical Approach.*, volume 1. IRL Press, McLean, Virginia, 1985.

Hanaki, H., Kuwahara-Arai, K., Boyle-Vavra, S., Daum, R. S., Labischinski, H., and Hiramatsu, K. (1998a). Activated cell-wall synthesis is associated with vancomycin resistance in methicillin-resistant Staphylococcus aureus clinical strains Mu3 and Mu50. *J Antimicrob Chemother*, 42 No. 2:199–209, Aug 1998.

Hanaki, H., Labischinski, H., Inaba, Y., Kondo, N., Murakami, H., and Hiramatsu, K. (1998b). Increase in glutamine-non-amidated muropeptides in the peptidoglycan of vancomycin-resistant Staphylococcus aureus strain Mu50. *J Antimicrob Chemother*, 42 No. 3:315–320, Sep 1998.

Harada, F. & Nishimura, S. (1972). Possible anticodon sequences of tRNA His, tRNA Asn, and tRNA Asp from Escherichia coli B. Universal presence of nucleoside Q in the first position of the anticodons of these transfer ribonucleic acids. *Biochemistry*, 11:301–308, 1972.

Haugen, H. N. (1961). The determination of thiamine and thiamine phosphates in blood and tissues by the thiochrome method. *Scand J Clin Lab Invest*, 13:50–56, 1961.

Healthcare, GE (2008). *G25 Micro Spin Columns*, 2008.

Hendrix, M., Priestley, E. S., Joyce, G. F., and Wong, C. H. (1997). Direct observation of aminoglycoside-RNA interactions by surface plasmon resonance. *J Am Chem Soc*, 119 No. 16:3641–3648, Apr 1997.

Hennessy, D. J. and Cerecedo, L. R. (1939). The determination of free and phosphorylated thiamin by a modified thiochrome assay. pages 179–183, 1939.

Bibliography

Hermann, T. and Tor, Y. (2005). RNA as a target for small-molecule therapeutics. *Expert Opin Ther Pat*, 15:49–62, 2005.

Hermann, T. and Westhof, E. (2000). Rational drug design and high-throughput techniques for RNA targets. *Comb Chem High Throughput Screen*, 3 No. 3:219–234, Jun 2000.

Hiramatsu, K. (1998). Vancomycin resistance in staphylococci. *Drug Resist Updat*, 1 No. 2: 135–150, 1998.

Hiramatsu, K. (2001). Vancomycin-resistant Staphylococcus aureus: a new model of antibiotic resistance. *Lancet Infect Dis*, 1 No. 3:147–155, Oct 2001. doi: 10.1016/S1473-3099(01) 00091-3. *URL:* `http://dx.doi.org/10.1016/S1473-3099(01)00091-3`.

Hiramatsu, K., Aritaka, N., Hanaki, H., Kawasaki, S., Hosoda, Y., Hori, S., Fukuchi, Y., and Kobayashi, I. (1997). Dissemination in Japanese hospitals of strains of Staphylococcus aureus heterogeneously resistant to vancomycin. *Lancet*, 350 No. 9092: 1670–1673, Dec 1997. doi: 10.1016/S0140-6736(97)07324-8. *URL:* `http://dx.doi.org/10.1016/S0140-6736(97)07324-8`.

Ho, C.-W., Popat, S. D., Liu, T.-W., Tsai, K.-C., Ho, M.-J., Chen, W.-H., Yang, A.-S., and Lin, C.-H. (2010). Development of GlcNAc-inspired iminocyclitiols as potent and selective N-acetyl-beta-hexosaminidase inhibitors. *ACS Chem Biol*, 5 No. 5:489–497, May 2010. doi: 10.1021/cb100011u. *URL:* `http://dx.doi.org/10.1021/cb100011u`.

Howden, B. P., Davies, J. K., Johnson, P. D. R., Stinear, T. P., and Grayson, M. L. (2010). Reduced vancomycin susceptibility in Staphylococcus aureus, including vancomycin-intermediate and heterogeneous vancomycin-intermediate strains: resistance mechanisms, laboratory detection, and clinical implications. *Clin Microbiol Rev*, 23 No. 1: 99–139, Jan 2010. doi: 10.1128/CMR.00042-09. *URL:* `http://dx.doi.org/10.1128/CMR.00042-09`.

Hutchison, C. A., Phillips, S., Edgell, M. H., Gillam, S., Jahnke, P., and Smith, M. (1978). Mutagenesis at a specific position in a DNA sequence. *J Biol Chem*, 253 No. 18:6551–6560, Sep 1978.

Hägglund, P., Bunkenborg, J., Elortza, F., Jensen, O. N., and Roepstorff, P. (2004). A new strategy for identification of N-glycosylated proteins and unambiguous assignment of their glycosylation sites using HILIC enrichment and partial deglycosylation. *J Proteome Res*, 3 No. 3:556–566, 2004.

Hör, Jens (2011). Bachelor Thesis: Untersuchung der Bindungsaffinitäten von Riboswitchen mittels Microscale Thermophorese. Master's thesis, University of Bonn, GERMANY, 2011.

Irnov., Kertsburg, A., and Winkler, W. C. (2006). Genetic control by cis-acting regulatory RNAs in Bacillus subtilis: general principles and prospects for discovery. *Cold Spring Harb Symp Quant Biol*, 71:239–249, 2006. doi: 10.1101/sqb.2006.71.021. *URL:* `http://dx.doi.org/10.1101/sqb.2006.71.021`.

Iwashima, A., Wakabayashi, Y., and Nose, Y. (1976). Formation of pyrithiamine pyrophosphate in brain tissue. *J Biochem*, 79 No. 4:845–847, Apr 1976.

Iwata-Reuyl, Dirk (2003). Biosynthesis of the 7-deazaguanosine hypermodified nucleosides of transfer RNA. *Bioorg Chem*, 31 No. 1:24–43, Feb 2003.

Jandera, Pavel (2011). Stationary and mobile phases in hydrophilic interaction chromatography: a review. *Anal Chim Acta*, 692 No. 1-2:1–25, Apr 2011. doi: 10.1016/j.aca.2011.02. 047. *URL:* `http://dx.doi.org/10.1016/j.aca.2011.02.047`.

Jenkins, J. L., Krucinska, J., McCarty, R. M., Bandarian, V., and Wedekind, J. E. (2011). Comparison of a preQ1 riboswitch aptamer in metabolite-bound and free states with implications for gene regulation. *J Biol Chem*, 286 No. 28:24626–24637, Jul 2011. doi: 10.1074/jbc.M111.230375. *URL:* `http://dx.doi.org/10.1074/jbc.M111.230375`.

Jensen, K. F. (1993). The Escherichia coli K-12 "wild types" W3110 and MG1655 have an rph frameshift mutation that leads to pyrimidine starvation due to low pyrE expression levels. *J Bacteriol*, 175 No. 11:3401–3407, Jun 1993.

Jones, D., Metzger H.J. Schatz A. Waksman S.A. (1944). Control of Gram- negative bacteria in experimental animals by streptomycin. *Science*, 100:103–5, Aug 1944.

Jorgensen, J. H., Redding, J. S., Maher, L. A., and Howell, A. W. (1987). Improved medium for antimicrobial susceptibility testing of Haemophilus influenzae. *J Clin Microbiol*, 25 No. 11:2105–2113, Nov 1987.

Jorgensen, J. H., Howell, A. W., and Maher, L. A. (1990). Antimicrobial susceptibility testing of less commonly isolated Haemophilus species using Haemophilus test medium. *J Clin Microbiol*, 28 No. 5:985–988, May 1990.

Junod, A., Lambert, A. E., Orci, L., Pictet, R., Gonet, A. E., and Renold, A. E. (1967). Studies of the diabetogenic action of streptozotocin. *Proc Soc Exp Biol Med*, 126 No. 1:201–205, Oct 1967.

Jurgenson, C. T., Begley, T. P., and Ealick, S. E. (2009). The structural and biochemical foundations of thiamin biosynthesis. *Annu Rev Biochem*, 78:569–603, 2009. doi: 10.1146/annurev.biochem.78.072407.102340. *URL:* `http://dx.doi.org/10.1146/annurev.biochem.78.072407.102340`.

Kang, M., Peterson, R., and Feigon, J. (2009). Structural Insights into riboswitch control of the biosynthesis of queuosine, a modified nucleotide found in the anticodon of tRNA. *Mol Cell*, 33 No. 6:784–790, Mar 2009. doi: 10.1016/j.molcel.2009.02.019. *URL:* `http://dx.doi.org/10.1016/j.molcel.2009.02.019`.

Karimi, R. and Ehrenberg, M. (1994). Dissociation rate of cognate peptidyl-tRNA from the A-site of hyper-accurate and error-prone ribosomes. *Eur J Biochem*, 226 No. 2:355–360, Dec 1994.

Kay, W. W. (1972). Genetic control of the metabolism of propionate by Escherichia coli K12. *Biochim Biophys Acta*, 264 No. 3:508–521, May 1972.

Kaye. and Kaye. (2000). Multidrug-resistant Pathogens: Mechanisms of Resistance and Epidemiology. *Curr Infect Dis Rep*, 2 No. 5:391–398, Oct 2000.

Bibliography

Kazuya Nishikawa, Benjamin L. Adams, Sidney M. Hecht (1982). Chemical excision of apurinic acids from RNA. A structurally modified yeast tRNAPhe. *J. Am. Chem. Soc.*, 104 No. 1:326–328, January 1982.

Kilian, Mogens (2001). *Manual of Clinical Microbiology.* 5th edition, 2001.

Kim, J. N., Blount, K. F., Puskarz, I., Lim, J., Link, K. H., and Breaker, R. R. (2009). Design and antimicrobial action of purine analogues that bind Guanine riboswitches. *ACS Chem Biol*, 4 No. 11:915–927, Nov 2009. doi: 10.1021/cb900146k. *URL:* http://dx.doi.org/10.1021/cb900146k.

Kirk, S. R. and Tor, Y. (1999). tRNA(Phe) binds aminoglycoside antibiotics. *Bioorg Med Chem*, 7 No. 9:1979–1991, Sep 1999.

Klein, D. J. and Ferré-D'Amaré, A. R. (2006). Structural basis of glmS ribozyme activation by glucosamine-6-phosphate. *Science*, 313 No. 5794:1752–1756, Sep 2006. doi: 10.1126/science.1129666. *URL:* http://dx.doi.org/10.1126/science.1129666.

Klein, D. J., Been, M. D., and Ferré-D'Amaré, A. R. (2007a). Essential role of an active-site guanine in glmS ribozyme catalysis. *J Am Chem Soc*, 129 No. 48:14858–14859, Dec 2007. doi: 10.1021/ja0768441. *URL:* http://dx.doi.org/10.1021/ja0768441.

Klein, D. J., Wilkinson, S. R., Been, M. D., and Ferré-D'Amaré, A. R. (2007b). Requirement of helix P2.2 and nucleotide G1 for positioning the cleavage site and cofactor of the glmS ribozyme. *J Mol Biol*, 373 No. 1:178–189, Oct 2007. doi: 10.1016/j.jmb.2007.07.062. *URL:* http://dx.doi.org/10.1016/j.jmb.2007.07.062.

Klein, D. J., Edwards, T. E., and Ferré-D'Amaré, A. R. (2009). Cocrystal structure of a class I preQ1 riboswitch reveals a pseudoknot recognizing an essential hypermodified nucleobase. *Nat Struct Mol Biol*, 16 No. 3:343–344, Mar 2009. doi: 10.1038/nsmb.1563. *URL:* http://dx.doi.org/10.1038/nsmb.1563.

Kluytmans, J., van Belkum, A., and Verbrugh, H. (1997). Nasal carriage of Staphylococcus aureus: epidemiology, underlying mechanisms, and associated risks. *Clin Microbiol Rev*, 10 No. 3:505–520, Jul 1997.

Kochetkov, N. and Budovskii, E. (1972). *Organic Chemistry of Nucleic Acids. Hydrolysis of N-glycosidic bonds in nucleosides, nucleotides and their derivatives.* Plenum, New York, 1972.

Kock, H., Gerth, U., and Hecker, M. (2004). The ClpP peptidase is the major determinant of bulk protein turnover in Bacillus subtilis. *J Bacteriol*, 186 No. 17:5856–5864, Sep 2004. doi: 10.1128/JB.186.17.5856-5864.2004. *URL:* http://dx.doi.org/10.1128/JB.186.17.5856-5864.2004.

Koedam, J. C. (1958). The mode of action of pyrithiamine as an inductor of thiamine deficiency. *Biochim Biophys Acta*, 29 No. 2:333–344, Aug 1958.

Koedam, J. C., Steyn-Parve, E. P., and Van Rheenen, D. L. (1956). Thiamine deficiency after feeding pyrithiamine. *Biochim Biophys Acta*, 19 No. 1:181–182, Jan 1956.

Koehl, J. L., Muthaiyan, A., Jayaswal, R. K., Ehlert, K., Labischinski, H., and Wilkinson, B. J. (2004). Cell wall composition and decreased autolytic activity and lysostaphin susceptibility of glycopeptide-intermediate Staphylococcus aureus. *Antimicrob Agents Chemother*, 48 No. 10:3749–3757, Oct 2004. doi: 10.1128/AAC.48.10.3749-3757.2004. *URL:* `http://dx.doi.org/10.1128/AAC.48.10.3749-3757.2004`.

Komatsuzawa, H., Ohta, K., Yamada, S., Ehlert, K., Labischinski, H., Kajimura, J., Fujiwara, T., and Sugai, M. (2002). Increased glycan chain length distribution and decreased susceptibility to moenomycin in a vancomycin-resistant Staphylococcus aureus mutant. *Antimicrob Agents Chemother*, 46 No. 1:75–81, Jan 2002.

Kubodera, T., Watanabe, M., Yoshiuchi, K., Yamashita, N., Nishimura, A., Nakai, S., Gomi, K., and Hanamoto, H. (2003). Thiamine-regulated gene expression of Aspergillus oryzae thiA requires splicing of the intron containing a riboswitch-like domain in the 5'-UTR. *FEBS Lett*, 555 No. 3:516–520, Dec 2003.

Küpfer, P. A. and Leumann, C. J. (2007). The chemical stability of abasic RNA compared to abasic DNA. *Nucleic Acids Res*, 35 No. 1:58–68, 2007. doi: 10.1093/nar/gkl948. *URL:* `http://dx.doi.org/10.1093/nar/gkl948`.

Laue, P. and Macdonald, R. E. (1968). Studies on the relation of thiomethyl-beta-D-galactoside accumulation to thiomethyl-beta-D-galactoside phosphorylation in Staphylococcus aureus HS1159. *Biochim Biophys Acta*, 165 No. 3:410–418, Oct 1968.

Leclercq, R., Derlot, E., Duval, J., and Courvalin, P. (1988). Plasmid-mediated resistance to vancomycin and teicoplanin in Enterococcus faecium. *N Engl J Med*, 319 No. 3:157–161, Jul 1988. doi: 10.1056/NEJM198807213190307. *URL:* `http://dx.doi.org/10.1056/NEJM198807213190307`.

Lee, E. R., Blount, K. F., and Breaker, R. R. (2009). Roseoflavin is a natural antibacterial compound that binds to FMN riboswitches and regulates gene expression. *RNA Biol*, 6 No. 2:187–194, 2009.

Lee, E. R., Baker, J. L., Weinberg, Z., Sudarsan, N., and Breaker, R. R. (2010). An allosteric self-splicing ribozyme triggered by a bacterial second messenger. *Science*, 329 No. 5993:845–848, Aug 2010. doi: 10.1126/science.1190713. *URL:* `http://dx.doi.org/10.1126/science.1190713`.

Lengeler, J. (1979). Streptozotocin, an antibiotic superior to penicillin in the selection of rare bacterial mutations. *FEMS Microbiol. Lett*, 5:417–419, 1979.

Lengeler, J. (1980). Characterisation of mutants of Escherichia coli K12, selected by resistance to streptozotocin. *Mol Gen Genet*, 179 No. 1:49–54, 1980.

Leone, M., Bourgoin, A., Cambon, S., Dubuc, M., Albanèse, J., and Martin, C. (2003). Empirical antimicrobial therapy of septic shock patients: adequacy and impact on the outcome. *Crit Care Med*, 31 No. 2:462–467, Feb 2003. doi: 10.1097/01.CCM.0000050298.59549.4A. *URL:* `http://dx.doi.org/10.1097/01.CCM.0000050298.59549.4A`.

Leone, M., Garcin, F., Bouvenot, J., Boyadjev, I., Visintini, P., Albanèse, J., and Martin, C. (2007). Ventilator-associated pneumonia: breaking the vicious circle of

antibiotic overuse. *Crit Care Med*, 35 No. 2:379–85; quizz 386, Feb 2007. doi: 10.1097/ 01.CCM.0000253404.69418.AA. *URL:* http://dx.doi.org/10.1097/01.CCM.0000253404. 69418.AA.

Liberman, J. A. and Wedekind, J. E. (2012). Riboswitch structure in the ligand-free state. *Wiley Interdiscip Rev RNA*, 3 No. 3:369–384, 2012. doi: 10.1002/wrna.114. *URL:* http://dx.doi.org/10.1002/wrna.114.

Lim, J., Grove, B. C., Roth, A., and Breaker, R. R. (2006). Characteristics of ligand recognition by a glmS self-cleaving ribozyme. *Angew Chem Int Ed Engl*, 45 No. 40: 6689–6693, Oct 2006. doi: 10.1002/anie.200602534. *URL:* http://dx.doi.org/10.1002/ anie.200602534.

Lipinski, C. A., Lombardo, F., Dominy, B. W., and Feeney, P. J. (2001). Experimental and computational approaches to estimate solubility and permeability in drug discovery and development settings. *Adv Drug Deliv Rev*, 46 No. 1-3:3–26, Mar 2001.

Livak, K. J. and Schmittgen, T. D. (2001). Analysis of relative gene expression data using real-time quantitative PCR and the 2(-Delta Delta C(T)) Method. *Methods*, 25 No. 4: 402–408, Dec 2001. doi: 10.1006/meth.2001.1262. *URL:* http://dx.doi.org/10.1006/ meth.2001.1262.

Lundberg, K. S., Shoemaker, D. D., Adams, M. W., Short, J. M., Sorge, J. A., and Mathur, E. J. (1991). High-fidelity amplification using a thermostable DNA polymerase isolated from Pyrococcus furiosus. *Gene*, 108 No. 1:1–6, Dec 1991.

Lutz, R. and Bujard, H. (1997). Independent and tight regulation of transcriptional units in Escherichia coli via the LacR/O, the TetR/O and AraC/I1-I2 regulatory elements. *Nucleic Acids Res*, 25 No. 6:1203–1210, Mar 1997.

Lünse, C. E., Schmidt, M. S., Wittmann, V., and Mayer, G. (2011). Carba-sugars activate the glmS-riboswitch of Staphylococcus aureus. *ACS Chem Biol*, 6 No. 7:675–678, Jul 2011. doi: 10.1021/cb200016d. *URL:* http://dx.doi.org/10.1021/cb200016d.

Mandal, M. and Breaker, R. R. (2004). Adenine riboswitches and gene activation by disruption of a transcription terminator. *Nat Struct Mol Biol*, 11 No. 1:29–35, Jan 2004. doi: 10.1038/nsmb710. *URL:* http://dx.doi.org/10.1038/nsmb710.

Mandal, M., Boese, B., Barrick, J. E., Winkler, W. C., and Breaker, R. R. (2003). Riboswitches control fundamental biochemical pathways in Bacillus subtilis and other bacteria. *Cell*, 113 No. 5:577–586, May 2003.

Mandal, M., Lee, M., Barrick, J. E., Weinberg, Z., Emilsson, G. M., Ruzzo, W. L., and Breaker, R. R. (2004). A glycine-dependent riboswitch that uses cooperative binding to control gene expression. *Science*, 306 No. 5694:275–279, Oct 2004. doi: 10.1126/science. 1100829. *URL:* http://dx.doi.org/10.1126/science.1100829.

Mayer, G. and Famulok, M. (2006). High-throughput-compatible assay for glmS riboswitch metabolite dependence. *Chembiochem*, 7 No. 4:602–604, Apr 2006. doi: 10.1002/cbic.200500490. *URL:* http://dx.doi.org/10.1002/cbic.200500490.

Mayer, G., Raddatz, M.-S. L., Grunwald, J. D., and Famulok, M. (2007). RNA ligands that distinguish metabolite-induced conformations in the TPP riboswitch. *Angew Chem Int Ed Engl*, 46 No. 4:557–560, 2007. doi: 10.1002/anie.200603166. *URL:* `http://dx.doi.org/10.1002/anie.200603166`.

McCarthy, T. J., Plog, M. A., Floy, S. A., Jansen, J. A., Soukup, J. K., and Soukup, G. A. (2005). Ligand requirements for glmS ribozyme self-cleavage. *Chem Biol*, 12 No. 11:1221–1226, Nov 2005. doi: 10.1016/j.chembiol.2005.09.006. *URL:* `http://dx.doi.org/10.1016/j.chembiol.2005.09.006`.

McCord, T., Ravel J. Skinner C. & Shive W. (1957). DL-4-oxalysine, an inhibitory analog of lysine. *J. Am. Chem. Soc.*, 79:5693–5696, 1957.

McCown, P. J., Roth, A., and Breaker, R. R. (2011). An expanded collection and refined consensus model of glmS ribozymes. *RNA*, 17 No. 4:728–736, Apr 2011. doi: 10.1261/rna.2590811. *URL:* `http://dx.doi.org/10.1261/rna.2590811`.

McGaughey, G. B., Sheridan, R. P., Bayly, C. I., Culberson, J. C., Kreatsoulas, C., Lindsley, S., Maiorov, V., Truchon, J.-F., and Cornell, W. D. (2007). Comparison of topological, shape, and docking methods in virtual screening. *J Chem Inf Model*, 47 No. 4:1504–1519, 2007. doi: 10.1021/ci700052x. *URL:* `http://dx.doi.org/10.1021/ci700052x`.

McGuigan, C., Serpi, M., Bibbo, R., Roberts, H., Hughes, C., Caterson, B., Gibert, A. T., and Verson, C. R. A. (2008). Phosphate prodrugs derived from N-acetylglucosamine have enhanced chondroprotective activity in explant cultures and represent a new lead in antiosteoarthritis drug discovery. *J Med Chem*, 51 No. 18:5807–5812, Sep 2008. doi: 10.1021/jm800594c. *URL:* `http://dx.doi.org/10.1021/jm800594c`.

McNamara, Peter J. (2008). *Staphylococcus: Molecular Genetics*. Caister Academic Press, 2008.

McNulty, D. E. and Annan, R. S. (2008). Hydrophilic interaction chromatography reduces the complexity of the phosphoproteome and improves global phosphopeptide isolation and detection. *Mol Cell Proteomics*, 7 No. 5:971–980, May 2008. doi: 10.1074/mcp.M700543-MCP200. *URL:* `http://dx.doi.org/10.1074/mcp.M700543-MCP200`.

Meier, F., Suter B. Grosjean H. Keith G. & Kubli E. (1985). Queuosine modification of the wobble base in tRNAHis influences in vivo decoding properties. *EMBO J.*, 4:823–827, 1985.

Melnick, J., Lis, E., Park, J.-H., Kinsland, C., Mori, H., Baba, T., Perkins, J., Schyns, G., Vassieva, O., Osterman, A., and Begley, T. P. (2004). Identification of the two missing bacterial genes involved in thiamine salvage: thiamine pyrophosphokinase and thiamine kinase. *J Bacteriol*, 186 No. 11:3660–3662, Jun 2004. doi: 10.1128/JB.186.11.3660-3662.2004. *URL:* `http://dx.doi.org/10.1128/JB.186.11.3660-3662.2004`.

Meyer, H., Liebeke, M., and Lalk, M. (2010). A protocol for the investigation of the intracellular Staphylococcus aureus metabolome. *Anal Biochem*, 401 No. 2:250–259, Jun 2010. doi: 10.1016/j.ab.2010.03.003. *URL:* `http://dx.doi.org/10.1016/j.ab.2010.03.003`.

Bibliography

Meyer, M. M., Roth, A., Chervin, S. M., Garcia, G. A., and Breaker, R. R. (2008). Confirmation of a second natural preQ1 aptamer class in Streptococcaceae bacteria. *RNA*, 14 No. 4:685–695, Apr 2008. doi: 10.1261/rna.937308. *URL:* `http://dx.doi.org/10.1261/rna.937308`.

Michael K, Wang H, Tor Y. (1999). Enhanced RNA binding of dimerized aminoglycosides. *Bioorg Med Chem.*, 7:1361–71, 1999.

Mikkelsen, N. E., Brännvall, M., Virtanen, A., and Kirsebom, L. A. (1999). Inhibition of RNase P RNA cleavage by aminoglycosides. *Proc Natl Acad Sci U S A*, 96 No. 11:6155–6160, May 1999.

Milewski, Sławomir (2002). Glucosamine-6-phosphate synthase–the multi-facets enzyme. *Biochim Biophys Acta*, 1597 No. 2:173–192, Jun 2002.

Miranda-Ríos, J., Navarro, M., and Soberón, M. (2001). A conserved RNA structure (thi box) is involved in regulation of thiamin biosynthetic gene expression in bacteria. *Proc Natl Acad Sci U S A*, 98 No. 17:9736–9741, Aug 2001. doi: 10.1073/pnas.161168098. *URL:* `http://dx.doi.org/10.1073/pnas.161168098`.

Miranda-Ríos, Juan (2007). The THI-box riboswitch, or how RNA binds thiamin pyrophosphate. *Structure*, 15 No. 3:259–265, Mar 2007. doi: 10.1016/j.str.2007.02.001. *URL:* `http://dx.doi.org/10.1016/j.str.2007.02.001`.

Montange, R. K. and Batey, R. T. (2008). Riboswitches: emerging themes in RNA structure and function. *Annu Rev Biophys*, 37:117–133, 2008. doi: 10.1146/annurev.biophys.37.032807.130000. *URL:* `http://dx.doi.org/10.1146/annurev.biophys.37.032807.130000`.

Moreira, B., Boyle-Vavra, S., deJonge, B. L., and Daum, R. S. (1997). Increased production of penicillin-binding protein 2, increased detection of other penicillin-binding proteins, and decreased coagulase activity associated with glycopeptide resistance in Staphylococcus aureus. *Antimicrob Agents Chemother*, 41 No. 8:1788–1793, Aug 1997.

Mueller, J. H. and Hinton, J. (1941). A protein-free medium for primary isolation of gonococcus and meningococcus. *Proc. Soc. Exp. Biol. Med*, 48:3330–333, 1941.

Mulhbacher, J., Brouillette, E., Allard, M., Fortier, L.-C., Malouin, F., and Lafontaine, D. A. (2010). Novel riboswitch ligand analogs as selective inhibitors of guanine-related metabolic pathways. *PLoS Pathog*, 6 No. 4:e1000865, Apr 2010. doi: 10.1371/journal.ppat.1000865. *URL:* `http://dx.doi.org/10.1371/journal.ppat.1000865`.

Muller, Y. A., Lindqvist, Y., Furey, W., Schulz, G. E., Jordan, F., and Schneider, G. (1993). A thiamin diphosphate binding fold revealed by comparison of the crystal structures of transketolase, pyruvate oxidase and pyruvate decarboxylase. *Structure*, 1 No. 2:95–103, Oct 1993.

Müller, Alexander (2011). Bachelor thesis: Screening for adenine riboswitch modulating compounds. Master's thesis, University of Bonn, GERMANY, 2011.

Nahvi, A., Barrick, J. E., and Breaker, R. R. (2004). Coenzyme B12 riboswitches are widespread genetic control elements in prokaryotes. *Nucleic Acids Res*, 32 No. 1:143–150, 2004. doi: 10.1093/nar/gkh167. *URL:* `http://dx.doi.org/10.1093/nar/gkh167`.

Narberhaus, F., Waldminghaus, T., and Chowdhury, S. (2006). RNA thermometers. *FEMS Microbiol Rev*, 30 No. 1:3–16, Jan 2006. doi: 10.1111/j.1574-6976.2005.004.x. *URL:* `http://dx.doi.org/10.1111/j.1574-6976.2005.004.x`.

Nelson, J. L., Rice, K. C., Slater, S. R., Fox, P. M., Archer, G. L., Bayles, K. W., Fey, P. D., Kreiswirth, B. N., and Somerville, G. A. (2007). Vancomycin-intermediate Staphylococcus aureus strains have impaired acetate catabolism: implications for polysaccharide intercellular adhesin synthesis and autolysis. *Antimicrob Agents Chemother*, 51 No. 2:616–622, Feb 2007. doi: 10.1128/AAC.01057-06. *URL:* `http://dx.doi.org/10.1128/AAC.01057-06`.

Neu, H. C. (1992). The crisis in antibiotic resistance. *Science*, 257 No. 5073:1064–1073, Aug 1992.

Nicholls, A., McGaughey, G. B., Sheridan, R. P., Good, A. C., Warren, G., Mathieu, M., Muchmore, S. W., Brown, S. P., Grant, J. A., Haigh, J. A., Nevins, N., Jain, A. N., and Kelley, B. (2010). Molecular shape and medicinal chemistry: a perspective. *J Med Chem*, 53 No. 10:3862–3886, May 2010. doi: 10.1021/jm900818s. *URL:* `http://dx.doi.org/10.1021/jm900818s`.

Ogston, A. (1882). Micrococcus Poisoning. *J Anat Physiol*, 17 No. Pt 1:24–58, Oct 1882.

Okada, N., Noguchi, S., Kasai, H., Shindo-Okada, N., Ohgi, T., Goto, T., and Nishimura, S. (1979). Novel mechanism of post-transcriptional modification of tRNA. Insertion of bases of Q precursors into tRNA by a specific tRNA transglycosylase reaction. *J Biol Chem*, 254 No. 8:3067–3073, Apr 1979.

Ott, E., Stolz, J., Lehmann, M., and Mack, M. (2009). The RFN riboswitch of Bacillus subtilis is a target for the antibiotic roseoflavin produced by Streptomyces davawensis. *RNA Biol*, 6 No. 3:276–280, 2009.

Pankey, G. A. and Sabath, L. D. (2004). Clinical relevance of bacteriostatic versus bactericidal mechanisms of action in the treatment of Gram-positive bacterial infections. *Clin Infect Dis*, 38 No. 6:864–870, Mar 2004. doi: 10.1086/381972. *URL:* `http://dx.doi.org/10.1086/381972`.

Pape, T., Wintermeyer, W., and Rodnina, M. (1999). Induced fit in initial selection and proofreading of aminoacyl-tRNA on the ribosome. *EMBO J*, 18 No. 13:3800–3807, Jul 1999. doi: 10.1093/emboj/18.13.3800. *URL:* `http://dx.doi.org/10.1093/emboj/18.13.3800`.

Payne, D. J., Gwynn, M. N., Holmes, D. J., and Pompliano, D. L. (2007). Drugs for bad bugs: confronting the challenges of antibacterial discovery. *Nat Rev Drug Discov*, 6 No. 1: 29–40, Jan 2007. doi: 10.1038/nrd2201. *URL:* `http://dx.doi.org/10.1038/nrd2201`.

Peske, F., Savelsbergh, A., Katunin, V. I., Rodnina, M. V., and Wintermeyer, W. (2004). Conformational changes of the small ribosomal subunit during elongation

factor G-dependent tRNA-mRNA translocation. *J Mol Biol*, 343 No. 5:1183–1194, Nov 2004. doi: 10.1016/j.jmb.2004.08.097. *URL:* http://dx.doi.org/10.1016/j.jmb.2004.08.097.

Pfeltz, R. F., Singh, V. K., Schmidt, J. L., Batten, M. A., Baranyk, C. S., Nadakavukaren, M. J., Jayaswal, R. K., and Wilkinson, B. J. (2000). Characterization of passage-selected vancomycin-resistant Staphylococcus aureus strains of diverse parental backgrounds. *Antimicrob Agents Chemother*, 44 No. 2:294–303, Feb 2000.

Ploy, M. C., Grélaud, C., Martin, C., de Lumley, L., and Denis, F. (1998). First clinical isolate of vancomycin-intermediate Staphylococcus aureus in a French hospital. *Lancet*, 351 No. 9110:1212, Apr 1998.

Poiata, E., Meyer, M. M., Ames, T. D., and Breaker, R. R. (2009). A variant riboswitch aptamer class for S-adenosylmethionine common in marine bacteria. *RNA*, 15 No. 11:2046–2056, Nov 2009. doi: 10.1261/rna.1824209. *URL:* http://dx.doi.org/10.1261/rna.1824209.

Pootoolal, J., Neu, J., and Wright, G. D. (2002). Glycopeptide antibiotic resistance. *Annu Rev Pharmacol Toxicol*, 42:381–408, 2002. doi: 10.1146/annurev.pharmtox.42.091601.142813. *URL:* http://dx.doi.org/10.1146/annurev.pharmtox.42.091601.142813.

Rakieten, N., R. M. L. and Nadkarni, M. R. (1963). Studies on the diabetogenic action of streptozotocin (NSC-37917). *Cancer Chemother Rep*, 29:91–98, May 1963.

Ramesh, A. and Winkler, W. C. (2010). Magnesium-sensing riboswitches in bacteria. *RNA Biol*, 7 No. 1:77–83, 2010.

Regulski, E. E., Moy, R. H., Weinberg, Z., Barrick, J. E., Yao, Z., Ruzzo, W. L., and Breaker, R. R. (2008). A widespread riboswitch candidate that controls bacterial genes involved in molybdenum cofactor and tungsten cofactor metabolism. *Mol Microbiol*, 68 No. 4:918–932, May 2008. doi: 10.1111/j.1365-2958.2008.06208.x. *URL:* http://dx.doi.org/10.1111/j.1365-2958.2008.06208.x.

Reichenbach, B., Maes, A., Kalamorz, F., Hajnsdorf, E., and Görke, B. (2008). The small RNA GlmY acts upstream of the sRNA GlmZ in the activation of glmS expression and is subject to regulation by polyadenylation in Escherichia coli. *Nucleic Acids Res*, 36 No. 8:2570–2580, May 2008. doi: 10.1093/nar/gkn091. *URL:* http://dx.doi.org/10.1093/nar/gkn091.

Reipert, A., Ehlert, K., Kast, T., and Bierbaum, G. (2003). Morphological and genetic differences in two isogenic Staphylococcus aureus strains with decreased susceptibilities to vancomycin. *Antimicrob Agents Chemother*, 47 No. 2:568–576, Feb 2003.

Reizer, J., Saier, M. H., Deutscher, J., Grenier, F., Thompson, J., and Hengstenberg, W. (1988). The phosphoenolpyruvate:sugar phosphotransferase system in gram-positive bacteria: properties, mechanism, and regulation. *Crit Rev Microbiol*, 15 No. 4:297–338, 1988. doi: 10.3109/10408418809104461. *URL:* http://dx.doi.org/10.3109/10408418809104461.

Ren, A., Rajashankar, K. R., and Patel, D. J. (2012). Fluoride ion encapsulation by Mg2+ ions and phosphates in a fluoride riboswitch. *Nature*, 486 No. 7401:85–89, Jun 2012. doi: 10.1038/nature11152. *URL:* http://dx.doi.org/10.1038/nature11152.

Rentmeister, A., Mayer, G., Kuhn, N., and Famulok, M. (2007). Conformational changes in the expression domain of the Escherichia coli thiM riboswitch. *Nucleic Acids Res*, 35 No. 11:3713–3722, 2007. doi: 10.1093/nar/gkm300. *URL:* http://dx.doi.org/10.1093/nar/gkm300.

Rentmeister, A., Mayer, G., Kuhn, N., and Famulok, M. (2008). Secondary structures and functional requirements for thiM riboswitches from Desulfovibrio vulgaris, Erwinia carotovora and Rhodobacter spheroides. *Biol Chem*, 389 No. 2:127–134, Feb 2008. doi: 10.1515/BC.2008.012. *URL:* http://dx.doi.org/10.1515/BC.2008.012.

Repoila, F. and Darfeuille, F. (2009). Small regulatory non-coding RNAs in bacteria: physiology and mechanistic aspects. *Biol Cell*, 101 No. 2:117–131, Feb 2009. doi: 10.1042/BC20070137. *URL:* http://dx.doi.org/10.1042/BC20070137.

Reuter, K., Slany, R., Ullrich, F., and Kersten, H. (1991). Structure and organization of Escherichia coli genes involved in biosynthesis of the deazaguanine derivative queuine, a nutrient factor for eukaryotes. *J Bacteriol*, 173 No. 7:2256–2264, Apr 1991.

Ripphausen, P., Nisius, B., Peltason, L., and Bajorath, J. (2010). Quo vadis, virtual screening? A comprehensive survey of prospective applications. *J Med Chem*, 53 No. 24:8461–8467, Dec 2010. doi: 10.1021/jm101020z. *URL:* http://dx.doi.org/10.1021/jm101020z.

Robbins, W. J. (1941). The Pyridine Analog of Thiamin and the Growth of Fungi. *Proc Natl Acad Sci U S A*, 27 No. 9:419–422, Sep 1941.

Rodionov, D. A., Vitreschak, A. G., Mironov, A. A., and Gelfand, M. S. (2002). Comparative genomics of thiamin biosynthesis in procaryotes. New genes and regulatory mechanisms. *J Biol Chem*, 277 No. 50:48949–48959, Dec 2002. doi: 10.1074/jbc.M208965200. *URL:* http://dx.doi.org/10.1074/jbc.M208965200.

Rodionov, D. A., Vitreschak, A. G., Mironov, A. A., and Gelfand, M. S. (2004). Comparative genomics of the methionine metabolism in Gram-positive bacteria: a variety of regulatory systems. *Nucleic Acids Res*, 32 No. 11:3340–3353, 2004. doi: 10.1093/nar/gkh659. *URL:* http://dx.doi.org/10.1093/nar/gkh659.

Roemer, T., Davies, J., Giaever, G., and Nislow, C. (2012). Bugs, drugs and chemical genomics. *Nat Chem Biol*, 8 No. 1:46–56, Jan 2012. doi: 10.1038/nchembio.744. *URL:* http://dx.doi.org/10.1038/nchembio.744.

Rogers, J., Chang, A. H., von Ahsen, U., Schroeder, R., and Davies, J. (1996). Inhibition of the self-cleavage reaction of the human hepatitis delta virus ribozyme by antibiotics. *J Mol Biol*, 259 No. 5:916–925, Jun 1996. doi: 10.1006/jmbi.1996.0369. *URL:* http://dx.doi.org/10.1006/jmbi.1996.0369.

Ross R. Herr, Heinz K. Jahnke, Alexander D. Argoudelis (1967). Structure of streptozotocin. *J. Am. Chem. Soc.*, 89 (18),:4808–4809, 1967.

Roth, A. and Breaker, R. R. (2009). The structural and functional diversity of metabolite-binding riboswitches. *Annu Rev Biochem*, 78:305–334, 2009. doi: 10.1146/annurev.biochem.78.070507.135656. *URL:* http://dx.doi.org/10.1146/annurev.biochem.78.070507.135656.

Roth, A., Nahvi, A., Lee, M., Jona, I., and Breaker, R. R. (2006). Characteristics of the glmS ribozyme suggest only structural roles for divalent metal ions. *RNA*, 12 No. 4: 607–619, Apr 2006. doi: 10.1261/rna.2266506. *URL:* `http://dx.doi.org/10.1261/rna.2266506`.

Roth, A., Winkler, W. C., Regulski, E. E., Lee, B. W. K., Lim, J., Jona, I., Barrick, J. E., Ritwik, A., Kim, J. N., Welz, R., Iwata-Reuyl, D., and Breaker, R. R. (2007). A riboswitch selective for the queuosine precursor preQ1 contains an unusually small aptamer domain. *Nat Struct Mol Biol*, 14 No. 4:308–317, Apr 2007. doi: 10.1038/nsmb1224. *URL:* `http://dx.doi.org/10.1038/nsmb1224`.

Saiki, R. K., Gelfand, D. H., Stoffel, S., Scharf, S. J., Higuchi, R., Horn, G. T., Mullis, K. B., and Erlich, H. A. (1988). Primer-directed enzymatic amplification of DNA with a thermostable DNA polymerase. *Science*, 239 No. 4839:487–491, Jan 1988.

Salazar, J. C., Ambrogelly, A., Crain, P. F., McCloskey, J. A., and Söll, D. (2004). A truncated aminoacyl-tRNA synthetase modifies RNA. *Proc Natl Acad Sci U S A*, 101 No. 20:7536–7541, May 2004. doi: 10.1073/pnas.0401982101. *URL:* `http://dx.doi.org/10.1073/pnas.0401982101`.

Sass, P. and Bierbaum, G. (2009). Native graS mutation supports the susceptibility of Staphylococcus aureus strain SG511 to antimicrobial peptides. *Int J Med Microbiol*, 299 No. 5:313–322, Jun 2009. doi: 10.1016/j.ijmm.2008.10.005. *URL:* `http://dx.doi.org/10.1016/j.ijmm.2008.10.005`.

Sassetti, C. M., Boyd, D. H., and Rubin, E. J. (2003). Genes required for mycobacterial growth defined by high density mutagenesis. *Mol Microbiol*, 48 No. 1:77–84, Apr 2003.

Schmidt, Magnus (2010). *Synthese von Kohlenhydrat-Derivaten zur Untersuchung der Wechselwirkung von Kohlenhydraten mit Proteinen und RNA*. PhD thesis, University of Konstanz. GERMANY, 2010.

Schneider, Gisbert (2010). Virtual screening: an endless staircase? *Nat Rev Drug Discov*, 9 No. 4:273–276, Apr 2010. doi: 10.1038/nrd3139. *URL:* `http://dx.doi.org/10.1038/nrd3139`.

Schneider, G. and Fechner, U. (2005). Computer-based de novo design of drug-like molecules. *Nat Rev Drug Discov*, 4 No. 8:649–663, Aug 2005. doi: 10.1038/nrd1799. *URL:* `http://dx.doi.org/10.1038/nrd1799`.

Schroeder, R., Waldsich, C., and Wank, H. (2000). Modulation of RNA function by aminoglycoside antibiotics. *EMBO J*, 19 No. 1:1–9, Jan 2000. doi: 10.1093/emboj/19.1.1. *URL:* `http://dx.doi.org/10.1093/emboj/19.1.1`.

Schyns, G., Potot, S., Geng, Y., Barbosa, T. M., Henriques, A., and Perkins, J. B. (2005). Isolation and characterization of new thiamine-deregulated mutants of Bacillus subtilis. *J Bacteriol*, 187 No. 23:8127–8136, Dec 2005. doi: 10.1128/JB.187.23.8127-8136.2005. *URL:* `http://dx.doi.org/10.1128/JB.187.23.8127-8136.2005`.

Schüller, Anna (2012). Modulation of the glmS–riboswitch activity by aminoglycosides and a glucosamine–nitrosourea derivative. Master's thesis, University of Bonn, GERMANY, 2012.

Scott, Fraser J. (2012). *An Investigation into Nucleic Acid Binding Compounds.* PhD thesis, University of Strathclyde, Glasgow, UK, 2012.

Serganov, Alexander (2010). Determination of riboswitch structures: light at the end of the tunnel? *RNA Biol*, 7 No. 1:98–103, 2010.

Serganov, A. and Patel, D. J. (2012). Molecular recognition and function of riboswitches. *Curr Opin Struct Biol*, 22 No. 3:279–286, Jun 2012. doi: 10.1016/j.sbi.2012.04.005. *URL:* `http://dx.doi.org/10.1016/j.sbi.2012.04.005`.

Serganov, A., Polonskaia, A., Phan, A. T., Breaker, R. R., and Patel, D. J. (2006). Structural basis for gene regulation by a thiamine pyrophosphate-sensing riboswitch. *Nature*, 441 No. 7097:1167–1171, Jun 2006. doi: 10.1038/nature04740. *URL:* `http://dx.doi.org/10.1038/nature04740`.

Serganov, A., Huang, L., and Patel, D. J. (2008). Structural insights into amino acid binding and gene control by a lysine riboswitch. *Nature*, 455 No. 7217:1263–1267, Oct 2008. doi: 10.1038/nature07326. *URL:* `http://dx.doi.org/10.1038/nature07326`.

Serganov, A., Huang, L., and Patel, D. J. (2009). Coenzyme recognition and gene regulation by a flavin mononucleotide riboswitch. *Nature*, 458 No. 7235:233–237, Mar 2009. doi: 10.1038/nature07642. *URL:* `http://dx.doi.org/10.1038/nature07642`.

Shahbabian, K., Jamalli, A., Zig, L., and Putzer, H. (2009). RNase Y, a novel endoribonuclease, initiates riboswitch turnover in Bacillus subtilis. *EMBO J*, 28 No. 22: 3523–3533, Nov 2009. doi: 10.1038/emboj.2009.283. *URL:* `http://dx.doi.org/10.1038/emboj.2009.283`.

Shanahan, C. A., Gaffney, B. L., Jones, R. A., and Strobel, S. A. (2011). Differential analogue binding by two classes of c-di-GMP riboswitches. *J Am Chem Soc*, 133 No. 39:15578–15592, Oct 2011. doi: 10.1021/ja204650q. *URL:* `http://dx.doi.org/10.1021/ja204650q`.

Shiota, T., Folk, J. E., and Tietze, F. (1958). Inhibition of lysine utilization in bacteria by S-(beta-aminoethyl) cysteine and its reversal by lysine peptides. *Arch Biochem Biophys*, 77 No. 2:372–377, Oct 1958.

Sieradzki, K. and Tomasz., A. (1997). Inhibition of cell wall turnover and autolysis by vancomycin in a highly vancomycin-resistant mutant of Staphylococcus aureus. *J. Bacteriol.*, 179:2557–2566, 1997.

Sieradzki, K. and Tomasz, A. (1999). Gradual alterations in cell wall structure and metabolism in vancomycin-resistant mutants of Staphylococcus aureus. *J Bacteriol*, 181 No. 24:7566–7570, Dec 1999.

Sieradzki, K. and Tomasz, A. (2003). Alterations of cell wall structure and metabolism accompany reduced susceptibility to vancomycin in an isogenic series of clinical isolates of Staphylococcus aureus. *J Bacteriol*, 185 No. 24:7103–7110, Dec 2003.

Bibliography

Sieradzki, K., Pinho, M. G., and Tomasz, A. (1999). Inactivated pbp4 in highly glycopeptide-resistant laboratory mutants of Staphylococcus aureus. *J Biol Chem*, 274 No. 27:18942–18946, Jul 1999.

Simons, R. W., Houman, F., and Kleckner, N. (1987). Improved single and multicopy lac-based cloning vectors for protein and operon fusions. *Gene*, 53 No. 1:85–96, 1987.

Spinelli, S. V., Pontel, L. B., Véscovi, E. G., and Soncini, F. C. (2008). Regulation of magnesium homeostasis in Salmonella: Mg(2+) targets the mgtA transcript for degradation by RNase E. *FEMS Microbiol Lett*, 280 No. 2:226–234, Mar 2008. doi: 10.1111/j.1574-6968. 2008.01065.x. *URL:* http://dx.doi.org/10.1111/j.1574-6968.2008.01065.x.

Spitale, R. C., Torelli, A. T., Krucinska, J., Bandarian, V., and Wedekind, J. E. (2009). The structural basis for recognition of the PreQ0 metabolite by an unusually small riboswitch aptamer domain. *J Biol Chem*, 284 No. 17:11012–11016, Apr 2009. doi: 10.1074/jbc.C900024200. *URL:* http://dx.doi.org/10.1074/jbc.C900024200.

Stage, T. K., Hertel, K. J., and Uhlenbeck, O. C. (1995). Inhibition of the hammerhead ribozyme by neomycin. *RNA*, 1 No. 1:95–101, Mar 1995.

Storz, G., Opdyke, J. A., and Wassarman, K. M. (2006). Regulating bacterial transcription with small RNAs. *Cold Spring Harb Symp Quant Biol*, 71:269–273, 2006. doi: 10.1101/sqb.2006.71.033. *URL:* http://dx.doi.org/10.1101/sqb.2006.71.033.

Sudarsan, N., Lee, E. R., Weinberg, Z., Moy, R. H., Kim, J. N., Link, K. H., and Breaker, R. R. (2008). Riboswitches in eubacteria sense the second messenger cyclic di-GMP. *Science*, 321 No. 5887:411–413, Jul 2008. doi: 10.1126/science.1159519. *URL:* http://dx.doi.org/10.1126/science.1159519.

Sudarsan, N., Barrick, J. E., and Breaker, R. R. (2003a). Metabolite-binding RNA domains are present in the genes of eukaryotes. *RNA*, 9 No. 6:644–647, Jun 2003.

Sudarsan, N., Wickiser, J. K., Nakamura, S., Ebert, M. S., and Breaker, R. R. (2003b). An mRNA structure in bacteria that controls gene expression by binding lysine. *Genes Dev*, 17 No. 21:2688–2697, Nov 2003. doi: 10.1101/gad.1140003. *URL:* http://dx.doi.org/10.1101/gad.1140003.

Sudarsan, N., Cohen-Chalamish, S., Nakamura, S., Emilsson, G. M., and Breaker, R. R. (2005). Thiamine pyrophosphate riboswitches are targets for the antimicrobial compound pyrithiamine. *Chem Biol*, 12 No. 12:1325–1335, Dec 2005. doi: 10.1016/j. chembiol.2005.10.007. *URL:* http://dx.doi.org/10.1016/j.chembiol.2005.10.007.

Sudarsan, N., Hammond, M. C., Block, K. F., Welz, R., Barrick, J. E., Roth, A., and Breaker, R. R. (2006). Tandem riboswitch architectures exhibit complex gene control functions. *Science*, 314 No. 5797:300–304, Oct 2006. doi: 10.1126/science.1130716. *URL:* http://dx.doi.org/10.1126/science.1130716.

Tenover, F. C. (1999). Implications of vancomycin-resistant Staphylococcus aureus. *J Hosp Infect*, 43 Suppl:S3–S7, Dec 1999.

Tenover, F. C., Lancaster, M. V., Hill, B. C., Steward, C. D., Stocker, S. A., Hancock, G. A., O'Hara, C. M., McAllister, S. K., Clark, N. C., and Hiramatsu, K. (1998). Characterization of staphylococci with reduced susceptibilities to vancomycin and other glycopeptides. *J Clin Microbiol*, 36 No. 4:1020–1027, Apr 1998.

Thomas, J. R. and Hergenrother, P. J. (2008). Targeting RNA with small molecules. *Chem Rev*, 108 No. 4:1171–1224, Apr 2008. doi: 10.1021/cr0681546. *URL:* http://dx.doi.org/10.1021/cr0681546.

Thore, S., Leibundgut, M., and Ban, N. (2006). Structure of the eukaryotic thiamine pyrophosphate riboswitch with its regulatory ligand. *Science*, 312 No. 5777:1208–1211, May 2006. doi: 10.1126/science.1128451. *URL:* http://dx.doi.org/10.1126/science.1128451.

Thore, S., Frick, C., and Ban, N. (2008). Structural basis of thiamine pyrophosphate analogues binding to the eukaryotic riboswitch. *J Am Chem Soc*, 130 No. 26:8116–8117, Jul 2008. doi: 10.1021/ja801708e. *URL:* http://dx.doi.org/10.1021/ja801708e.

Tindall, K. R. and Kunkel, T. A. (1988). Fidelity of DNA synthesis by the Thermus aquaticus DNA polymerase. *Biochemistry*, 27 No. 16:6008–6013, Aug 1988.

Tor, Y., Hermann, T., and Westhof, E. (1998). Deciphering RNA recognition: aminoglycoside binding to the hammerhead ribozyme. *Chem Biol*, 5 No. 11:R277–R283, Nov 1998.

Tor, Yitzhak (2003). Targeting RNA with small molecules. *Chembiochem*, 4 No. 10: 998–1007, Oct 2003. doi: 10.1002/cbic.200300680. *URL:* http://dx.doi.org/10.1002/cbic.200300680.

Tracy, A. and Elderfield, R. (1941). Studies in the pyridine series. II. Synthesis of 2-methyl-3-(beta-hydroxyethyl)pyridine and of the pyridine analog of thiamine (vitamin B-1). *J. Organ. Chem.*, 6:54–62, 1941.

Tudor I. Oprea, Andrew M. Davis, S. J. T. and Leeson, P. D. (2001). Is There a Difference between Leads and Drugs? A Historical Perspective. *J. Chem. Inf. Comput. Sci.*, 41:1308–1315, 2001.

Turner, Philip C. (1997). *Ribozyme Protocols*, volume 74. 1997.

van de Sande, J. H., Kleppe, K., and Khorana, H. G. (1973). Reversal of bacteriophage T4 induced polynucleotide kinase action. *Biochemistry*, 12 No. 25:5050–5055, Dec 1973.

Vicens, Q. and Westhof, E. (2002). Crystal structure of a complex between the aminoglycoside tobramycin and an oligonucleotide containing the ribosomal decoding a site. *Chem Biol*, 9 No. 6:747–755, Jun 2002.

Vioque, A. (1989). Protein synthesis inhibitors and catalytic RNA. Effect of puromycin on tRNA precursor processing by the RNA component of Escherichia coli RNase P. *FEBS Lett*, 246 No. 1-2:137–139, Mar 1989.

von Ahsen, U. and Noller, H. F. (1993). Footprinting the sites of interaction of antibiotics with catalytic group I intron RNA. *Science*, 260 No. 5113:1500–1503, Jun 1993.

von Ahsen, U., Davies, J., and Schroeder, R. (1991). Antibiotic inhibition of group I ribozyme function. *Nature*, 353 No. 6342:368–370, Sep 1991. doi: 10.1038/353368a0. *URL:* `http://dx.doi.org/10.1038/353368a0`.

Wachter, A., Tunc-Ozdemir, M., Grove, B. C., Green, P. J., Shintani, D. K., and Breaker, R. R. (2007). Riboswitch control of gene expression in plants by splicing and alternative 3' end processing of mRNAs. *Plant Cell*, 19 No. 11:3437–3450, Nov 2007. doi: 10.1105/tpc.107.053645. *URL:* `http://dx.doi.org/10.1105/tpc.107.053645`.

Wallis, M. G., von Ahsen, U., Schroeder, R., and Famulok, M. (1995). A novel RNA motif for neomycin recognition. *Chem Biol*, 2 No. 8:543–552, Aug 1995.

Walsh, C. (1999). Deconstructing vancomycin. *Science*, 284 No. 5413:442–443, Apr 1999.

Walter, F., Vicens, Q., and Westhof, E. (1999). Aminoglycoside-RNA interactions. *Curr Opin Chem Biol*, 3 No. 6:694–704, Dec 1999.

Wang, H.; Tor. Y. (1997). Electrostatic Interactions in RNA-Aminoglycosides Binding. *J. Am. Chem. Soc.*, 119:8734–8735, 1997.

Wang, J. X. and Breaker, R. R. (2008). Riboswitches that sense S-adenosylmethionine and S-adenosylhomocysteine. *Biochem Cell Biol*, 86 No. 2:157–168, Apr 2008. doi: 10.1139/O08-008. *URL:* `http://dx.doi.org/10.1139/O08-008`.

Wang, J. X., Lee, E. R., Morales, D. R., Lim, J., and Breaker, R. R. (2008). Riboswitches that sense S-adenosylhomocysteine and activate genes involved in coenzyme recycling. *Mol Cell*, 29 No. 6:691–702, Mar 2008. doi: 10.1016/j.molcel.2008.01.012. *URL:* `http://dx.doi.org/10.1016/j.molcel.2008.01.012`.

Watson, P. Y. and Fedor, M. J. (2011). The glmS riboswitch integrates signals from activating and inhibitory metabolites in vivo. *Nat Struct Mol Biol*, 18 No. 3:359–363, Mar 2011. doi: 10.1038/nsmb.1989. *URL:* `http://dx.doi.org/10.1038/nsmb.1989`.

Webb, E., Claas, K., and Downs, D. M. (1997). Characterization of thiI, a new gene involved in thiazole biosynthesis in Salmonella typhimurium. *J Bacteriol*, 179 No. 13: 4399–4402, Jul 1997.

Weigel, L. M., Clewell, D. B., Gill, S. R., Clark, N. C., McDougal, L. K., Flannagan, S. E., Kolonay, J. F., Shetty, J., Killgore, G. E., and Tenover, F. C. (2003). Genetic analysis of a high-level vancomycin-resistant isolate of Staphylococcus aureus. *Science*, 302 No. 5650:1569–1571, Nov 2003. doi: 10.1126/science.1090956. *URL:* `http://dx.doi.org/10.1126/science.1090956`.

Weinberg, Z., Barrick, J. E., Yao, Z., Roth, A., Kim, J. N., Gore, J., Wang, J. X., Lee, E. R., Block, K. F., Sudarsan, N., Neph, S., Tompa, M., Ruzzo, W. L., and Breaker, R. R. (2007). Identification of 22 candidate structured RNAs in bacteria using the CMfinder comparative genomics pipeline. *Nucleic Acids Res*, 35 No. 14:4809–4819, 2007. doi: 10.1093/nar/gkm487. *URL:* `http://dx.doi.org/10.1093/nar/gkm487`.

Weinberg, Z., Regulski, E. E., Hammond, M. C., Barrick, J. E., Yao, Z., Ruzzo, W. L., and Breaker, R. R. (2008). The aptamer core of SAM-IV riboswitches mimics

the ligand-binding site of SAM-I riboswitches. *RNA*, 14 No. 5:822–828, May 2008. doi: 10.1261/rna.988608. *URL:* `http://dx.doi.org/10.1261/rna.988608`.

Weinberg, Z., Wang, J. X., Bogue, J., Yang, J., Corbino, K., Moy, R. H., and Breaker, R. R. (2010). Comparative genomics reveals 104 candidate structured RNAs from bacteria, archaea, and their metagenomes. *Genome Biol*, 11 No. 3:R31, 2010. doi: 10.1186/gb-2010-11-3-r31. *URL:* `http://dx.doi.org/10.1186/gb-2010-11-3-r31`.

Welz, R. and Breaker, R. R. (2007). Ligand binding and gene control characteristics of tandem riboswitches in Bacillus anthracis. *RNA*, 13 No. 4:573–582, Apr 2007. doi: 10.1261/rna.407707. *URL:* `http://dx.doi.org/10.1261/rna.407707`.

Wiener, S. L., Wiener, R., Urivetzky, M., and Meilman, E. (1972). Inhibition of ribonuclease by diethyl pyrocarbonate and other methods. *Biochim Biophys Acta*, 259 No. 3:378–385, Feb 1972.

Wienken, C. J., Baaske, P., Rothbauer, U., Braun, D., and Duhr, S. (2010). Protein-binding assays in biological liquids using microscale thermophoresis. *Nat Commun*, 1:100, 2010. doi: 10.1038/ncomms1093. *URL:* `http://dx.doi.org/10.1038/ncomms1093`.

Wiley, P. F., Herr R. R. Jahnke H. K. Chidester C. G. Mizsak S. A. Spaulding L. B. Argoudelis A. D. (1979). Streptozocin: structure and chemistry. *J. Organ. Chem.*, 44:9–16, 1979.

Winkler, W., Nahvi, A., and Breaker, R. R. (2002a). Thiamine derivatives bind messenger RNAs directly to regulate bacterial gene expression. *Nature*, 419 No. 6910:952–956, Oct 2002. doi: 10.1038/nature01145. *URL:* `http://dx.doi.org/10.1038/nature01145`.

Winkler, W. C., Cohen-Chalamish, S., and Breaker, R. R. (2002b). An mRNA structure that controls gene expression by binding FMN. *Proc Natl Acad Sci U S A*, 99 No. 25:15908–15913, Dec 2002. doi: 10.1073/pnas.212628899. *URL:* `http://dx.doi.org/10.1073/pnas.212628899`.

Winkler, W. C., Nahvi, A., Sudarsan, N., Barrick, J. E., and Breaker, R. R. (2003). An mRNA structure that controls gene expression by binding S-adenosylmethionine. *Nat Struct Biol*, 10 No. 9:701–707, Sep 2003. doi: 10.1038/nsb967. *URL:* `http://dx.doi.org/10.1038/nsb967`.

Winkler, W. C., Nahvi, A., Roth, A., Collins, J. A., and Breaker, R. R. (2004). Control of gene expression by a natural metabolite-responsive ribozyme. *Nature*, 428 No. 6980:281–286, Mar 2004. doi: 10.1038/nature02362. *URL:* `http://dx.doi.org/10.1038/nature02362`.

Wong, W., Young, F. E., and Chatterjee, A. N. (1974). Regulation of bacterial cell walls: turnover of cell wall in Staphylococcus aureus. *J Bacteriol*, 120 No. 2:837–843, Nov 1974.

Wong, W., Chatterjee, A. N., and Young, F. E. (1978). Regulation of bacterial cell walls: correlation between autolytic activity and cell wall turnover in Staphylococcus aureus. *J Bacteriol*, 134 No. 2:555–561, May 1978.

Bibliography

Woolley, D. W. (1951). An enzymatic study of the mode of action of pyrithiamine (neopyrithiamine). *J Biol Chem*, 191 No. 1:43–54, Jul 1951.

Woolley, D. W. and White, A. G. (1943). Selective reversible inhibition of microbial growth with pyrithiamine. *J Exp Med*, 78 No. 6:489–497, Dec 1943.

Wu, C. H. and Bergdoll, M. S. (1971). Stimulation of Enterotoxin B Production II. Synthetic Medium for Staphylococcal Growth and Enterotoxin B Production. *Infect Immun*, 3 No. 6:784–792, Jun 1971.

Xu, J., McRae, M. A. A., Harron, S., Rob, B., and Huber, R. E. (2004). A study of the relationships of interactions between Asp-201, Na+ or K+, and galactosyl C6 hydroxyl and their effects on binding and reactivity of beta-galactosidase. *Biochem Cell Biol*, 82 No. 2: 275–284, Apr 2004. doi: 10.1139/o04-004. *URL:* `http://dx.doi.org/10.1139/o04-004`.

Zaher, H. S. and Green, R. (2009). Fidelity at the molecular level: lessons from protein synthesis. *Cell*, 136 No. 4:746–762, Feb 2009. doi: 10.1016/j.cell.2009.01.036. *URL:* `http://dx.doi.org/10.1016/j.cell.2009.01.036`.

Zalkin, H. and Smith, J. L. (1998). Enzymes utilizing glutamine as an amide donor. *Adv Enzymol Relat Areas Mol Biol*, 72:87–144, 1998.

Zapp, M. L., Stern, S., and Green, M. R. (1993). Small molecules that selectively block RNA binding of HIV-1 Rev protein inhibit Rev function and viral production. *Cell*, 74 No. 6:969–978, Sep 1993.

Zhang, Q., Kang, M., Peterson, R. D., and Feigon, J. (2011). Comparison of solution and crystal structures of preQ1 riboswitch reveals calcium-induced changes in conformation and dynamics. *J Am Chem Soc*, 133 No. 14:5190–5193, Apr 2011. doi: 10.1021/ja111769g. *URL:* `http://dx.doi.org/10.1021/ja111769g`.

Zhang, R., Ou, H.-Y., and Zhang, C.-T. (2004). DEG: a database of essential genes. *Nucleic Acids Res*, 32 No. Database issue:D271–D272, Jan 2004. doi: 10.1093/nar/gkh024. *URL:* `http://dx.doi.org/10.1093/nar/gkh024`.

Ziehler, William A. ; Engelke, David R. (2000). Probing RNA structure with chemical reagents and enzymes. *Current Protocols in Nucleic Acid Chemistry*, 2:6.1.1–6.1.16, 2000.